State of Florida

Department of Transportation

DEVELOPMENT OF A PROCEDURE FOR EVALUATING AND APPROVING LIQUID ANTI-STRIP AGENTS

BE585

FINAL REPORT

Submitted by the

TEXAS A&M TRANSPORTATION INSTITUTE

June 2020

Texas A&M Transportation Institute

DISCLAIMER

The opinions, findings, and conclusions expressed in this publication are those of the authors and not necessarily those of the State of Florida Department of Transportation.

METRIC CONVERSION CHART

SI* (MODERN METRIC) CONVERSION FACTORS

APPROXIMATE CONVERSIONS TO SI UNITS

Symbol	When You Know	Multiply By	To Find	Symbol
		LENGTH		
in	inches	25.4	millimeters	mm
ft	feet	0.305	meters	m
yd	yards	0.914	meters	m
mi	miles	1.61	kilometers	km
		AREA		
in^2	square inches	645.2	square millimeters	mm^2
ft^2	square feet	0.093	square meters	m^2
yd^2	square yard	0.836	square meters	m^2
ac	acres	0.405	hectares	ha
mi^2	square miles	2.59	square kilometers	km^2
		VOLUME		
fl oz	fluid ounces	29.57	milliliters	mL
gal	gallons	3.785	liters	L
ft^3	cubic feet	0.028	cubic meters	m^3
yd^3	cubic yards	0.765	cubic meters	m^3
	NOTE: volumes greater than 1000 L shall be shown in m^3			
		MASS		
oz	ounces	28.35	grams	g
lb	pounds	0.454	kilograms	kg
T	short tons (2000 lb)	0.907	megagrams (or "metric ton")	Mg (or "t")
		TEMPERATURE (exact degrees)		
°F	Fahrenheit	5 (F-32)/9 or (F-32)/1.8	Celsius	°C
		ILLUMINATION		
fc	foot-candles	10.76	lux	lx
fl	foot-Lamberts	3.426	$candela/m^2$	cd/m^2
		FORCE and PRESSURE or STRESS		
lbf	poundforce	4.45	newtons	N
lbf/in^2	poundforce per square inch	6.89	kilopascals	kPa

APPROXIMATE CONVERSIONS FROM SI UNITS

Symbol	When You Know	Multiply By	To Find	Symbol
		LENGTH		
mm	millimeters	0.039	inches	in
m	meters	3.28	feet	ft
m	meters	1.09	yards	yd
km	kilometers	0.621	miles	mi
		AREA		
mm^2	square millimeters	0.0016	square inches	in^2
m^2	square meters	10.764	square feet	ft^2
m^2	square meters	1.195	square yards	yd^2
ha	hectares	2.47	acres	ac
km^2	square kilometers	0.386	square miles	mi^2
		VOLUME		
mL	milliliters	0.034	fluid ounces	fl oz
L	liters	0.264	gallons	gal
m^3	cubic meters	35.314	cubic feet	ft^3
m^3	cubic meters	1.307	cubic yards	yd^3
		MASS		
g	grams	0.035	ounces	oz
kg	kilograms	2.202	pounds	lb
Mg (or "t")	megagrams (or "metric ton")	1.103	short tons (2000 lb)	T
		TEMPERATURE (exact degrees)		
°C	Celsius	1.8C+32	Fahrenheit	°F
		ILLUMINATION		
lx	lux	0.0929	foot-candles	fc
cd/m^2	$candela/m^2$	0.2919	foot-Lamberts	fl
		FORCE and PRESSURE or STRESS		
N	newtons	0.225	poundforce	lbf
kPa	kilopascals	0.145	poundforce per square inch	lbf/in^2

*SI is the symbol for the International System of Units. Appropriate rounding should be made to comply with Section 4 of ASTM E380.
(Revised March 2003)

TECHNICAL REPORT DOCUMENTATION PAGE

1. Report No.	2. Government Accession No.	3. Recipient's Catalog No.
4. Title and Subtitle DEVELOPMENT OF A PROCEDURE FOR EVALUATING AND APPROVING LIQUID ANTI-STRIP AGENTS		5. Report Date June 2020 6. Performing Organization Code
7. Author(s) Pravat Karki, Edith Arámbula-Mercado, and Tito Nyamuhokya		8. Performing Organization Report No.
9. Performing Organization Name and Address Texas A&M Transportation Institute 3135 TAMU College Station, TX 77843-3135		10. Work Unit No. (TRAIS) 11. Contract or Grant No. BE585
12. Sponsoring Agency Name and Address Florida Department of Transportation 605 Suwannee Street, MS 30 Tallahassee, FL 32399		13. Type of Report and Period Covered Final Report June 2018–June 2020 14. Sponsoring Agency Code
15. Supplementary Notes		

16. Abstract

The objectives of this project were to determine the extent to which liquid anti-strip agents (ASAs) can affect asphalt mixture stability during and after construction, determine the effective laboratory methods/procedures to evaluate asphalt mixture stability, and develop an approval system for liquid ASA with respect to mixture stability. The project initiated with a review of the literature on the use of liquid ASA in asphalt pavements, protocols used to evaluate and approve their use, need, and dosage, and their effects on asphalt mixture stability during and after construction. The experimental plan involved (1) the Superpave gyratory compaction of four control and sixteen liquid ASA-treated mixtures to identify stability parameters from compaction data and (2) two control and eight liquid ASA-treated mixtures to identify stability parameters from five types of tests conducted after compaction. Results showed liquid ASA-treated mixtures were softer and less resistant to shear than control mixtures, and that shear energy and compactability energy indices measured from compaction curves and shear strength measured from a newly developed IDEAL shear rutting test were able to evaluate asphalt mixture stability. An approval system for liquid ASA was developed for evaluating the effectiveness of liquid ASA in terms of asphalt mixture stability during and after construction.

17. Key Words	18. Distribution Statement		
Asphalt Mixture Stability; Anti-Strip Agents	No restrictions.		
19. Security Classif. (of this report)	20. Security Classif. (of this page)	21. No. of Pages 154	22. Price

Form DOT F 1700.7 (8-72) Reproduction of completed page authorized.

ACKNOWLEDGMENTS

The authors would like to extend their gratitude to Ahmad Chami, Howard Moseley, Richard Hewitt, Michael Horst, Greg Sholar, and Wayne Rilko for their guidance and support throughout the execution of this project. Gratitude is also extended to Fujie Zhou and Soohyok Im for sharing their expertise in support of the laboratory tests.

Appreciation is also extended to Moises Saca Estevanott, Saureen Naik, Zeinab Mraiza, Ethan Karnei, Tony Barbosa, and Rick Canatella for their assistance in laboratory-related activities. Finally, the authors are thankful to the suppliers of aggregates, asphalt binder, and liquid anti-strip agents used to execute the experimental plan of this project.

EXECUTIVE SUMMARY

Many state highway agencies allow, if not require, the use of liquid anti-strip agents (ASAs) in asphalt mixtures to mitigate moisture-induced stripping of asphalt binder from aggregates. The Florida Department of Transportation only employs the liquid ASAs that are listed in its Approved Product List. FM 5-508 (FDOT, 2018a)—a modified Lottman test-based protocol is used to decide if a product can be approved and placed in this list. Currently, this protocol only evaluates the effectiveness of liquid ASA on the moisture damage susceptibility of asphalt mixtures. Field personnel in Florida reported that there were isolated instances where mixtures produced with some of these approved liquid ASAs were

- tender and moved excessively under the rollers during field compaction while the mixtures were still hot; and
- still soft and would crumble when inspected by the contractors the day after compaction, when mixtures had already cooled to ambient temperature.

They were concerned whether liquid ASAs were contributing to these issues. Therefore, it was deemed critical to update the current approval system with the capability to evaluate the effectiveness of liquid ASA with respect to asphalt mixture stability during and after construction.

The objectives of this project were to determine the extent to which liquid ASA can affect asphalt mixture stability during and after construction, determine the effective laboratory methods/procedures to evaluate asphalt mixture stability, and develop an approval system for liquid ASA with respect to mixture stability. To accomplish these objectives, researchers reviewed the studies that investigated the effect of liquid ASA in asphalt mixtures, the protocols that have been developed to evaluate and approve the use, need, and dosage of liquid ASA in asphalt mixtures, and the protocols that have been developed to evaluate asphalt mixture stability during and after construction. Based on this review, an experimental plan was devised with two components:

- Superpave gyratory compaction of four control and sixteen liquid ASA-treated mixtures with a predetermined number of gyrations to obtain compaction parameters that could be correlated to asphalt mixture stability during and after construction.
- Superpave gyratory compaction of two control and eight liquid ASA-treated mixtures with predetermined air void content to obtain performance parameters from laboratory tests (resilient modulus, asphalt pavement analyzer, Hamburg wheel-track, Cantabro abrasion loss, and the recently developed IDEAL shear rutting tests) at various durations after compaction (up to 72 hours) that could be correlated to asphalt mixture stability during and after construction.

The first part of the experimental plan revealed that, out of 121 different parameters obtained from compaction data, three parameters (two shear energy and two compactability energy indices calculated using the area under the compaction stress versus gyration number

curve) were able to differentiate mixtures that were equivalent or different from the control mixture in terms of stability during compaction.

Likewise, the second part of the experimental plan showed that liquid ASA-treated mixtures were generally softer and less resistant to shear (or had lower resilient modulus and lower shear strength values) than control mixtures. The results of this second part of the experimental plan also revealed that, unlike the undamaged stiffness value obtained from the resilient modulus tests, the rut depth values obtained from the asphalt pavement analyzer and the Hamburg wheel-track test, mass loss percentage obtained from the Cantabro abrasion loss tests, the shear strength values obtained from the IDEAL shear rutting tests discriminated the liquid ASA-treated mixtures from control mixtures more consistently.

Based on the conclusions drawn from the literature review and the results of both parts of the experimental plan, a protocol was developed to approve liquid ASAs based on their effectiveness on asphalt mixture stability. Because only one type, source, and grade of the binder were used to develop this protocol, it is recommended to further verify these conclusions with other types, sources, and grades of the binder. Similarly, because the protocol was developed based only on laboratory tests, it is furthermore recommended to validate these conclusions with field observations.

TABLE OF CONTENTS

DISCLAIMER ..... **ii**

METRIC CONVERSION CHART ..... **iii**

TECHNICAL REPORT DOCUMENTATION PAGE ..... **iv**

ACKNOWLEDGMENTS ..... **v**

EXECUTIVE SUMMARY ..... **vi**

LIST OF FIGURES ..... **xii**

LIST OF TABLES ..... **xiv**

1 INTRODUCTION **1**

1.1 Background 1

1.2 Issues 2

1.3 Objectives 2

1.4 Report Organization 3

2 LITERATURE REVIEW **7**

2.1 Asphalt Mixture Stripping 7

2.1.1 Influencing Factors 7

2.1.2 Test Protocols 8

2.1.3 Mitigation Methods 10

2.2 Use of Liquid ASA 10

2.2.1 Anti-stripping Effects 11

2.2.2 Previously Raised Common Issues 13

2.2.3 Approved Product Lists 14

2.3 Asphalt Mixture Stability 20

2.3.1 Parameters Measured during Mixing 22

2.3.2 Parameters Obtained from Data Collected during Compaction 24

2.3.3 Parameters Obtained from Tests after Mixtures Have Partially Cooled 48

2.3.4 Parameters Obtained from Tests after Mixtures Have Completely Cooled 55

2.4 Summary 55

3 MATERIALS 58

3.1 Asphalt Binder 58

3.1.1 DSR Tests of Unaged Binder 58

3.1.2 MSCR Test of RTFO-Aged Binder 58

3.1.3 BBR Test of PAV-Aged Binder 59

3.1.4 DSR Test of PAV-Aged Binder 59

3.2 Aggregates 60

3.3 Liquid ASA 63

3.4 Mix Design Verification 63

3.5 Summary 65

4 PARAMETERS OBTAINED FROM COMPACTION DATA 66

4.1 Gyratory Compaction Tests 66

4.1.1 Compacted Density Parameters 70

4.1.2 Compaction Effort Parameters 72

4.1.3 Compaction Rate Parameters 74

4.1.4 Densification Indices 75

4.1.5 Compaction Energy Indices 77

4.2 Data Analysis 79

4.2.1 Compacted Density Parameters 83

4.2.2 Compaction Effort Parameters 83

4.2.3 Compaction Rate Parameters 84

4.2.4 Densification Indices 85

4.2.5 Compaction Energy Indices 85

4.3 Summary 87

5 PARAMETERS OBTAINED FROM TESTS CONDUCTED AFTER COMPACTION 89

5.1 Asphalt Binder Tests 89

5.1.1 Fourier-Transform Infrared Tests 89

5.1.2 Dynamic Shear Modulus Tests 93
5.1.3 Monotonic Pull-Off Tests 94
5.2 Asphalt Mixture Tests 97
5.2.1 Resilient Modulus Tests 99
5.2.2 Cantabro Abrasion Loss Tests 103
5.2.3 Asphalt Pavement Analyzer Tests 105
5.2.4 Hamburg Wheel-Track Tests 108
5.2.5 IDEAL Shear Rutting Tests 109
5.3 Summary 114
6 CONCLUSIONS AND RECOMMENDATIONS 116
6.1 Conclusions 116
6.1.1 Literature Review 116
6.1.2 Parameters Obtained from Compaction Data 116
6.1.3 Parameters Obtained from Tests Conducted after Compaction 117
6.2 Limitations 118
6.3 Recommendations 118
7 LIQUID ANTI-STRIP AGENT APPROVAL SYSTEM 119
7.1 Scope 119
7.2 Referenced Documents 119
7.2.1 AASHTO Standards 119
7.2.2 ASTM Standards 119
7.2.3 Florida Method of Tests 119
7.2.4 Journal Articles 119
7.3 Significance and Use 119
7.4 Summary of Method 120
7.5 Apparatus 120
7.6 Submittal of Test Specimens 120
7.7 Preparation of Specimens to Analyze Stability Parameters from Compaction Data 121

7.8 Preparation of Specimens to Analyze Stability Parameters from Tests Conducted after Compaction 121
7.9 Evaluation of Test Specimens 124
7.10 Stability Parameters Obtained from Compaction Data 124
7.11 Stability Parameters Obtained from Tests Conducted after Compaction 125
7.12 Decision of Approval 126
REFERENCES 127
APPENDIX A PARAMETERS OBTAINED FROM COMPACTION DATA 137

LIST OF FIGURES

Figure 1-1. Project Outline Including the Components of the Experimental Plan. 3
Figure 2-1. Distribution of Moisture Damage Treatments (Hicks et al. 2003) 11
Figure 2-2. Asphalt Pavement Stability Issues: (a) Checking, (b) Humping, and (c) Shoving 21
Figure 2-3. Viscosity and Compaction Temperature Effect (McLeod, 1967) 23
Figure 2-4. Torque as a Workability Parameter (Bennert et al., 2010) 24
Figure 2-5. Workability Index (Cabrera, 1996) 26
Figure 2-6. Relative Density at Design Number of Gyrations (McGennis, 1997) 27
Figure 2-7. Compacted Air Voids in (a) Marshall Compacted Samples; (b) Gyratory Compacted Samples (Bennert et al., 2010) 28
Figure 2-8. Locking Point (Mohammad and Al Shamsi, 2007) 29
Figure 2-9. Gyratory Compaction Rate (Bennert et al., 2010) 30
Figure 2-10. Correlation of Resistance to Compaction with (a) Mix Constituents; (b) Mix Stiffness (Bissada, 1984) 31
Figure 2-11. Compaction Slope (McGennis, 1997) 32
Figure 2-12. Correlation of Compaction Slope with Stiffness (Anderson et al., 1999) 33
Figure 2-13. Compaction Slope × Air Voids (Anderson et al., 2002) 33
Figure 2-14. Compaction Curves (Button et al., 2004) 34
Figure 2-15. Correlation of Gyratory Shear with (a) Percent Asphalt Content; (b) Percent Natural Sand (Ruth et al., 1992) 35
Figure 2-16. Correlation of Maximum Shear Stress with (a) Gyration Angle; (b) Vertical Stress (Butcher, 1998) 36
Figure 2-17. Gyrations at Maximum Shear Stress Ratio: (a) Determining Its Value; (b) Its Correlation with Rutting Rate (Anderson et al., 2002) 37
Figure 2-18. Normalized Maximum Shear Stress (Newcomb et al., 2015) 38
Figure 2-19. Frictional Resistance (Guler et al., 2000) 39
Figure 2-20. Schematic Separation of Compaction Data (Bayomy et al., 2002) 40
Figure 2-21. Contact Energy Index Sensitivity (Dessouky et al., 2004) 41
Figure 2-22. Shear Energy and Force Index Schematic (Bahia and Faheem, 2007) 42
Figure 2-23. Gyratory Stability (Abu Abdo et al., 2010) 43
Figure 2-24. Workability and Compactability Correlations (Dessouky et al., 2013) 44
Figure 2-25. Asphalt Binder Pull-Off Test (a) Illustration; (b) Sample Results (Gorsuch et al., 2013) 49
Figure 2-26. Asphalt Pavement Cooling Behavior (McLeod, 1967) 50
Figure 2-27. Asphalt Pavement Cooling Behavior (Dickson and Corlew, 1970) 51
Figure 2-28. Asphalt Pavement Cooling Behavior (Chadbourn et al., 1998) 52
Figure 2-29. Asphalt Pavement Cooling Behavior (Chang et al., 2009) 53
Figure 2-30. Asphalt Mixture Stiffness and Strength Properties (Chang et al., 2009) 54
Figure 4-1. Illustration of Compacted Density Parameters 71

Figure 4-2. Illustration of Compaction Effort Parameters 72
Figure 4-3. Illustration of Compaction Slope Parameters 75
Figure 4-4. Illustration of Densification Indices 77
Figure 4-5. Illustration of Compaction Energy Indices 79
Figure 5-1. FTIR Test Results: Liquid ASAs 90
Figure 5-2. FTIR Test Results of Liquid ASA-Treated Asphalt Binders versus Liquid ASAs: (a) L1, (b) L2, (c) L3, and (d) L4 90
Figure 5-3. FTIR Test Results: Liquid ASA-Treated Asphalt Binders 92
Figure 5-4. Dynamic Shear Modulus Test Results: (a) Complex Shear Modulus; (b) Phase Angle 94
Figure 5-5. Monotonic Pull-Off Test Results: (a) 30 Minutes after Cooling; (b) 30 versus 60 Minutes after Cooling 96
Figure 5-6. Monotonic Pull-Off Test Results: (a) Peak Force; (b) Work 97
Figure 5-7. Resilient Modulus Test Plan 100
Figure 5-8. Resilient Modulus Test Results: (a-b) Moduli during 4-5 Hours of Cooling after Compaction, (c-d) Moduli after 4, 24, 48, and 72 Hours of Cooling after Compaction, and (e-f) Percent Difference in Moduli of Lx-Treated and Control Mixes 102
Figure 5-9. CAL Test: (a) Instrument, (b) Specimen before and after the Test, (c-d) CAL Values, and (e-f) Percent Difference in CAL Values between Lx-Treated and Control Mixtures 104
Figure 5-10. APA Test: (a) Instrument; (b) Setup 105
Figure 5-11. APA Test Results: (a-b) Rut Depths at 74°C and 64°C, (c-d) Percent Difference in Rut Depths between 74°C to 64°C, and (e-f) Percent Difference in Rut Depths between Lx-Treated and Control Mixtures 107
Figure 5-12. HWT Test: (a) Instrument; (b) Setup 108
Figure 5-13. HWT Test Results: (a-b) Rut Depths at 50°C; (c-d) Percent Difference in Rut Depths between Lx-Treated and Control Mixtures 109
Figure 5-14. IDEAL Shear Rutting Test: (a) Setup, (b) Typical Result, and (c) Shear Stress Distribution (Zhou et al., 2019) 111
Figure 5-15. IDEAL Shear Rutting Test Results: (a-b) Shear Strengths after 0 and 35 Minutes of Cooling, (c-d) Percent Difference in Shear Strengths between 0 and 35 Minutes of Cooling, and (e-f) Percent Difference in Shear Strengths between Lx-Treated and Control Mixtures 113
Figure 7-1. Sample Fabrication and Test Plan for Liquid Anti-Strip Agent Approval 122

LIST OF TABLES

Table 2-1. Moisture Damage Susceptibility Tests 9
Table 2-2. ASA Approval Systems in Florida and Its Eight Neighboring States 16
Table 2-3. Workability and Compactability Parameters 45
Table 3-1. Performance Grade Results: Control Asphalt Binder 60
Table 3-2. Job Mix Formula of Aggregates: Original 61
Table 3-3. JMF of Aggregates: Adjusted 62
Table 3-4. Characteristics of Mix Design Samples: Control Mixtures 65
Table 4-1. Characteristics of GA9.5 Samples at N = 75 Gyrations 68
Table 4-2. Characteristics of GA12.5 Samples at N = 75 Gyrations 68
Table 4-3. Characteristics of LS9.5 Samples at N = 75 Gyrations 69
Table 4-4. Characteristics of LS12.5 Samples at N = 75 Gyrations 69
Table 4-5. Parameters Extracted from Compaction Data of GA9.5 Mixtures 81
Table 4-6. Parameters Extracted from Compaction Data of GA12.5 Mixtures 82
Table 4-7. Analysis Results of Compaction Density Parameters 83
Table 4-8. Analysis Results of Compaction Effort Parameters 84
Table 4-9. Analysis Results of Compaction Rate Parameters 85
Table 4-10. Analysis Results of Compaction Densification Indices 86
Table 4-11. Analysis Results of Compaction Energy Indices 87
Table 5-1. Mixtures Tests Selected to Study Stability after Construction 99
Table A-1. Compaction Effort Parameters Obtained from Compaction Data 137
Table A-2. Compaction Density Parameters Obtained from Compaction Data 138
Table A-3. Compaction Slope Parameters Obtained from Compaction Data 138
Table A-4. Densification Parameters Obtained from Compaction Data 139
Table A-5. Compaction Energy Parameters Obtained from Compaction Data 140

1 INTRODUCTION

1.1 Background

Moisture damage is one of the major sources of distresses that can cause premature failure of asphalt pavements (Epps et al., 2003; Hicks et al., 2003; Little et al., 2006; Birgisson et al., 2005; Putnam and Amirkhanian, 2006; Kim et al., 2008; Ravi Shankar et al., 2018). State Departments of Transportation (DOTs) have tried different methods to mitigate moisture damage in their pavements such as preventing the entry of excess water, allowing the rapid removal of surface water, avoiding the use of stripping-prone aggregates and asphalt binders, and treating mixtures with adhesion enhancing agents that make aggregates and binders less prone to stripping (Kennedy and Anagnos, 1984). For these reasons, the Florida Department of Transportation (FDOT) requires the use of liquid anti-strip agents (ASAs) or hydrated lime in mixtures used in its contracts:

- *Superpave (SP) mixes:* FDOT's Standard Specifications for Road and Bridge Construction (FDOT, 2020) requires the use of 0.50% heat-stable, liquid ASA by weight of binder in mixtures prepared for traffic levels A and B (see Section 334-3.2.6.1). Similarly, the specification requires the use of either 1.00% hydrated lime by weight of aggregates or 0.50% heat-stable, liquid ASA by weight of binder in mixtures produced for traffic levels C, D, and E if either their untreated, unconditioned indirect tensile strength (ITS) is less than 100 psi (690 kPa) and the untreated conditioned-to-unconditioned tensile strength ratio (*TSR*) is less than 0.80 (i.e., 80%) (see Section 334-3.2.6.2).
- *Friction course (FC) mixes:* The specification requires the use of 1.00% hydrated lime by weight of aggregates with granite aggregates and 0.50% liquid ASA by weight of binder with limestone aggregates (Section 337-3.2.1.4).
- *Asphalt-treated permeable base (ATPB) mixes:* The specification requires the use of 0.50% liquid ASA by weight of binder in all ATPB mixtures (see Section 287.2).

FDOT also mandates that hydrated lime satisfies the American Association of State Highway and Transportation Officials (AASHTO) M 303-89 (2010a) requirements of Type 1 lime as specified in Section 337-2.5 and that the liquid ASA is listed in the Approved Product List (APL) and satisfies the requirements specified in Section 916-4.

State highway agencies have tried different methods to assess the moisture damage susceptibility of untreated asphalt mixtures, evaluate the effect of selected products (hydrated lime or liquid ASA) on this susceptibility, decide their inclusion in the corresponding APL, and approve their uses in state contracts.

FDOT uses the test protocol FM 5-508 (FDOT, 2018a) to assess the effect of selected products on the moisture damage susceptibility of asphalt mixtures and determine whether the product can be placed in its APL for liquid ASAs. The protocol involves determining *ITS* and *TSR* values of Type SP-9.5 and Type SP-12.5 mixtures (i.e., Superpave mixtures produced

with a nominal maximum aggregate size of 9.5 and 12.5 mm, respectively) produced with 0.50% liquid ASA-treated PG 67-22 asphalt binder and multiple aggregate sources using FM 1-T 283 (FDOT, 2018b)—FDOT's own version of AASHTO T 283 (2014a). If the *ITS* and *TSR* values are equal to or greater than 100 psi (690 kPa) and 0.80 (80%), respectively, the product is added to the APL and approved for use in its contracts.

1.2 Issues

Field personnel in Florida reported that there were isolated instances where mixtures produced with some of these liquid ASAs, despite being approved through a rigorous test method and passing a moisture damage test, exhibited lack of stability during and after construction. Notably:

- During compaction of the mixture in the field (while the mixture was still hot), the mixture was tender and moved excessively under the rollers. An example of this issue included the scuffing of mixtures under power steering or braking action as seen in a couple of projects in the past few years.
- After the mixture had cooled to ambient temperatures, the mixture was still soft the following couple of days and crumbled when inspected by the contractor. An example of this issue included the instances where the turning of the wheels of a pickup truck while parked left visible distress marks in the pavement. The field personnel's concern was that the mixture might cool adequately but still might exhibit instability for one or more days after paving.

They were concerned whether liquid ASAs were contributing to these issues. However, the current Florida Test Method, FM 5-508 (FDOT, 2018a), approves liquid ASAs by evaluating their effectiveness only with respect to moisture damage susceptibility. The test method does not investigate or address their effectiveness with respect to stability during and after construction.

1.3 Objectives

The researchers at Texas A&M Transportation Institute (TTI) conducted this study to achieve three main objectives:

1. document the extent to which liquid ASA can affect asphalt mixture stability during and after construction,
2. determine the effective laboratory methods or procedures to evaluate asphalt mixture stability, and
3. develop an approval system for liquid ASA with respect to mixture stability.

To achieve these three objectives, researchers developed a rigorous experimental plan in cooperation with FDOT. Figure 1-1 illustrates the different tasks, including the experimental plan, included in this project. Chapters 1 to 6 of this report summarize the results of the literature review conducted in Task 1, and details the experimental plan prepared in Task 2 and

the results of laboratory tests conducted in Task 3 in line with the first and second objectives of this project. Chapter 7 of this report presents the proposed approval system for liquid ASA with respect to asphalt mixture stability in line with the third objective of this project.

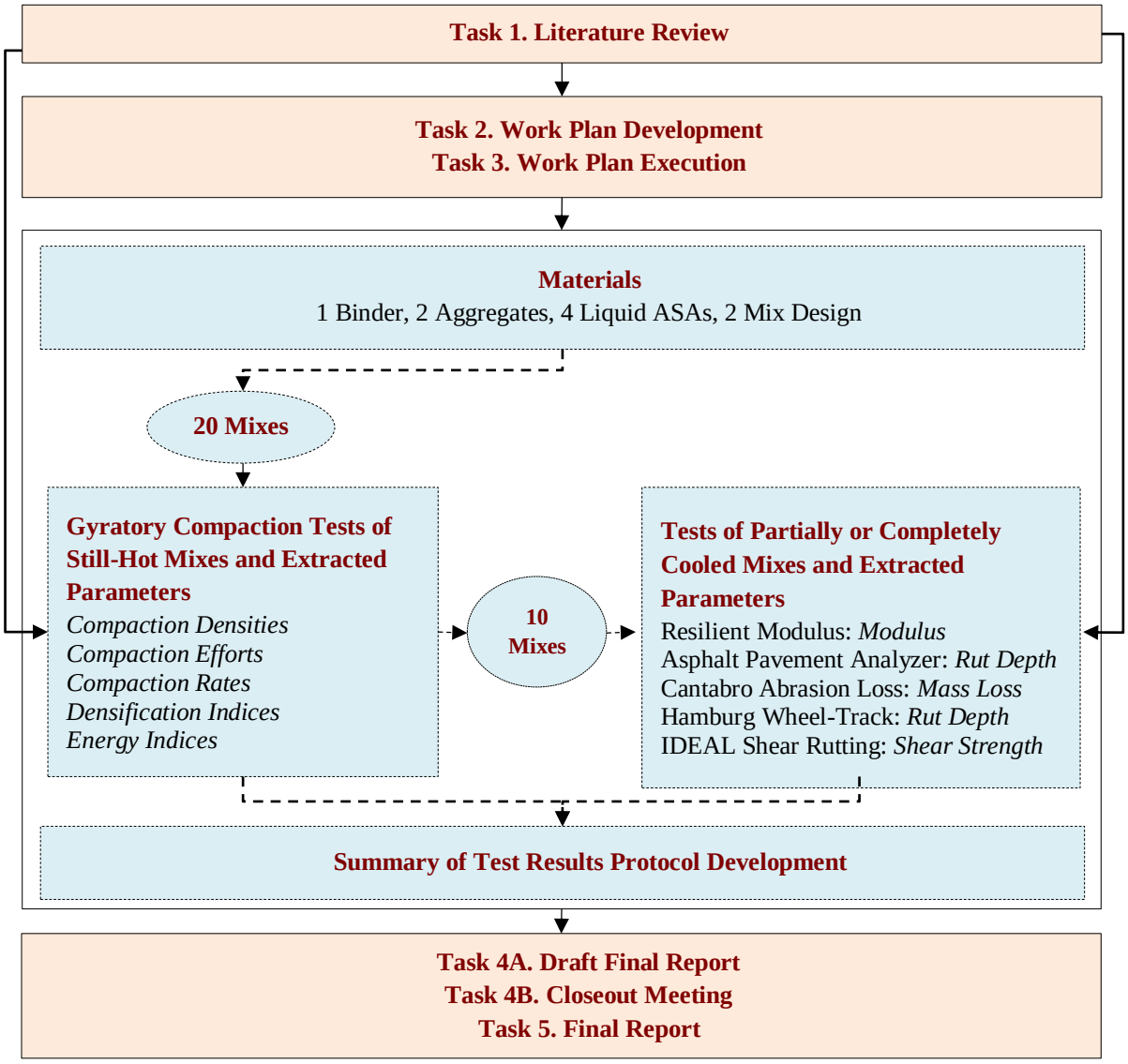

Figure 1-1. Project Outline Including the Components of the Experimental Plan.

1.4 Report Organization

Chapter 1 (this chapter) introduces the background and objectives of this project and outlines various components of the work plan devised to achieve these objectives.

Chapter 2 (the next chapter) summarizes the literature review conducted at the beginning of this project. The review was focused on three main areas relevant to this project: asphalt mixture stripping, asphalt mixture stability, and assessment protocols. The review showed that state highway agencies only use moisture damage susceptibility tests to approve the use of liquid ASA and determine their doses in their contracts; they do not use asphalt mixture stability tests for this purpose. The review also showed that asphalt mixture stability during

construction has been mostly assessed in terms of parameters that can be extracted from compaction data and tied to the workability of mixtures under rollers during construction. The review also showed that asphalt mixture stability after construction has been mostly assessed in terms of parameters that can be extracted from the latter part of the compaction data, the change in asphalt binder/mixture properties, and the change in plastic deformation properties (or rutting performance) after mixtures have partially or completely cooled.

Chapter 3 presents the description of materials (types, percentages, and sources), including the mix designs obtained for use in this project as outlined in Figure 1-1. The materials descriptions formed the following experimental (mixture) variables for this research:

- one type of binder (styrene-butadiene-styrene [SBS]–modified PG 76-22 polymer-modified asphalt [PMA] binder),
- two types of aggregates (granite from Georgia and limestone from Southeast Florida),
- two types of liquid ASA (obtained from two different sources), and
- two types of mix designs per aggregate (Type SP/FC-9.5 and Type SP/FC-12.5 mixes).

Chapter 3 also presents the results of the tests conducted to verify the properties of these materials and mix design:

- *Performance grade (PG) of binder*: The tests involved the dynamic shear rheometer (DSR) tests of the unaged and the long-term oven-aged asphalt binders, the multiple stress creep recovery (MSCR) tests of the short-term oven-aged asphalt binders, and the bending beam rheometer (BBR) tests of the long-term aged asphalt binders as specified in Section 916-2 of FDOT's Standard Specifications for Road and Bridge Construction (FDOT, 2019). Rolling thin film oven (RTFO) and pressure aging vessel (PAV) were used to simulate short-term and long-term oven aging of asphalt binders specified in Section 916-2. The chapter will show that the control binder satisfied each requirement of PG 76-22 (PMA) binder.
- *Aggregate gradation*: The tests involved wet sieve analysis of the oven-dried batches of aggregates prepared according to the job mix formula (JMF) provided by FDOT and Section 334-3.2 of FDOT's specifications (FDOT, 2019). This chapter shows that there were more differences in washed gradation and JMF in granite than in limestone gradations, and adjustments were needed in batching to meet the target gradation noted in the JMF.
- *Mix design of control mixtures at design number of gyrations*: The tests involved compaction of control mixtures until the FDOT-specified design number of gyrations (herein, 75) following AASHTO T 312 (2015) and checking compliance with the requirement of 4.0 ± 0.5% air void content by compacted volume at the same number of gyrations according to AASHTO M 323 (2017a) and Section 334-3.2.4 of FDOT's specifications (FDOT, 2019). This chapter shows that all but one control mixture satisfied this requirement, thereby allowing the use of the same optimum binder content as mentioned in the control mix designs in the mixtures that satisfied this requirement

and slight reduction in the optimum asphalt binder content in the mixture that did not meet this requirement.

Chapter 4 presents the work performed on four control and 16 liquid ASA-treated asphalt mixtures (i.e., 20 types of mixtures in total) to extract parameters from data captured while mixtures were still hot and compacted with the Superpave gyratory compactor. In this part of the experimental plan, the Superpave gyratory compacted (SGC) samples of the control and the liquid ASA-treated mixtures were fabricated using the design number of gyrations with a target air void content of 4.0 ± 0.5% by volume (i.e., 96.0 ± 0.5% G_{mm}). The compaction data (stress, height, and number of gyrations, etc.) were continuously collected during compaction and used to extract parameters that would differentiate the types of liquid ASA in terms of stability during compaction.

This chapter shows that several compaction effort-related parameters (i.e., the number of gyrations, N required to reach certain relative density, $\%G_{mm}$), compaction density-related parameter (i.e., relative density or $\%G_{mm}$ achieved at certain numbers of gyrations, N), compaction rate-related parameters (i.e., slope of compacted density or air void), densification-related parameters (i.e., indices extracted from compaction density versus gyration number data), and compaction energy-related parameters (i.e., indices extracted from compaction energy versus gyration number data) were able to differentiate mixtures that had equivalent stability from mixtures that had different stability compared to control (stable) mixtures; this was detected only in granite mixtures, however.

Chapter 5 presents the work performed on two control and eight liquid ASA-treated asphalt binders/mixtures (i.e., 10 mixtures in total) to obtain stability parameters from tests conducted after mixtures had partially or completely cooled down to ambient temperature. In this part of the experimental plan, SP-9.5 and SP-12.5/FC-12.5 granite mixtures were fabricated with a target air void content of 7.0 ± 0.5% by volume (i.e., 93.0 ± 0.5% G_{mm}) and target heights dictated by the specific test methods. Each mixture was subjected to a total of five tests—one nondestructive (non-damage) and four destructive (damage) tests at different testing conditions (i.e., different controlled test temperatures, different durations of cooling in the laboratory, etc.). The nondestructive test included the M_r test, while the destructive tests included the asphalt pavement analyzer (APA), Hamburg wheel tracking (HWT), Cantabro abrasion loss (CAL), and the recently developed IDEAL shear rutting tests.

This chapter shows that, unlike the M_r, mass loss, APA rut depth, and HWT rut depth values obtained respectively from the M_r, CAL, HWT, and APA tests, the shear strength values obtained from the IDEAL shear rutting test better discriminated liquid ASA-treated granite SP-9.5 and SP-12.5 mixtures from control mixtures. Based on this similarity in the effect of liquid ASAs in both mix types, the shear strength obtained from the IDEAL shear rutting tests was selected to develop the test protocol for evaluating the effect of the liquid ASA on the stability of asphalt mixtures after construction.

Chapter 6 summarizes the test results presented in Chapter 4 and Chapter 5, and provides the conclusions drawn based on these results.

Finally, Chapter 7 presents the draft protocol for evaluating the effectiveness of liquid ASA on asphalt mixture stability during and after construction. The draft protocol includes the criteria to approve liquid ASA in terms of asphalt mixture stability. The draft protocol follows the same format as the Florida Method of Test for the Resistance of Compacted Bituminous Mixture to Moisture-Induced Damage, FM 1-T 283 (FDOT, 2018b).

2 LITERATURE REVIEW

The literature review was conducted to document existing experiences regarding the use of liquid ASA to mitigate stripping problems in asphalt mixtures, the policies or practices implemented by state highway agencies to approve liquid ASA in their contracts, and the laboratory test methods that assess the stability of asphalt mixtures during and after construction. The ensuing sections elaborate on the findings of this review.

2.1 Asphalt Mixture Stripping

Asphalt mixture stripping is a mechanism by which asphalt binder film gets detached from the surfaces of aggregates due to the infiltration of moisture and subsequent loss of adhesion (McGennis et al., 1984). Since the late 1970s, stripping has been identified as a major contributor of distresses that can cause premature failures of asphalt pavements (Epps et al., 2003; Little et al., 2006). Several studies have been conducted to

- investigate the factors that can make asphalt mixtures more susceptible to moisture damage,
- develop protocols and parameters that can evaluate the moisture damage susceptibility of asphalt mixtures, and
- develop methods that can mitigate stripping in asphalt mixtures (Aschenbrenner, 2003).

2.1.1 Influencing Factors

Factors that can influence asphalt mixture stripping but also can be controlled during construction include aggregate, asphalt binder, construction, and mix production.

2.1.1.1 Aggregate

Garf (1986) reported that stripping was more prevalent in limestone mixtures than in granite mixtures. Other studies have discounted this observation since then. However, Garf also reported that the severity of stripping in mixtures produced with granite depends on the aggregate source. Similarly, other studies reported that stripping is more prevalent in aggregates that have rougher surfaces such as crushed aggregates than in aggregates that have smoother surfaces such as river gravels (McGennis et al., 1984; Kennedy and Anagnos, 1984; Putnam and Amirkhanian, 2006).

2.1.1.2 Asphalt Binder

Since stripping is directly related to the adhesive property of asphalt binder, those that have better adhesive properties and that do not lose these properties in the presence of moisture are more resistant to stripping. However, current asphalt binder purchase specifications are based on PG system—a system that does not measure any adhesive properties and therefore cannot evaluate stripping potential.

2.1.1.3 Construction

Dense well-graded asphalt mixtures are more resistant to stripping (Kennedy and Anagnos, 1984). Therefore, in addition to testing individual components, the stripping potential of prospective asphalt mixtures should be tested. Production of mixtures that always comply with mix design and their compaction to desired density level are parameters that can influence the stripping potential of asphalt mixtures.

2.1.1.4 Mix Production

The longer the asphalt mixtures are stored in silos or trucks, the higher the chance of asphalt binder oxidation, which results in stiffer asphalt binder and more stripping-prone asphalt mixtures (Putnam and Amirkhanian, 2006). Similarly, aggregates that are not coated well during mixing because of inadequate quantities of asphalt binder or because the asphalt binder or aggregate is not heated properly produce stripping-prone mixtures (Putnam and Amirkhanian, 2006).

2.1.2 Test Protocols

Over the years, several test protocols have been developed to evaluate asphalt mixture stripping and determine moisture damage susceptibility of both untreated and treated asphalt mixtures. These tests can be categorized as either qualitative or quantitative (see Table 2-1).

2.1.2.1 Qualitative Tests

The primary purpose of these tests is to screen asphalt binders and aggregates in terms of their stripping potential. The boiling test is the most common example in this category. Boiling tests involve submerging a predetermined mass of loose asphalt mixture sample in water, boiling it at a certain temperature for a certain period, and visually estimating the percentage of aggregates that are uncoated. This method is primarily based on ASTM D3625 (2012) and is subjective. Though simple and fast, these tests only address the stripping potential but not the stability of asphalt mixtures.

2.1.2.2 Quantitative Tests

These tests are always conducted on compacted asphalt mixture samples and involve keeping an equal number of compacted asphalt mixture samples in dry (air) and wet (water-submerged) conditions for a certain period, subjecting each of the specimen sets to identical tests, and ultimately comparing dry versus wet properties. Some examples of these tests include the immersion compression, triaxial, Marshall stability, resilient modulus, and *ITS* (the most popular) tests. Recently, a quantitative approach based on boiling tests was also introduced. This approach involves conducting absorption tests on loose aggregates before and after mixing them with asphalt binders based on AASHTO T 209 (2012a) and determining the coatability index based on the difference in absorption values of aggregates (Velasquez et al. 2010). This approach assumes that fully coated aggregates do not absorb water because of the

impervious film of binder. Like qualitative tests, each of these quantitative tests do not address asphalt mixture stability as well.

Table 2-1. Moisture Damage Susceptibility Tests

Test	References	Scope/Features
Qualitative		
Boiling	ASTM D3625 (2012)	Visually observing the loss of adhesion in uncompacted bituminous-coated aggregate mixtures due to the action of boiling water
Static-Immersion	ASTM D1664 (withdrawn) AASHTO T 182 (withdrawn)	Retention of asphalt film on aggregate surface in the presence of water
Quantitative		
Tunnicliff-Root	Tunnicliff and Root (1984)	Indirect tension test with Tunnicliff-Root conditioning; saturation over 24 hours
Lottman	Lottman (1982)	Indirect tension test with Lottman conditioning
Modified Lottman	AASHTO T 283 (2014a); ASTM D4867 (2014)	Change in indirect tensile strength value because of water saturation and accelerated water conditioning of compacted mixtures
Immersion Compression	AASHTO T 165 (2002) ASTM D1075 (2011a)	Loss of compressive strength resulting from the action of water on compacted asphalt mixtures
Texas Freeze-Thaw Pedestal	Kennedy et al. (1984a)	Poor field correlation; time consuming
Initial Asphalt Absorption and Desorption	Emery and Seddik (1997)	Guidance for stripping potential; not for moisture damage resistance
Triaxial	Al-Swailmi and Terrel (1993, 1992)	Strategic Highway Research Program (SHRP) method of Test M-006 using an environmental conditioning system; resilient modulus ratio
Immersion Marshall	MTO LS 283 (2017)	Double plunger tests of air-cured and water-immersed mixtures; % retained stability
Wheel-Track	Aschenbrenner et al. (1995)	Stripping slope and stripping inflection point from rut depth versus load cycle curve
Coatability Index	Newcomb et al. (2015)	Water absorption capacity of aggregates before and after mixing with binders

In terms of tests implemented at the national and local levels, the boiling tests (qualitative) and modified Lottman tests (quantitative) are the most popular in each category for evaluating stripping potential and moisture damage susceptibility of asphalt mixtures.

National Practice: A survey of 55 state highway agencies in the United States and Canada previously revealed that the majority of them, including FDOT, used some version of indirect tension-based tests to evaluate moisture damage susceptibility of asphalt mixtures (Aschenbrenner, 2003). Most of the modifications to the standard AASHTO or ASTM test methods are related to conditioning and pass-or-fail criteria of moisture damage susceptibility. Relevant to this project, neither the survey from 2003 nor other research studies revealed whether any state highway agency evaluates the effectiveness of ASA in terms of asphalt mixture stability.

Florida's Neighboring States' Practice: TTI's review of specifications used by FDOT and its eight neighboring state highway agencies to design asphalt mixtures showed that all nine state highway agencies use AASHTO T 283 (2014a) or a modified version to evaluate moisture damage susceptibility of asphalt mixtures, but each uses a different conditioning method. The review also revealed that only one agency, the Mississippi Department of Transportation (MDOT), uses the boiling test as an additional test to evaluate the moisture damage susceptibility of asphalt mixtures. Similarly, all but one agency uses the minimum *TSR* value as a pass-or-fail criterion for moisture damage susceptibility. However, only four state highway agencies use minimum *ITS* as an additional pass-or-fail criterion for moisture damage susceptibility. The review showed that neighboring state highway agencies have no protocols to evaluate the effectiveness of liquid ASA in terms of asphalt mixture stability.

2.1.3 Mitigation Methods

Based on these studies, different methods can be used to mitigate stripping in asphalt pavements (Kennedy and Anagnos, 1984):

- avoiding the use of aggregates and asphalt binders that are more prone to stripping,
- providing drainage for preventing the entry of excess water into the pavements,
- allowing the rapid removal of surface water from pavements,
- applying seal coats on the top and bottom surfaces of the asphalt mixture layers, and
- using adhesion-enhancing ASAs in asphalt mix production.

2.2 Use of Liquid ASA

The aforementioned survey of 55 highway agencies in the United States and Canada (Aschenbrenner, 2003; Hicks et al., 2003) revealed that 25 DOTs predominantly use liquid ASA, 13 DOTs predominantly use hydrated lime, seven DOTs equivalently use liquid ASA and hydrated lime, and three DOTs seldom use liquid ASA to counter stripping in asphalt mixtures. This survey highlighted the overwhelming acceptance of hydrated lime and liquid ASA to counter moisture susceptibility (see Figure 2-1).

Hydrated lime is a commercially available ASA found in pulverized form (power or dust). First introduced as a proprietary additive to increase the stiffness of asphalt binder in the 1910s (Epps et al., 2003), hydrated lime has been used since that time to reduce stripping potential (Epps et al., 2003; Hicks et al., 2003; Little et al., 2006; Birgisson et al., 2005; Putnam and Amirkhanian, 2006; Kim et al., 2008; Ravi Shankar et al., 2018), fatigue cracking potential (Aragao et al., 2010), permanent deformation, and low-temperature cracking potential (Little et al., 2006). In terms of the method of application, hydrated lime can be added as dust to the damp aggregates or as a part of slurry to dry aggregates with or without marination (Epps et al., 2003; National Lime Association, 2003).

Conversely, liquid ASAs are commercially available products that are directly blended with asphalt binder prior to mixing with aggregates. Increasingly, liquid ASAs are being preferred over hydrated lime because of their equivalent, if not better, anti-stripping capability; lower cost; and ease of application in the asphalt mixture (Christensen et al., 2015; Amirkhanian et al., 2018). FDOT requires the introduction of liquid ASA directly into the binder at the terminal.

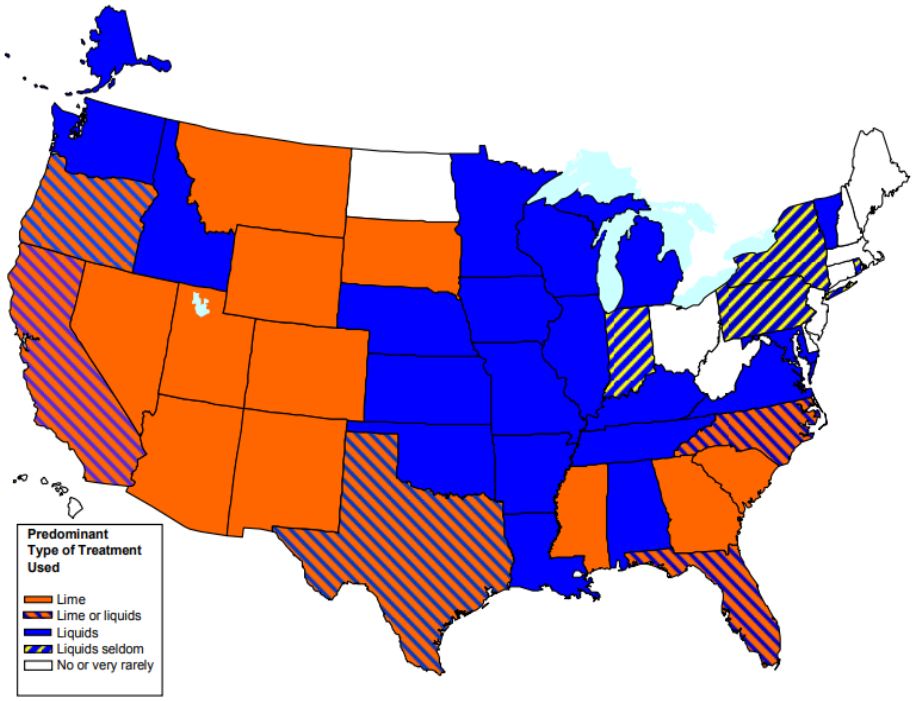

Figure 2-1. Distribution of Moisture Damage Treatments (Hicks et al. 2003)

2.2.1 Anti-stripping Effects

Over the years, there has been a significant increase in the number of commercially available liquid ASA products, each of which has a different proprietary formula. Therefore, several studies were and are being conducted to determine whether a new product can enhance the anti-stripping potential of asphalt mixtures as intended and whether it is suitable to be added to the APL.

For example, Birgisson et al. (2005) conducted a study for FDOT to develop the best methods to evaluate moisture damage potential of asphalt mixtures and the effectiveness of hydrated lime and liquid ASA on these asphalt mixtures. The researchers developed a framework for the evaluation of the effects of moisture damage on the fracture resistance of asphalt mixtures prepared with or without hydrated lime and liquid ASA. For this study, the researchers used an asphalt mixture prepared with a PG 67-22 asphalt binder, two aggregate types, one reclaimed asphalt pavement (RAP) source, and one liquid ASA type. Their study showed that granite mixtures had noticeably greater fracture resistance than limestone mixtures. The study also revealed that cyclic pore pressure in the range of 5–15 psi at a conditioning temperature of 40°C conditioned the mixtures better than submerging in water. Additionally, the study showed that the energy ratio, a parameter based on fracture mechanics, discriminated asphalt mixtures and anti-stripping effects independent of the conditioning procedure. The study recommended different criteria of energy ratios to decide whether asphalt mixtures would need liquid ASA to resist moisture damage.

Similarly, Putnam and Amirkhanian (2006) conducted another study for the South Carolina Department of Transportation (SCDOT) to evaluate the moisture damage resistance of 30 different asphalt mixtures produced with hydrated lime (1.0% by weight of aggregate), three types of liquid ASA (0.5% by weight of binder), two sources of PG 64-22 binder, and three types of aggregates. The researchers conducted *ITS* tests on unconditioned and water-conditioned (1, 7, 28, 90, and 180 days) samples using SCDOT's AASHTO T 283 (2014a) equivalent test method, SCT 70. Test results showed that ASA-treated asphalt mixtures had higher *ITS* values than the untreated asphalt mixtures and met SCDOT's requirement for conditioned *ITS* value ($\geq$ 65 psi or $\geq$ 448 kPa). Test results also showed that hydrated lime-treated mixtures performed better than liquid ASA-treated mixtures. Furthermore, binder and aggregate source contributes to the effectiveness of different liquid ASA, but the extended duration of conditioning did not have an effect. There was no significant influence of the liquid ASA source and extended duration of conditioning of treated asphalt binders on asphalt binder PG and asphalt mixtures' moisture damage resistance.

Sebaaly et al. (2010) conducted a research for the National Lime Association to evaluate the impact of hydrated lime and liquid ASAs on hot-mix asphalt (HMA) pavements. The researchers used one aggregate and one asphalt binder from five states and formulated three mix designs—control, 0.50% liquid ASA by weight of binder, and 1.00% hydrated lime by weight of aggregate. The researchers prepared 15 asphalt mixtures by blending these materials (i.e., 3 mix designs from five locations) and investigated their performances (resistance to moisture damage, permanent deformation, fatigue cracking, and thermal cracking). Test results revealed that liquid ASA-treated asphalt mixtures possessed lower *TSR* values than hydrated lime-treated mixtures but greater *TSR* values than control mixtures. Test results also revealed that liquid ASA-treated asphalt mixtures ranked lower, while hydrated lime-treated asphalt mixtures ranked higher than or equal to the control mixtures in terms of their resistance to permanent deformation. In terms of fatigue, 14 hydrated lime-treated mixtures performed better than or equivalent to control mixtures, while liquid ASA-treated mixtures performed

differently depending upon their source. And in terms of thermal cracking, liquid ASA-treated asphalt mixtures always performed better than control mixtures, but hydrated lime-treated asphalt mixtures performed better (higher tensile stress to fracture) than liquid ASA-treated asphalt mixtures.

Recently, Amirkhanian et al. (2018) conducted another study for SCDOT to evaluate the performance of liquid ASA in high-volume PG 64-22 asphalt mixtures in terms of moisture damage and recommended appropriate doses. The authors used hydrated lime, five liquid ASAs, a PG 64-22 asphalt binder, six aggregate types, and six RAP sources to prepare the asphalt mixtures. Their test results showed that hydrated lime-treated asphalt mixtures always met the required criteria, while liquid ASA-treated asphalt mixtures of certain aggregate types did not always meet the requirements for minimum *TSR* (≥ 85%) and minimum wet *ITS* (≥ 65 psi or ≥ 448 kPa). As a solution, a minimum dose of 0.7% liquid ASA by weight of binder was recommended for those cases that did not meet the required criteria.

To synopsize, the review revealed that liquid ASA mostly has a positive effect not only on the resistance of asphalt mixtures to moisture damage but also on the resistance to other distresses, the intensity of which depends on their sources and dosages.

2.2.2 Previously Raised Common Issues

2.2.2.1 Compatibility

Hicks et al. (2003) suggested that some liquid ASAs did not yield satisfactory resistance to moisture damage when these additives were used with asphalt binders that were already modified with polyphosphoric acid (PPA). The researchers referenced this anomaly to the incompatibility of amines and acids. Buncher (2009) reported that the use of amine-based liquid ASA with PPA-modified asphalt binders neutralized either the high-temperature gain obtained from the addition of PPA or the anti-stripping benefits obtained from the addition of the liquid ASA. The researchers reported that the use of phosphate ester-based liquid ASAs with PPA-modified asphalt binders did not have such issues. As a result, suppliers have introduced several liquid ASAs claiming better compatibility with PPA-modified asphalt binders and the ability to maintain the high temperature grade of asphalt binders and thermal stability while enhancing aggregate-binder adhesion.

2.2.2.2 Tenderness

Paul (1995) mentioned that some liquid ASAs could contain emulsifying agents, which usually activate when the dose of the liquid ASAs exceeded certain limits. Emulsification of asphalt binders due to the presence of excess amount of liquid ASA overlubricates asphalt binders and makes asphalt mixtures more “tender” during compaction and even more prone to stripping due to a higher degree of exposure to moisture. Brown et al. (2000) enlisted liquid ASA as one of the mix-design factors that can make asphalt mixtures tender. Despite such mention, the stability of liquid ASA-treated asphalt mixtures during and after construction has not been studied extensively.

2.2.3 Approved Product Lists

Though liquid ASA are widely used for their anti-stripping capability, some state highway agencies only allow certain types and sources of liquid ASAs to be used in their contracts. These agencies usually approve the admission of new liquid ASAs in their APL only when mixtures produced with these additives pass the specific moisture damage susceptibility tests. The review of specifications and APL maintained by FDOT and its eight neighboring state highway agencies reveals that, even in this small group of state agencies, there is variation in test methods and criteria used to approve new sources of liquid ASAs. Some of these agencies use *TSR* test (e.g., Florida), some use boiling test (e.g., Louisiana and Tennessee), and some use both tests (e.g., Georgia). Even the agencies that use the same type of tests use different criteria for this purpose (see Table 2-2).

2.2.3.1 Alabama

Alabama Department of Transportation (ALDOT)'s Standard Specifications for Highway Construction (ALDOT, 2018) requires that asphalt mixtures other than polymer-modified open-graded friction courses, plant mix asphalt base, and permeable asphalt-treated base be tested for moisture susceptibility and, if warranted, treated with liquid ASA (i.e., amines or organosilanes) or hydrated lime. ALDOT does not maintain an APL but requires that the *TSR* of the asphalt mixtures, treated or untreated, be at least 0.80. ALDOT uses the *ITS* tests to calculate the dosage of liquid ASAs and check their effectiveness (ALDOT, 2008). ALDOT also limits the use of hydrated lime within 0.5–2.0% or liquid ASA to 0.25–1.0%, when needed.

2.2.3.2 Georgia

Georgia Department of Transportation (GDOT)'s Standard Specifications Construction of Transportation Systems (GDOT, 2013) requires the use of hydrated lime in all paving courses except as otherwise stated in the contracts of certain roads such as the Local Assistance Road Program roads, airports, and parking lots. When it is specified in contracts, GDOT allows the use of 0.50% liquid ASA from its APL. GDOT uses *TSR* as well as boiling tests to approve new products. The mixtures prepared with these liquid ASAs must have the minimum *TSR* of 0.80 and both the minimum conditioned and unconditioned *ITS* value of 60 psi (GDOT, 2011). Coating percent based on the boiling test must be at least 95% for approval (GDOT, 2012).

2.2.3.3 Louisiana

Louisiana Department of Transportation and Development (LaDOTD)'s Standard Specifications for Roads and Bridges (LaDOTD, 2016) allows the use of liquid ASA in all courses and uses the boiling test to approve these products in the Approved Materials List (AML). Percent retained coating must be at least 90% for approval in accordance with DOTD TR 317 (2014a). LaDOTD also includes the Fourier-transform infrared (FTIR) spectroscopy test of liquid ASA, DOTD TR 610 (LaDOTD, 1994), as a part of DOTD TR 317 (LaDOTD,

2014a). The spectra obtained from FTIR test samples should qualitatively conform to the spectrum obtained from the original sample.

2.2.3.4 Mississippi

MDOT's Standard Specifications for Road and Bridge Construction (MDOT, 2017) allows the use of liquid or powdered ASA when needed to pass the *TSR* minimum requirement of 0.85 (MDOT, 2005) and boiling test minimum coating percentage of 95% (MDOT, 2010). MDOT does not maintain an APL but uses the modified AASHTO T 283 (2014a) method to evaluate the moisture damage susceptibility of the treated mixtures.

2.2.3.5 North Carolina

North Carolina Department of Transportation (NCDOT)'s Specifications for Roads and Structures (NCDOT, 2018a) allows the use of liquid ASA or hydrated lime or both in all types of courses. NCDOT maintains an APL for liquid ASA products, but each of the liquid ASAs in this list are at different stages of evaluation. When these types of products are used, NCDOT recommends including at least 0.25% liquid ASA by weight of total asphalt binder and requires that the treated mixtures pass the minimum *TSR* of 0.85 (NCDOT, 2018b).

2.2.3.6 South Carolina

SCDOT's Specifications for Highway Construction (SCDOT, 2007) requires the use of hydrated lime unless the use of liquid ASA is mentioned in the contract. However, SCDOT does not allow the use of liquid ASA in interstate intersections. SCDOT maintains a Qualified Product List (QPL) based on whether the liquid ASA can guarantee 80% aggregate coating measured with boiling test (SCDOT, 2008).

2.2.3.7 Tennessee

Tennessee Department of Transportation (TDOT)'s Standard Specifications for Road and Bridge Construction (TDOT, 2015) allows the use of liquid ASA or hydrated lime when the mixtures containing untreated asphalt binders do not have a minimum *TSR* of 0.80 and the conditioned *ITS* is below 100 psi when the binder is polymer modified and below 80 psi in other cases. TDOT maintains a QPL based on a 10-minute boiling test conducted on asphalt mixtures. A minimum coating of 95% is used as the approval criteria (TDOT, 2018).

2.2.3.8 Texas

Texas Department of Transportation (TxDOT)'s Standard Specifications for Construction and Maintenance of Highways (TxDOT, 2014) allows the use of hydrated lime or liquid ASA based on *TSR* using TEX-531-C standard test method. TxDOT does not maintain an APL of liquid ASA. Rather, it allows the contractors to use liquid ASA obtained from any source if the mixtures pass the stripping or boiling test minimum percent coating criteria of 95% (TxDOT, 2008) and minimum *TSR* criteria of 0.80 (TxDOT, 1999). Unlike other agencies, TxDOT allows the contractors to use the dose recommended by the ASA supplier provided the treated mixtures have enough resistance to stripping or moisture damage.

Table 2-2. ASA Approval Systems in Florida and Its Eight Neighboring States

State (Referred Specification)	Moisture Damage Susceptibility Tests and Mix Acceptance Criteria	Hydrated Lime (by weight of aggregates)	Liquid ASA (by weight of binder)	APL List APL Approval Tests APL Approval Criteria
Alabama (ALDOT, 2018)	ALDOT 361 (ALDOT, 2008) • $TSR \geq 0.80$	Calculated: 0.5–2.0%	Calculated: 0.25-1.0%	APL List: n/a APL Test: n/a
Florida (FDOT, 2019)	FM 1-T 283 (FDOT, 2018b) • $TSR \geq 0.80$ • $ITS_{\text{unconditioned}} \geq 100$ psi	1.0 %	As specified in the APL	APL List: • 12 additives APL Test: FM 5-508 (FDOT, 2018a) • $TSR \geq 0.80$ • $ITS_{\text{unconditioned}} \geq 100$ psi
Georgia (GDOT, 2013)	GDT 66 (GDOT, 2011) $ITS \geq 100$ psi • $TSR \geq 0.70$ $ITS < 100$ psi • $TSR \geq 0.80$ • $ITS_{\text{conditioned}} \geq 60$ psi • $ITS_{\text{unconditioned}} \geq 60$ psi	≥ 1 % (virgin aggregates) + 0.5% (RAP aggregates)	0.50% (Allowed only in specified contracts)	APL List: • 14 additives APL Tests: GDT 56 (GDOT, 2012) • $Coating \geq 95\%$ GDT 66 (GDOT, 2011) • $TSR \geq 0.80$ • $ITS_{\text{conditioned}} \geq 60$ psi • $ITS_{\text{unconditioned}} \geq 60$ psi

Table 2-2. ASA Approval Systems in Florida and Its Eight Neighboring States, Continued

State (Referred Specification)	Moisture Damage Susceptibility Tests and Mix Acceptance Criteria	Hydrated Lime (by weight of aggregates)	Liquid ASA (by weight of binder)	APL List APL Approval Tests APL Approval Criteria
Louisiana (LaDOTD, 2016)	DOTD TR 322 (LaDOTD, 2014b) • *TSR* ≥ 0.80	≥ 1.5%	Calculated: 0.6-1.2%	APL List: • 48 additives APL Tests: DOTD TR 610 (LaDOTD, 1994) • FTIR Test: Pass DOTD TR 317 (LaDOTD, 2014a) • *Coating* ≥ 90%
Mississippi (MDOT, 2017)	MT 59 (MDOT, 2010) • *Coating* ≥ 95% MT 63 (MDOT, 2005) • *TSR* ≥ 0.85 • $Coating_{\text{conditioned}} \geq$ 95%	1.0%	Calculated	APL List: n/a APL Test: n/a
North Carolina (NCDOT, 2018a)	NC T283 (NCDOT, 2018b) • *TSR* ≥ 0.85	≥ 1.0%	≥ 0.25%	APL List: • 3 accepted for field trial • 2 under evaluation • 1 additional information requested APL Test: NC T283 (NCDOT, 2018b) • *TSR* ≥ 0.85

Table 2-2. ASA Approval Systems in Florida and Its Eight Neighboring States, Continued

State (Referred Specification)	Moisture Damage Susceptibility Tests and Mix Acceptance Criteria	Hydrated Lime (by weight of aggregates)	Liquid ASA (by weight of binder)	APL List APL Approval Tests APL Approval Criteria
South Carolina (SCDOT, 2007)	SCT 70 (SCDOT, 2009) During Mix Design: • $TSR \geq 0.85$ • $ITS_{conditioned} \geq 65$ psi During Mix Production: • $TSR \geq 0.80$ • $ITS_{condioned} \geq 60$ psi [Not reqd. in low-volume surface, seal and base courses]	≥ 1.0%	Calculated everywhere except in Interstate intersections	APL List: • 12 additives Effectiveness Test: SCT 69 (SCDOT, 2008) • *Coating*≥ 80%
Tennessee (TDOT, 2015)	ASTM D4867 (ASTM, 2014) TSR Test with Root-Tunnicliff conditioning except in a few cases • $TSR \geq 0.80$ • $ITS_{conditioned} \geq 80$ psi (without Polymer) • $ITS_{conditioned} \geq 100$ psi (with Polymer)	1.0%	Calculated using 10-min boil test	APL List: • 51 additives APL Test: 10-min. boil test (TDOT, 2018) • *Coating* ≥ 95%

Table 2-2. ASA Approval Systems in Florida and Its Eight Neighboring States, Continued

State (Referred Specification)	Moisture Damage Susceptibility Tests and Mix Acceptance Criteria	Hydrated Lime (by weight of aggregates)	Liquid ASA (by weight of binder)	APL List APL Approval Tests APL Approval Criteria
Texas (TxDOT, 2014)	Tex-531-C (TxDOT, 1999) TSR Test • *TSR* ≥ 0.80	1.0%	Manufacturer recommended: 0.2-2.0%	APL: n/a APL Test: Effectiveness Test: Tex-530-C (TxDOT, 2008) • *Coating* ≥ 95%

Notes: Below are the weblinks of APLs, AMLs or QPLs as retrieved on March 2020:

- **Florida:** https://fdotwp1.dot.state.fl.us/ApprovedProductList/ProductTypes/Index/2
- **Georgia:** http://www.dot.ga.gov/PartnerSmart/Materials/Documents/qpl26.pdf
- **Louisiana:** http://wwwapps.dotd.la.gov/engineering/materials_lab/QualifiedProjectList/ApprovedMaterialsListFiltered.aspx
- **North Carolina:** https://apps.ncdot.gov/vendor/ApprovedProducts/
- **South Carolina:** http://info2.scdot.org/Materials/QualProd/104%20QPL.pdf
- **Tennessee:** https://www.tn.gov/content/dam/tn/tdot/hq-materials-tests/qpl/QPL%2014.pdf

2.3 Asphalt Mixture Stability

The previous sections showed that current test protocols used to approve liquid ASA products evaluate their effectiveness primarily in terms of moisture damage susceptibility but seldom in terms of stability issues such as the two issues recently raised by field personnel in Florida.

The first of these issues involves excessive movement of mixtures under rollers during compaction due to their tenderness (higher workability and compactability) while the mixtures are still hot. The second issue involves crumbling of mixtures during inspection of pavements due to their softness (lower stiffness and lower shear strength) after the mixtures have cooled to ambient temperatures.

The literature review revealed that very similar issues have been previously reported though not with regards to the use of liquid ASA. For example, Scherocman (2006) mentioned that if mixtures are too soft or tender during construction (i.e., while the mixtures were still hot), mixtures tend to move transversely, shove in front of the steel wheels of the rollers, and create humps on the outside edge of the rollers (see Figure 2-2). Scherocman (2006) identified three temperature zones over which mixtures show different compaction behaviors:

- *Upper temperature zone*: This zone covers the temperature range from 140–160°C (285–320°F), depending upon the PG of the asphalt binder, to about 115°C (240°F). In this zone, mixtures do not show tenderness (i.e., do not move or shove excessively) and are easy to compact irrespective of the type of the rollers.
- *Tender temperature zone*: This zone covers the temperature range from 115°C (240°F) to 90°C (195°F). In this zone, mixtures lack enough internal stability to support the weight of the rollers and therefore move or shove. As a result, it is hard to compact them to the desired level of compaction (i.e., relative density and air void content) with a predetermined level of compaction effort. However, researchers also mentioned that mixtures do not show this tendency under pneumatic tire rollers.
- *Lower temperature zone*: This zone covers temperature below the tender temperature zone. In this zone, mixtures are relatively colder, and the pavement layer is more mature, and therefore it is hard to compact them any further.

Scherocman (2006) also recommended different methods to avoid lack of stability during compaction, including keeping the breakdown or initial compaction rollers close to the back of the paver and immediately compacting the asphalt mixtures while the temperature of the asphalt mixtures is still elevated with two double-drum vibratory rollers operating in the echelon directly behind the paver and then, if warranted, with a static steel wheel finish compaction roller.

(a) Checking (Scherocman, 2006) (b) Humping (Scherocman, 2006) (c) Shoving (Pavement Interactive, 2020)

Figure 2-2. Asphalt Pavement Stability Issues: (a) Checking, (b) Humping, and (c) Shoving

Similarly, Kennedy et al. (1984b) previously defined unstable asphalt mixtures as those mixtures "that have very low resistance to deformation by punching loads and scuff under horizontally-applied shearing loads after compaction has been completed." They also provided a list of characteristics that only unstable mixtures show during and after construction, such as:

- Characteristics of unstable mixtures during construction:
  - They are difficult to roll without excessive lateral displacement.
  - They are difficult to compact to design density.
  - They are easy to indent under a punching load.
- Characteristics of unstable mixtures after construction:
  - They rut after construction is complete.
  - They displace under the heel of a shoe.
  - They shove under traffic, sometimes months after construction.
  - They slip under traffic usually soon after construction.
  - They scuff under power steering or braking action.

Kennedy et al. (1984b) also mentioned that the use of insufficient fines, higher asphalt binder content, and less absorptive aggregates would leave behind a larger amount of asphalt binder to coat the aggregates (i.e., thicker asphalt binder film), which would result in excessively lubricated mixtures (less viscous) that are too workable (too tender) during construction. They also implied that excessive use of medium-size sand and smooth and less angular aggregates would decrease resistance to shear and make mixers more unstable. In addition to these mix-design-related factors, the researchers also identified two construction-related factors such as the use of excessive high temperature and the presence of mixture that could make mixtures more unstable.

Brown et al. (2000) added the contamination of asphalt binders during construction, the inadequate bond of the surface and underlying pavement layers, and the type of compaction

equipment and techniques to the list of factors that can affect the asphalt mixture stability during and after construction. Most importantly, they also listed liquid ASA as one of those additives that can make mixtures tender. To synopsize, several factors can make asphalt mixtures unstable:

- Mix design-related factors (Kennedy et al., 1984b):
  - Use of very soft asphalt binder,
  - Use of insufficient fine content,
  - Use of less absorptive aggregates,
  - Use of excessive amount of medium-sized sand,
  - Use of smoother and less angular aggregates, and
  - High asphalt binder content.
- Construction practice-related factors (Brown et al., 2000; Kennedy et al., 1984b):
  - Excessively high mixing temperature,
  - Presence of moisture in the mixture,
  - Contamination of asphalt binders during construction,
  - Inadequate bond of the surface and underlying pavement layers, and
  - Compaction equipment and techniques.

Asphalt mixture stability has been assessed in terms of parameters that describe the ease with which mixtures can be mixed, placed, or compacted during construction as well as in terms of parameters that describe the ease with which mixtures would be compacted or sheared under traffic loads after construction. The following sections describe each type of parameter.

2.3.1 Parameters Measured during Mixing

Several studies have used the ease with which asphalt mixtures could be mixed to estimate the ease with which the materials could be compacted in the field.

Among them, McLeod (1967) recognized that the ease with which mixtures could be mixed and compacted was strongly dependent on asphalt binder viscosity. The author reported that the decrease of temperature during compaction would increase asphalt binder viscosity and asphalt mixture density gradually and thereby make asphalt mixtures more difficult to compact (i.e., more stable). The author also reported that, for the same compaction effort and temperature, mixtures prepared with more viscous binders would be more difficult to mix or compact than those prepared with less viscous binders (see Figure 2-3). The author also mentioned that mixtures prepared at the same temperature with the same binder type but placed at different temperatures would need different durations for compaction because of the difference in rate of gain in overall viscosity due to cooling. In other words, the temperature at which the asphalt mixtures are placed in the field directly impacts the rate of increase in asphalt binder viscosity and, by extension, the rate of gain in asphalt mixture stability during construction.

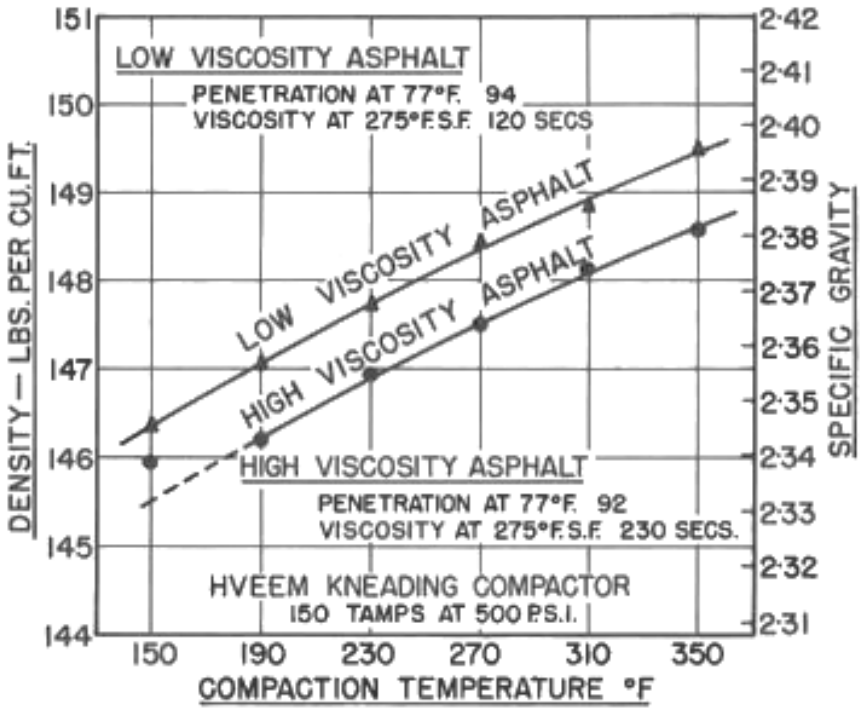

Figure 2-3. Viscosity and Compaction Temperature Effect (McLeod, 1967)

Marvillet and Bougault (1979) used asphalt mixture viscosity during mixing to discriminate hard-to-mix, hard-to-compact materials from easy-to-mix, easy-to-compact materials. Since viscosity (i.e., the resistance to flow) is directly proportional to torque at a constant speed, the authors measured the torque needed to prepare a certain amount of asphalt mixture at a constant speed (15 kilograms at 22 revolutions per minute) as a measure of mixture viscosity. The authors also developed one of the first known mechanical systems to measure this torque. From their study, they revealed that the torque required for mixing decreased (i.e., it became easier to mix and compact the mixtures) with the use of less angular aggregates, lower filler content, and less viscous binders but remained indifferent with the change in binder content.

Gudimettla et al. (2003, 2004) also used a similar system to measure the torque during mixing to differentiate less from highly workable asphalt mixtures. The authors verified that the torque required for mixing decreased (i.e., it became easier to mix and compact the mixtures) with the use of more viscous or stiffer binders, less angular aggregates, and smaller nominal maximum aggregate size but remained indifferent with the change in aggregate gradation. In other words, the authors found that asphalt mixture workability was more sensitive to aggregate type, angularity, or size than gradation.

Bennert et al. (2010) defined the workability of asphalt mixtures as "the property that describes the ease with which a hot-mix asphalt can be placed and compacted to the desired mat density." The authors measured the torque required to produce warm-mix asphalt (WMA) with different dosages and sources of warm-mix additives and ranked their workability in terms

of this torque. The authors found that workability always increased (torque always decreased) with the use of warm-mix additives, higher dosages of warm-mix additives, and higher temperatures (see Figure 2-4). The authors also reported that mixtures prepared with different types of warm-mix additives at the same dose registered different values of torques, suggesting the selected test and associated parameter (torque) was sensitive to additive type in addition to its dosage

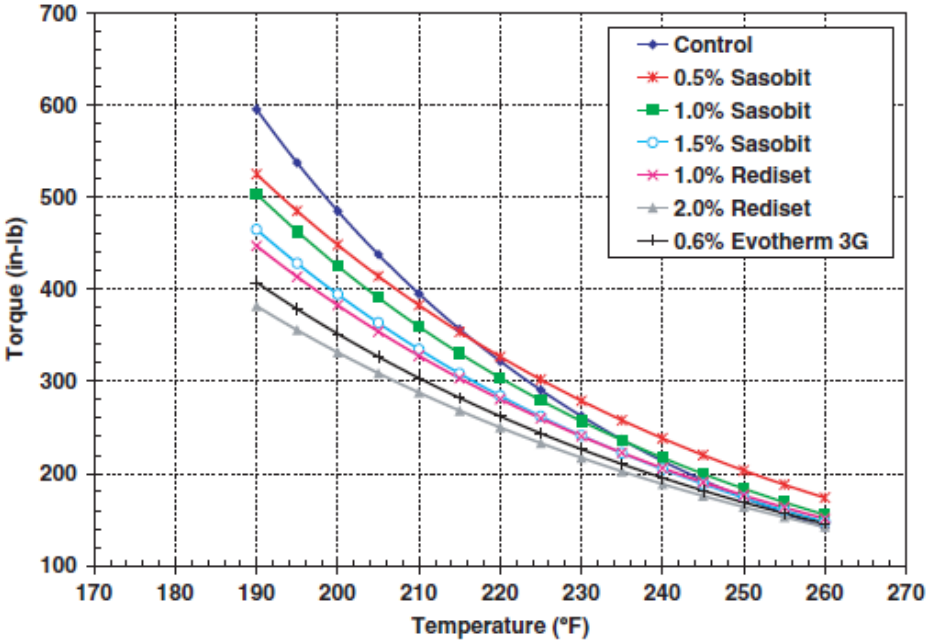

Figure 2-4. Torque as a Workability Parameter (Bennert et al., 2010)

Additionally, Bennert et al. (2010) evaluated the workability of mixtures treated with different warm-mix additives in terms of lubricity of the asphalt binder. To determine the lubricity, the authors conducted steady-state rotational tests from 1 to 150 radians/second on asphalt binder samples at four different thicknesses (i.e., 500, 100, 50, and 25 μm) and two different temperatures (115°C and 125°C). The authors conducted these tests first at 500-μm thickness and then at other thicknesses after squeezing the samples at a rate of 10 μm/sec at the completion of each step. The authors evaluated the rotational speed at which viscosity or normal force value would show sudden discontinuity—a sign of slippage of the upper geometry plate. The test results showed that discontinuity happened at higher shear rates with the use of warm-mix additives, thereby verifying the lubricating effect of warm-mix additives on asphalt binders and, by extension, on asphalt mixtures. The authors also found that the shear rates at which this discontinuity happened were dependent on the type of warm-mix additive.

2.3.2 Parameters Obtained from Data Collected during Compaction

Several studies have defined asphalt mixture stability in terms of the ease with which mixtures can be compacted in the field with rollers. Some of these studies have also defined asphalt mixture stability in terms of the ease with which mixtures can be compacted under the

traffic after construction. Both types of studies overwhelmingly used the data collected during compaction of asphalt mixture samples in the laboratory to extract parameters that describe the compactability of asphalt mixtures during and after construction. These parameters mostly fall into one of these categories:

- *Single-data parameters:* These parameters represent the properties of the mixtures at certain instances during compaction such as:
  - Compacted density achieved after a certain amount of compaction effort, and
  - Compaction effort required to achieve a certain density.
- *Slope parameters:* These parameters represent the rate at which certain properties of mixtures change over time during compaction such as:
  - Rate of change in air void content, and
  - Rate of change in relative density.
- *Area parameters:* These parameters represent the total energy required to compact the mixtures from one density level to another density level or from one compacted height to another compacted height:
  - Densification indices calculated from the area under $\%G_{mm}$ versus *N* curve.
  - Compaction energy indices calculated from the area under *height* versus *N* curve.

The following sections present the synopsis of studies conducted on these parameters.

2.3.2.1 Relative Density or Air Void Content

Heukelom (1968) defined the workability of asphalt mixtures of compaction as "the ability of the pre-arranged particles to be forced into their mutual interstices forming a compact mass under the weight of a roller" and proposed the ratio of compacted sample volumes at 5 and 100 blows of the Marshall compactor, defined as compaction factor (C_f), to assess this property. The author reported that the easy-to-work/compact (more tender) mixtures possessed smaller values of this factor than did the difficult-to-work/compact mixtures.

Cabrera (1996, 1991) defined the workability of mixtures in terms of compaction as "the property which allows the production, handling, placing and compaction of an asphalt mixture with the application of minimum energy" and proposed an index, called the workability index (*WI*), to assess this property. The author fitted the plot of measured values of porosity (P) against the logarithmic value of gyration number ($logN$) with a linear function and used it to calculate uncompacted or initial porosity (P_0). The author reported that the easy-to-work/compact (more tender) mixtures possessed higher workability indices, usually higher than 6.0, than did the difficult-to-work/compact mixtures. The author showed that the workability index (tenderness) increased with an increase in binder content or temperature or both (see Figure 2-5).

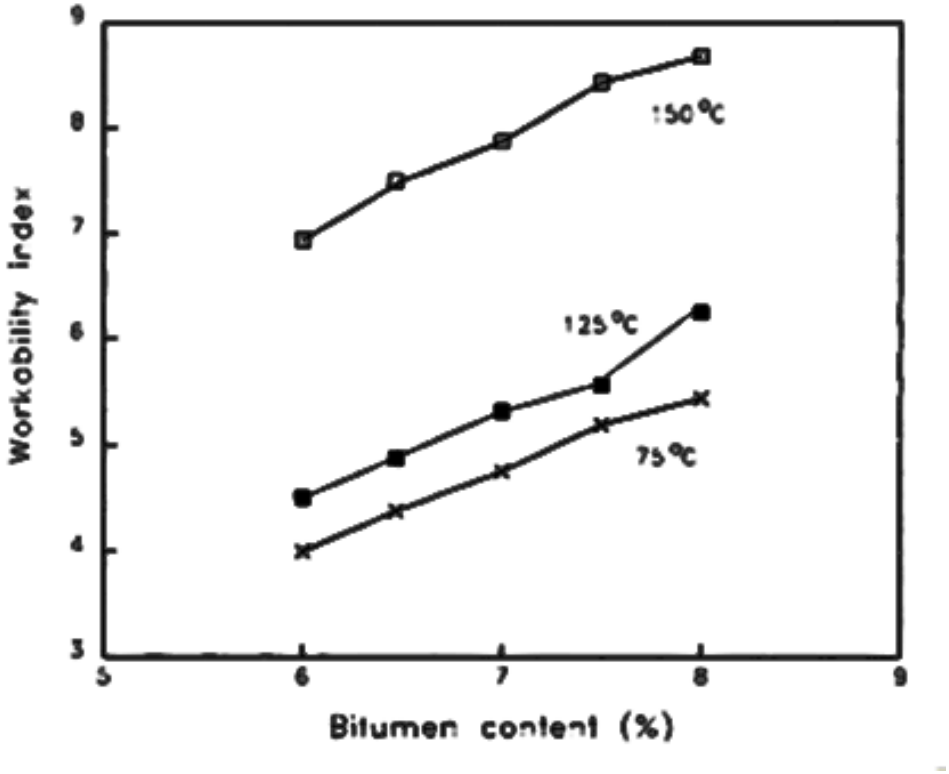

Figure 2-5. Workability Index (Cabrera, 1996)

Cominsky et al. (1994) studied the compaction behavior of mixtures under two different gyratory compactors as the part of the Strategic Highway Research Program (SHRP). The authors linear-fitted the plot of the percent maximum theoretical specific gravity (%G_{mm}) and logarithmic values of gyration number (expressed as $logN$) and extracted two parameters—%G_{mm} at 10 gyrations (C_{10}) and %G_{mm} at 230 gyrations (C_{230})—to describe this behavior. The authors showed that mixtures produced with higher binder contents could be compacted to higher %G_{mm} with the same effort (i.e., higher C_{10} and C_{230} values), which strongly implied an increased level of workability and compactability (i.e., tenderness) with increased binder content.

McGennis (1997) compared the %G_{mm} values of six different asphalt mixtures at N_{intial} value. The author mentioned that too-soft-to-compact (tender) mixtures had higher values of %G_{mm} at N_{intial} values compared to too-hard-to-compact counterparts. The author also mentioned that mixtures that contained higher sand content, a total of four mixtures, exhibited higher than specified values of %G_{mm} at N_{intial}, manifesting the unfavorable effect of higher sand content on tenderness during compaction (see Figure 2-6).

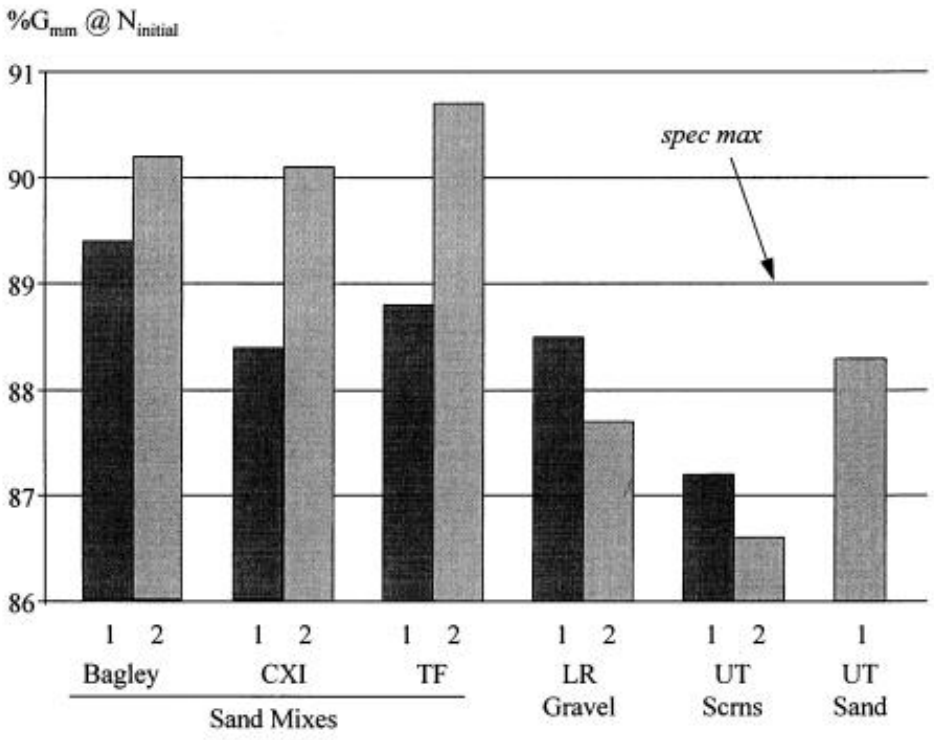

Figure 2-6. Relative Density at Design Number of Gyrations (McGennis, 1997)

Button et al. (2004) seconded the fact that the $\%G_{mm}$ value at N_{initial} can be used to assess mix compactability and tenderness. The authors recognized two extreme possibilities based on the value of this parameter:

- The mixtures with very high values of $\%G_{mm}$ at N_{initial} would be too easy to compact (too tender), resulting in stability issues such as pushing and shoving under traffic loads.
- The mixtures with very low values of $\%G_{mm}$ at N_{initial} would be too difficult to compact (too stiff), resulting in poorer in-situ performance in the field.

Similarly, Bennert et al. (2010) evaluated the compactability of asphalt mixtures in terms of air void content achieved after applying certain compaction efforts. The authors used six combinations of warm-mix additives (0.5%, 1.0%, 1.5% Sasobit, 2.0% Rediset, and 0.6% Evotherm 3G), three different combinations of mixing and compaction temperatures (315°F/300°F, 270°F/255°F, and 230°F/215°F), and two different compaction methods (Marshall and gyratory) in this study. The authors used 75 blows per side to produce the Marshall compacted samples and 100 gyrations to produce gyratory compacted samples. Test results showed that, in general, mixtures prepared with higher dosages of warm-mix additives and/or higher mixing and compaction temperatures were compacted more (see Figure 2-7). These results strongly implied that the use of too much warm-mix additives and very high mixing/compaction temperatures can make mixtures more tender.

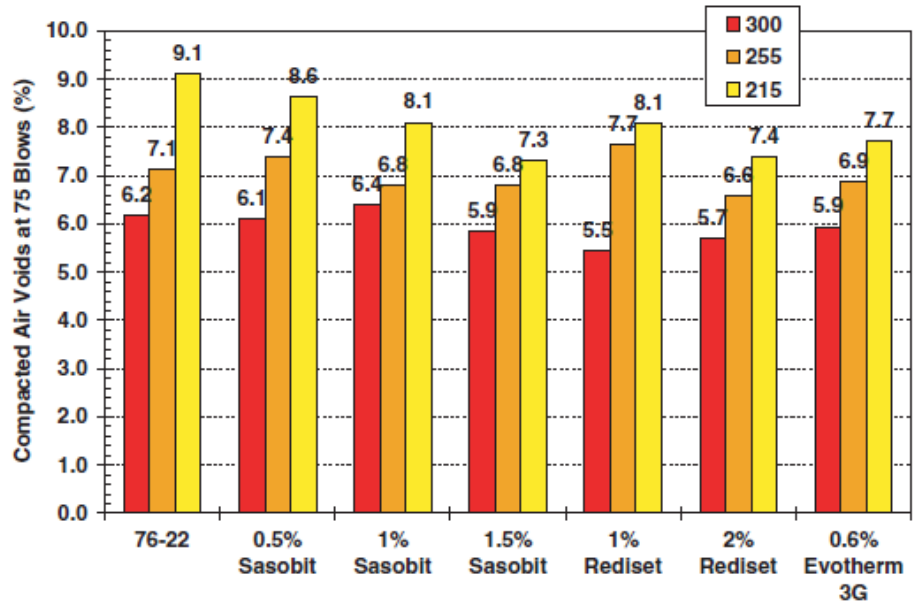

(a) Marshall Compacted Samples

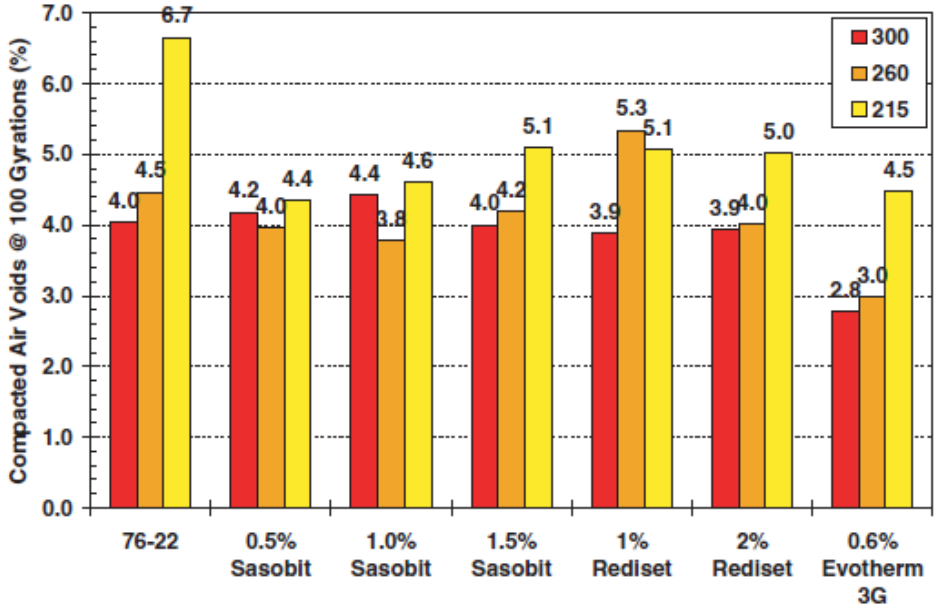

(b) Gyratory Compacted Samples

Figure 2-7. Compacted Air Voids in (a) Marshall Compacted Samples; (b) Gyratory Compacted Samples (Bennert et al., 2010)

2.3.2.2 Compaction Effort or Number of Gyrations

Vavrik and Carpenter (1998) introduced locking point as a parameter to evaluate the compaction behavior of asphalt mixtures. The authors defined the locking point (*LP*) as the first of three gyrations that were at the same height preceded by two gyrations at the same height. They referred this point as a condition at which mixtures would start significantly resisting further densification.

Mohammad and Al Shamsi (2007) used the locking point of aggregates during compaction to compare mixtures with different compactability. The authors noticed that asphalt mixtures prepared with coarser aggregates required a comparatively higher number of gyrations than mixtures prepared with finer aggregates to reach the locking point (see Figure 2-8), implying coarser gradation of aggregates would require a higher number of gyrations to reach locking point.

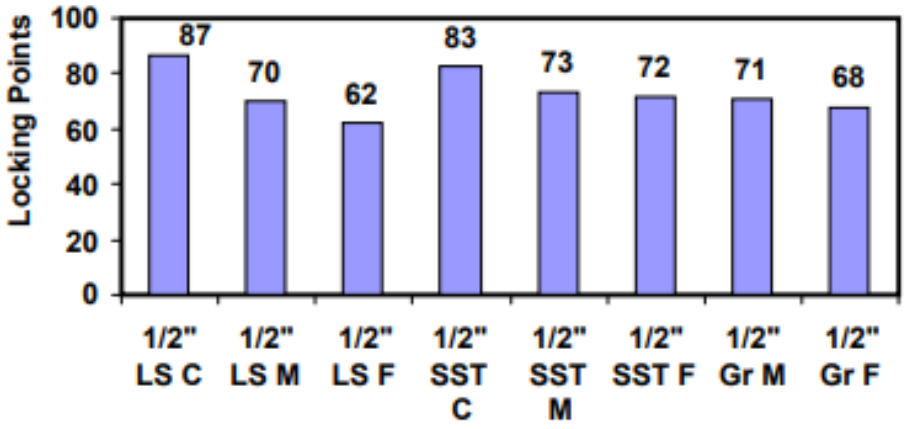

Figure 2-8. Locking Point (Mohammad and Al Shamsi, 2007)

Mallick (1999) defined the stability of asphalt mixtures as the property by which mixtures retain their strength during and after compaction. The author categorically mentioned that asphalt mixtures with higher stability would gain strength during compaction and retain it continuously, whereas the asphalt mixtures with lower stability would lose strength after a certain level of densification and become susceptible to shear failure. Based on this theory, the author proposed using the ratio of the number of gyrations required to compact mixtures to 98%G_{mm} and 95%G_{mm} (2% and 5% air void content levels, respectively), called gyratory ratio (*GR*), as the indicator of asphalt mixture stability. The author reported that the *GR* values of five mixtures, each obtained from a different field project, had a good correlation with total rutting (in millimeters) and the rutting rate (in millimeters/equivalent single axle loads [ESALs]). The author also reported that mixtures with better rutting performance in the field (higher instability) had *GR* values of 4.0 or higher.

Similarly, Bennert et al. (2010) used yet another parameter, called the gyration compaction rate (*CR*), to evaluate the compactability of one HMA versus six WMA mixtures. The authors determined this value by dividing the total number of gyrations required to compact asphalt mixtures to the 7% air void level or 93%G_{mm} ($N93$) by the corresponding height of the compacted sample ($h93$). The authors found that *CR* increased with higher doses of WMA additive and higher mixing and compaction temperatures (see Figure 2-9). These results inherently implied that asphalt mixtures can become too tender when very high dosages of some WMA additives are used, and when very high mixing and compaction temperatures are used.

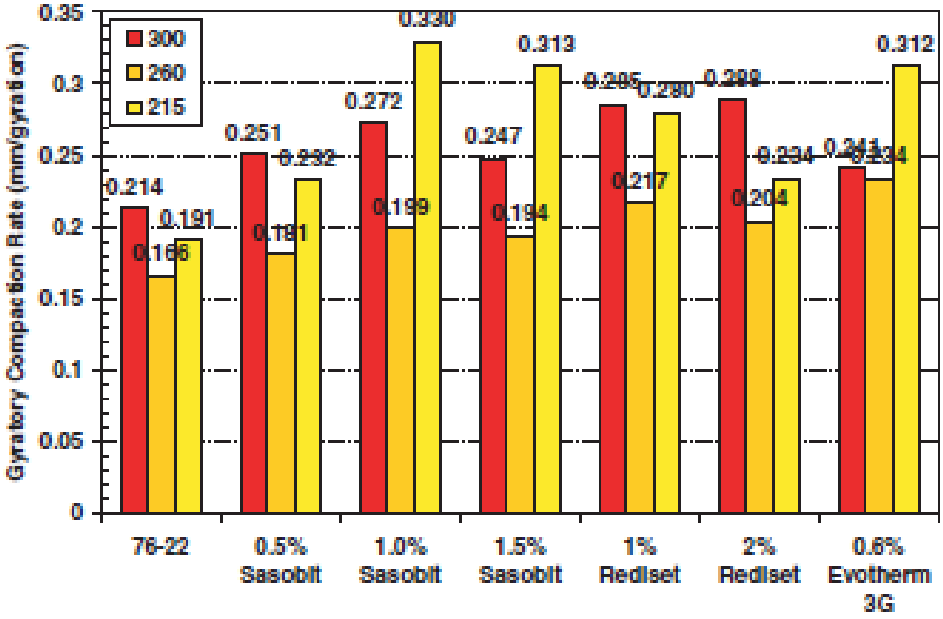

Figure 2-9. Gyratory Compaction Rate (Bennert et al., 2010)

Ling et al. (2013) used the number of gyrations required to achieve 87%G_{mm}, referred to as $N87$ to evaluate compactability of two cold-mix asphalts. Their test results showed that mixtures produced with more residual asphalt binder content (5.0%) required less effort (14 gyrations), while the mixtures produced with less residual binder content (3.5%) required more effort (35 gyrations) to be compacted to the same density level (87%G_{mm}). These results highlighted the fact that thicker binder coatings, higher binder content, or softer mixtures are easier to compact (tender) than their counterparts.

2.3.2.3 Compaction Slope

Bissada (1984) used the slope of the compaction curve obtained during Marshall compaction to evaluate the resistance of asphalt mixtures to compaction. The author defined the rate of increase in mixture density with respect to applied compaction effort ($d\gamma$/dC) as an exponential function of the difference between the maximum achievable density ($\gamma_{\max}$) and the density measured after applying certain compaction effort (γ). The author referred to the inverse of the slope of this function as an indicator of compactability:

$$\frac{d\gamma}{dC} = \frac{1}{R}(\gamma_{\max} - \gamma) \qquad 2\text{-}1$$

The author noticed that the resistance to compaction increased with higher filler content and less binder content at different levels depending upon the type of asphalt binder [see Figure 2-10(a)]. The author also noticed that the stiffer asphalt mixtures possessed higher resistance to compaction [see Figure 2-10(b)]. Such mixtures were more stable and therefore would also resist rutting more effectively than their counterparts.

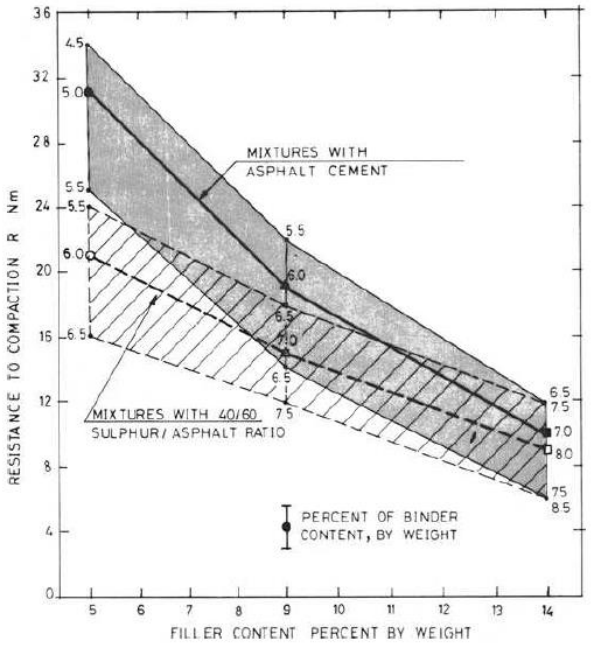

(a) R versus Mix Constituents

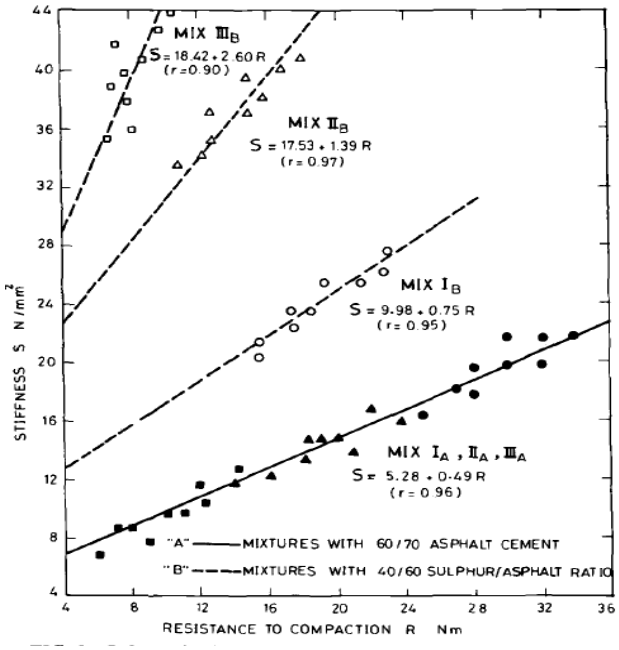

(b) R versus Mix Stiffness

Figure 2-10. Correlation of Resistance to Compaction with (a) Mix Constituents; (b) Mix Stiffness (Bissada, 1984)

Cominsky et al. (1994) also used the slope of compaction curve (k) to evaluate the compaction behaviors of mixtures. The authors showed that the slope increased with an increase in asphalt binder content irrespective of the diameter of the sample (100 mm or 150 mm in diameter) and the type of compactor (SHRP or modified Texas gyratory compactors). This observation suggested that the mixtures containing higher binder contents

would be easier to compact (more tender) than would be mixtures containing lower binder contents.

McGennis (1997) also used the compaction slope (k) as an indicator of internal stability of six asphalt mixtures prepared with different aggregate types, sources, and sand or screenings [Bagley field sand (Bagley), CXI field sand (CXI), Thompson Fulbright field sand (TF), Little Rock (LR) gravel, University of Texas limestone screenings (UT Scrns.), and the University of Texas natural sand (UT sand)]. Test results showed that mixtures containing little to no sand had steeper compaction slopes (i.e., higher K values) than mixtures containing more sands, which implied that a higher content of sand would make asphalt mixture hard to compact (see Figure 2-11). Test results also showed that mixtures with coarser aggregate gradation had steeper compaction slopes than mixtures with finer aggregate gradation, meaning coarser aggregate gradation would provide more stability and make asphalt mixtures more difficult to compact (see Figure 2-11). Their study essentially showed that the compaction slope was sensitive to the skeletal stability of the aggregates (or the internal stability of asphalt mixtures).

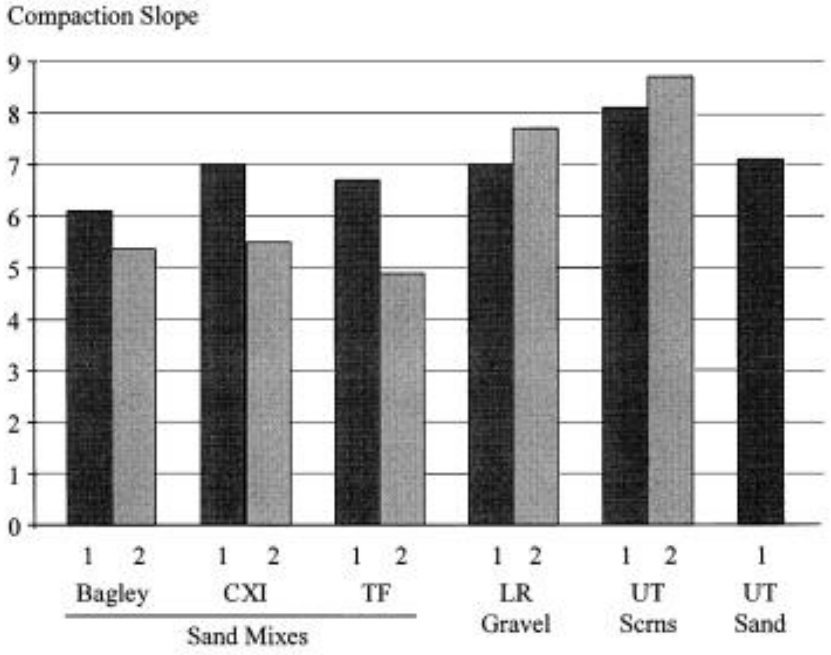

Figure 2-11. Compaction Slope (McGennis, 1997)

Anderson and Bahia (1997) evaluated the compaction rates of four different mix design mixtures in terms of the slope obtained from density versus gyration data collected during laboratory compaction of asphalt mixture samples. The test results showed that compaction rate (or compaction slope, k) decreased with finer gradation of aggregations. For example, mixtures with coarse gradations had a slope of 9.93, while mixtures with fine gradations (just above the restricted zone) had a slope of 6.66.

Anderson et al. (1999) measured the compaction slope (k_{SGC}) of several different asphalt mixtures from the compacted density versus compaction gyration curves and studied its relationship with stiffness measured at a given frequency and temperature. The authors found

that stiffness or stability and compaction slopes were only fairly correlated (see Figure 2-12), owing to the influence of aggregates on compaction slope but the influence of both aggregates and binders on stiffness.

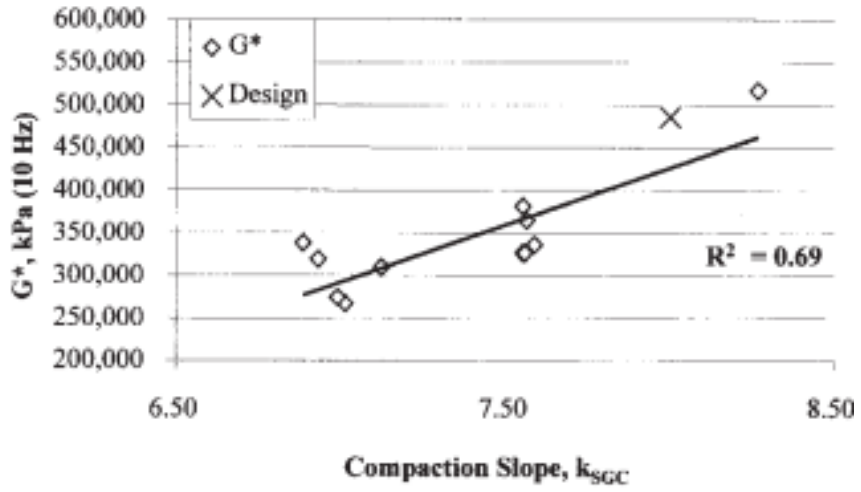

Figure 2-12. Correlation of Compaction Slope with Stiffness (Anderson et al., 1999)

Anderson et al. (2002) later noted that the asphalt binder content had a significant impact on the total amount of permanent shear strain—another measure of asphalt mixture stability measured using the repeated shear at constant height (RSCH) mode in Superpave shear tests. Therefore, the authors included the effect of asphalt binder content in the compaction slope, which previous studies reported as nonexistent (Cominsky et al., 1998; Anderson et al., 1999), by introducing a new parameter that the authors determined by multiplying the compaction slope by the design percent air voids ($k \times AV$). Test results showed that this new parameter had a relatively better correlation with permanent strain (γ) or asphalt mixture stability when the sand content was low (see Figure 2-13).

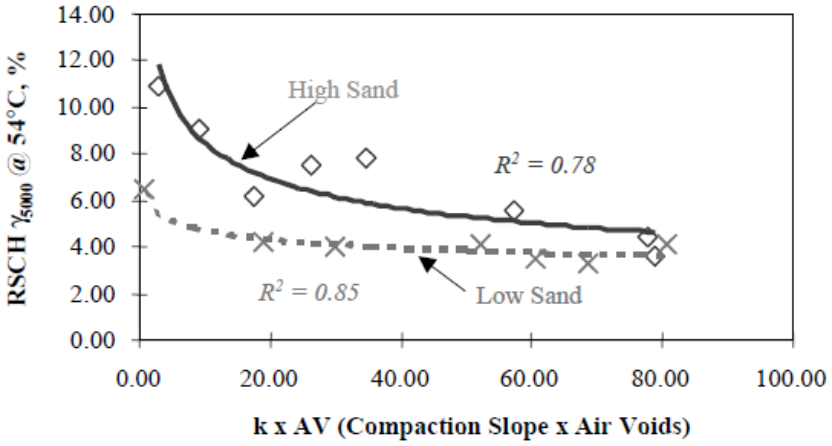

Figure 2-13. Compaction Slope × Air Voids (Anderson et al., 2002)

Button et al. (2004) confirmed the conclusion of previous studies that density versus gyration (%G_{mm} versus N) plot can be used to identify tender asphalt mixtures that would collapse quickly to lower air void levels and accumulate excessive rut depths. In a study for the TxDOT on the development of laboratory procedure for using the Superpave gyratory compactor in Texas, the authors reported that the slope of compaction curves was sensitive to mix constituents such as binder content and curing times (see Figure 2-14).

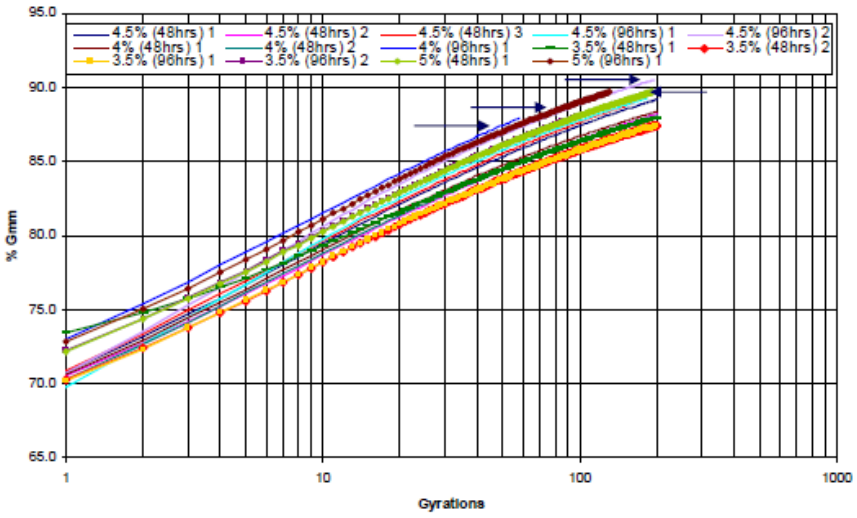

Figure 2-14. Compaction Curves (Button et al., 2004)

Kaseem et al. (2012) fitted %Va versus N data until 92%Gmm with a linear function and determined a new parameter, laboratory compaction index (CI) from a combined function of resultant slope (m) and intercept (c). They mentioned that mixtures that were easier to achieve target air voids in the field (i.e., easier-to-compact mixtures) had higher laboratory CI.

2.3.2.4 Shear Stress Parameters

Ruth et al. (1992) determined gyratory shear (*Gs*) stress to evaluate the stability of asphalt mixture samples produced with different percentages of asphalt binders, sand content, limestone coarse aggregates, and limestone fine aggregates. The author found that the gyratory shear stress at 200 gyrations was sensitive to asphalt binder content, natural sand content, mineral filler (*MF*) content, aggregate source, voids in mineral aggregates (*VMA*), and coarse and fine aggregate percentages (see Figure 2-15). The author suggested using this parameter to differentiate asphalt mixtures with the higher shear resistance against shoving (plastic deformation) from their counterparts.

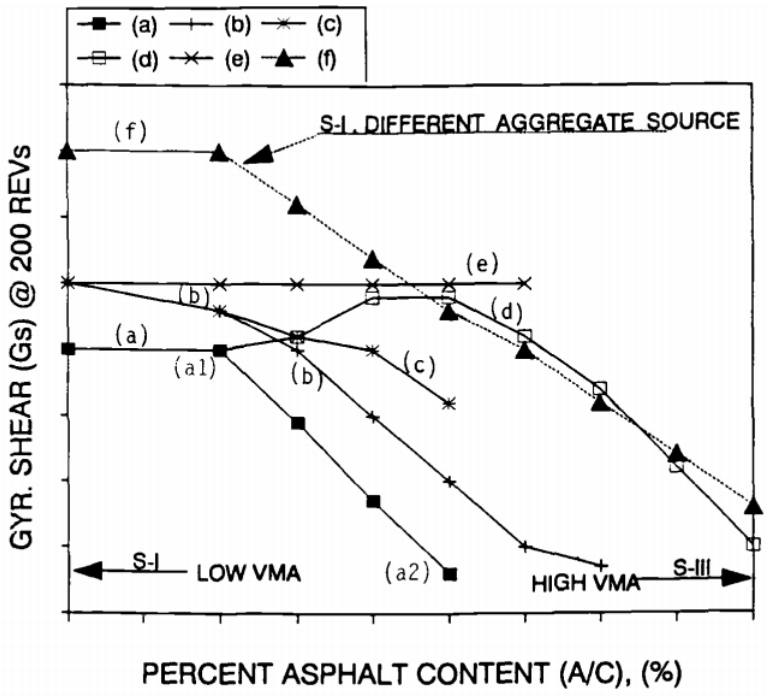

(a) Gs versus Percent Asphalt Content

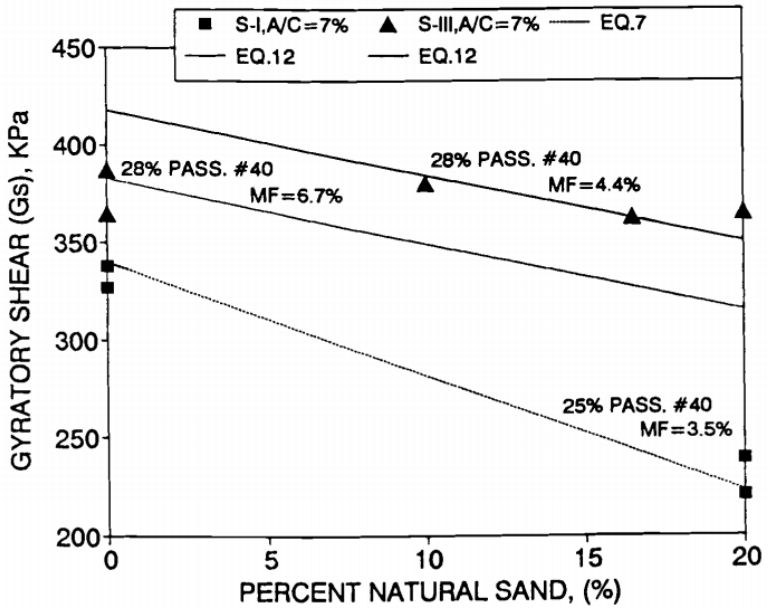

(b) Gs versus Percent Natural Sand

Figure 2-15. Correlation of Gyratory Shear with (a) Percent Asphalt Content; (b) Percent Natural Sand (Ruth et al., 1992)

Butcher (1998) calculated the shear stress in the stone matrix asphalt mixtures using the data collected during compaction with Servopac gyratory compactor. The author demonstrated that asphalt mixtures prepared with stiffer asphalt binders (i.e., AC20) allowed higher shear stresses than the asphalt mixtures prepared with softer asphalt binders (i.e., AC14), highlighting the sensitivity of shear stress to asphalt binder grade (see Figure 2-16). The author

also determined that the rate of change in air void content in asphalt mixtures at the maximum shear stress position changed only with aggregate gradation but not with gyration angle and vertical stress, meaning this property was dependent on volumetric mix design properties but not on the effort applied to compact them. Therefore, the author concluded that maximum shear stress could be used to evaluate the compaction behavior of asphalt mixtures with different binders and aggregate combinations.

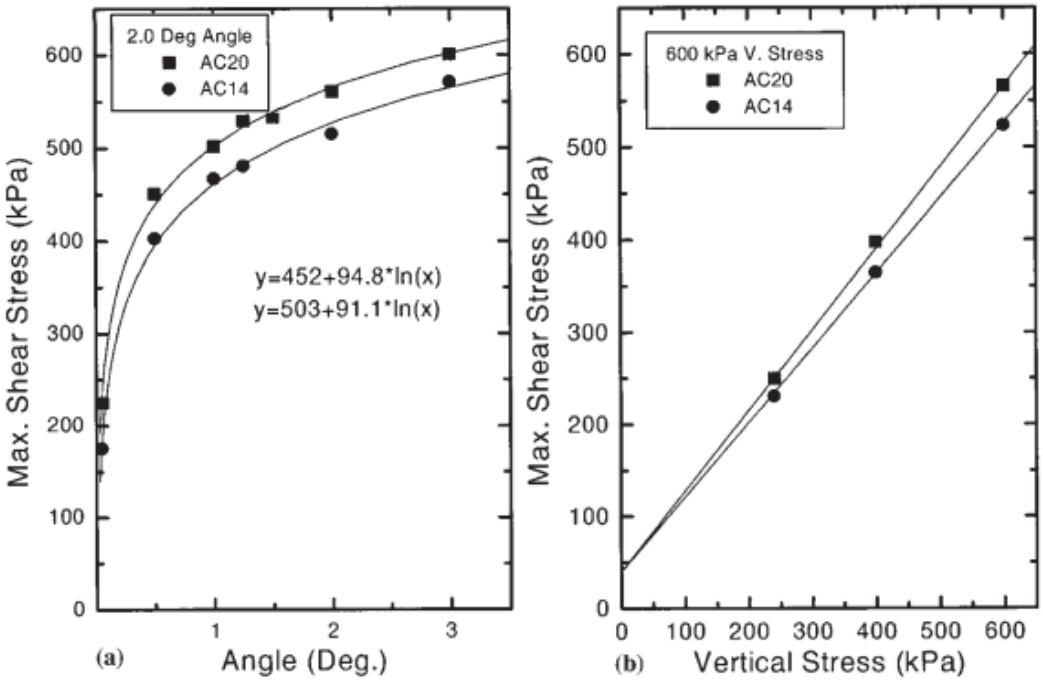

(a) Gyration Angle (b) Vertical Stress

Figure 2-16. Correlation of Maximum Shear Stress with (a) Gyration Angle; (b) Vertical Stress (Butcher, 1998)

De Sombre et al. (1998) determined that maximum shear stress to assess the compactability and stability of asphalt mixtures during construction. The researcher determined that the shear strength of asphalt mixtures had a Mohr-Coulomb type relationship with cohesion and internal friction. The author reported that an increase in aggregate angularity increased internal friction and therefore shear strength, and consequently stability of asphalt mixtures. The author also reported that an increase in either asphalt binder or filler content or both increased their cohesion and therefore their shear strength or stability. Based on this study, optimum binder and filler contents and more cohesive binder help asphalt mixtures achieve higher stability.

Anderson et al. (2002) conducted National Cooperative Highway Research Program (NCHRP) Project 09-16, in which the authors reviewed the effectiveness of five parameters based on shear stress (τ) measured during gyratory compaction as stability and rutting resistance parameters:

- the maximum shear stress ratio, that is, the ratio of maximum shear stress ($\tau_{\max}$) and normal stress (σ), $SR_{\max} = \frac{\tau_{\max}}{\sigma}$;
- the number of gyrations at the maximum stress ratio, $N\text{-}SR_{\max}$;
- the stress ratio at the final gyration normalized with respect to the maximum stress ratio, $SR_f/SR_{\max}$;
- the stress ratio at 160 gyrations normalized with respect to the maximum stress ratio, $SR_{160}/SR_{\max}$;
- the percentage of compaction at the maximum stress ratio, $\%G_{mm}$ at $SR_{\max}$.

The authors reported that among the five different shear stress-related parameters listed, only $N\text{-}SR_{\max}$ had relatively good correlation with rutting rates. The authors validated this correlation with several different field projects, including NCHRP Project 09-7, the 1992 Long-Term Pavement Performance (LTPP) Specific Pavement Studies pilot projects, the WesTrack project, and several original LTPP General Pavement Studies projects (see Figure 2-17). The authors found that this parameter was able to capture the effectiveness of change in aggregate structure and binder content on asphalt mixture stability after construction. Based on this correlation, the authors proposed a protocol to identify good, fair, and poor asphalt mixtures during volumetric mix design and decide whether to re-design the asphalt mixture or run further performance-related testing on a given mix design (see NCHRP Report 09-16 Appendix D). However, the authors mentioned that this parameter could not respond well to the change in binder stiffness.

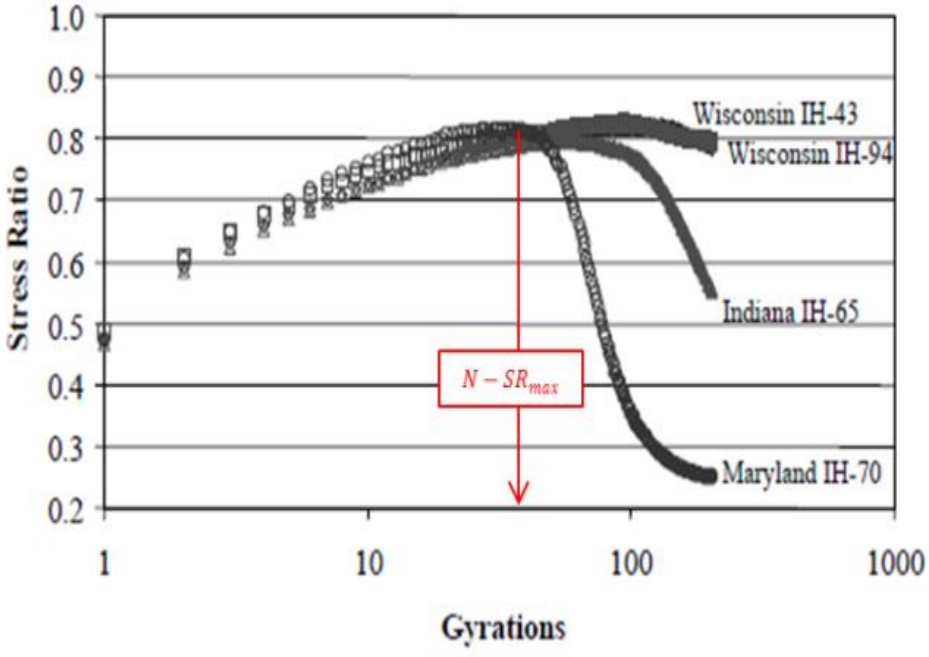

(a) Determining $N\text{-}SR_{\max}$

Figure 2-17. Gyrations at Maximum Shear Stress Ratio: (a) Determining Its Value; (b) Its Correlation with Rutting Rate (Anderson et al., 2002)

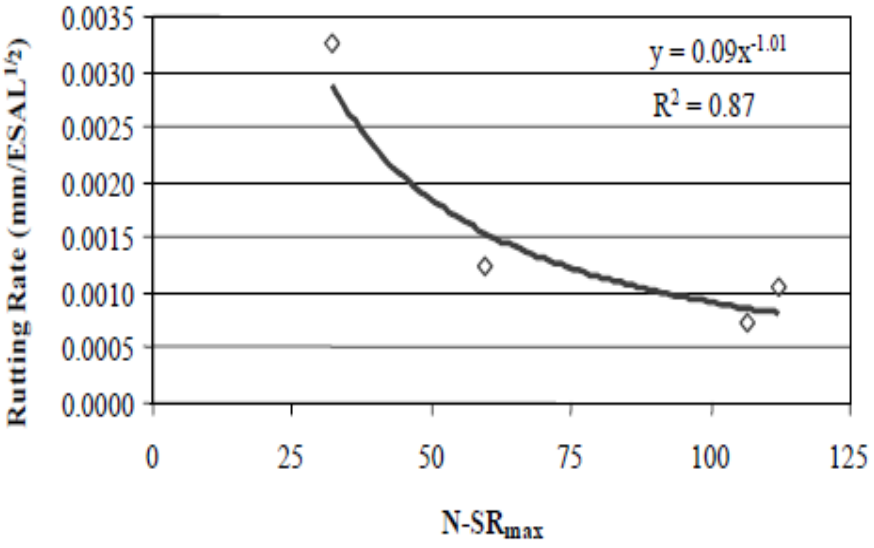

(b) Rutting Rate versus $N\text{-}SR_{\max}$

Figure 2-17. Gyrations at Maximum Shear Stress Ratio: (a) Determining Its Value; (b) Its Correlation with Rutting Rate (Anderson et al., 2002), Continued

Newcomb et al. (2015) followed the work of De Sombre et al. (1998) and used the maximum shear stress to compare the compactability of different asphalt mixtures. The authors normalized the maximum shear stress values of foamed WMA samples with respect to the maximum shear stress of control samples for this comparison. The authors concluded that normalized maximum shear stress was sensitive to mix characteristics and, by extension, asphalt binder grade. The authors demonstrated that control and foamed WMA mixtures exhibited different values of normalized maximum shear stress for different binder types and water contents (see Figure 2-18), and therefore recommended selecting the foaming water content that produced the lowest maximum shear stress to ensure stability during compaction.

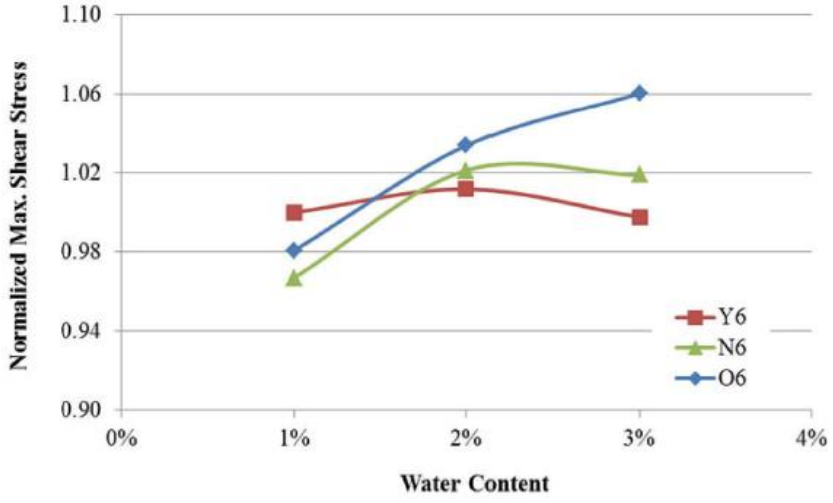

Figure 2-18. Normalized Maximum Shear Stress (Newcomb et al., 2015)

Guler et al. (2000) evaluated the change in frictional resistance of asphalt mixtures during compaction to study the stability of asphalt mixtures. For this evaluation, the authors developed a gyratory load cell and plate assembly and placed it on top of the asphalt mixture inside the compaction mold to capture the force applied by the ram of the compactor for compaction. The authors multiplied this force with its eccentricity to calculate the moment applied on the mixture during gyration and determined resultant frictional resistance using the balance of strain energy (frictional resistance × cross-sectional area × compacted height = force × eccentricity). Test results showed that the value of frictional resistance continuously increased until a certain number of gyrations and then reached a maximum value that remained almost steady in some asphalt mixtures but precipitately dropped to lower values in others (see Figure 2-19). The authors attributed the steadiness in frictional resistance to high internal stability, and the precipitous drop in frictional resistance to compromised internal stability. On that basis, the authors also defined the plot of friction resistance versus gyrations as a volumetric-stability plot and recommended using the laboratory-measured frictional resistance of asphalt mixtures as an indicator of stability. However, the authors did not verify this relationship with stability in the field.

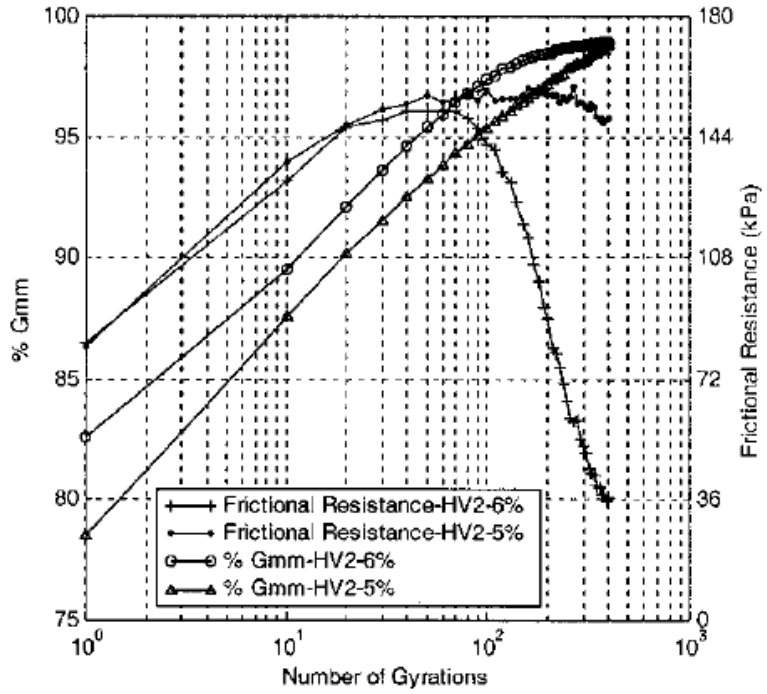

Figure 2-19. Frictional Resistance (Guler et al., 2000)

2.3.2.5 Densification Indices

Bahia et al. (1998) were among the first to evaluate compactability of mixtures in terms of the effort required to compact them from one density level to another. The authors were also among the first to separate compacted data into two parts—the first part comprised of data from eight gyrations to 92%G_{mm} (8 gyrations to 8% air void content) that represented

precipitous densification of mixtures, and the second part comprised of data from 92%G_{mm} to 98%G_{mm} (8% to 2% air void content) that represented comparatively slower densification. The authors used the first part to determine a parameter that represented the effort required to compact mixtures under rollers during construction and defined it as the construction densification index (*CDI*). The authors used the second part to determine another parameter that represented the effort required to compact mixtures under traffic and defined it as the traffic densification index (*TDI*). Ideally, tender mixtures would need less effort to compact and therefore would have lower *CDI* and *TDI* than their counterparts.

Mohammad and Al Shamsi (2007) verified that mixtures such as those with coarser aggregate gradations that became stable and more difficult to compact soon during construction exhibited higher *CDI* values (or required more energy to compact) than their counterparts. Likewise, the authors also verified that mixtures that did not get compacted much under traffic loading exhibited higher *TDI* values.

2.3.2.6 Energy Indices

Bayomy et al. (2002) proposed different parameters to separate the compaction data into two parts. The first part included densification data only up to the number of gyrations at which the slope of two consecutive gyrations was less than or equal to 0.001%, N_{G1} in this part (see Figure 2-20). Since this part involved precipitous increase in compacted density, the authors postulated that applied energy would be used significantly more for carrying out the volumetric change than for overcoming frictional resistance from aggregates and adjusting their orientation in this part. The second part included the densification data from N_{G1} to N_{G2}, which referred to the number of gyrations that would yield the same value of N_{G2}-N_{G1} for the asphalt mixtures that the authors evaluated in their study. Since this part involved a relatively slower increase in compacted density, the authors postulated that applied energy would be used significantly more for overcoming frictional resistance from aggregates and adjusting their orientation than for volumetric change in this part.

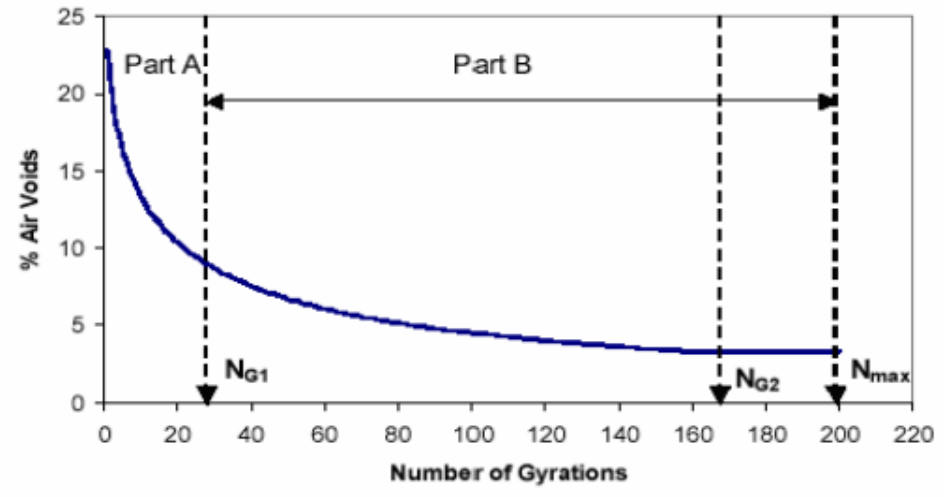

Figure 2-20. Schematic Separation of Compaction Data (Bayomy et al., 2002)

Unlike Bahia et al. (1998), Bayomy et al. (2002) used shear stress versus compacted height ($S_{N\theta}$ versus h) data from N_{G1} to N_{G2} (i.e., the second part of the curve) to calculate a new indicator of asphalt mixture stability, called the contact energy index (*CEI*). Dessouky et al. (2003, 2004) reported that the easy-to-compact (tender or too soft) mixtures had lower values of this index than their counterparts. The authors also reported that the *CEI* was sensitive to most of the mix design variables (see Figure 2-21):

- asphalt binder content,
- sand content,
- aggregate gradation,
- nominal maximum aggregate size, and
- aggregate type

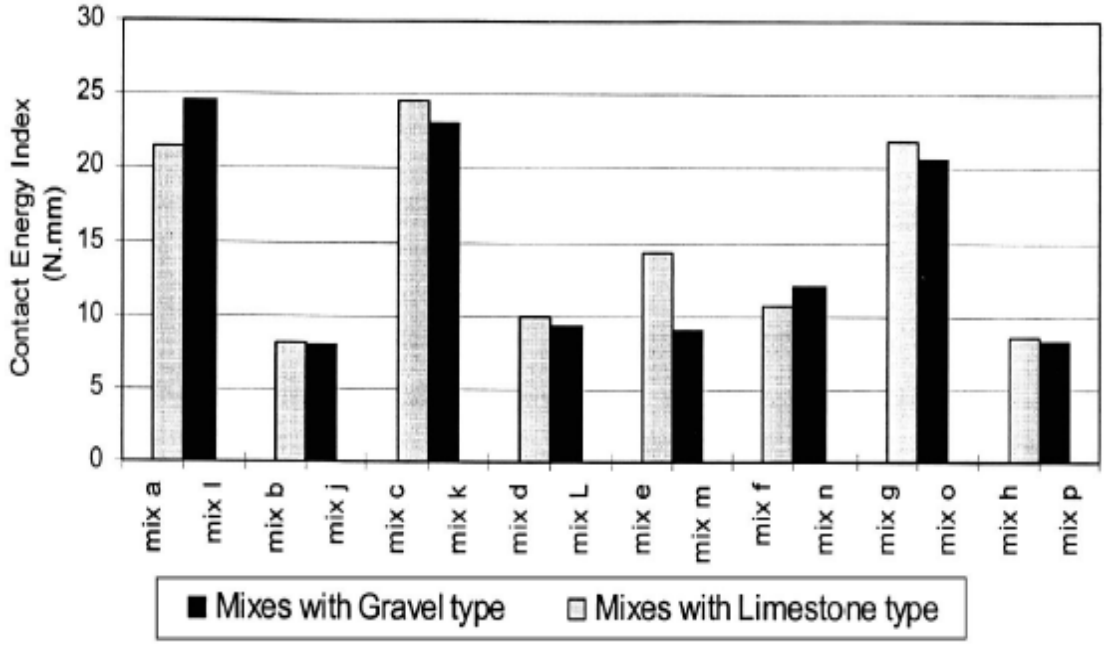

Figure 2-21. Contact Energy Index Sensitivity (Dessouky et al., 2004)

Bahia and Faheem (2007) mentioned that the *CDI* and *TDI* developed by Bahia et al. (1998) could not truly represent the plastic instability of asphalt mixtures because these indices were calculated based on volumetric changes instead of the shear resistance of the mixtures during compaction. Therefore, the authors used the gyratory load plate assembly developed by Guler et al. (2000) to measure shear stress in asphalt mixture samples during compaction and defined two new indices. These indices included the construction force index (*CFI*), which was calculated using the area under shear stress against the compacted height curve from $N_{initial}$ to 92%G_{mm}, and the traffic force index (*TFI*), which was calculated using the data 92%G_{mm} to 98%G_{mm} (see Figure 2-22).

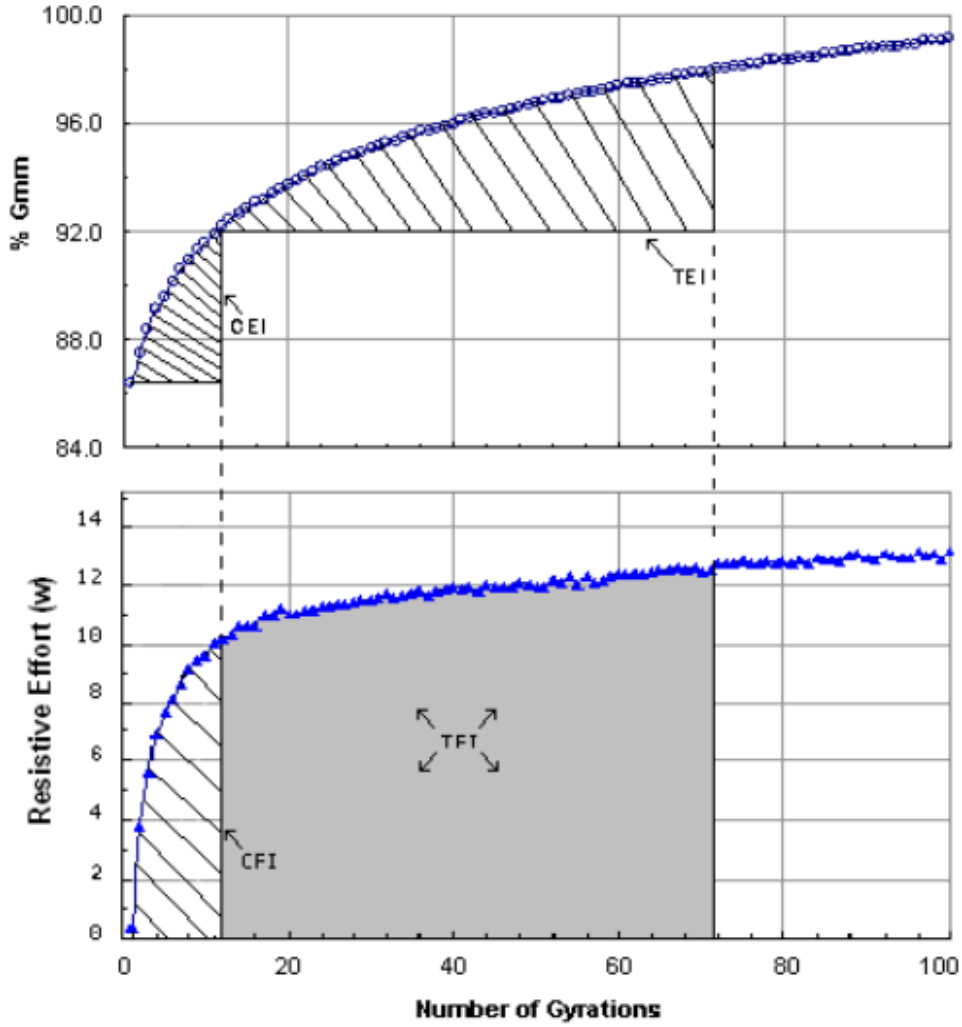

Figure 2-22. Shear Energy and Force Index Schematic (Bahia and Faheem, 2007)

Bahia and Faheem (2007) determined the values of the *CFI*, *TFI*, *CDI*, and *TDI* of several different mixtures and studied their correlations with flow number (in cycles) and rutting rate (millimeters/ESAL) obtained from HWT tests. The authors found that the *CDI* value was better correlated with resistance to compaction by compaction rollers during construction, while the *TDI* or *TFI* was better correlated to compaction by traffic after construction. Therefore, the authors recommended using the *CDI* for evaluating resistance to compaction during construction (i.e., stability during construction) and the *TDI* or *TFI* for evaluating resistance to deformation after construction (i.e., stability after construction). The authors also proposed minimum values for these indices to ensure stability during and after construction for 3, 10, and 30 million ESALs of traffic, represented as E3, E10, and E30.

Bayomy and Abu Abdo (2006) modified the previously developed equation for contact energy index, *CEI* (Bayomy et al., 2002), by replacing N_{G2} with design number of gyrations, N_{design}, based on the hypothesis that the energy applied after N_{G2} has no effect on compaction and does not help in assessing asphalt mixture stability. The authors defined the new energy

index term as gyratory stability (*GS*). The authors used 47 Hveem mixtures and 2 Superpave mixtures to investigate the potential use of gyratory stability as a screening tool at the mix design stage to assess mix performance. By studying the correlation of their gyratory stability with their fracture toughness, the authors concluded that *GS* was able to capture the effect of asphalt binder content and aggregate gradations. Likewise, Abdo et al. (2010) ranked asphalt mixtures obtained from five locations based on gyratory stability, flow number, asphalt binder content, APA rut depth, and mechanistic-empirical pavement design guide software-estimated rut depth. The authors found that *GS* value decreased with an increase in binder content, flow number, and rut depth (see Figure 2-23).

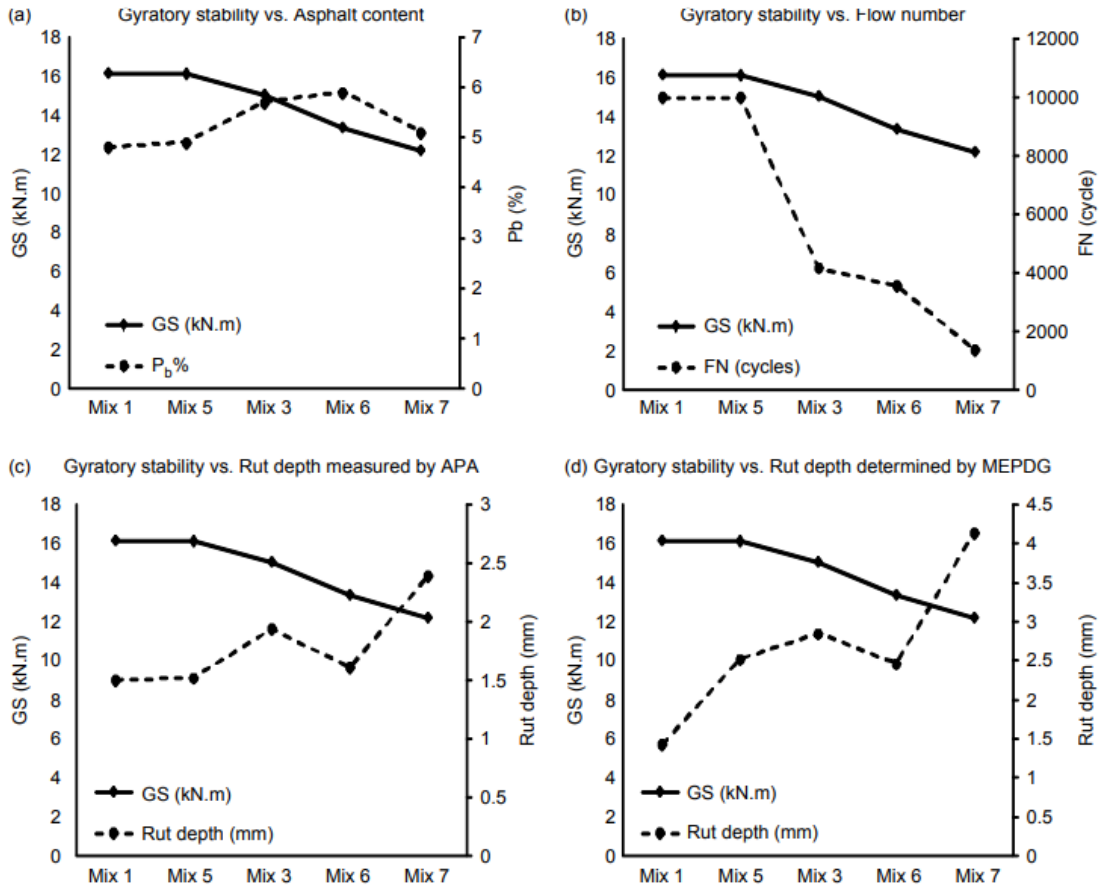

Figure 2-23. Gyratory Stability (Abu Abdo et al., 2010)

Most recently, Dessouky et al. (2013) proposed evaluating the workability and compactability of asphalt mixtures using the workability energy index (*WEI*) and the compactability energy index (*CEI*). The authors defined the workability in terms of the effort (energy = compaction pressure × area × change in height/effective number or gyrations) needed to compact the mixture to 92%G_{mm} (i.e., from uncompacted condition to 8% air void content) and compactability in terms of the effort (energy) needed to compact the mixture from 92%G_{mm} to 96%G_{mm} (i.e., from 8% to 4% air void content). The authors associated the *WEI* with the workability and compactability of asphalt mixtures during construction, and the *CEI*

with the compactability and stability of asphalt mixtures against loading after construction. On this basis, mixtures with higher *WEI* and lower *CEI* values would be easier to compact during construction and become stable soon after construction.

Dessouky et al. (2013) and Dessouky (2015) used this theory to evaluate the workability and compactability of mixtures prepared with local materials from Texas and mixtures obtained from three accelerated pavement testing facilities in Alabama, Louisiana, and Texas. Test results revealed that these indices were sensitive to mix design variables (binder content, binder grade, aggregate type, and aggregate gradation). The authors specifically studied the correlation of the *WEI* with field air voids and the correlation of the *CEI* with stiffness (dynamic modulus), rate of rutting, and the HWT test rutting rate (see Figure 2-24). The authors noticed a strong correlation between the *WEI* and field air void content, from which they determined a minimum threshold value of 4.5 for the *WEI*. Similarly, the authors noticed that stiffness, rate of rutting and the HWTT rutting rate had better correlations with *CEI* values than with the $k \times AV$ values and these same variables. Based on these correlations, the authors determined a maximum threshold value of 4.5 for the *CEI*.

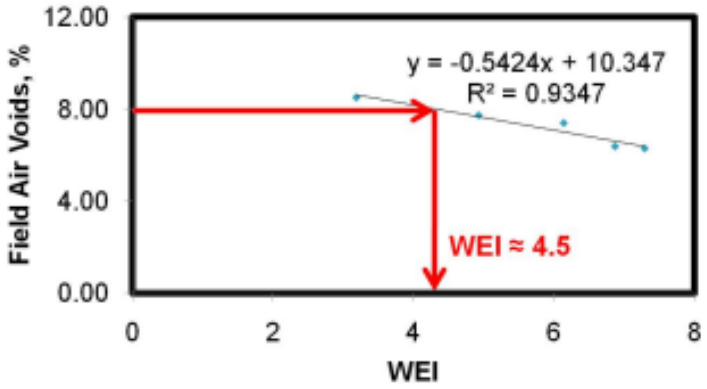

(a) WEI Correlation with Field Air Voids

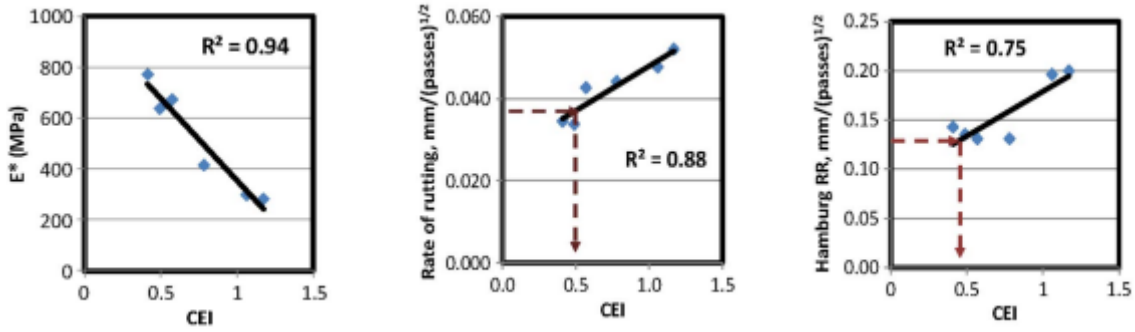

Dynamic Modulus at 37°C Rate of Rutting Hamburg Rutting Rate

(b) CEI Correlations with Stiffness and Rutting Rates

Figure 2-24. Workability and Compactability Correlations (Dessouky et al., 2013)

Table 2-3 summarizes the types, definitions, and references of different types of workability and compactability parameters identified from this literature review.

Table 2-3. Workability and Compactability Parameters

Types	Parameters	Definition	Reference
Workability during Mixing			
Workability Parameters	Lubricity	Shear rate at which upper plate geometry of the rheometer slips on asphalt binder samples	Bennert et al. (2010)
	Torque, T	Torque required for blending asphalt mixture samples at a constant speed and temperature	Marvillet and Bougault (1979) Gudimettla et al. (2003, 2004) Poeran and Sluer (2016)
Workability and Compactability during Compaction			
Single-Point Parameters: Compacted Density	Compaction Factor, C_f	Volume after 5 blows/Volume after 100 blows	Heukelom (1968)
	Air Void at 75 blows, $AV75$	$\%Va$ at 75 blows	Bennert et al. (2010)
	Workability Index, WI	1/Estimated porosity at 0 gyrations	Cabrera (1996, 1991)
	Density 10 gyrations, C_{10}	G_{mm} at 10 gyrations	Cominsky et al. (1994)
	Density at 230 gyrations, C_{230}	$\%G_{mm}$ at 230 gyrations	Cominsky et al. (1994)
	Density at N_{initial}	$\%G_{mm}$ at N_{initial}	McGennis (1997) Button et al. (2004)
	Compacted Air Voids, $AV100$	Air Void Content at 100 gyrations	Bennert et al. (2010)
Single-Point Parameters: Compaction Effort Parameters	Gyratory Ratio, GR	Gyration at 98%G_{mm}/ Gyration at 95%G_{mm}	Mallick (1999)
	Locking Point, LP	First of three gyrations that are at the same height preceded by two gyrations at the same height	Vavrik and Carpenter (1998)
	Compaction Rate, CR	Height at 93%G_{mm} /Gyration at 93%G_{mm} = $h93/N93$	Bennert et al. (2010)

Table 2-3. Workability and Compactability Parameters, Continued

Types	Parameters	Definition	Reference
Single-Point Parameters: Compaction Effort Parameters	$N87$	Gyration at 87%G_{mm}	Ling et al. (2013)
	Gyratory Shear, Gs	Gyratory shear stress at 200 gyrations	McRea (1965, 1962) Ruth et al. (1992)
	Maximum Shear Stress, $\tau_{\max}$	Maximum shear stress	De Sombre et al. (1998) Butcher (1998)
	Max. Shear Stress Ratio, $SR_{\max}$	Shear stress/Max. shear stress	Anderson et al. (2002) Newcomb et al. (2015)
	Gyrations at Max. Shear Stress Ratio, N-$SR_{\max}$	Gyration at max. shear stress/normal stress	Anderson et al. (2002)
Slope Parameters: Compaction Rate Parameters	Resistance to Compaction, R	$R = \frac{1}{\frac{d\gamma}{dC}}(\gamma_{\max} - \gamma)$	Bissada (1984)
	Compaction Slope, k or k_{SGC}	$k = \left\lvert\frac{d(\%Gmm)}{dN}\right\rvert$	Cominsky et al. (1994) McGennis (1997) Anderson and Bahia Button et al. (2004)
	Laboratory Compaction Index, CI	$CI = \frac{m^{1.2}}{c}$ where, $m = \left\lvert\frac{d(\%AV)}{dN}\right\rvert$ $c = \%AV_0$	Kaseem et al. (2012)
	$k \times AV$	k × %Air void content at N_{design}	Anderson et al. (2002)
	Frictional Shear Resistance	Ram force × Eccentricity/ Area / Height	Guler et al. (2000) Ling et al. (2013)

Table 2-3. Workability and Compactability Parameters, Continued

Types	Parameters	Definition	Reference
Area Parameters: Compaction Densification and Energy Parameters	Construction Densification Index, *CDI*	Area under densification curve from 8 gyrations up to 92%G_{mm}	Bahia et al. (1998) Mohammad and Al Shamsi (2007)
	Traffic Densification Index, *TDI*	Area under densification curve from 92% to 98%G_{mm}	Bahia et al. (1998) Mohammad and Al Shamsi (2007)
	Contact Energy Index, *CEI*	Area under shear resistance curve from N_{G1} to N_{G2}	Bayomy et al. (2002) Dessouky et al. (2003, 2004)
	Gyratory Stability, *GS*	Area under shear resistance curve from N_{G1} to N_{design}	Bayomy and Abu Abdo (2006) Abu Abdo et al. (2010)
	Construction Force Index, *CFI*	Area under shear resistance curve up to 92%G_{mm}	Bahia and Faheem (2007)
	Traffic Force Index, *TFI*	Area under shear resistance curve from 92% to 98%G_{mm}	Bahia and Faheem (2007)
	Workability Energy Index, *WEI*	Cross-Sectional Area × Pressure × $(h_0 - h92)$ / $N92$	Dessouky et al. (2013) Dessouky (2015)
	Compactability Energy Index, *CEI*	Cross-Sectional Area × Pressure × $(h96 - h92)$ / $(N92 - N96)$	Dessouky et al. (2013) Dessouky (2015)

2.3.3 Parameters Obtained from Tests after Mixtures Have Partially Cooled

Asphalt pavements cannot be opened to traffic or tested immediately after compaction because asphalt mixtures need time to lose temperature and gain stability. The time over which asphalt pavements gain stability depends on the rate at which asphalt binders that have been heated at high temperatures for several hours during construction regain their viscosity and adhesive-cohesive properties when left undisturbed at ambient temperature. The rate at which asphalt binders regain their properties after placement and compaction also influences the rate at which asphalt mixtures gain enough resistance to shearing and the rate at which the asphalt pavement becomes stable enough to allow traffic or testing at ambient temperature. Therefore, the research team reviewed literature on the cooling rates of asphalt binders, asphalt mixtures, and asphalt pavements and the factors that affect these rates as discussed in the following paragraphs.

Apeagyei et al. (2009) measured the cooling behavior of a beam of asphalt binder from an intermediate temperature of 15°C to a subnormal temperature of −50°C using an acoustic-emission system. The author restrained a beam of asphalt binder sample on granite substratum in a chamber and measured the temperature using a thermocouple. Despite letting the samples cool at subnormal temperature, their test result showed that the cooling rate did not follow a linear relationship. This result is quite relevant to this project because it shows an easier method to measure cooling behavior of asphalt binders, and the possibility of a nonlinear cooling rate of asphalt binders at higher temperatures, usually from compaction temperature to ambient temperature.

Gorsuch et al. (2013) evaluated the tackiness of the unmodified and modified asphalt binders and the emulsion residues by conducting pull-off tests at constant displacement rates using a dynamic shear rheometer. From these tests, the authors determined the maximum force and the total energy required by asphalt binders for complete pull-offs at different combinations of displacement rates and temperatures (see Figure 2-25). The authors determined a parameter, called a tack parameter, by calculating the area under the force versus time curve obtained from the pull-off tests and then dividing this area by the sample thickness, thereby making it independent of sample thickness. These parameters would be higher in asphalt binders that would stick to the tires or construction vehicles and get tracked across the pavement, or in other words, more cohesive/adhesive binders. Test results showed that the tack parameter was sensitive to displacement rate, temperature, polymer-modification, and treatment dosage. The following is a summary of the observations:

- The sensitivity to displacement rate suggests that tackiness can be potentially used to evaluate the viscosities (softness or hardness) of treated binders at a given temperature and by extension their effect on mix workability.
- The sensitivity to temperature suggests that tackiness can be potentially used to evaluate the stiffening (or cooling) rates of different asphalt binders at a given displacement rate and by extension their effect on mix compactability.
- The sensitivity to modification/treatment suggests that tackiness can be potentially used to evaluate the effectiveness of the effect of liquid ASA treatments on binder cooling rates and by extension asphalt mixture stability.

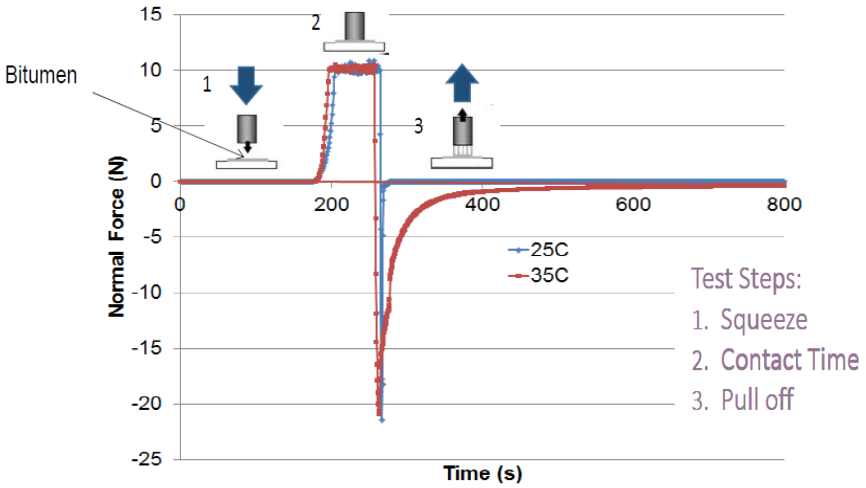

(a) Illustration

(**Note**: Only the step 3 was used for tack parameter analysis.)

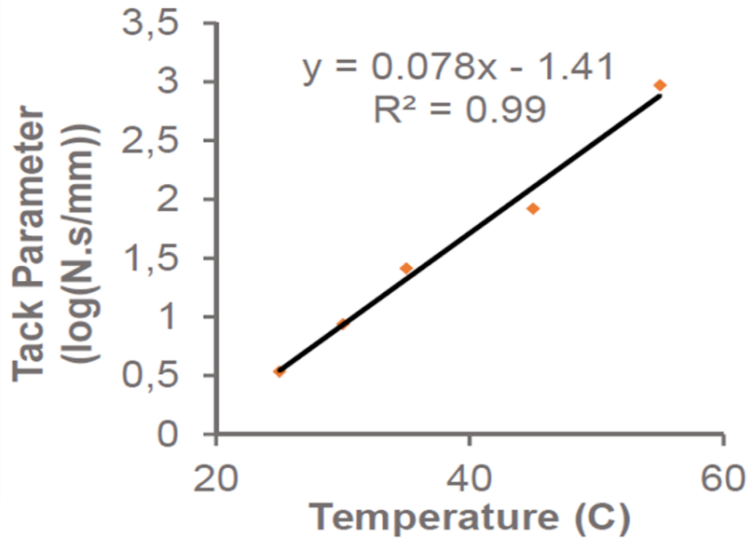

(b) Sample Results

Figure 2-25. Asphalt Binder Pull-Off Test (a) Illustration; (b) Sample Results (Gorsuch et al., 2013)

Sun et al. (2017) monitored the decrease in temperature as a function of time in a binder beam sample attached to a granite substratum and in a semicircular asphalt concrete sample over 20°C to −50°C using piezoelectric acoustic emission and thermocouple. The test result showed that temperature change in the mixture took longer than the asphalt binders, as expected. Due to a larger volume of asphalt mixture samples, it is customary to use a dummy sample with a thermocouple in the environmental chamber to ensure the test specimens have attained isothermal condition before starting a test at a certain temperature in the laboratory.

McLeod (1967) was among the first to study the cooling rate of asphalt pavements over time until the maximum resistance to further compaction. The author determined that since all asphalt binders do not gain viscosity at the same rate with temperature, asphalt mixtures prepared with different asphalt binders and placed even at the same temperature can cool at different rates and take different durations to reach the temperature at which further compaction is possible (see Figure 2-26).

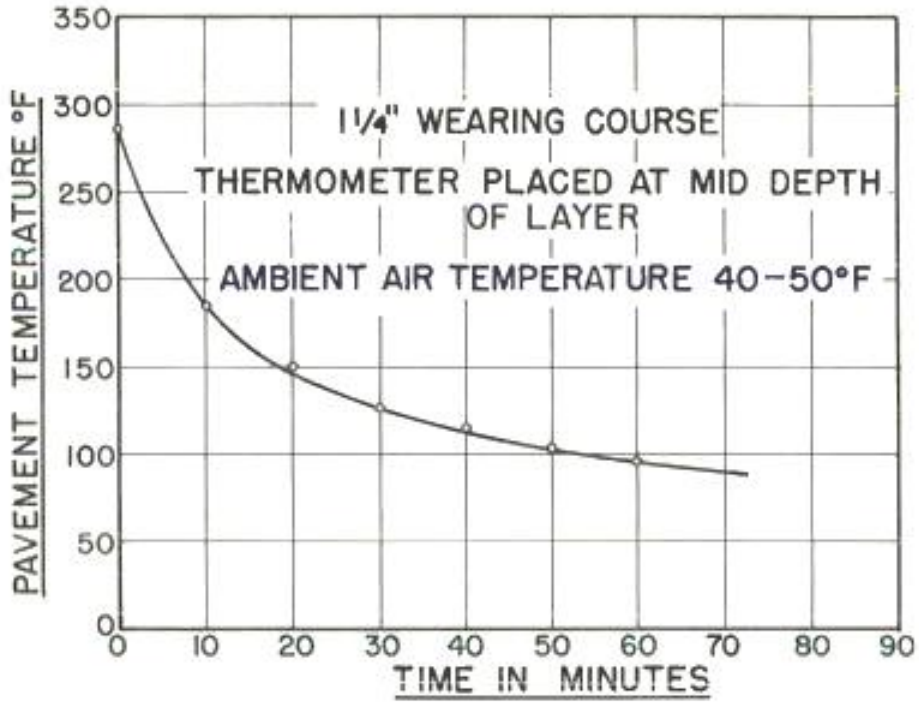

Figure 2-26. Asphalt Pavement Cooling Behavior (McLeod, 1967)

Dickson and Corlew (1970) are other early researchers who studied the cooling rate of asphalt pavements during construction. The authors reported that as the mat (or mix) temperature decreases during compaction, asphalt binder becomes more viscous and asphalt mixtures become more resistant to compaction. And, after mat temperature drops to a certain value, asphalt mixtures become too stiff to compact any more. The authors aptly defined the temperature after which asphalt mixtures cannot be further compacted with the rollers as the cessation temperature. After reaching this temperature, asphalt binders become too viscous and the aggregate skeleton (internal structure of asphalt mixtures) becomes too strong for further

compaction. Before reaching this temperature, asphalt binders are comparatively softer and the internal structure of asphalt mixtures is comparatively weak, and as a result, asphalt mixtures allow further compaction. The authors also showed that the asphalt mixture cooling rates depend on several factors that field personnel can control such as mat thickness, base temperature, and mix temperature (see Figure 2-27), as well as several other factors they cannot control such as wind velocity, solar flux, and ambient temperature.

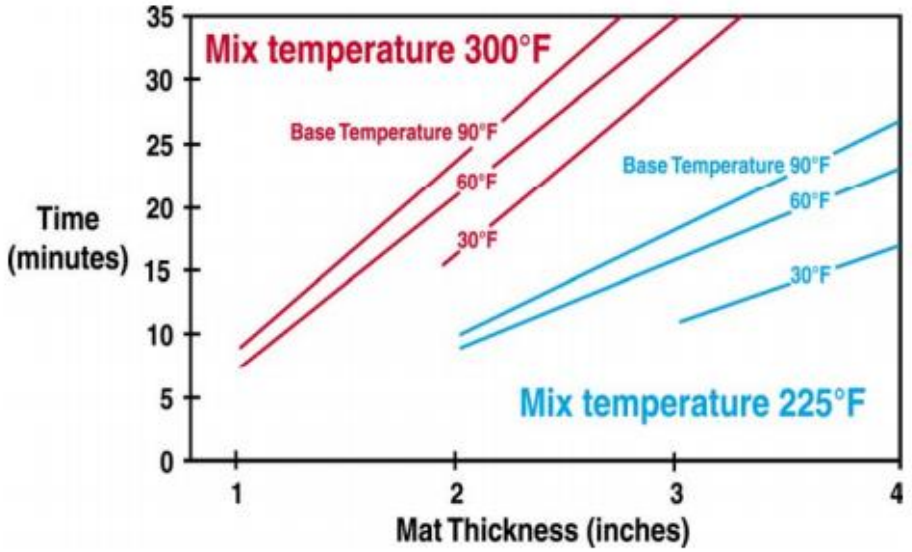

Figure 2-27. Asphalt Pavement Cooling Behavior (Dickson and Corlew, 1970)

Hughes (1989) seconded that the duration over which asphalt mixtures can be and need to be compacted to reach the desired level of density directly depends on the time asphalt mixtures take to reach the cessation temperature after being placed in the field. Similarly, Chadbourn et al. (1998) monitored the cooling rate of asphalt pavement in several paving projects. The authors also developed software to simulate this cooling after paving under a variety of conditions. The authors validated the accuracy of this program by comparing the temperature-versus-time data predicted using this program with the temperature-versus-time data obtained from the field. The authors determined that the cooling rate of the pavement depends on several factors, such as time of day, time of year, latitude of location, cloud cover, ambient temperature, lift thickness, existing base material properties, and new HMA material properties. The authors noted that when these factors are not adequately controlled, asphalt pavements can be compacted with as high as 16% air void content instead of the target air void content, typically 7–9%. However, the authors only considered one lift of asphalt mixture during construction.

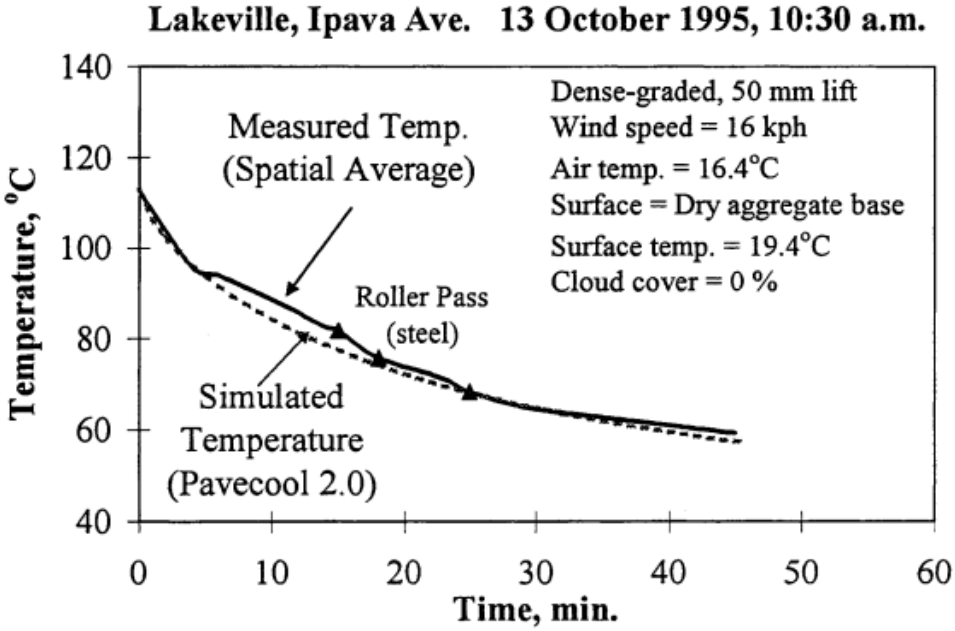

Figure 2-28. Asphalt Pavement Cooling Behavior (Chadbourn et al., 1998)

Timm et al. (2001) monitored the change in temperature in conventional asphalt pavements during their construction and found that the number of lifts of asphalt mixtures and the time gaps between these lifts both influenced the cooling rates of asphalt pavements. Therefore, the authors modified the previously developed asphalt pavement cooling rate prediction software (Chadbourn et al., 1998) by including these two new factors.

Chang et al. (2009) studied the effect of mixture characteristics on the cooling rates of asphalt pavements to estimate the time available for compaction of the HMA during night construction. The authors installed thermocouples to monitor the decrease in temperature in the field until the mat temperature dropped close to the surrounding temperature. The authors categorized the cooling process of the compacted mixture into three stages (see Figure 2-29). The first stage is characterized by a rapid drop in temperature due to a higher amount of heat loss directly to air by convection. The second stage is characterized by a comparatively slower drop in temperature due to a lower amount of heat by conduction. The third and last stage is characterized by gradual or no drop in temperature due to equilibrium with the ambient temperature. From the field and laboratory cooling rate study, the authors concluded that various factors influenced the asphalt pavement cooling rates and, consequently, the time available for compaction and the time required for temperature equilibrium with the surroundings:

- The rate of cooling at the first stage primarily depends on the difference between the asphalt mixture and the ambient temperature.
- The porous asphalt mixtures cooled at significantly higher rates than dense-graded asphalt mixtures, owing to the difference in their air void contents.
- Thicker asphalt pavements cooled at slower rates than thinner pavements, owing to the time taken by the asphalt mixtures to transit from one state to another stage of cooling mode (or heat loss).

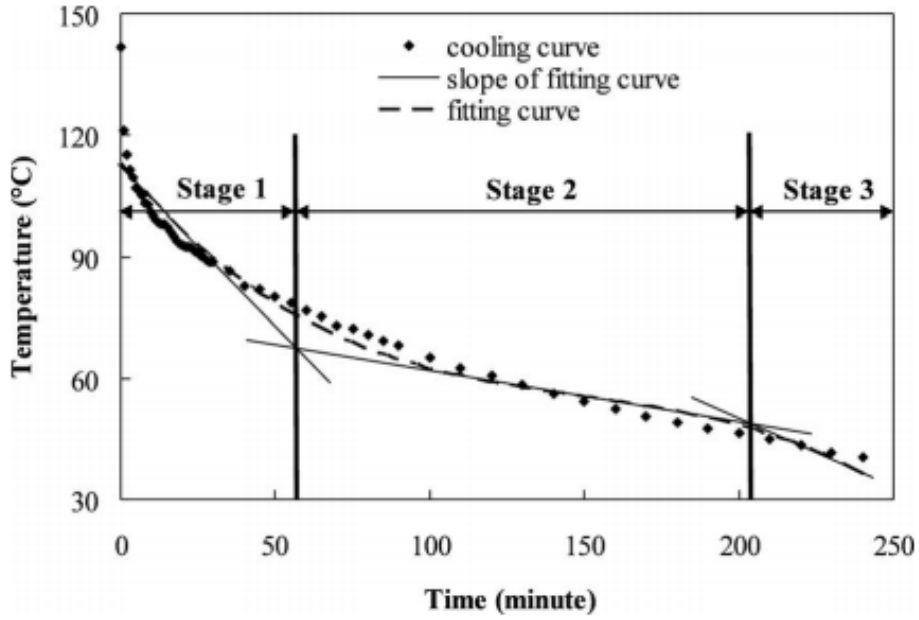

Figure 2-29. Asphalt Pavement Cooling Behavior (Chang et al., 2009)

Chang et al. (2009) also conducted tests to determine the Marshall stability, the indirect tensile strength, and the resilient modulus values of compacted samples at different temperatures to monitor the changes in these properties with increasing temperature (see Figure 2-30). Some important findings that are relevant to this project are:

- The stability value almost increased by 50%, and the *ITS* value almost increased by 35% when the mix temperature dropped from 80 to 50°C, which means that asphalt mixtures could not be opened to traffic or testing at high temperature because they would not have attained adequate stability and strength to carry these loads.
- The indirect tensile strength value increased 10 times when the mix temperature dropped from 90 to 10°C, owing to a significant change in asphalt binder viscosity over this temperature drop.
- The stiffness or resilient modulus value increased by 43% from 50 to 60°C and by 12% at 70°C.

Based on these findings, the authors recommended opening the pavements to traffic at a temperature of 50°C or below.

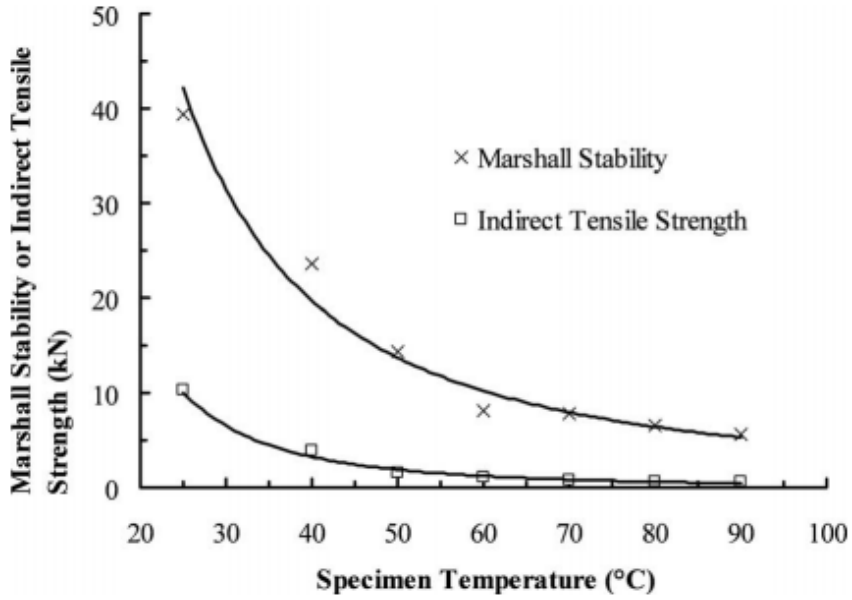

(a) Marshall Stability or Indirect Tensile Strength versus Specimen Temperature

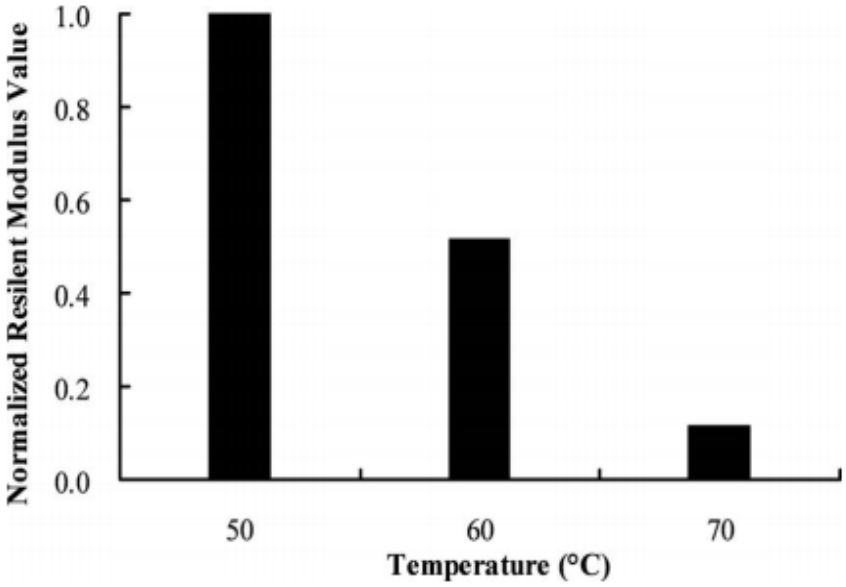

(b) Normalized Resilient Modulus versus Test Temperature

Figure 2-30. Asphalt Mixture Stiffness and Strength Properties (Chang et al., 2009)

Vargas-Nordcbeck and Timm (2011) monitored the temperature change in nonconventional pavement mixtures (WMA mixtures, mixtures containing high percentages of RAP, and mixtures containing modified and alternative binders). The authors also used the software developed by Timm et al. (2001) to predict cooling behaviors (Timm et al., 2001). Their study once again verified that the cooling behavior of asphalt pavement is indeed a function of the factors identified previously by Chadbourn et al. (1998) and Timm et al. (2001). Likewise, Sánchez and Timm (2014) determined that the use of recycled asphalt shingles,

RAP, and ground tire rubber (GTR)-modified asphalt binders also impacted the cooling behavior of asphalt mixtures. The authors validated such impacts through the direct measurement of temperature during construction as well as their simulations with the software. These studies have resulted in different tools to evaluate the cooling rates of mixtures in the field until cessation temperature, which is usually higher than the ambient temperature (see the National Asphalt Pavement Association's link for Multicool software at https://www.asphaltpavement.org/multicool and the Minnesota Department of Transportation's link for Pavecool software at http://www.dot.state.mn.us/app/pavecool).

2.3.4 Parameters Obtained from Tests after Mixtures Have Completely Cooled

Previous researchers always try to correlate parameters obtained from compaction curves while the mixtures were still hot with mixture properties obtained from tests conducted after mixtures were completely cooled and conditioning them at different conditions. For example, Anderson et al. (1999) studied the correlation of the rate of compaction (k) extracted from compaction data with the stiffness of mixtures (see Figure 2-12). Anderson et al. (2002) also evaluated such correlation between a compaction rate-related parameter ($k \times AV$) and the total amount of permanent shear strain measured from the Superpave shear tests in repeated shear at constant height, *%RSCH* γ (see Figure 2-13). Furthermore, Anderson et al. (2002) again evaluated the correlation of the gyration number at maximum shear stress (N-$SR_{\max}$) with rutting rates measured from wheel-track tests (see Figure 2-17). Likewise, Bahia and Faheem (2007) also evaluated the correlations of force and densification indices obtained from different areas under compaction curves with the flow number (in cycles) and rutting rate (mm/ESAL) obtained from HWT tests). Similarly, Dessouky et al. (2013) and Dessouky (2015) studied the correlation of energy indices with field air voids, stiffness, and rutting rates (see Figure 2-24).

In general, there seems to be a practice of using tests that measure stiffness or shear-related properties of mixtures to evaluate compactability after mixtures have cooled completely.

2.4 Summary

This literature review was conducted to document existing experiences regarding the use of liquid ASAs to mitigate stripping problems in asphalt mixtures, the policies or practices implemented by state highway agencies to approve liquid ASAs in their contracts, and the laboratory test methods that assess the stability of asphalt mixtures during and after construction. The summary of this review is as follows:

- Use of liquid ASA:
  - State highway agencies, including FDOT and the agencies in its eight neighboring states, use either boiling or *TSR* or both tests to evaluate the stripping potential of asphalt mixtures.
  - Most state highway agencies require contractors to redesign the mixtures with better materials or use liquid ASAs if the original designs do not pass stripping tests.

- Many state highway agencies maintain separate APLs for liquid ASAs. The sources and recommended dosages of approved liquid ASAs vary from agency to agency.
- Many state highway agencies decide whether a new liquid ASA can be placed in the APL solely based on its effect on moisture damage susceptibility.
- Tenderness during construction and incompatibility with PPA-modified binders are the two most common issues mentioned regarding the use of liquid ASAs in asphalt mixtures.

- Asphalt mixture stability (see Table 2-3):
  - Asphalt mixture stability is influenced by several mix design factors such as asphalt binder viscosity, asphalt binder content, aggregate angularity, aggregate size, aggregate gradation, filler content, sand content, additive type and dosage, and construction-related factors such as compaction and surrounding temperatures and roller types.
  - Liquid ASA is listed as one of several mix design-based factors that impact asphalt mixture stability. However, studies that have evaluated its type (positive, negative, and indifferent effects) and severity (high or low or equivalent) are lacking.
  - The stability of mixtures during construction while the mixtures are still hot has been mainly studied in terms of the ease by which mixtures can be mixed and compacted until mixtures reach a certain compaction effort (i.e., a certain number of blows in the Marshall compaction method and a certain number of gyrations or a certain level of density in the Superpave gyratory compaction method).
  - The stability of mixtures after compaction while mixtures have partially cooled (or are still cooling) has not been studied.
  - The stability of mixtures after construction, after mixtures have completely cooled to ambient temperature, has been mainly studied in terms of the ease with which mixtures can be compacted after they have already undergone a significant level of volumetric change, attained interlocked structure of aggregates and developed shear resistance, and correlated to stiffness, rutting rates, and rut depths.

- Assessment of asphalt mixture stability:
  - The stability of mixtures in the field (the ease by which pavements can be compacted to a desired level of density) has been mostly assessed in terms of parameters that describe the ease with which asphalt mixtures can be mixed and compacted in the laboratory.
  - The ease with which mixtures can be mixed in the field has been assessed mostly in terms of the torque required to blend aggregates and binders using a bucket and paddle mixer in the laboratory (i.e., a measure of mix viscosity) and sometimes in terms of the viscosity or lubricity of asphalt binders. The torque required to prepare mixtures (i.e., the workability of mixtures during mixing) has also been

used to estimate the ease with which mixtures can be compacted (i.e., the workability of mixtures during compaction). However, the ease by which mixtures can be mixed and the ease by which mixtures can be compacted (workability during mixing versus workability during compaction) are not the same.

- Workability (i.e., tenderness or instability) of mixtures during compaction has been assessed in terms of parameters that describe the volumetric properties of mixtures at certain instances during compaction, parameters that describe the rate of change in volumetric properties during compaction, and parameters that describe the total amount of compaction effort (densification) or compaction energy required to change volumetric properties from one level to another.
- Parameters that describe the total amount of compaction effort (densification) or compaction energy required to change volumetric properties from one level to another have been classified into two groups. The first group represents the compactability of mixtures under rollers during construction while mixtures are still hot, and the second group represents the compactability of mixtures under traffic loads after construction after mixtures have significantly cooled down.
- Parameters such as the *CDI*, *CFI*, *VEI*, and *WEI* that represent the effort required to bring significant change in density (usually from uncompacted condition to 92%G_{mm} or N_{G1}) are the parameters used to assess the workability and compactability (or tenderness) of mixtures under rollers during construction while mixtures are still hot.
- Parameters such as the *TDI*, *TFI*, *SEI*, and *CEI* that represent the effort required to compact mixtures against significant shear resistance (usually after 92%G_{mm} or N_{G1}) are the parameters used to assess the compactability of mixtures (or tenderness) under traffic loads after mixtures have significantly cooled.
- The stability of mixtures, while they have partially or completely cooled to ambient temperature after construction, can be potentially evaluated in terms of the rate of change in binder stiffness and tackiness, the rate of change in mixture stiffness properties such as dynamic modulus, resilient modulus, and plastic deformation properties such as Marshall stability, rut depth, rutting rate, etc.

3 MATERIALS

3.1 Asphalt Binder

One Superpave PG 76-22 polymer-modified asphalt (PMA) binder with same mixing and compaction temperature (166ºC or 330°F) was used in this study. The binder (herein simply referred to as "PMA" control binder) was obtained from one of the sources listed in FDOT's APL for Superpave PG 76-22 (PMA) binders (see https://fdotwp1.dot.state.fl.us/ApprovedProductList/ProductTypes/Index/87).

The PMA binder was subjected to different aging and testing conditions as specified in Section 916 of FDOT's Standard Specifications for Road and Bridge Construction (FDOT, 2019) to determine its various properties and verify its performance grade (PG). The aging conditions included accelerated short-term oven aging (STOA) in an RTFO at 163°C (325°F) for 85 minutes following AASHTO T 240 (2013) and accelerated long-term oven aging (LTOA) in a PAV at 100°C (212°F) and 2.1 MPa (305 psi) for 20 hours following AASHTO R 28 (2012b). And, the testing conditions included the DSR tests of its unaged and PAV-aged samples, the MSCR tests of its RTFO-aged samples and BBR tests of its PAV-aged samples at various loading and temperature conditions as summarized below.

3.1.1 DSR Tests of Unaged Binder

DSR tests were conducted on unaged specimens of asphalt binder at an angular frequency of 10 rad/sec and minimum two grade temperatures following AASHTO T 315 (2012c) to measure its dynamic shear modulus (G^*), phase angle (δ) and rutting parameter ($G^*/\text{Sin}\delta$) values at those temperatures and ultimately determine its high temperature PG (PG_{HT}). Three parallel plate specimens, each measuring 25.0 mm in diameter and 1.0 mm in thickness and a Malvern Kinexus Pro DSR were used for these tests at each temperature. Test results showed that the binder satisfied FDOT's both requirements (i.e., $G^*/\text{Sin}\delta \geq 1.00$ kPa and $\delta \leq 75°$ degrees at 76°C) for a PG 76-22 (PMA) binder (see Table 3-1).

3.1.2 MSCR Test of RTFO-Aged Binder

MSCR tests were conducted on RTFO-aged residue of asphalt binder sample at shear stresses of 0.10 kPa and 3.20 kPa and a temperature of 67°C following AASHTO T 350 (2014b) to measure its unrecoverable creep compliance ($Jnr_{0.1}$ and $Jnr_{3.2}$), percent recovery ($\%Rec_{0.1}$ and $\%Rec_{3.2}$) and percent difference in Jnr ($\%Rec_{\text{diff}}$ and $\%Jnr_{\text{diff}}$) values at that temperature, and ultimately determine its AASHTO M 332 (2014c) grade. Three parallel plate specimens, each measuring 25.0 mm in diameter and 1.0 mm in thickness, and the Malvern Kinexus Pro DSR were used for these tests. Test results showed that the binder satisfied each requirement ($Jnr_{3.2} \leq 1.0$/kPa, $\%Rec_{3.2} \geq 29.37 \times {Jnr_{3.2}}^{-0.2633}$ and $\%Jnr_{\text{diff}} \leq 75\%$ at 67°C for a PG 76-22 (PMA) binder; it was actually a "E" graded modified binder (see Table 3-1).

3.1.3 BBR Test of PAV-Aged Binder

BBR tests were conducted on the PAV-aged residue of asphalt binder at a creep load of 980 N and minimum two grade temperatures plus 10°C following AASHTO T 313 (2012d) to measure its creep stiffness and creep slope values after 60 seconds of loading at those temperatures (S and m), and determine its creep-stiffness-and creep slope-based critical low temperature (T_{cs} and T_{cm}) and ultimately its low temperature PG (PG_{LT}). Two beam specimens, each measuring 127.0 mm in length, 12.5 mm in width and 6.35 mm in thickness and a Cannon Instruments TE-BBR were used for these tests at each temperature. Test results showed that the binder satisfied FDOT's both requirements (i.e., $m \geq 0.300$ and $S \leq 300$ MPa at −12°C) for a Superpave PG 76-22 (PMA) binder at −12°C (see Table 3-1). Test results also showed the binder also satisfied a recently added binder quality-related parameter (i.e., $\Delta T_c = T_{cs} - T_{cm} \geq -5$°C) as specified in ASTM D7643 (2016).

3.1.4 DSR Test of PAV-Aged Binder

DSR tests were also conducted on the PAV-aged residue of the asphalt binder at an angular frequency of 10 rad/sec and a temperature of 26.5°C following AASHTO T 315 (2012c) to determine its cracking parameter ($G^*\text{Sin}\delta$) value at that temperature. Three parallel plate specimens, each measuring 8.0 mm in diameter and 2.0 mm in thickness and the Malvern Kinexus Pro DSR were used for the tests. Test results showed that the binder satisfied FDOT's requirements ($G^*\text{Sin}\delta \leq 5000$ kPa) for a Superpave PG 76-22 (PMA) binder at 26.5°C (see Table 3-1).

Based on these four tests, its true grade was 79.7-22.3 and satisfied all requirements of PG 76-22 (PMA) binder as specified in Section 916-2 (FDOT, 2019).

Table 3-1. Performance Grade Results: Control Asphalt Binder

Test	Geometry	Loading	T °C	FDOT Criteria	Measured	Remarks
Original						
DSR	D 25 mm H 1 mm	ω 10 r/s γ 12%	76.0	$G^*/\text{Sin}\delta \geq 1.0$ kPa	1.39	Pass (PG_{HT} = 79.7)
				$\delta \leq 75$ deg.	71.6	
			82.0	$G^*/\text{Sin}\delta$ (kPa)	0.81	
				δ (deg.)	73.5	
RTFO Residue						
MSCR	D 25 mm H 1 mm	τ 0.1 kPa τ 3.2 kPa	67.0	$Jnr_{3.2} \leq 1.0$ 1/kPa	0.2771	Pass
				Grade $\geq$ V	E	
				$\%Rec_{3.2} \geq 29.37 \times Jnr_{3.2}^{-0.2633}$	33.8	
				$\%Jnr_{\text{diff}} \leq 75\%$	62.0	
PAV Residue						
BBR	L 127 mm B 12.5 mm H 6.35 mm	P 980 mN	−12.0	$m \geq 0.300$	0.303	Pass (PG_{LT} = −22.3; ΔTc = −2.7)
				$S \leq 300$ MPa	205	
			−18.0	m	0.253	
				S (MPa)	443	
DSR	D 8 mm H 2 mm	ω 10 r/s γ 1%	26.5	$G^*\text{Sin}\delta \leq 5000$ kPa	4430	Pass
Note: D = Diameter; L = Length; B = Breadth; H = Height; ω = Frequency; γ = Shear Strain; τ = Shear Stress; P = Load; T = Temperature						

3.2 Aggregates

Two types of aggregates were used in this project—the granite aggregates obtained from Anderson Columbia Company, Inc. in Georgia and the limestone aggregates obtained from the White Rock Quarries in Southeast Florida. FDOT's Approved Aggregate Production Facility List identifies these two sources of aggregates as GA553 and 87339, respectively (https://mac.fdot.gov/smoreports):

- Granite from GA553 ➔ Referred to as "GA"
- Limestone from 87339 ➔ Referred to as "LS"

FDOT provided a total of four mix design types—three SP and one FC mixes with 9.5 mm (3/8 in. = 0.375 in.) or 12.5 mm (1/2 in. = 0.50 in.) nominal maximum aggregates size (NMAS)—for use in this study:

- Type SP-9.5 mix of granite with NMAS of 9.5 mm ➔ Referred to as "GA9.5"
- Type SP-12.5 mix of granite with NMAS of 12.5 mm ➔ Referred to as "GA12.5"
- Type SP-9.5 mix of limestone with NMAS of 9.5 mm ➔ Referred to as "LS9.5"
- Type FC-12.5 mix of limestone with NMAS of 12.5 mm ➔ Referred to as "LS12.5"

The first three mixtures were designed as structural courses while the fourth mixture was designed as friction course for use with traffic level of C by FDOT.

Table 3-2 presents the JMF and bin-to-bin percentages of different types and subtypes aggregates as used in the four types of FDOT-provided control mix designs. As evident from the table, the mixtures of granite aggregates were made of coarser subtypes such as C47 (S1A Stone) and C53 (S1B Stone), and finer subtypes such as F22 (screenings), F23 (screenings) and sand. Likewise, the mixtures of limestone aggregates were made of coarser subtypes such as C41 (S1A Stone), C51 (S1B Stone) and C54 (S1B Stone), and finer subtypes such as F22 (screenings).

Table 3-2. Job Mix Formula of Aggregates: Original

Parameter	Sieve (Size)	GA9.5	GA12.5	LS9.5	LS12.5
JMF (Cum. passing % by total weight of aggregates)	¾" (19.0 mm)	100.0	100.0	100.0	100.0
	½" (12.5 mm)	100.0	100.0	100.0	97.0
	3/8" (9.5 mm)	100.0	89.0	99.0	87.0
	#4 (4.75 mm)	77.0	68.0	80.0	60.0
	#8 (2.36 mm)	54.0	52.0	49.0	44.0
	#16 (1.19 mm)	42.0	41.0	36.0	34.0
	#30 (0.60 mm)	32.0	32.0	29.0	27.0
	#50 (0.30 mm)	19.0	16.0	22.0	20.0
	#100 (0.15 mm)	9.0	8.0	8.0	9.0
	#200 (0.075 mm)	5.5	5.1	3.8	4.0
Aggregate Subtype Proportion (%by total weight aggregates)	C47: S1A Stone	0.0	27.0	0.0	0.0
	C53: S1B Stone	36.0	14.0	0.0	0.0
	F22: Screenings	34.0	25.0	0.0	0.0
	F23: Screenings	15.0	14.0	0.0	0.0
	Sand	15.0	20.0	0.0	0.0
	C41: S1A Stone	0.0	0.0	0.0	20.0
	C51: S1B Stone	0.0	0.0	20.0	35.0
	C54: S1B Stone	0.0	0.0	35.0	0.0
	F22: Screenings	0.0	0.0	45.0	45.0
Bulk Specific Gravity, G_{sb}	-	2.727	2.726	2.487	2.461

The aggregates were not subjected to any other tests except washed sieve analysis. The tests were required to verify their compliance with the FDOT-provided JMF of control

mixtures and with the requirements specified in Section 334-3.2.2 (FDOT, 2019). For these tests, unwashed batches of aggregates were prepared for each mix type following the FDOT-provided mix design, which were then washed, oven-dried and sieve-analyzed.

Test results showed that the gradations of washed and oven-dried batches and the JMF differed from each other more significantly in limestone than granite mixtures, sometimes by more than 1.0% in coarse aggregates and by more than 0.5% in fine aggregates, due to higher percentage loss of fines in limestone than in granite during washing. Therefore, the gradations were adjusted such that the final gradations of washed and oven-dried batches would meet FDOT-provided JMFs. Table 3-3 present the adjusted, unwashed gradations and bulk specific gravities of aggregates. As expected, the adjusted gradation satisfied the requirement for minimum passing percentage of aggregates at point control sieve (PCS) and could be still designated as fine-graded as specified in AASHTO M 323 (2017a) and referred to in Section 334-1.1:

- Percent Passing at PCS (sieve No. 4) for SP-9.5/FC-9.5 mixtures ≥ 47%
- Percent Passing at PCS (sieve No. 8) for SP-12.5/FC-12.5 mixtures ≥ 39%

Table 3-3. JMF of Aggregates: Adjusted

Parameter	Sieve (Size)	GA9.5	GA12.5	LS9.5	LS12.5
JMF (Cum. passing % by total weight of aggregates)	¾" (19.0 mm)	100.0	100.0	100.0	100.0
	½" (12.5 mm)	100.0	100.0	100.0	96.7
	3/8" (9.5 mm)	100.0	89.0	99.4	87.0
	#4 (4.75 mm)	77.0	68.0	80.3	61.3
	#8 (2.36 mm)	54.0	52.0	49.4	45.5
	#16 (1.19 mm)	42.0	41.0	36.4	35.8
	#30 (0.60 mm)	32.0	32.0	29.6	28.7
	#50 (0.30 mm)	19.0	16.0	22.1	21.1
	#100 (0.15 mm)	9.0	8.0	7.2	9.6
	#200 (0.075 mm)	5.5	5.1	1.1	2.2
Aggregate Subtype Proportion (% by total weight aggregates)	C47: S1A Stone	0.0	26.0	0.0	0.0
	C53: S1B Stone	34.0	13.0	0.0	0.0
	F22: Screenings	36.0	27.0	0.0	0.0
	F23: Screenings	15.0	14.0	0.0	0.0
	Sand	15.0	20.0	0.0	0.0
	C41: S1A Stone	0.0	0.0	0.0	18.0
	C51: S1B Stone	0.0	0.0	18.0	32.0
	C54: S1B Stone	0.0	0.0	29.0	-
	F22: Screenings	0.0	0.0	53.0	50.0
Bulk Specific Gravity, G_{sb}	-	2.726	2.725	2.492	2.467

3.3 Liquid ASA

Four different types of liquid ASA were used in this project as recommended by FDOT. They are randomly referred to as L1, L2, L3 and L4 in this report. The first three liquid ASA (i.e., L1, L2 and L3) were used at 0.50% by weight of asphalt binder and the fourth liquid ASA (i.e., L4) was used at 0.40% by weight of asphalt binder as recommended by the APL (see https://fdotwp1.dot.state.fl.us/ApprovedProductList/ProductTypes/Index/2). According to FDOT, there were isolated instances where mixtures containing two of the four liquid ASA exhibited stability issues.

Because of proprietary nature of these products, only limited information (color, physical state, odor, viscosity, density, specific gravity, flash point, water solubility, etc.) was publicly available about the physical and chemical properties of these liquid ASA in their safety data sheets. This information did not indicate the way these ASAs would impact the properties of binders and mixtures in terms of stability.

3.4 Mix Design Verification

The mix design verification involved the compaction of control mixtures until N_{design} and verification of $\%G_{mm}$ and $\%Va$ values with the requirements specified in AASHTO M 323-12 (2017a) in accordance to Section 334-3.2.2 (FDOT, 2019).

For this verification, mix design samples of GA9.5, GA12.5, LS9.5 and GA12.5 mixtures were prepared without using any liquid ASA (i.e., control mixtures) and used to measure their volumetric properties at N_{design} through a series of steps as described below:

- Batching:

  Batches of aggregates were first prepared using the adjusted JMF and then heated overnight at FDOT-specified mixing temperature of 166ºC (330°F) in an oven. The PMA binder, bucket and paddle mixer and other mixing tools were heated at least 2 hours at the mixing temperature of 166ºC (330°F) prior to mixing.

- Mixing:

  The pre-heated aggregates were mixed with the pre-heated binders using a bucket and paddle mixer until aggregates were thoroughly coated with binder. FDOT-provided binder contents ($\%Pb$) were used in these mixtures, i.e., 5.6%, 5.3%, 6.6% and 6.3% by weight of GA9.5, GA12.5, LS9.5 and LS12.5 mixtures, respectively.

- Aging:

  The freshly prepared loose mixtures were spread in a pan and heated at 166ºC (330°F) for 2 hours to simulate short-term oven aging following AASHTO R 30 (2014d). The aged loose mixture sample was then separated into two parts—one part for measuring G_{mm} and the other part for compacting gyratory compacted samples and measuring bulk specify gravity (G_{mb}).

- SGC Compaction:

  The short-term oven-aged loose mixtures were compacted into cylindrical samples, each measuring 150.0 mm (5.91 in.) in diameter, until design number of gyrations (N_{design} = 75 gyrations) by applying a normal stress of 600.0 kPa (87.0 psi) at an internal angle of 1.25 degrees using a Superpave gyratory compactor following the AASHTO T 312 (2015). [Note: The samples prepared to extract stability parameters from data collected during compaction were compacted until N_{max} number of gyrations and samples prepared to extract parameters from tests conducted after partial or complete cooling were compacted until the target height dictated by selected test method as described in Chapters 4 and 5.]

- G_{mm} Testing:

  The short-term oven-aged loose mixtures was cooled down to laboratory temperature and separated into two equal specimens. Each specimen was then subjected to the Florida Method of Test for Maximum Specific Gravity of Asphalt Paving Mixtures, FM 1-T 209 (FDOT, 2017). FDOT-specified acceptable range of G_{mm} from a single operator ($\leq$ 0.013) was used to accept the results obtained from these tests or redo the tests.

- G_{mb} Testing:

  The SGC samples were allowed to cool down to laboratory temperature overnight and subjected to the Florida Method of Test for Bulk Specific Gravity of Compacted Asphalt Specimens, FM 1-T 166 (FDOT, 2016). FDOT-specified acceptable range of G_{mb} from a single operator ($\leq$ 0.011) was used to accept the results obtained from these tests or redo the tests.

Table 3-4 presents volumetric properties of control mixtures (i.e., GA9.5-C0, GA12.5-C0, LS9.5-C0 and LS12.5-C0 mixtures at N_{design}, where C0 stands for mixtures prepared with control binder. Test results showed that all but LS12.5 did not meet the 4.0% air void content by volume criterion. Therefore, the binder content in LS12.5 was reduced from 6.3% to 6.0% by weight with approval from FDOT. The adjusted LS12.5 mix satisfactorily satisfied the 4.0 ± 0.5% air void content (i.e., 96 ± 0.5%G_{mm}) criterion (see Table 3-4). Test results also showed that both G_{mm} and G_{mb} values satisfy FDOT-specified ranges allowed from a single operator. The table also presents the resultant values of effective specific gravity of aggregates (*Gse*), void in mineral aggregates (*VMA*) and voids filled with asphalt (*VFA*).

Table 3-4. Characteristics of Mix Design Samples: Control Mixtures

Parameter	Criteria		GA9.5 C0	GA12.5 C0	LS9.5 C0	LS12.5 C0	
	SP/FC-9.5	SP/FC-12.5				Original	Adjusted
%Pb	-	-	5.6	5.3	6.6	6.3	6.0
G_{sb}	-	-	2.725	2.725	2.492	2.461	2.467
G_{se}	-	-	2.788	2.764	2.588	2.577	2.582
G_{mm}	-	-	2.545	2.538	2.353	2.354	2.368
G_{mm} ***(Range)***	0.013	0.013	0.007	0.010	0.009	0.006	0.004
G_{mb}	-	-	2.432	2.438	2.249	2.277	2.270
G_{mb} ***(Range)***	0.011	0.011	0.001	0.012	0.003	0.003	0.005
%Va	4 ± 0.5	4 ± 0.5	4.4	3.9	4.4	3.3	4.1
%VMA	≥15.0	≥14.0	15.8	15.3	15.7	13.3	13.5
%VFA	73-76	65-75	72	74	72	75	69

3.5 Summary

The following materials were obtained for use in this study:

- 1 type of binder [SBS-modified PG 76-22 polymer-modified asphalt (PMA) binder],
- 4 types of liquid ASA (obtained from two different sources).
- 2 types of aggregates (granite from Georgia and limestone from Southeast Florida), and

Asphalt binder was subjected to PG verification tests. These tests showed that the control binder satisfied each requirement of PG 76-22 (PMA) binder as specified in Section 916-2 of FDOT's Standard Specifications for Road and Bridge Construction (FDOT, 2019). Liquid ASA were not subjected to any tests in this part of the experimental plan. Aggregates were batched and sieve-analyzed to check their compliance with FDOT-provided mix design gradations: two per each aggregate type (Type SP/FC-9.5 and Type SP/FC-12.5 mixes). Test results showed that washed gradation and JMF differed more in granite than in limestone. Adjustments were made accordingly to meet the target JMF.

Furthermore, control mixtures were compacted until FDOT-specified design number of gyrations (herein, 75) in accordance with AASHTO T 312 (2015) and their compliance with the requirement of 4.0 ± 0.5% air void content by volume were verified according to AASHTO M 323 (2017a) and Section 334-3.2.4 of FDOT's Specifications (FDOT, 2019). Test results showed that all but one control mixture satisfied this requirement, thereby allowing the use of the same optimum binder content as mentioned in the control mix designs in the mixtures that satisfied this requirement, while slight reduction in the optimum asphalt binder content in the mixture that did not meet this requirement.

4 PARAMETERS OBTAINED FROM COMPACTION DATA

4.1 Gyratory Compaction Tests

For this part of the experimental plan, a total of four control mixtures (4 mix designs × 1 PMA) and 16 liquid ASA-treated mixtures (4 mix designs × 4 liquid ASAs × 1 PMA) were prepared. The liquid ASA-treated mixtures were prepared with one extra step than those mentioned in Section 3.4 of Chapter 3. This step included the treatment of PG76-22 (PMA) binder with the APL-specified dosage of selected liquid ASA at 166°C (330°F) prior to mixing asphalt binder and aggregates together. As such, a total of 5 types of binders were produced:

- Asphalt binders
  - SBS-modified PG 76-22 (PMA) = PMA (C*ontrol Binder*)
  - PMA binder + 0.5% L1 by weight of binder = PMA + L1
  - PMA binder + 0.5% L2 by weight of binder = PMA + L2
  - PMA binder + 0.5% L3 by weight of binder = PMA + L3
  - PMA binder + 0.4% L4 by weight of binder = PMA + L4

Using these 5 combinations of binders (1 control + 4 liquid ASA-treated binders), 20 different mixtures were prepared for this part of the experimental plan. These included 1 control (denoted with the suffix "C0") and 4 four liquid ASA-treated samples (mixtures denoted with the suffix "L*x*", where *x* = 1, 2, 3 and 4) from each of the four mix designs (4 mix designs × 5 binder combinations) as listed below:

- Granite SP-9.5 mixtures:
  - Granite Aggregates + 5.6% (PMA) = GA9.5 + C0 *(Control Mix)*
  - Granite Aggregates + 5.6% (PMA + L1) = GA9.5 + L1
  - Granite Aggregates + 5.6% (PMA + L2) = GA9.5 + L2
  - Granite Aggregates + 5.6% (PMA + L3) = GA9.5 + L3
  - Granite Aggregates + 5.6% (PMA + L4) = GA9.5 + L4
- Granite SP-12.5 mixtures:
  - Granite Aggregates + 5.3% (PMA) = GA12.5 + C0 *(Control Mix)*
  - Granite Aggregates + 5.3% (PMA + L1) = GA12.5 + L1
  - Granite Aggregates + 5.3% (PMA + L2) = GA12.5 + L2
  - Granite Aggregates + 5.3% (PMA + L3) = GA12.5 + L3
  - Granite Aggregates + 5.3% (PMA + L4) = GA12.5 + L4
- Limestone SP-9.5 mixtures:
  - Limestone Aggregates + 6.6% (PMA) = LS9.5 + C0 *(Control Mix)*
  - Limestone Aggregates + 6.6% (PMA + L1) = LS9.5 + L1
  - Limestone Aggregates + 6.6% (PMA + L2) = LS9.5 + L2
  - Limestone Aggregates + 6.6% (PMA + L3) = LS9.5 + L3
  - Limestone Aggregates + 6.6% (PMA + L4) = LS9.5 + L4

- Limestone FC-12.5 mixtures:
  - Limestone Aggregates + 6.0% (PMA) = LS12.5 + C0 *(Control Mix)*
  - Limestone Aggregates + 6.0% (PMA + L1) = LS12.5 + L1
  - Limestone Aggregates + 6.0% (PMA + L2) = LS12.5 + L2
  - Limestone Aggregates + 6.0% (PMA + L3) = LS12.5 + L3
  - Limestone Aggregates + 6.0% (PMA + L4) = LS12.5 + L4

The production of the SGC samples involved a series of steps as descried in Section 3.4 of Chapter 3: (a) blending asphalt binder with the APL-specified dosage of selected liquid ASA at 166ºC (330°F), (b) preheating aggregates and binders at 166ºC (330°F), (c) mixing pre-heated aggregates with treated or untreated asphalt binder at 166ºC (330°F) using a bucket and paddle mixer, (d) aging the freshly-prepared loose mixtures at 166ºC (330°F) in an oven for 2 hours, and (e) compacting the oven-aged loose mixtures at 166ºC (330°F) to cylindrical SGC specimens until certain number of gyrations (i.e., 115 gyrations for this part of the experimental plan) or certain height (i.e.,75.0 mm for APA, 115.0 for CAL tests, 63.5 mm for HWT, M_r and IDEAL shear rutting tests for next part of the experimental plan). FDOT's test methods FM 1-T 209 (FDOT, 2017) and FM 1-T 166 (FDOT, 2016) were used to measure the G_{mm} values of the 2-hour aged loose mixtures and the G_{mb} values of the SGC specimens, respectively as stated previously. The mass of the asphalt mixture required in each SGC specimen was determined such that the compacted height would be within 115 ± 5 mm at the completion of compaction. For this part of the experimental plan, the samples were compacted until $N_{\max}$ number of gyrations (i.e., 115) instead of only until design number of gyrations (i.e., 75) to be able to obtain all potential stability-related parameters as identified in literature review (see Chapter 2). The compaction data (i.e., stress, height and number of gyration) obtained from each specimen was used to extract these parameters.

Table 4-1 to Table 4-4 present the volumetric properties of compacted GA9.5, GA12.5, LS9.5 and LS12.5 control mixtures at N_{design}: asphalt binder content ($\%Pb$), bulk specific gravity of aggregates (G_{sb}), effective specific gravity of aggregates (G_{se}), average G_{mm} obtained from at least two specimens (G_{mm}), standard deviation of G_{mm} (G_{mm} *SD*), difference between maximum and minimum G_{mm} values (G_{mm} *Range*), standard deviation value of G_{mm} obtained from at least two specimens (G_{mm} *SD*), average G_{mb} obtained from at least two specimens (G_{mb}), difference between maximum and minimum G_{mb} values (G_{mb} *Range*), air void content (%Va or *AV*), voids in mineral aggregates (*VMA*), voids filled with asphalt (*VFA*), and dust proportion (*DP*). Note that:

$$Gmb \text{ at } N_{design} = Gmb \text{ at } N_{max} \times \left(\frac{Height\ at\ N_{max}}{Height\ at\ N_{design}} \right) \qquad 4\text{-}1$$

Test results showed that C0, L1 and L2 mixtures always satisfied the volumetric criteria specified at N_{design} as mentioned in AASHTO M 323 (2017a); however, L3 and L4 mixtures did not always satisfy these criteria, hinting differences in compaction behaviors of mixtures produced with these two liquid ASAs.

Table 4-1. Characteristics of GA9.5 Samples at N = 75 Gyrations

Parameter	Criteria	C0	L1	L2	L3	L4
%Pb	-	5.6	5.6	5.6	5.6	5.6
G_{sb}	-	2.725	2.726	2.726	2.726	2.726
G_{se}	-	2.788	2.803	2.791	2.786	2.792
G_{mm}	-	2.545	2.557	2.547	2.544	2.548
G_{mm} SD	0.00449	0.00274	0.00387	0.00556	0.00476	0.00461
G_{mm} Range	0.013	0.007	0.008	0.011	0.010	0.009
G_{mb}	-	2.432	2.458	2.449	2.465	2.473
G_{mb} Range	0.011	0.001	0.004	0.004	0.004	0.002
%Va	4.0	4.4	3.9	3.9	3.1	3.0
%VMA	≥15.0	15.8	14.9	15.2	14.6	14.4
%VFA	73-76	71.8	74.1	74.7	78.9	79.4
DP	06-1.2	1.1	1.2	1.2	1.1	1.2

Table 4-2. Characteristics of GA12.5 Samples at N = 75 Gyrations

Parameter	Criteria	C0	L1	L2	L3	L4
%Pb	-	5.3	5.3	5.3	5.3	5.3
G_{sb}	-	2.725	2.725	2.725	2.725	2.725
G_{se}	-	2.764	2.786	2.763	2.777	2.755
G_{mm}	-	2.538	2.555	2.537	2.548	2.530
G_{mm} SD	0.00449	0.00346	0.00600	0.00428	0.00209	0.00887
G_{mm} Range	0.013	0.010	0.012	0.009	0.004	0.013
G_{mb}	-	2.438	2.461	2.444	2.477	2.470
G_{mb} Range	0.011	0.012	0.004	0.004	0.006	0.010
%Va	4.0	3.9	3.7	3.6	2.8	2.4
%VMA	≥14.0	15.3	14.5	15.1	13.9	14.2
%VFA	65-75	74.4	74.5	75.8	80.1	83.2
DP	06-1.2	1.1	1.1	1.1	1.1	1.0

Table 4-3. Characteristics of LS9.5 Samples at N = 75 Gyrations

Parameter	Criteria	C0	L1	L2	L3	L4
%Pb	-	6.6	6.6	6.6	6.6	6.6
G_{sb}	-	2.492	2.492	2.492	2.492	2.492
G_{se}	-	2.588	2.594	2.593	2.587	2.591
G_{mm}	-	2.353	2.357	2.357	2.352	2.355
G_{mm} SD	0.00449	0.00457	0.00427	0.00078	0.00540	0.00418
G_{mm} Range	0.013	0.009	0.009	0.002	0.011	0.008
G_{mb}	-	2.249	2.270	2.263	2.262	2.258
G_{mb} Range	0.011	0.003	0.000	0.001	0.001	0.000
%Va	4.0	4.4	3.7	4.0	3.8	4.2
%VMA	≥15.0	15.7	14.9	15.2	15.2	15.4
%VFA	73-76	71.8	75.1	73.7	74.9	73.0
DP	06-1.2	0.7	0.7	0.7	0.7	0.7

Table 4-4. Characteristics of LS12.5 Samples at N = 75 Gyrations

Parameter	Criteria	C0	L1	L2	L3	L4
%Pb	-	6.0	6.0	6.0	6.0	6.0
G_{sb}	-	2.467	2.467	2.467	2.467	2.467
G_{se}	-	2.582	2.581	2.579	2.583	2.576
G_{mm}	-	2.368	2.367	2.365	2.369	2.364
G_{mm} SD	0.00449	0.00184	0.00383	0.00335	0.00257	0.00583
G_{mm} Range	0.013	0.004	0.008	0.007	0.005	0.012
G_{mb}	-	2.270	2.274	2.278	2.280	2.297
G_{mb} Range	0.011	0.005	0.003	0.001	0.004	0.002
%Va	4.0	4.1	3.9	3.7	3.7	2.8
%VMA	≥14.0	13.5	13.3	13.2	13.1	12.5
%VFA	65-75	69.4	70.7	72.0	71.5	77.4
DP	06-1.2	0.9	0.9	0.9	0.9	0.9

The literature review revealed several parameters that could be extracted form compaction data and used to describe asphalt mixture stability during/after construction. The following sections briefly reintroduce these parameters and evaluate the effectiveness of these parameters in differentiating liquid ASA in terms of the stability of asphalt mixtures produced with liquid ASA-treated asphalt binders.

4.1.1 Compacted Density Parameters

Literature showed that the degree of compaction is one of the parameters used to describe asphalt mixture compactability and stability. The degree of compaction (*C*) can be expressed in terms of relative density (%G_{mm}) achieved after certain compaction effort. Since same vertical stress and same internal angle are used at each gyration, compaction effort can be also defined in terms of number of gyrations, *N* (Cominsky et al., 1994; McGennis, 1997; Button et al., 2005; Bennert et al., 2010; Ling et al., 2013).

In this study, seven different compacted density parameters extracted at pre-defined number of gyrations were used to evaluate the effect of liquid ASA on asphalt mixture stability (see Figure 4-1):

$$CN = \%Gmm_N = \left(\frac{Gmb_N}{Gmm}\right) x\ 100\% \quad \text{4-2}$$

where,

$$Gmb_N = Gmb_{N_{\text{design}}} \times \left(\frac{h_{N_{\text{design}}}}{h_N}\right) \quad \text{4-3}$$

where,

N =1 (uncompacted), 7 (N_{initial} or Ni), 8 (Bahia et al., 1998), 10 (Cominsky et al., 1994), 75 (N_{design} or Nd), 100 (Bennert et al., 2010) or 115 (N_{max} or Nm)

$Gmb_{N_{\text{design}}}$ = Bulk specific gravity at N_{design}

$h_{N_{\text{design}}}$ = Compacted height at N_{design}

h_N = Compacted height at *N*

In confined compaction such as gyratory compaction, same number of gyrations can compact tender mixtures to a higher relative density (or less air void level) than their counterparts:

$CN_{\text{unstable}} > CN_{\text{stable}}$

where,

$N_{\text{unstable}} = N_{\text{stable}}$

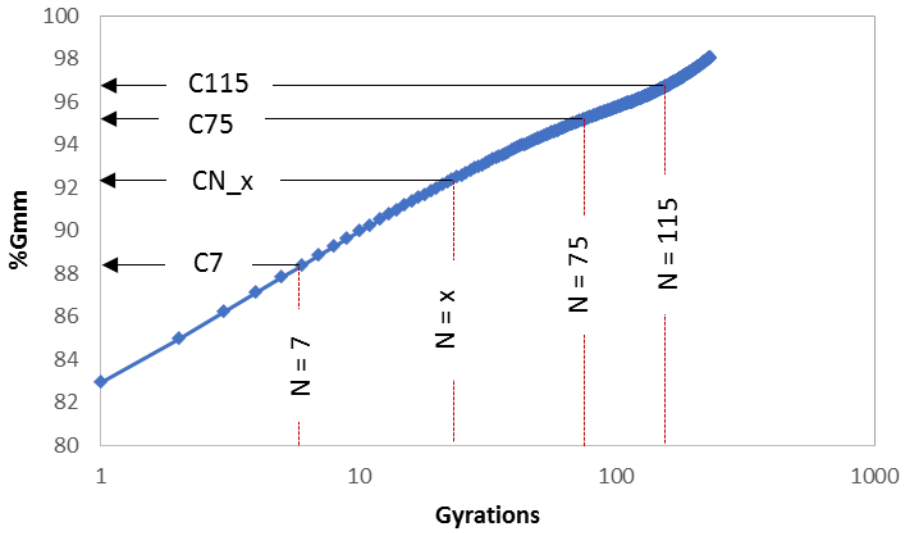

Figure 4-1. Illustration of Compacted Density Parameters

Similarly, the degree of compaction can be also defined in terms of %G_{mm} at the first instance of 0.05 mm or less change in compacted height for three consecutive gyrations during compaction. This condition refers to development of significant amount of shear resistance as result of interlocking of aggregate particles and is fittingly referred to as locking point (*LP*). After reaching locking point, the samples show minimal change in height or volume even with incessant application of compaction effort or gyrations (Vavrik and Carpenter, 1998).

CN_{LP} = %G_{mm} at the first number of gyrations with $\Delta h \leq 0.05$ mm

Likewise, the degree of compaction was also defined in terms of %G_{mm} measured at the first instance of 0.001% or less change in the slope of air void between two consecutive gyrations during compaction. The number of gyrations corresponding to this condition is referred to as N_{G1} (Abu Abdo et al., 2010; Bahia et al., 1998; Bayomy and Abu Abdo, 2006; Dessouky et al., 2003, 2004; Mohammad and Al Shamsi, 2007).

CN_{G1} = %Gmm at the first number of gyrations with $\Delta\left(\frac{dVa}{dN}\right) \leq 0.001\%$

In lieu of relative density (%G_{mm}), the degree of compaction can be alternatively defined in terms of the air void content measured at the selected number of gyrations such as *N* = 7, 75, 100, and 115 (Bennert et al., 2010):

$$AVN = \left(\frac{Gmm - Gmb_N}{Gmm}\right) \times 100\% \qquad 4\text{-}4$$

Furthermore, the degree of compaction can be also defined in terms of %G_{mm} measured at maximum shear stress (Butcher, 1998; De Sombre et al., 1998) and maximum ratio of shear stress and normal stress, aptly defined as shear stress ratio or normalized maximum shear stress (Anderson et al., 2002; Newcomb et al., 2015):

$C\tau_{\max}$ = $\%G_{mm}$ at $N_{\tau_{\max}}$

$CSR_{\max}$ = $\%G_{mm}$ at $N_{SR_{\max}}$

where,

$N_{\tau_{\max}}$ = Number of gyrations at $\tau_{\max}$

$N_{SR_{\max}}$ = Number of gyrations at $SR_{\max}$

$\tau_{\max}$ = Maximum shear stress

$SR_{\max} = \frac{\tau_{\max}}{\sigma}$

σ = Normal or vertical stress

In this study, 11 different compacted density parameters ($C1$, $C7$, $C8$, $C10$, $C75$, $C100$, $C115$, CLP, $CNG1$, $C\tau_{\max}$, and $CSR_{\max}$) were selected to evaluate the effect of liquid ASA on asphalt mixture stability. Unless otherwise stated, their values are in percentages.

4.1.2 Compaction Effort Parameters

Since same normal stress and same internal angle are used in each gyration, compaction effort could be defined in terms of total number of gyrations, N required to compact asphalt mixture samples to certain degree of compaction, $\%G_{mm}$ (Mallick, 1999; Bennert et al., 2010; Ling et al., 2013), which can be expressed as:

N_x = No. of gyrations required to reach $x\%$ G_{mm}

where,

x = 87, 92, 93, 95, 96, and 98 (see Figure 4-2)

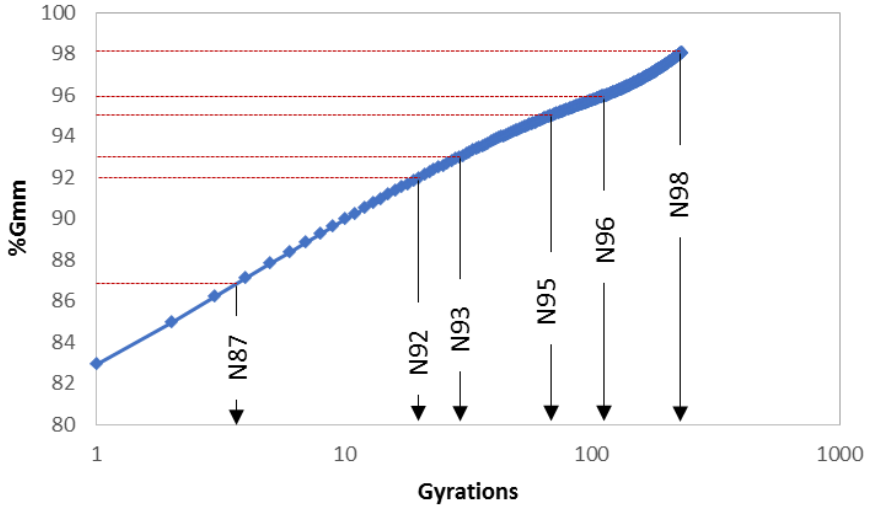

Figure 4-2. Illustration of Compaction Effort Parameters

In a confined volume, unstable mixtures require fewer number of gyrations (or less compaction effort) than stable mixtures to be compacted to same degree of compaction:

$Nx_{\text{unstable}} > Nx_{\text{stable}}$ to reach same $\%Gmm$

The compaction effort (i.e., number of gyrations) required to achieve different compaction densities or air voids (i.e., $\%G_{mm}$ or $\%Va$) were furthermore used to extract parameters such as the effective number of gyrations (ΔN), the gyration ratios (GR) (Mallick, 1999), the logarithmic gyration ratios ($GR_{\log}$) (Anderson et al., 2002), and the compaction rate (CR) (Bennert et al., 2010) that could evaluate the effect of liquid ASA on asphalt mixture stability:

$$\Delta N = N_b - N_a \tag{4-5}$$

where,

N_a = 7 (N_{initial} or Ni), $N92$, $NG1$, NLP, $N96$, and 75 (N_{design} or Nd)

N_b = 75 (N_{design} or Nd), $N96$, $N98$, and 115 ($N_{\max}$ or Nm)

$$GR_{9895} = \frac{N98}{N95} \tag{4-6}$$

$$GR_{9896} = \frac{N98}{N96} \tag{4-7}$$

$$GR_{log9692} = \frac{logN96}{logN92} \tag{4-8}$$

$$GR_{log9895} = \frac{logN98}{logN95} \tag{4-9}$$

$$GR_{log9896} = \frac{logN98}{logN96} \tag{4-10}$$

$$CR = \frac{h93}{N93} \tag{4-11}$$

where,

$h93$ = Compacted height at 93%G_{mm}

Similarly, compaction effort (i.e., the number of gyrations) required to compact asphalt mixtures to the certain volumetric conditions such as the locking point, NLP and $NG1$ was also used to evaluate the effect of liquid ASA on asphalt mixture stability:

NLP = the first number of gyrations that yields $\Delta h \leq 0.05$ mm

$NG1$ = the first number of gyrations that yields $\Delta\left(\frac{dVa}{dN}\right) \leq 0.001\%$

Additionally, compaction effort (i.e., the number of gyrations) that corresponds to the instance of the maximum shear stress, $\tau_{\max}$ and maximum shear stress ratio, $SR_{\max}$ can be also used to evaluate the effect of liquid ASA on asphalt mixture stability:

$N\tau_{\max}$ = Number of gyrations at $\tau = \tau_{\max}$

$NSR_{\max}$ = Number of gyrations at $SR = SR_{\max}$

As such, a total of 31 different compaction effort parameters ($11 \times N + 14 \times \Delta N + 5 \times GR + 1 \times CR$) were extracted in this study to evaluate the effect of liquid ASA on asphalt mixture stability.

4.1.3 Compaction Rate Parameters

Literature review showed that the rate of change in relative density or air void content (%G_{mm} and $\%Va$) during compaction could be also used to extract parameters that can evaluate the behavior of asphalt mixtures during compaction. As such, %G_{mm} and $logN$ data until 92%G_{mm} were fitted with a linear function ($\%Gmm = \%Gmm_0 + k \times logN$) and used to extract parameters such as and the rate of change in %G_{mm} (i.e., compaction slope, k) including the initial degree of compaction (P_o) (see Figure 4-3). These parameters were furthermore processed to determine the values of other parameters such as porosity index (PI) (Cominsky et al., 1994; McGennis, 1997; Anderson and Bahia, 1997; Button et al., 2005) and workability index ($k \times AV_{N_{\text{design}}}$) (Anderson et al., 2002):

$$k \times AV_{N_{design}} = k \times AV75 \quad \text{4-12}$$

$$PI = \frac{1}{P_o} \quad \text{4-13}$$

where,

k = Slope = $\left|\frac{92\% - \%Gmm_0}{log(N92)}\right|$

P_o = Intercept = $\%Gmm_o$

$N92$ = Number of gyrations at 92%Gmm

$AV75$ = Air void content at 75 gyrations

Similarly, the air void content (AV or $\%Va$) and $logN$ data until 92%G_{mm} were also fitted with similar linear functions ($\%AV = c + m \times logN$) and used to extract parameters such as the rate of change in air void content (m) including the uncompacted air void content (c), which were furthermore utilized to determine the laboratory compaction index (LCI), or simply compaction index (CI) parameter (Kaseem et al., 2012):

$$CI = \frac{m^{1.2}}{c} \quad \text{4-14}$$

where,

m = Slope = $\left|\frac{8\%-c}{log(N92)}\right|$

c = Intercept = $\%AV_0$

$N92$ = Number of gyrations at 92%G_{mm}

In a confined volume, unstable mixtures take fewer number of gyrations to be compacted to 92%G_{mm} than stable mixtures, i.e.,

$$N92_{\text{unstable}} < N92_{\text{stable}}$$

$$k_{\text{unstable}} > k_{\text{stable}}$$

$$m_{\text{unstable}} > m_{\text{stable}}$$

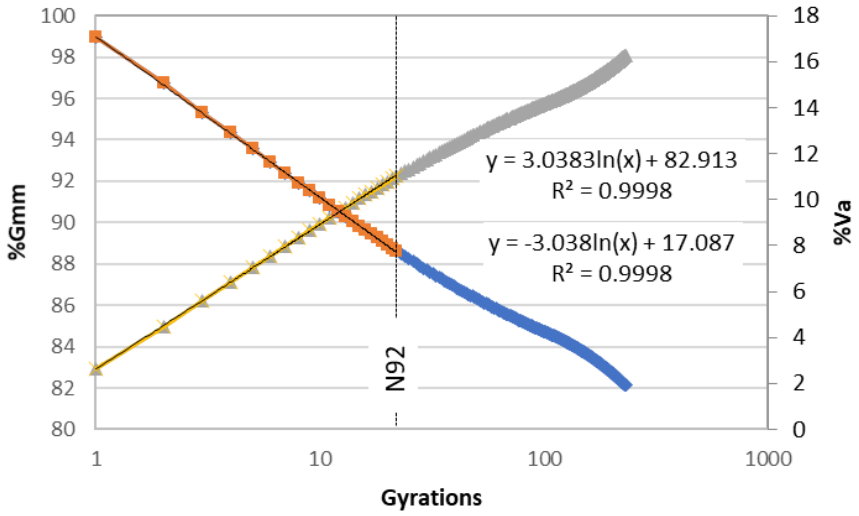

Figure 4-3. Illustration of Compaction Slope Parameters

As such, 7 different compaction-slope related parameters (2 × slopes + 2 intercepts + 3 × related others) were extracted in this study to evaluate the effect of liquid ASA on asphalt mixture stability.

4.1.4 Densification Indices

Literature review revealed that densification (%G_{mm} versus N) data can be separated in two parts using several criteria (see Figure 4-4) and used to extract parameters that are related to effort required to change relative density from one level to another. Based on this review, the first part of the data is related to the effort required to compact loose mixtures with significant amount of change in compacted height or volume. In this part of the compaction, the aggregates are still interlocking and therefore able to provide only the minimal amount of shear resistance. This part is used to extract parameters that mainly describe the workability/compactability of mixtures during construction such as construction densification index, *CDI* and workability index, *WI* (Bahia et al., 1998; Mohammad and Al Shamsi, 2007):

$$CDI_{N_aN_b} = \sum_{N_a}^{N_a} \Delta(\%Gmm)_N \quad 4\text{-}15$$

$$WI_{N_aN_b} = \frac{CDI_{N_aN_b}}{N_b - N_a} \quad 4\text{-}16$$

where,

$N_a = 0$ or N_{initial}

$N_{\text{b}} = N92, N96, NG1, NLP$ or N_{design}

The second part of the $\%G_{mm}$ versus N data is primarily related to effort required to compact the loose mixture against shear strength provided by interlocked aggregates. In this part of the compaction, the aggregates have fully developed interlocking and therefore allow minimal amount of change in height due to increased shear resistance. This part is used to extract parameters that describe the compaction of mixtures after construction usually under traffic load. These parameters include the traffic densification index, *TDI* and traffic index, *TI* (Bahia et al., 1998; Mohammad and Al Shamsi, 2007):

$$TDI_{N_bN_c} = \sum_{N_b}^{N_c} \Delta(\%Gmm)_N \quad 4\text{-}17$$

$$TI_{N_bN_c} = \frac{TDI_{N_bN_c}}{N_c - N_b} \quad 4\text{-}18$$

where,

$N_{\text{b}} = N92, N96, NG1, NLP$ or N_{design}

$N_c = N96, N98, N_{\text{design}}$ or N_{max}

Since stability is a function of shear resistance, stability of asphalt mixtures is related to parameters obtained from the second part of the compaction data, *TDI* or *TI*. Ideally, unstable mixtures take smaller number of gyrations for the same level of compaction, and consequently have smaller *TDI* values than stable mixtures, i.e.:

$(N_c - N_b)_{\text{stable}} > (N_c - N_b)_{\text{unstable}}$ for same change in $\%G_{mm}$

$TDI_{\text{stable}} > TDI_{\text{unstable}}$ for same change in $\%G_{mm}$

Note: TTI researchers used several different criteria, including the ones reported in literature review (i.e., $N_b = N92, NG1, N96, NLP$ or N_{design}) to separate the compaction data into parts and determine corresponding parameters. As such, the prefixes *C* and *T* used for construction and traffic might not always correlate with compactability under roller compactors and traffic loads.

In total, 36 such parameters ($6 \times CDI + 6 \times WI + 12 \times TDI + 12 \times TI$) were extracted in this study to evaluate the effect of liquid ASA on asphalt mixture stability.

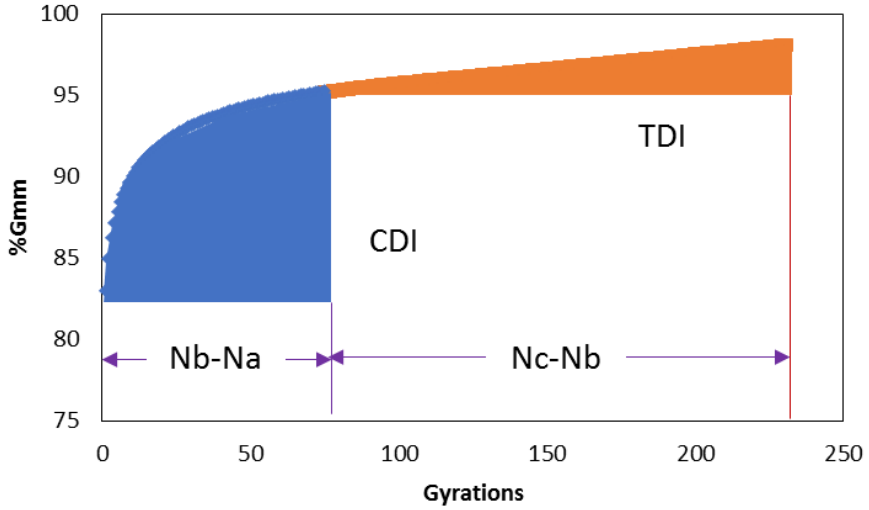

Figure 4-4. Illustration of Densification Indices

4.1.5 Compaction Energy Indices

Literature review also revealed that the energy required to compact asphalt mixtures from one height to another can be used to obtain parameters that are potentially related to asphalt mixture stability (Dessouky et al., 2013; Dessouky, 2015). Compaction energy, E is usually defined as:

$$\Delta E = \sigma \times \Delta V = \sigma \times A \times \Delta h = \sigma \times \left(\frac{\pi D^2}{4} \times \Delta h\right) \quad \text{4-19}$$

where,

σ = Normal or vertical stress

V = Change in compacted volume = $A \times \Delta h$

A = Cross-sectional area of compacted sample = $\frac{\pi D^2}{4}$

D = Diameter of compacted sample

Δh = Change in compacted height

Similar to $\%G_{mm}$ versus N data, the h versus N data can be divided into two parts for extracting two types of compaction energy parameters (see Figure 4-5). The first part can be used to determine the volumetric energy index, *VEI* and the workability energy index, *WEI*—the parameters that represent the energy required to compact asphalt mixtures against minimal shear resistance, usually characterized by a significant volumetric change:

$$VEI_{N_aN_b} = \sum_{N_a}^{N_b} \sigma \times \Delta V_N = \sigma \times \frac{\pi d^2}{4} \times \sum_{N_a}^{N_b} \Delta h_N \quad \text{4-20}$$

$$WEI_{N_aN_b} = \frac{VEI_{N_aN_b}}{N_b - N_a} \quad \text{4-21}$$

where,

$N_a = 0$ or N_{initial}

$N_{\text{b}} = N92, N96, NG1, NLP$ or N_{design}

The second part can be used to determine the shear energy index, *SEI* and compactability energy index, *CEI*—parameters that represent the energy required to compact asphalt mixtures against significant shear resistance, usually characterized by a minimal volumetric change:

$$SEI_{N_bN_c} = \sum_{N_b}^{N_c} \sigma \times \Delta V_N = \sigma \times \frac{\pi d^2}{4} \times \sum_{N_b}^{N_c} \Delta h_N \quad \text{4-22}$$

$$CEI_{N_bN_c} = \frac{SEI_{N_bN_c}}{N_c - N_b} \quad \text{4-23}$$

where,

$N_{\text{b}} = N92, N96, NG1, NLP$ or N_{design}

$N_c = N96, N98, N_{\text{design}}$ or N_{max}

Since stability is a function of shear resistance, stability of asphalt mixtures is related to parameters obtained from the second part of the compaction data, *SEI* or *CEI*. Ideally, unstable mixtures take smaller number of gyrations for the same level of compaction, and consequently have smaller *CEI* values than stable mixtures, i.e.:

$(N_c - N_b)_{\text{unstable}} < (N_c - N_b)_{\text{stable}}$ for same change in $\%G_{mm}$

$CEI_{\text{unstable}} > CEI_{\text{stable}}$ for same change in $\%G_{mm}$

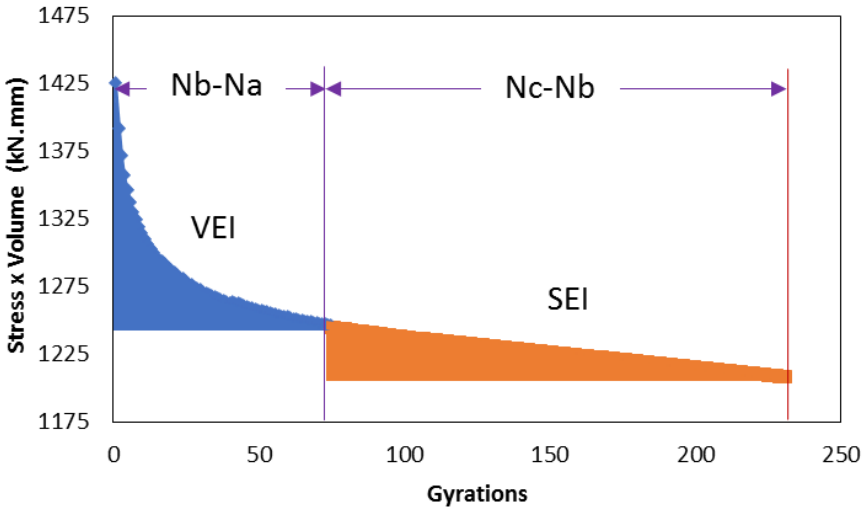

Figure 4-5. Illustration of Compaction Energy Indices

Like densification indices, researchers used five different criteria, including the ones reported in literature review to separate the compaction data into two parts and determine corresponding energy indices. In total, 36 such indices ($6 \times VEI + 6 \times WEI + 12 \times SEI + 12 \times CEI$) were extracted in this study to evaluate the effect of liquid ASA on asphalt mixture stability.

4.2 Data Analysis

The effectiveness of each parameter was evaluated in terms of its ability to distinguish the liquid ASA-treated mixtures that were equivalent to control mixtures from the liquid ASA-treated mixtures that were not equivalent to control mixtures. For this evaluation, the upper and lower limits of each parameter were determined for control (stable) and liquid ASA-treated mixtures, using:

$$UL_{C0} = y_{C0} + z \times d_{C0} \quad \text{4-24}$$

$$LL_{C0} = y_{C0} - z \times d_{C0} \quad \text{4-25}$$

$$UL_{Lx} = y_{Lx} + z \times d_{Lx} \quad \text{4-26}$$

$$LL_{Lx} = y_{C0} - z \times d_{Lx} \quad \text{4-27}$$

where,

UL = Upper limit of selected parameter

LL = Lower limit of selected parameter

y = Average value of selected parameter

d = Standard deviation value of selected parameter

$C0$ = Untreated, control (stable) mixture

Lx = Liquid ASA-treated mixture

z = 95% confidence level variate = 1.96

Based on normal distribution, the $y_{C0} \pm 1.96d_{C0}$ interval includes the values that are within 95% confidence level of average value. For each parameter, it was evaluated whether the $y_{Lx} \pm 1.96d_{Lx}$ intervals obtained from each liquid ASA-treated mixture were within $y_{C0} \pm 1.96d_{C0}$ interval obtained from control mixture.

If the $y_{Lx} \pm 1.96d_{Lx}$ intervals obtained from liquid ASA-treated mixtures were within $y_{\mathrm{C0}} \pm 1.96d_{\mathrm{C0}}$ interval obtained from control mixture, the liquid ASA-treated mixture would be considered equivalent to the control mixture in terms of stability (as stable as control mixture). However, if the $y_{C0} \pm 1.96d_{C0}$ interval obtained from liquid ASA-treated mixtures were outside the $y_{C0} \pm 1.96d_{C0}$ interval obtained from control mixture, the liquid ASA-treated mixture would be considered not equivalent (more stable or less stable) than control mixture. Whether these mixtures could be considered less stable or more stable were decided based on the physical meaning of the parameter as mentioned in Chapter 2.

According to FDOT, the mixtures prepared with L3 and L4 liquid ASA had isolated instances of stability issues while mixtures prepared with L1 and L3 liquid ASA did not have such issues. As such, the parameters that can distinguish unstable and stable mixtures should be able to show that L1 and L2 mixtures pass but L3 and L4 mixtures fail this test. Table 4-5 and Table 4-6 present the results of analysis conducted on 21 selected different parameters to equivalency of liquid ASA-treated and untreated GA9.5 and GA12.5 mixtures, respectively.

Table 4-7 to Table 4-11 present the results of analysis conducted on all 121 different parameters to check which parameters were within 95% confidence level of control mixtures. A value of one in these tables refers to mixtures that passed these tests and the values of zero indicate mixtures that failed these tests. As highlighted in the tables, only a few parameters could differentiate C0 (which can be assumed stable), L1 and L2 mixtures from L3 and L4 mixtures.

Table 4-5. Parameters Extracted from Compaction Data of GA9.5 Mixtures

Parameters	C0			L1 = C0?				L2 = C0?				L3 = C0?				L4 = C0?			
	y	y+2d	y-2d	y	y+2d	y-2d	Yes?	y	y+2d	y-2d	Yes?	y	y+2d	y-2d	Yes?	y	y+2d	y-2d	Yes?
N98-NG1	129.33	161.26	97.41	143.00	148.88	137.12	1	140.33	153.09	127.58	1	99.67	107.83	91.51	0	94.67	97.66	91.67	0
N98-NLP	98.67	124.69	72.64	119.67	127.59	111.75	0	116.00	134.70	97.30	0	77.67	82.60	72.73	1	70.67	81.46	59.87	0
CNG1	93.47	94.21	92.73	94.24	94.45	94.04	0	94.28	94.39	94.16	0	95.02	95.18	94.86	0	95.15	95.25	95.04	0
CLP	95.09	96.05	94.13	95.53	95.77	95.29	1	95.58	96.03	95.13	1	96.25	96.31	96.19	0	96.46	96.87	96.06	0
m	7.29	7.51	7.07	7.09	7.37	6.80	0	7.05	7.26	6.84	0	7.13	7.40	6.87	0	7.35	7.44	7.26	1
CI	62.08	66.37	57.80	64.46	66.19	62.74	1	64.56	66.09	63.02	1	67.96	69.41	66.51	0	69.70	69.85	69.54	0
TDI_NG1N96	54.09	73.33	34.85	34.93	40.61	29.24	0	34.61	39.29	29.93	0	15.29	19.03	11.55	0	12.43	14.30	10.56	0
TDI_NG1N98	124.26	155.89	92.63	138.15	143.70	132.59	1	135.56	147.80	123.32	1	96.60	104.45	88.75	0	91.81	94.69	88.94	0
TDI_NG1Nm	77.54	79.15	75.93	78.69	78.82	78.55	1	78.70	78.83	78.56	1	79.31	79.44	79.19	0	79.41	79.47	79.36	0
TDI_NLPN96	25.14	49.98	0.29	12.77	19.86	5.67	1	11.49	23.20	-0.21	0	5.77	7.65	3.88	1	10.59	20.59	0.59	1
SEI_N92N96	54.50	55.99	53.01	54.90	55.05	54.75	1	55.08	55.75	54.42	1	55.57	58.39	52.74	0	55.94	58.30	53.59	0
SEI_NG1N96	33.58	43.37	23.79	23.01	25.78	20.25	0	22.71	24.09	21.33	0	12.68	15.13	10.22	0	10.80	12.46	9.13	0
SEI_NG1N98	59.13	68.96	49.31	48.53	51.22	45.84	0	48.21	49.73	46.70	0	38.28	40.43	36.13	0	36.52	37.98	35.06	0
SEI_NG1Nm	42.38	49.79	34.96	35.45	36.75	34.14	0	35.38	36.42	34.35	0	34.65	35.54	33.75	0	34.04	35.01	33.07	0
SEI_NLPN98	37.21	49.67	24.74	31.46	34.61	28.31	1	30.95	36.84	25.05	1	22.17	22.96	21.37	0	19.34	24.59	14.10	0
CEI_N92N96	0.78	0.97	0.59	0.99	1.08	0.91	0	1.00	1.07	0.92	0	1.46	1.56	1.37	0	1.58	1.68	1.49	0
CEI_N92N98	0.57	0.70	0.43	0.50	0.51	0.48	1	0.51	0.54	0.47	1	0.67	0.70	0.63	0	0.70	0.73	0.67	0
CEI_NG1N96	0.59	0.64	0.55	0.63	0.66	0.59	0	0.63	0.67	0.58	0	0.79	0.85	0.74	0	0.83	0.84	0.82	0
CEI_NG1N98	0.46	0.64	0.29	0.34	0.35	0.33	1	0.34	0.36	0.32	1	0.38	0.40	0.37	1	0.39	0.39	0.38	1
CEI_NG1Nm	0.52	0.62	0.42	0.43	0.45	0.42	0	0.43	0.44	0.42	0	0.42	0.43	0.41	0	0.42	0.43	0.40	0
CEI_NLPN96	0.43	0.49	0.37	0.45	0.48	0.42	1	0.45	0.49	0.41	1	0.57	0.60	0.55	0	0.59	0.64	0.54	0

Note: 1 = Pass (Equivalent); 0 = Fail (Not Equivalent); Units of $N98\text{-}NG1$ and $N98\text{-}NLP$ = gyrations; Unit of $CNG1$ and CLP = %; Unit of m = %/gyrations; Unit of CI = None; Units of TDI, SEI and CEI = N.mm

Table 4-6. Parameters Extracted from Compaction Data of GA12.5 Mixtures

Parameters	C0			L1 = C0?				L2 = C0?				L3 = C0?				L4 = C0?			
	x	x+zd	x-zd	x	x+zd	x-zd	Yes?	x	x+zd	x-zd	Yes?	x	x+zd	x-zd	Yes?	x	x+zd	x-zd	Yes?
N98-NG1	123.33	159.06	87.60	141.67	152.81	130.52	1	140.33	145.27	135.40	1	84.67	101.10	68.23	0	60.67	86.69	34.64	0
N98-NLP	97.00	135.26	58.74	123.00	139.04	106.96	0	122.33	127.27	117.40	1	66.00	88.60	43.40	0	37.00	64.23	9.77	0
CNG1	94.10	94.82	93.38	94.55	94.73	94.38	1	94.63	94.81	94.46	1	95.52	95.77	95.28	0	95.91	96.32	95.51	0
CLP	95.41	96.22	94.61	95.54	96.00	95.08	1	95.58	95.73	95.43	1	96.49	96.97	96.01	0	97.07	97.53	96.61	0
m	6.65	7.18	6.11	6.39	6.52	6.26	1	6.37	6.50	6.24	1	6.53	6.63	6.42	1	6.48	6.74	6.22	1
CI	61.66	67.77	55.55	62.78	62.92	62.64	1	63.06	64.91	61.21	1	67.74	69.40	66.07	0	69.55	72.88	66.22	0
TDI_NG1N96	42.19	63.83	20.55	29.88	35.57	24.19	1	28.30	32.99	23.62	1	7.34	11.67	3.01	0	2.24	6.57	-2.10	0
TDI_NG1N98	118.83	153.84	83.82	137.01	147.70	126.31	1	135.75	140.40	131.10	1	82.19	98.11	66.28	0	58.95	84.18	33.72	0
TDI_NG1Nm	78.54	79.05	78.03	79.79	79.93	79.65	0	79.83	79.95	79.70	0	79.91	80.95	78.87	0	80.56	81.54	79.58	0
TDI_NLPN96	17.21	41.92	-7.51	12.13	24.61	-0.35	1	11.18	15.08	7.28	1	10.59	21.13	0.06	1	21.90	29.83	13.96	1
SEI_N92N96	55.34	56.65	54.03	56.82	57.76	55.87	0	55.65	57.82	53.47	0	55.69	58.27	53.11	0	58.97	62.53	55.42	0
SEI_NG1N96	25.04	34.81	15.27	18.94	21.42	16.46	1	18.04	20.43	15.65	1	6.05	9.28	2.81	0	2.09	5.76	-1.58	0
SEI_NG1N98	50.66	60.16	41.17	44.47	46.93	42.00	1	43.60	45.81	41.38	1	31.58	34.89	28.27	0	26.64	32.13	21.15	0
SEI_NG1Nm	38.08	45.16	30.99	32.63	33.18	32.07	1	32.19	32.89	31.50	1	31.13	31.76	30.50	0	31.11	31.78	30.43	0
SEI_NLPN98	33.03	43.45	22.62	31.44	37.54	25.34	1	31.01	32.98	29.03	1	18.99	25.35	12.63	0	11.62	17.75	5.50	0
CEI_N92N96	0.89	1.15	0.64	1.08	1.20	0.97	0	1.09	1.20	0.99	0	1.73	1.87	1.58	0	2.20	2.72	1.69	0
CEI_N92N98	0.58	0.72	0.43	0.51	0.54	0.47	1	0.50	0.52	0.48	1	0.75	0.84	0.65	0	0.99	1.29	0.69	0
CEI_NG1N96	0.57	0.64	0.50	0.61	0.64	0.57	1	0.61	0.63	0.59	1	0.79	0.86	0.73	0	0.96	1.16	0.75	0
CEI_NG1N98	0.42	0.58	0.26	0.31	0.33	0.30	1	0.31	0.32	0.31	1	0.37	0.41	0.34	1	0.45	0.54	0.36	1
CEI_NG1Nm	0.46	0.55	0.38	0.39	0.40	0.39	1	0.39	0.40	0.38	1	0.38	0.38	0.38	0	0.38	0.38	0.37	0
CEI_NLPN96	0.42	0.48	0.35	0.47	0.50	0.44	0	0.47	0.51	0.42	0	0.60	0.63	0.57	0	0.62	0.70	0.55	0

Note: 1 = Pass (Equivalent); 0 = Fail (Not Equivalent); Units of $N98\text{-}NG1$ and $N98\text{-}NLP$ = gyrations; Unit of $CNG1$ and CLP = %; Unit of m = %/gyrations; Unit of CI = None; Units of TDI, SEI and CEI = N.mm

4.2.1 Compacted Density Parameters

A total of 11 different parameters, each representing relative density (%G_{mm}) reached at a completely different condition, were extracted using compaction data and analyzed. Table 4-7 presents the results of these analyses. The value of one in this table refers to the liquid ASA-treated mixture that was equivalent to the control mixture and a value of zero refers to the liquid ASA-treated mixture that was not equivalent to the control mixture. The parameter that can distinguish unstable from stable liquid ASA-treated mixtures should pass this test in all eight L1 and L2 mixtures and should fail in all eight L3 and L4 mixtures.

Analysis results revealed that compacted density parameter i.e., *CLP* (%G_{mm} at locking point) categorized C0 (stable), L1- and L2-treated GA9.5 and GA12.5 mixtures in one group while the L3- and L4-treated GA9.5 and GA12.5 mixtures in another category; it failed to replicate it in LS mixtures though. All other parameters failed to show a similar trend in each mixture.

Table 4-7. Analysis Results of Compaction Density Parameters

S.N.	Parameter	L1 = C0?				L2 = C0?				L3 = C0?				L4 = C0?			
		GA		LS		GA		LS		GA		LS		GA		LS	
		9.5	12.5	9.5	12.5	9.5	12.5	9.5	12.5	9.5	12.5	9.5	12.5	9.5	12.5	9.5	12.5
1	C1	0	0	0	0	0	0	0	0	0	0	0	1	0	0	0	0
2	C7	0	0	0	0	0	0	0	0	0	0	0	0	0	0	0	0
3	C8	0	0	0	0	0	0	0	0	0	0	0	0	0	0	0	0
4	C10	0	0	0	0	0	0	0	0	0	0	0	0	0	0	0	0
5	C75	0	1	0	0	0	1	0	0	0	0	0	0	0	0	0	0
6	C100	0	1	0	0	0	1	0	1	0	0	0	0	0	0	1	0
7	C115	0	1	0	0	0	1	1	1	0	0	0	1	0	0	0	0
8	CNG1	0	1	0	1	0	1	0	0	0	0	0	0	0	0	0	0
9	CLP	1	1	0	1	1	1	0	0	0	0	0	0	0	0	0	0
10	Cτmax	1	0	1	0	1	1	1	0	1	1	1	0	1	1	1	0
11	CSRmax	1	0	1	0	1	1	1	0	1	1	1	0	1	1	1	0

Note: 1 = Pass (Equivalent); 0 = Fail (Not Equivalent)

4.2.2 Compaction Effort Parameters

A total of 31 different parameters, each representing compaction effort required to reach a completely different compaction level, were extracted and used to assess the equivalency between treated and untreated mixtures. Table 4-8 presents the results of these assessments.

Analysis results revealed that five such parameters ($N98$, $N98$-$NG1$, $GR_{log9895}$, and $GR_{log9896}$) placed the C0 (stable), L1- and L2-treated GA9.5 and GA12.5 mixtures in one group while the L3-and L4-treated GA9.5 and GA12.5 mixtures in another group; they failed to do the same with LS mixtures though.

Table 4-8. Analysis Results of Compaction Effort Parameters

S.N.	Parameter	L1 = C0?				L2 = C0?				L3 = C0?				L4 = C0?			
		GA		LS		GA		LS		GA		LS		GA		LS	
		9.5	12.5	9.5	12.5	9.5	12.5	9.5	12.5	9.5	12.5	9.5	12.5	9.5	12.5	9.5	12.5
1	N87	0	0	0	1	0	0	0	1	0	0	0	0	0	0	0	0
2	N92	0	0	0	0	0	0	0	0	0	0	0	0	0	0	0	0
3	N93	0	0	0	0	1	0	0	0	0	0	0	0	0	0	0	0
4	N95	0	1	0	1	1	1	0	0	0	0	0	0	0	0	0	0
5	N96	0	1	0	0	0	1	0	0	0	0	0	0	0	0	0	0
6	N98	1	1	0	0	1	1	0	0	0	0	0	0	0	0	0	0
7	N100	1	1	0	0	1	1	0	0	1	1	0	0	1	1	0	0
8	NG1	1	0	1	0	1	0	1	0	1	0	1	0	1	0	1	0
9	NLP	0	0	1	0	0	0	1	0	0	0	1	0	0	0	1	0
10	Nτmax	1	0	1	0	1	0	1	0	1	0	1	0	1	0	1	0
11	NSRmax	1	0	1	0	1	0	1	0	0	0	1	0	0	0	1	0
12	N92-7	0	0	0	0	0	0	0	0	0	0	0	0	0	0	0	0
13	N96-7	0	1	0	0	0	1	0	0	0	0	0	0	0	0	0	0
14	N96-N92	0	1	0	0	0	1	0	0	0	0	0	0	0	0	0	0
15	N96-NG1	0	1	0	0	0	1	0	0	0	0	0	0	0	0	0	0
16	N96-NLP	1	1	0	1	0	1	0	0	0	0	0	0	0	0	0	0
17	N98-NG1	1	1	0	0	1	1	0	0	0	0	0	0	0	0	0	0
18	N98-NLP	0	0	0	0	0	1	0	0	1	0	0	0	0	0	0	0
19	N98-N92	1	1	0	0	1	1	0	0	1	0	0	0	1	0	0	0
20	N98-N96	1	1	0	0	1	1	0	0	1	1	0	0	1	1	0	0
21	Nd-NG1	1	0	1	0	1	0	1	0	1	0	1	0	1	0	1	0
22	Nd-NLP	0	0	1	0	0	0	1	0	0	0	1	0	0	0	1	0
23	Nm-NG1	1	0	1	0	1	0	1	0	1	0	1	0	1	0	1	0
24	Nm-NLP	0	0	1	0	0	0	1	0	0	0	1	0	0	0	1	0
25	Nm-Nd	0	0	0	0	0	0	0	0	0	0	0	0	0	0	0	0
26	GR_98/95	1	1	0	0	1	1	0	0	1	1	0	0	1	0	0	0
27	GR_98/96	1	1	0	0	1	1	0	0	0	1	0	0	0	1	0	0
28	GR_Log96/92	0	0	1	0	0	0	0	0	0	0	0	0	0	0	0	0
29	GR_Log98/95	1	1	0	0	1	1	0	0	0	0	0	0	0	0	0	0
30	GR_Log98/96	1	1	0	0	1	1	0	0	0	0	0	0	0	0	0	0
31	CR	0	0	0	0	0	0	0	0	0	0	0	0	0	0	0	0

Note: 1 = Pass (Equivalent); 0 = Fail (Not Equivalent)

4.2.3 Compaction Rate Parameters

A total of 7 different parameters, including two slope parameters, were extracted by fitting the compaction data with functions described in Section 4.1.3. Table 4-9 presents the results of the equivalency assessment conducted on each of these parameters. Analysis results showed that the compaction index (*CI*) consistently differentiated the C0 (stable), L1- and L2-treated GA9.5 and GA12.5 mixtures in one group while the L3-and L4-treated GA9.5 and GA12.5 mixtures in another group; they did not do the same with LS mixtures though.

Table 4-9. Analysis Results of Compaction Rate Parameters

S.N.	Parameter	L1 = C0?				L2 = C0?				L3 = C0?				L4 = C0?			
		GA		LS		GA		LS		GA		LS		GA		LS	
		9.5	12.5	9.5	12.5	9.5	12.5	9.5	12.5	9.5	12.5	9.5	12.5	9.5	12.5	9.5	12.5
1	Gmm_0	0	0	0	0	0	0	0	0	0	0	0	1	0	0	0	0
2	k	0	1	0	0	0	1	0	0	0	1	0	0	1	1	0	0
3	PI	0	0	0	0	0	0	0	0	0	0	0	1	0	0	0	0
4	k x AV75	0	0	0	1	0	0	0	0	0	0	0	0	0	0	0	0
5	c	0	0	0	0	0	0	0	0	0	0	0	1	0	0	0	0
6	m	0	1	0	0	0	1	0	0	0	1	0	0	1	1	0	0
7	CI	1	1	0	0	1	1	0	0	0	0	0	0	0	0	0	0

Note: *1 = Pass (Equivalent); 0 = Fail (Not Equivalent)

4.2.4 Densification Indices

A total of 36 different densification indices were obtained by separating the compaction data into two parts. Table 4-10 presents the results of equivalency analysis conducted on each of these parameters. The table shows that four densification indices (TDI_{NG1N98}, TI_{NG1N98}, TI_{NLPN96}, and TI_{NLPN98}) consistently differentiated the C0 (stable), L1- and L2-treated GA9.5 and GA12.5 mixtures from the L3-and L4-treated GA9.5 and GA12.5 mixtures but shied away from doing the same with LS mixtures.

4.2.5 Compaction Energy Indices

A total of 36 different energy-related indices were obtained by separating the compaction data into two parts. Table 4-11 presents the results of equivalency analysis conducted on each of these parameters. Analysis results showed that the three parameters (SEI_{NLPN96}, SEI_{NLPN98}, and CEI_{N92N98}) consistently separated the C0 (stable), L1- and L2-treated GA9.5 and GA12.5 mixtures in one group but the L3-and L4-treated GA9.5 and GA12.5 mixes in another group; they failed to do the same with LS mixes.

Table 4-10. Analysis Results of Compaction Densification Indices

S.N.	Parameter	L1 = C0?				L2 = C0?				L3 = C0?				L4 = C0?			
		GA		LS		GA		LS		GA		LS		GA		LS	
		9.5	12.5	9.5	12.5	9.5	12.5	9.5	12.5	9.5	12.5	9.5	12.5	9.5	12.5	9.5	12.5
1	CDI_N1N92	0	0	0	0	0	0	0	0	0	0	0	0	0	0	0	0
2	CDI_N1NG1	1	0	1	0	1	0	1	0	1	0	1	0	1	0	1	0
3	CDI_N1NLP	0	0	1	0	0	0	1	0	0	0	1	0	0	1	1	0
4	CDI_N1Nd	0	0	0	1	0	0	0	0	0	0	0	0	0	0	0	0
5	CDI_N7N92	0	0	0	0	0	0	0	0	0	0	0	0	0	0	0	0
6	CDI_N7N96	0	1	0	0	0	1	0	0	0	0	0	0	0	0	0	0
7	WI_N1N92	0	0	0	0	0	0	0	0	0	0	0	0	0	0	0	0
8	WI_N1NG1	0	0	0	0	0	0	0	0	0	0	0	0	0	0	0	0
9	WI_N1NLP	1	1	0	0	0	1	0	0	0	0	0	0	0	0	0	0
10	WI_N1Nd	0	0	0	1	0	0	0	0	0	0	0	0	0	0	0	0
11	WI_N8N92	0	0	0	0	0	0	0	0	0	0	1	1	0	0	0	0
12	WI_N8N96	0	0	0	0	0	0	0	0	0	0	0	0	0	0	0	0
13	TDI_N92N96	0	1	0	0	0	1	0	0	0	0	0	0	0	0	0	0
14	TDI_N92N98	1	1	0	0	1	1	0	0	1	0	0	0	1	0	0	0
15	TDI_N96N98	1	1	0	0	1	1	0	0	1	1	0	0	1	1	0	0
16	TDI_NdNm	0	1	0	0	0	1	0	1	0	0	0	0	0	0	1	0
17	TDI_NG1N96	0	1	0	0	0	1	0	0	0	0	0	0	0	0	0	0
18	TDI_NG1N98	1	1	0	0	1	1	0	0	0	0	0	0	0	0	0	0
19	TDI_NG1Nd	1	0	1	0	1	0	1	0	1	0	1	0	1	0	1	0
20	TDI_NG1Nm	1	0	1	0	1	0	1	0	0	0	1	0	0	0	1	1
21	TDI_NLPN96	1	1	0	1	0	1	0	0	1	1	0	0	1	1	0	0
22	TDI_NLPN98	0	0	0	0	0	1	0	0	1	0	0	0	0	0	0	0
23	TDI_NLPNd	0	0	1	0	0	0	1	0	0	0	1	0	0	0	1	0
24	TDI_NLPNm	0	0	1	0	0	0	1	0	0	0	1	0	0	0	1	0
25	TI_N92N96	1	1	0	0	1	1	0	1	1	1	0	0	1	0	0	0
26	TI_N92N98	1	1	0	0	1	1	0	0	1	1	0	0	1	1	0	0
27	TI_N96N98	0	1	0	0	0	0	0	0	0	0	0	0	0	0	0	0
28	TI_NdNm	0	1	0	0	0	1	0	1	0	0	0	0	0	0	1	0
29	TI_NG1N96	0	1	0	1	0	1	0	0	0	0	0	0	0	0	0	0
30	TI_NG1N98	1	1	0	0	1	1	0	0	0	0	0	0	0	0	0	0
31	TI_NG1Nd	0	1	0	0	0	1	0	0	0	0	0	0	0	0	0	0
32	TI_NG1Nm	0	1	0	0	0	1	0	0	0	0	0	0	0	0	0	0
33	TI_NLPN96	1	1	0	1	1	1	0	0	0	0	0	0	0	0	0	0
34	TI_NLPN98	1	1	0	0	1	1	0	0	0	0	0	0	0	0	0	0
35	TI_NLPNd	1	1	0	1	0	1	0	0	0	0	0	0	0	0	0	0
36	TI_NLPNm	1	1	0	0	0	1	0	0	0	0	0	0	0	0	0	0

Note: 1 = Pass (Equivalent); 0 = Fail (Not Equivalent)

Table 4-11. Analysis Results of Compaction Energy Indices

S.N.	Parameter	L1 = C0?				L2 = C0?				L3 = C0?				L4 = C0?			
		GA		LS		GA		LS		GA		LS		GA		LS	
		9.5	12.5	9.5	12.5	9.5	12.5	9.5	12.5	9.5	12.5	9.5	12.5	9.5	12.5	9.5	12.5
1	VEI_N1N92	0	0	0	0	0	0	0	0	0	0	0	1	0	0	0	0
2	VEI_N1NG1	0	0	0	0	0	0	0	0	0	0	0	1	0	0	0	0
3	VEI_N1NLP	0	0	0	0	0	0	0	0	0	0	0	1	0	0	0	0
4	VEI_N1Nd	0	0	0	0	0	0	0	0	0	0	0	0	0	0	0	0
5	VEI_N7N92	0	0	0	0	0	0	0	0	0	0	0	0	0	0	0	0
6	VEI_N7N96	0	0	0	0	0	0	0	0	0	0	0	1	0	0	0	0
7	WEI_N1N92	0	1	0	0	0	0	0	0	0	0	0	0	0	0	0	0
8	WEI_N1NG1	0	0	0	0	0	1	0	0	0	0	1	1	0	0	1	0
9	WEI_N1NLP	0	0	1	0	0	0	0	0	0	0	1	0	0	1	1	0
10	WEI_N1Nd	0	0	0	0	0	0	0	0	0	0	0	0	0	0	0	0
11	WEI_N8N92	0	1	0	0	0	1	0	0	0	0	0	0	0	0	0	0
12	WEI_N8N96	0	1	0	0	0	1	0	0	0	0	0	0	0	0	0	0
13	SEI_N92N96	1	0	0	0	1	0	0	0	0	0	0	1	0	0	0	1
14	SEI_N92N98	1	0	0	0	1	0	0	0	0	0	0	1	0	0	0	1
15	SEI_N96N98	0	1	0	0	0	1	1	0	0	1	1	0	0	0	0	0
16	SEI_NdNm	1	1	0	0	1	1	0	0	1	1	0	0	1	1	0	0
17	SEI_NG1N96	0	1	0	1	0	1	0	0	0	0	0	0	0	0	0	0
18	SEI_NG1N98	0	1	0	1	0	1	0	0	0	0	0	0	0	0	0	0
19	SEI_NG1Nd	0	0	0	0	0	0	0	0	0	0	0	0	0	0	0	0
20	SEI_NG1Nm	0	1	0	0	0	1	0	0	0	0	0	0	0	0	0	0
21	SEI_NLPN96	1	1	0	1	1	1	0	0	1	1	0	0	1	0	0	0
22	SEI_NLPN98	1	1	0	1	1	1	0	0	0	0	0	0	0	0	0	0
23	SEI_NLPNd	0	0	1	0	0	0	0	0	0	0	1	0	0	1	1	0
24	SEI_NLPNm	1	1	0	0	1	1	0	0	1	1	0	0	1	1	0	0
25	CEI_N92N96	0	0	0	0	0	0	0	0	0	0	0	0	0	0	0	0
26	CEI_N92N98	1	1	0	0	1	1	0	0	0	0	0	0	0	0	0	0
27	CEI_N96N98	1	1	0	0	1	1	0	0	1	1	0	0	1	0	0	0
28	CEI_NdNm	1	1	0	0	1	1	0	0	1	1	0	0	1	1	0	0
29	CEI_NG1N96	0	1	0	0	0	1	0	0	0	0	0	0	0	0	0	0
30	CEI_NG1N98	1	1	0	0	1	1	0	0	1	1	0	0	1	1	0	0
31	CEI_NG1Nd	0	0	0	0	0	0	0	0	0	0	0	0	0	0	0	0
32	CEI_NG1Nm	0	1	0	0	0	1	0	0	0	0	0	0	0	0	0	0
33	CEI_NLPN96	1	0	0	0	1	0	0	0	0	0	0	0	0	0	0	0
34	CEI_NLPN98	1	1	0	0	1	1	0	0	1	1	0	0	1	1	0	0
35	CEI_NLPNd	1	0	1	0	0	1	0	0	1	0	0	0	0	0	0	0
36	CEI_NLPNm	1	1	0	0	1	1	0	0	1	1	0	0	1	1	0	0

Note: 1 = Pass (Equivalent); 0 = Fail (Not Equivalent)

4.3 Summary

A total of 121 parameters (11 compacted density parameters, 31 compaction effort parameters, 7 compaction slope-based parameters, 36 densification parameters, 36 compaction energy-based parameters) were obtained from each sample compacted for this part of the

experimental plan. Table A-1 to Table A-5 presented in Appendix A present average values of each of these parameters.

Data analyses of these parameters (2 mix design × 2 aggregates × 5 binder combinations × 121 parameters per sample) showed that 4 compaction effort parameters ($N98$, $N98$-$NG1$, $GR_{log9895}$, and $GR_{log9896}$), 1 compaction density parameter (CLP), 1 compaction rate parameter (CI), 4 densification parameters (TDI_{NG1N98}, TI_{NG1N98}, TI_{NLPN96}, and TI_{NLPN98}) and 3 energy indices (SEI_{NLPN96}, SEI_{NLPN98}, and CEI_{N92N98}) categorized C0 (stable), L1- and L2-treated GA9.5 and GA12.5 mixtures in one group while the L3-and L4-treated GA9.5 and GA12.5 mixtures in another group; however, these parameters did not yield the same results for the limestone mixtures. These results imply that stability parameters were more effective in differentiating the mixtures that are prepared with comparatively less absorbent and stiffer aggregates such as granite than the mixtures that are prepared with comparatively more absorbent and softer aggregates such as limestone.

Among the thirteen parameters that could categorize the C0 (stable), L1- and L2-treated GA9.5 and GA12.5 mixtures in one group and the L3- and L4-treated GA9.5 and GA12.5 mixtures in another group, the first two types of parameters (compaction effort parameters and compaction density parameters: $N98$, $N98$-$NG1$, $GR_{log9895}$, $GR_{log9896}$,and CLP) represent volumetric properties of mixtures at certain conditions during compaction. The third type of parameter (compaction slope parameter: *CI*) represents the rate of change in volumetric properties from one air void content (or density level) to another. Similarly, the parameters obtained from the area under compaction curves (such as TDI_{NG1N98}, TI_{NG1N98}, TI_{NLPN96}, TI_{NLPN98}, SEI_{NLPN96}, SEI_{NLPN98}, and CEI_{N92N98}) represent effort or energy required to compact mixtures from one density level to another.

5 PARAMETERS OBTAINED FROM TESTS CONDUCTED AFTER COMPACTION

5.1 Asphalt Binder Tests

The primary materials of interest in this project were asphalt mixtures; however, the asphalt binder tests were also included in the experimental plan because the rate at which asphalt mixtures gain stability immediately after construction potentially depends on the rate at which asphalt binders gain their stiffness and adhesive properties during this period. Additionally, the comparatively less expensive, more efficient tests could serve as a preliminary indicator of the effect of liquid ASA, if any, on the stability of asphalt mixtures. Three types of binder tests were included in the plan—the Fourier-Transform Infrared spectroscopy tests, Dynamic Shear Modulus tests and the Monotonic Pull-Off tests. The tests were conducted on the RTFO-aged specimens since this aging condition represented the condition during which the isolated instances of stability issues as reported by the contractors were observed in the field.

5.1.1 Fourier-Transform Infrared Tests

Fourier Transform Infrared (FTIR) spectroscopy tests were conducted to fingerprint the chemical composition of the test materials and determine anomalies, if any, that could be linked to the stability of asphalt mixtures during or after construction. FTIR tests were conducted first on the four liquid ASA and the control binder, and then on the liquid ASA-treated asphalt binders. Figure 5-1 to Figure 5-3 present the absorbance spectra obtained from these tests.

Test results show that, as expected, each liquid ASA yielded a distinct absorption spectrum as expected from different proprietary materials (see spectra of L1, L2, L3, and L4 in Figure 5-1). Test results also show that the absorption spectra of four specimens of liquid ASA-treated binders treated with the same liquid ASA were similar to each other and different from the liquid ASA themselves as expected (see spectra of Lx versus PMA + Lx, where x =1, 2, 3 and 4 in Figure 5-2).

Test results also showed that the absorbance spectra of asphalt binders treated with different types of liquid ASA were similar to each other (see spectra of PMA + L1, PMA + L2, PMA + L3, and PMA + L4 in Figure 5-3). This similarly in absorbance spectra irrespective of the type of liquid ASA can be attributed to the very small dosage of liquid ASA in the binder (i.e., 0.4-0.5% by weight of asphalt binder). In summary, FTIR test results revealed that liquid ASA-treated binders did not exhibit any significant difference between each other in their chemical composition that might contribute to the stability of asphalt mixtures during and after construction.

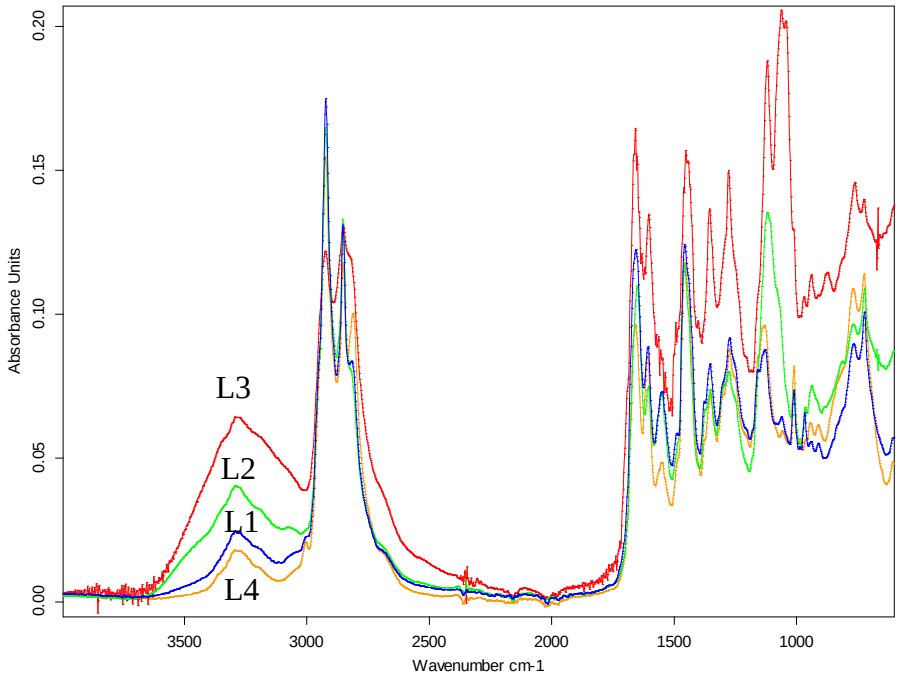

Figure 5-1. FTIR Test Results: Liquid ASAs

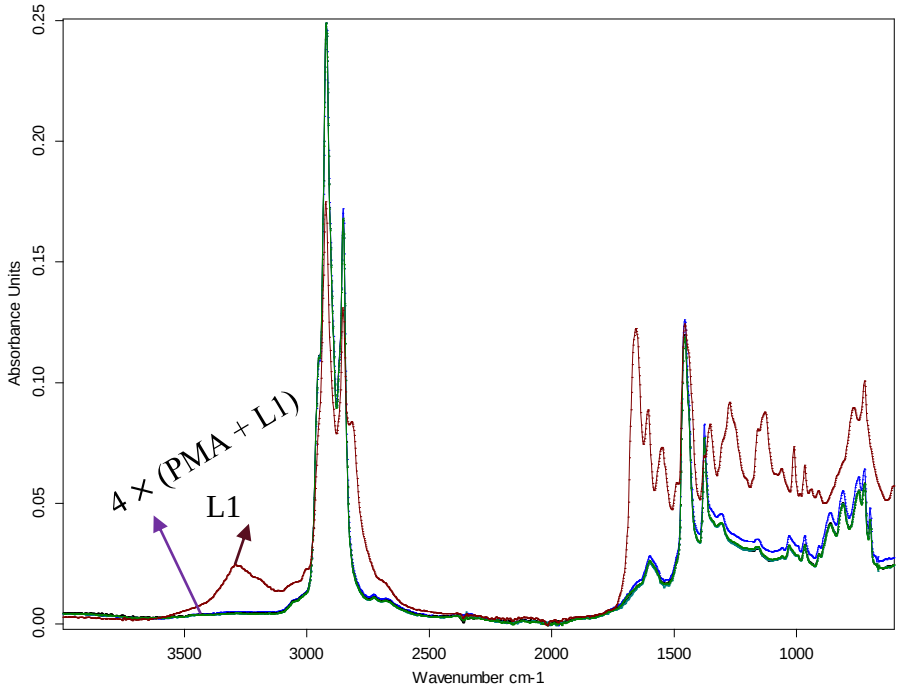

(a) L1-treated PMA versus L1

Figure 5-2. FTIR Test Results of Liquid ASA-Treated Asphalt Binders versus Liquid ASAs: (a) L1, (b) L2, (c) L3, and (d) L4

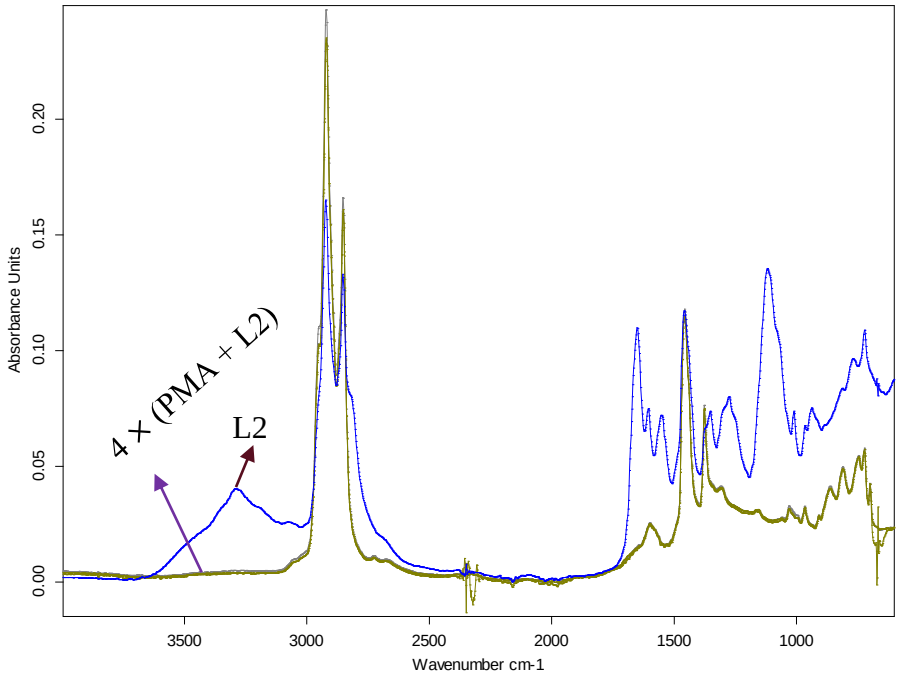

(b) L2-treated PMA versus L2

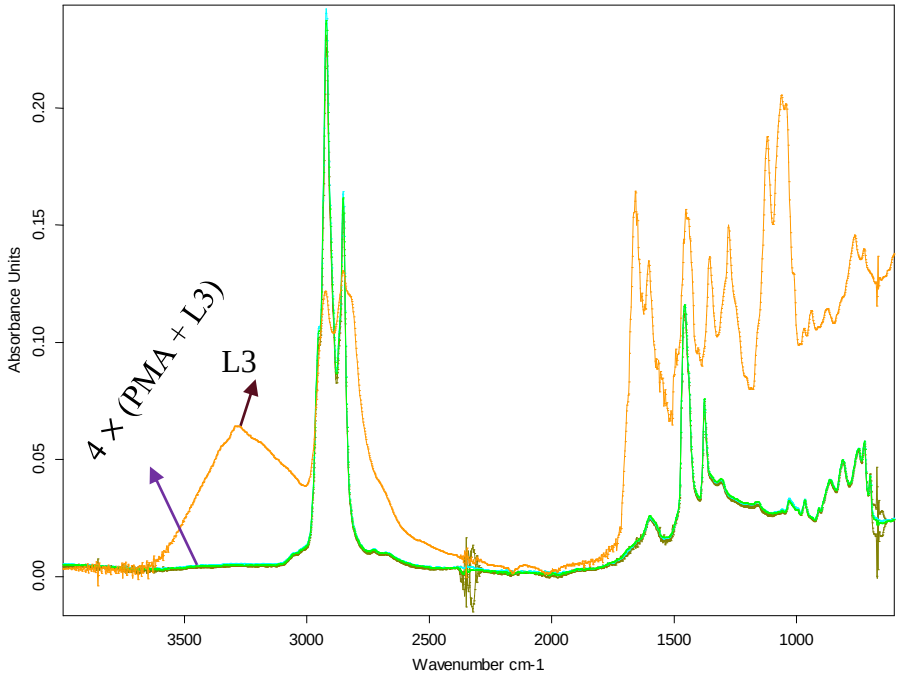

(c) L3-treated PMA versus L3

Figure 5-2. FTIR Test Results of Liquid ASA-Treated Asphalt Binders versus Liquid ASAs: (a) L1, (b) L2, (c) L3, and (d) L4, Continued

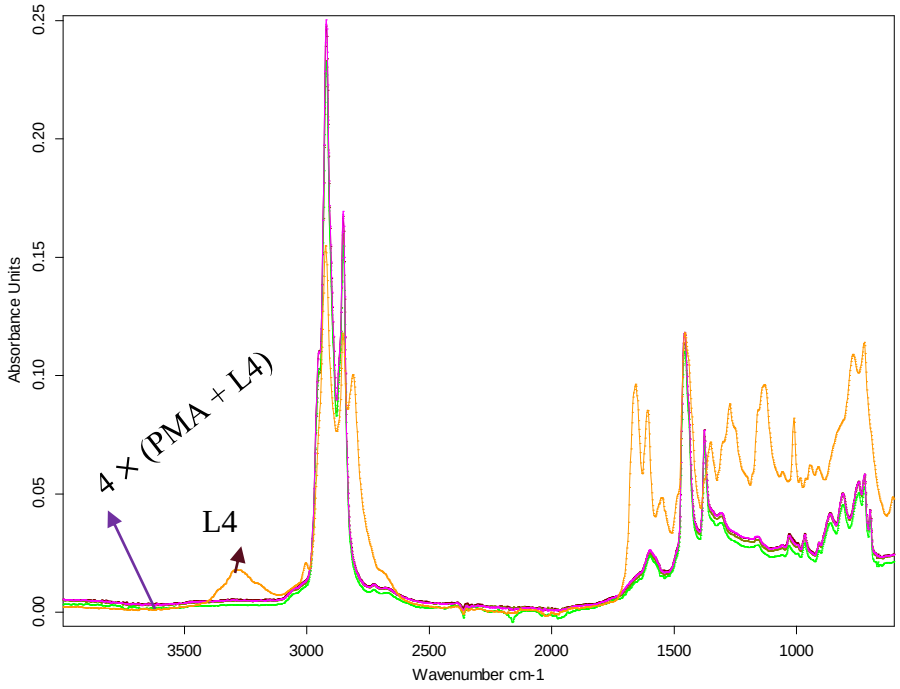

(d) L4-treated PMA versus L4

Figure 5-2. FTIR Test Results of Liquid ASA-Treated Asphalt Binders versus Liquid ASAs: (a) L1, (b) L2, (c) L3, and (d) L4, Continued

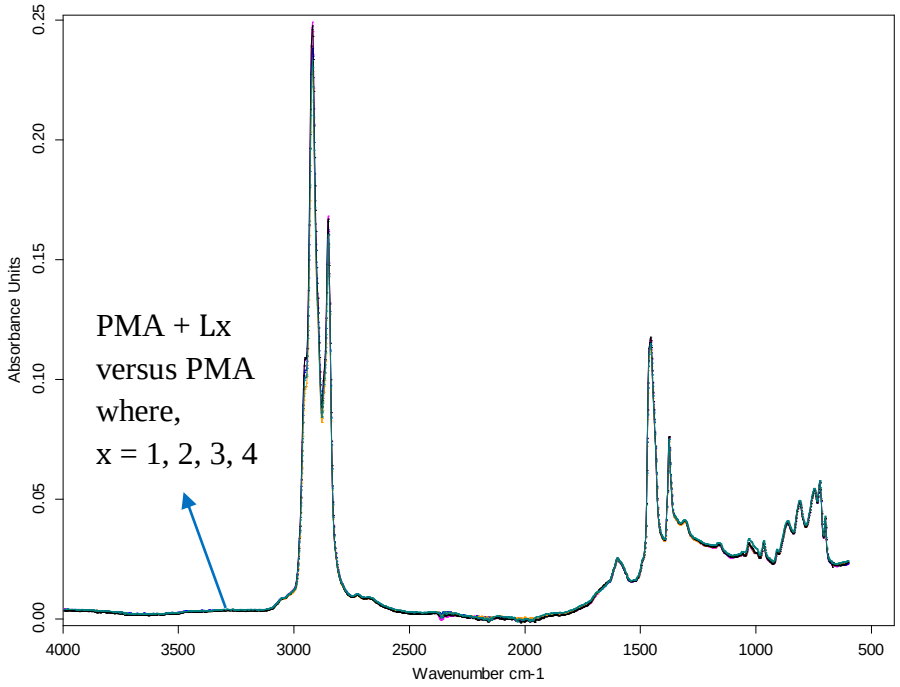

Figure 5-3. FTIR Test Results: Liquid ASA-Treated Asphalt Binders

5.1.2 Dynamic Shear Modulus Tests

Linear viscoelastic dynamic shear modulus tests were conducted to determine whether liquid ASA would decelerate the rate of increase in stiffness and decrease in phase angle during cooling. For these tests, the RTFO-aged asphalt binder specimens (measuring 8.0 mm in diameter and 2.0 mm in thickness) were first conditioned at 76°C (168.8°C) in a CTD180 chamber of the Anton Paar MCR 302 DSR for at least 30 minutes. Then, the heating and cooling system of the DSR was switched off and the chamber was opened to allow the specimens to cool down to a laboratory temperature of 21.5°C. During this phase, the specimens were subjected to dynamic shear modulus tests at a shear strain of 0.10% and a frequency of 10 Hz every 5 minutes until the G^* and δ values became constant.

Figure 5-4 (a) and (b) present the average values of G^* and δ values obtained from two specimens of control and liquid ASA-treated asphalt binders from these tests. The figures show that, at any given interval, the liquid ASA-treated binders (PMA + Lx, where x = 1, 2, 3, 4) had lower G^* (or were softer) and higher δ (or were more ductile or less brittle) than the control binder. However, the figures also showed that the asphalt binders treated with different types of liquid ASA did not show significantly different G^* and δ values between each other at a given interval or significantly different rates of change in their G^* values between each other over certain duration from each other (342-344 kPa/min and 0.49-0.56 degrees/min), though their values and rates of change in their values were different from the corresponding values of control binder (420 kPa/min and 0.55 degrees./min). Moreover, the rates of change in G^* and δ values, and the time required to cool off (~50-60 minutes) were very similar, which indicated the inability of this test to differentiate the difference in liquid ASA in terms of cooling rate after construction.

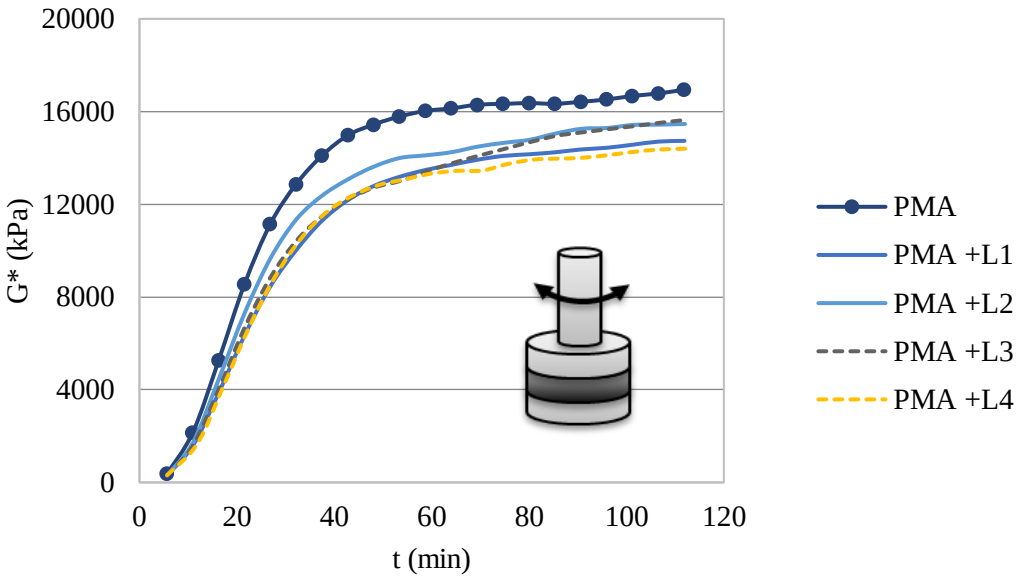

(a) Complex Shear Modulus

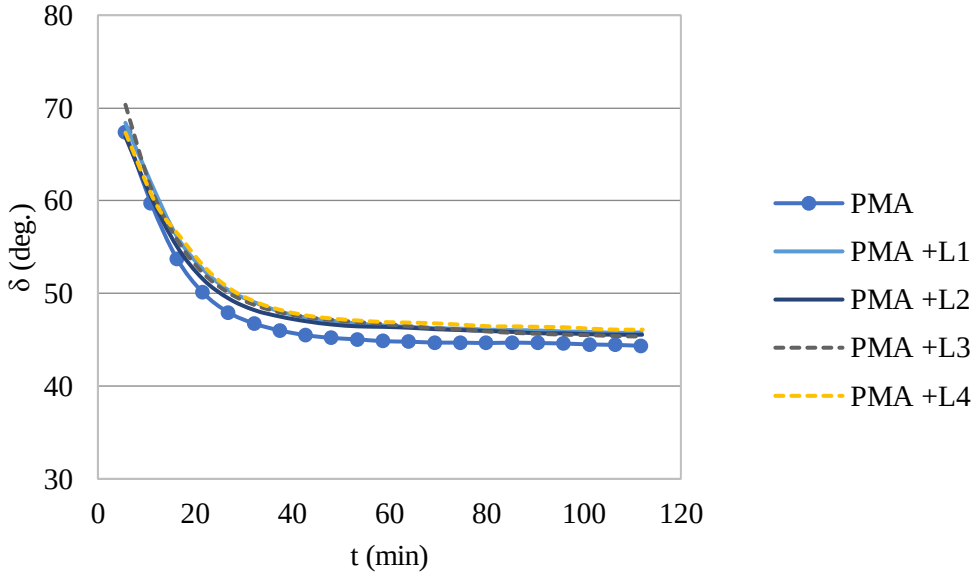

(b) Phase Angle

Figure 5-4. Dynamic Shear Modulus Test Results: (a) Complex Shear Modulus; (b) Phase Angle

5.1.3 Monotonic Pull-Off Tests

Tackiness is defined as the resistance against separation of two solids glued together by an adhesive (Bikerman, 1947). Work done to completely pull-off an adhesive material from the lower plate of the rheometer at a pre-determined rate of pull-off, which can be calculated using the area under the force versus time curve, was recently used to evaluate the tackiness of

asphaltic materials (Gorsuch et al., 2013; Wilson et al., 2016). These studies showed that the tack parameter (work normalized with sample thickness) was sensitive to change in temperature and asphalt binder treatments. Because of these features, monotonic pull-off tests were selected in this study to determine whether some liquid ASA would negatively impact the cooling rate of asphalt binders and keep asphalt mixtures unstable for longer period after construction.

In this study, RTFO-aged asphalt binder specimens (measuring 8.0 mm in diameter and 2.0 mm in thickness) were first conditioned at 76°C (168.8°C) in a CTD180 chamber of the Anton Paar MCR 302 for at least 30 minutes. Then, the heating and cooling system was switched off and the CTD180 chamber was opened to let the specimens cool down to a laboratory temperature of 21.5°C. During this period, the specimens were monotonically pulled off from lower geometry plate at a rate of 0.18 mm/sec after 30, 35, 40, 45, 50, 55 and 60 minutes of cooling. The pull off rate of 0.18 mm/sec was selected based on the normal force limits of the DSR at normal laboratory temperature. The test output (force-displacement data) was then used to determine the peak force ($P_{\max}$) and total work ($w = \int P.dx$) at each interval (see Figure 5-5). Unlike dynamic shear modulus tests, the pull-off tests induced damage in specimens and therefore, a new specimen was used for each selected interval. And, since same sample thickness was used in each case, the work needed for a complete pull-off instead of thickness-normalized tack factor was used to evaluate the tackiness of the asphalt binders in this study.

Figure 5-6(a) and Figure 5-6(b) respectively present P_{max} and W values of the control and the liquid ASA-treated binders (PMA versus PMA + Lx, where x = 1, 2, 3 or 4) at five different intervals after cooling the specimens from 76°C. Figure 5-6(a) shows that the $P_{\max}$ value increased with waiting time and then became stable at some interval after cooling for each sample; however, its value did not discriminate one type of liquid ASA from another. Figure 5-6(b) shows that the W value increased with waiting time and then became stable after some time for each sample—a trend like that of the $P_{\max}$ value. However, the figures also show that C0, L3- and L4-treated asphalt binders attained higher W values at a faster rate than did the L1- and L2-treated asphalt binders, which illustrates a mismatch of ranking based on the reported field stability issues.

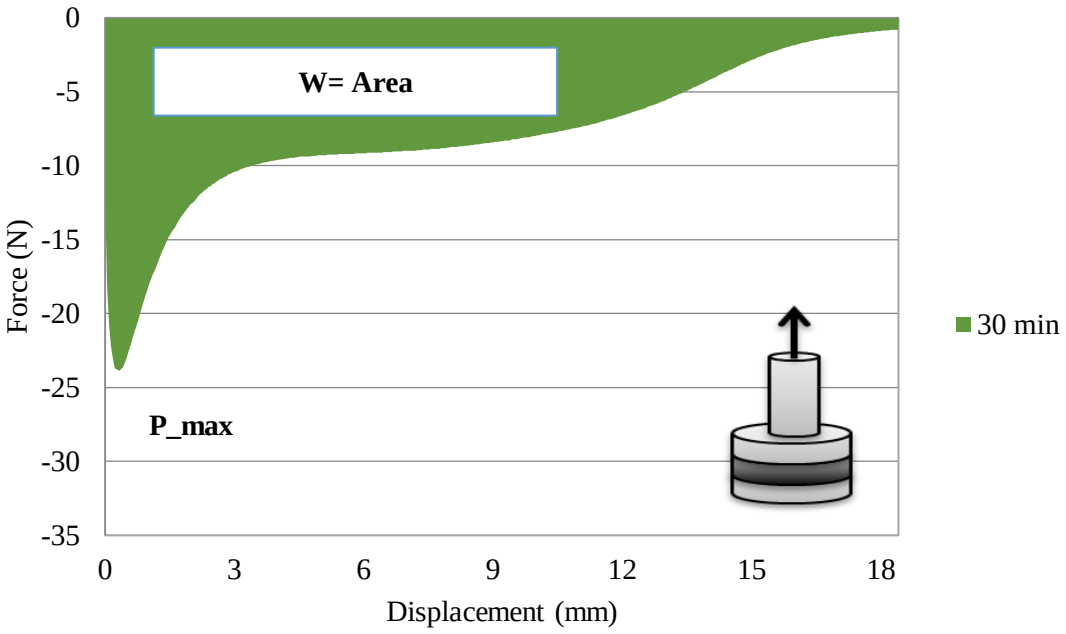

(a) 30 Minutes after Cooling

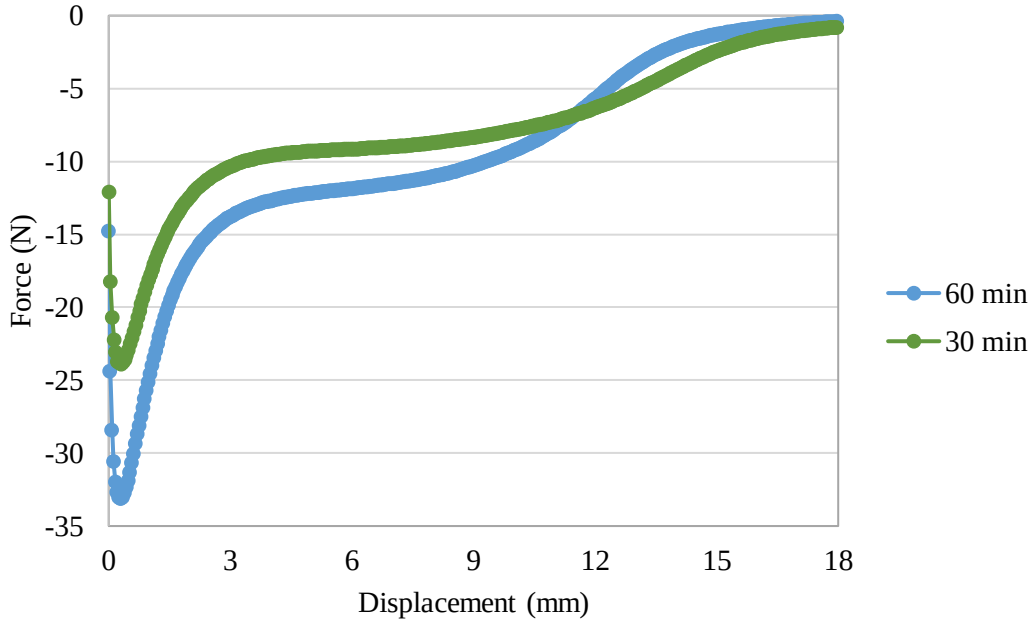

(b) 30 versus 60 Minutes after Cooling

Figure 5-5. Monotonic Pull-Off Test Results: (a) 30 Minutes after Cooling; (b) 30 versus 60 Minutes after Cooling

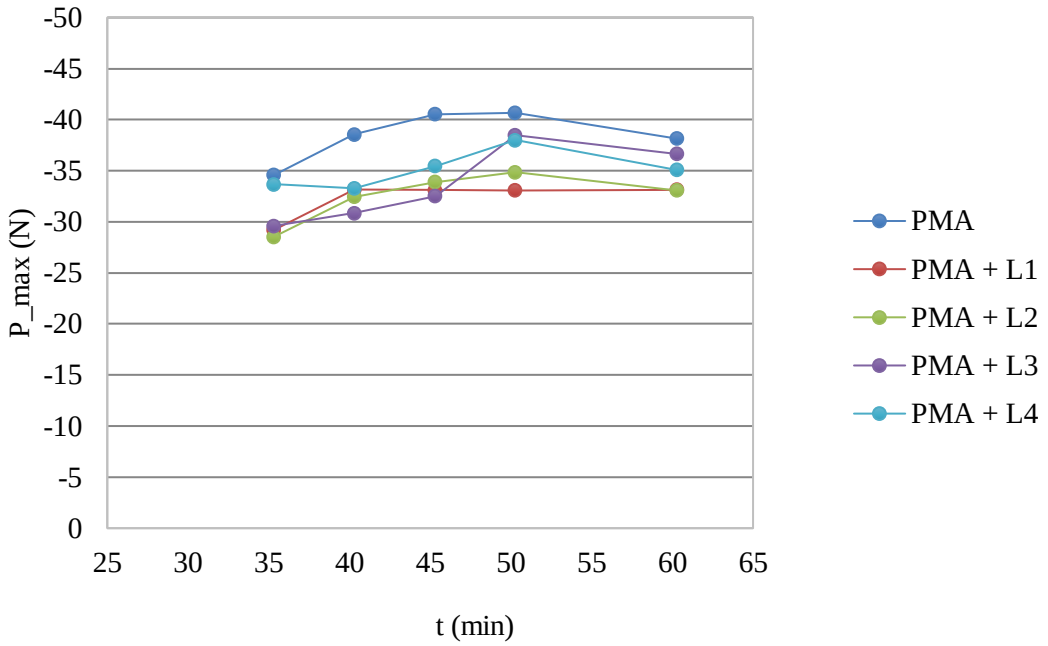

(a) Peak Force

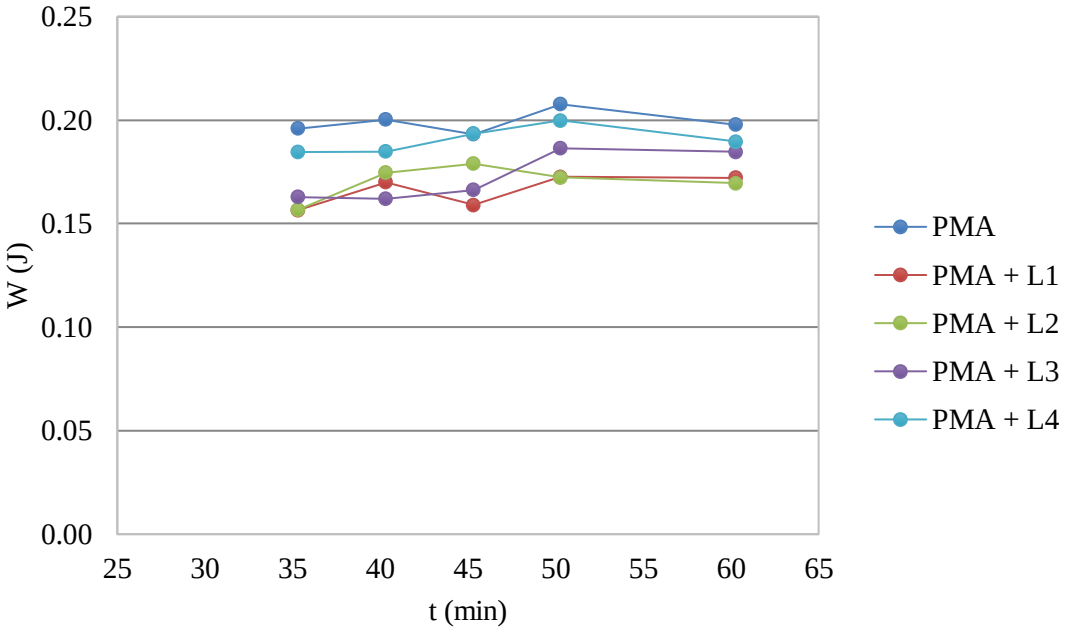

(b) Work

Figure 5-6. Monotonic Pull-Off Test Results: (a) Peak Force; (b) Work

5.2 Asphalt Mixture Tests

The stability of asphalt pavements after construction is related to the curing or cooling rate of the asphalt mixtures after compaction and corresponding change in their mechanical properties during this phase. It would be ideal to determine the change in temperature in asphalt

mixture samples using embedded thermocouples at different durations after compaction. However, embedding thermocouples in asphalt mixture samples that are usually large in size is not only difficult but also impractical in terms of routine laboratory testing. That is why a similarly fabricated specimen is embedded with a thermocouple and used to verify the temperature in compacted samples during routine laboratory testing. A practical alternative to this method is to measure the mechanical properties of asphalt mixtures at different durations during cooling in a controlled temperature environment because the mechanical properties of the asphalt mixtures always depend on temperature.

Several mechanical tests were therefore conducted on the SGC samples of the control and the liquid ASA-treated mixtures at different intervals after compaction to evaluate the impact of liquid ASA on asphalt mixture stability after construction. These tests include both the nondestructive tests such as M_r tests, and the destructive tests such as the CAL, APA, HWT, and IDEAL shear rutting tests (see Table 5-1).

Resilient modulus tests were selected to evaluate asphalt mixture stability in terms of their stiffness following several previous works (Anderson et al., 1999; Dessouky et al., 2013; Dessouky, 2015). Similarly, wheel-track (APA and HWT) and CAL tests were used to evaluate asphalt mixture stability in terms of their resistance to rutting or plastic deformation following several previous works (Anderson et al., 2002; Bahia and Faheem, 2007; Dessouky et al., 2013; Dessouky, 2015).

Chapter 4 already demonstrated that only the mixtures prepared with Georgia granite aggregates were able to differentiate the liquid ASA that had potential issues from their counterparts (i.e., L1 and L2 mixtures versus L3 and L4 mixtures). Based on these results, the mixtures prepared with the Georgia granite aggregates were selected as the materials of interest for this portion of the study (i.e., stability issues after construction). A total of 10 different mixtures were prepared.

The ensuring section presents the summary of results obtained from these tests after compacting and cooling SGC samples for different durations at different conditions and the discussion on the effectiveness of parameters obtained from each of these tests in evaluating the effectiveness of liquid ASA in terms of asphalt mixture stability after construction.

Table 5-1. Mixtures Tests Selected to Study Stability after Construction

Tests	Parameters	Mixtures	Total
Non-Destructive Tests			
Resilient Modulus (M_r)	Resilient Modulus (M_r) until 72 hrs. of cooling after compaction	GA9.5—C0, L1, L2, L3, L4 GA12.5—C0, L1, L2, L3, L4	10 mixtures × n intervals
Destructive Tests			
Cantabro Abrasion Loss (CAL)	Mass loss (Δm_L) after 2, 4, 6, 24 hrs. of cooling after compaction	GA9.5—C0, L1, L2, L3, L4 GA12.5—C0, L1, L2, L3, L4	10 mixtures × 4 intervals
Asphalt Pavement Analyzer (APA)	Rut depth (d) at 64°C and 74°C (No water)	GA9.5—C0, L1, L2, L3, L4 GA12.5—C0, L1, L2, L3, L4	10 mixtures × 2 temperatures
Hamburg Wheel-Track (HWT)	Rut depth (d) at 50°C (Under water)	GA9.5—C0, L1, L2, L3, L4 GA12.5—C0, L1, L2, L3, L4	10 mixtures × 1 temperature
IDEAL Shear Rutting	Shear Strength (τ) at 50°C, and after 35 minutes of cooling at laboratory temperature from 50°C (No water)	GA9.5—C0, L1, L2, L3, L4 GA12.5—C0, L1, L2, L3, L4	10 mixtures × 2 temperatures
Note: "n" refers to the number of intervals let to cool the samples after compaction. For example, CAL samples were tested after allowed them to cool for 2, 4, 6 or 24 hours after compaction, and therefore n = 4.			

5.2.1 Resilient Modulus Tests

Resilient modulus or modulus of resilience, M_r represents the stiffness of undamaged linear viscoelastic materials. To determine the M_r value, SGC samples are subjected to indirect tension for 100 cycles using haversine function defined by 0.1 seconds of loading period with 334 N (75 lb.) and 0.9 second of rest period with zero load at a given temperature following ASTM D7369 (2011b).

In this study, three SGC samples, each measuring 150.0 mm (5.91 in.) diameter by 63.5 mm (2.5 in.) in height and 7.0% in target air void content were produced for these tests. The first specimen was tested after 75 minutes of cooling at a laboratory temperature of 21.5°C. This interval corresponds to the time taken by the control samples to cool down to 50°C at the surface (T_{surface}) from compaction temperature of 166°C in the laboratory. The second and the

third samples were tested after another 5 and 10 minutes after the first specimen respectively, thereby resulting in the M_r values at 75, 80, and 85 minutes after cooling. Then, the tests were repeated after 10 minutes, 15 minutes, 30 minutes, 24 hours, 48 hours, and 72 hours intervals, thereby resulting in the M_r values at different durations of cooling over 3 days of cooling (see Figure 5-7). Since the M_r test does not induce damage, the same samples were repetitively used for these tests. Because tests were conducted at various intervals on the same day of compaction and various intervals in ensuing three days, this part of the experimental plan involved incessant use of the test instrument and manpower continuously for a month, which might be an issue in terms of routine laboratory testing.

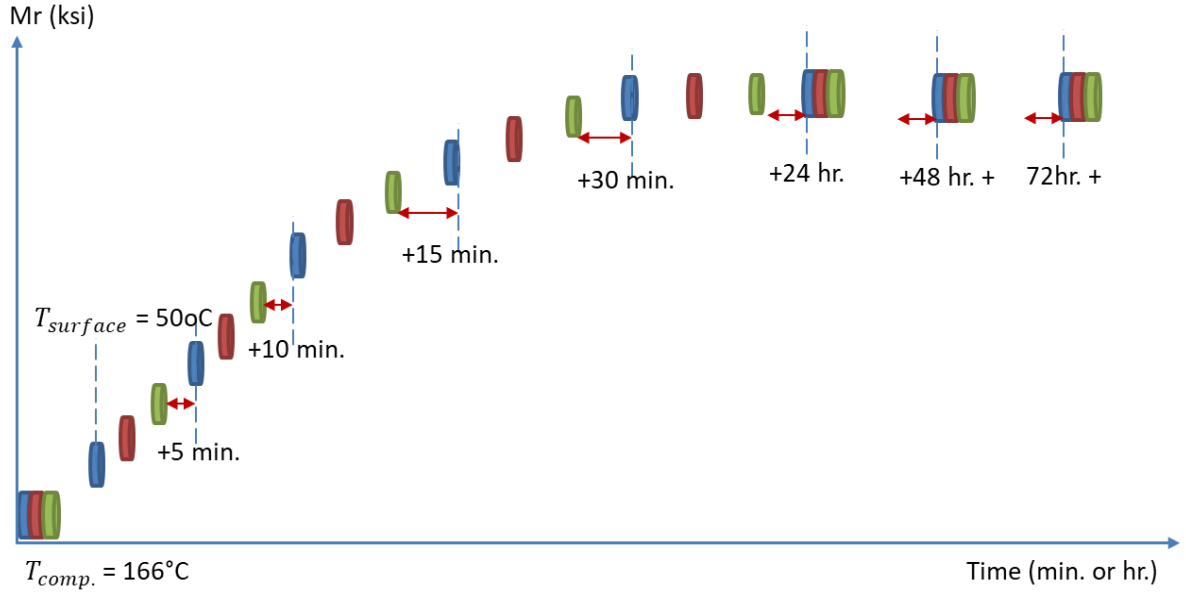

Figure 5-7. Resilient Modulus Test Plan

Figure 5-8(a-b) presents the M_r values of the control and the liquid ASA-treated GA9.5 and GA12.5 mixtures measured after allowing them to cool down at a temperature of 21.5°C for 4-5 hours after compaction. The figure shows that the M_r value generally increased with longer cooling duration as expected. Figure 5-8(c-d) presents the M_r values of the control and the liquid ASA-treated GA9.5 and GA12.5 mixtures measured after cooling them for 4 hours, 24 hours, 48 hours, and 72 hours at a temperature of 21.5°C.

Test results showed that the M_r value generally increased until 72 hours in several of these mixtures, although in some instances there was a reduction in the M_r value. The decrease in the M_r value in some of these mixtures were within sample-to-sample variability usually allowed in asphalt mixture tests. For some of the mixtures, the tests could not be conducted at 72 hours after compaction because of technical difficulties that were beyond the control of the researchers. Therefore, to evaluate the effect of liquid ASA, the percent difference in the M_r values of treated and control mixtures were only analyzed after 4, 24, and 48 hours of cooling:

$$\Delta Mr_{Lx}\ (\%) = \left(\frac{\left(M_{r_t}\right)_{Lx} - \left(M_{r_t}\right)_{C0}}{\left(M_{r_t}\right)_{C0}} \right) \times 100\% \qquad 5\text{-}1$$

where,

$\left(M_{r_t}\right)_{Lx}$ = Resilient modulus of the Lx-treated mixture after time "t"

$\left(M_{r_t}\right)_{C0}$ = Resilient modulus of the C0 mixture after time "t"

t = selected time period for cooling (i.e., 75 minutes, 4, 24, or 48 hours. etc.)

The results of this analysis showed that liquid ASA reduced the M_r value of GA9.5 and GA12.5 asphalt mixtures except in a few cases [see Figure 5-8(e-f)]. However, the results also showed that the difference in M_r value of treated and control GA9.5 and GA12.5 mixtures did not rank the liquid ASA in similar manner. For example, the ranking based on M_r value measured changed from L4>L2>L1>L3 in GA9.5 mixtures to L2>L4>L1>L3 in GA9.5 mixtures after 24 hours of cooling. Similarly, the ranking changed from L4>L1>L2>L3 in GA9.5 mixtures to L4>L2>L1>L3 in GA 12.5 after 48 hours of cooling. These results prove that the M_r test, though informative and nondestructive in nature, cannot be effectively used to differentiate the impact of liquid ASA on asphalt mixture stability after compaction.

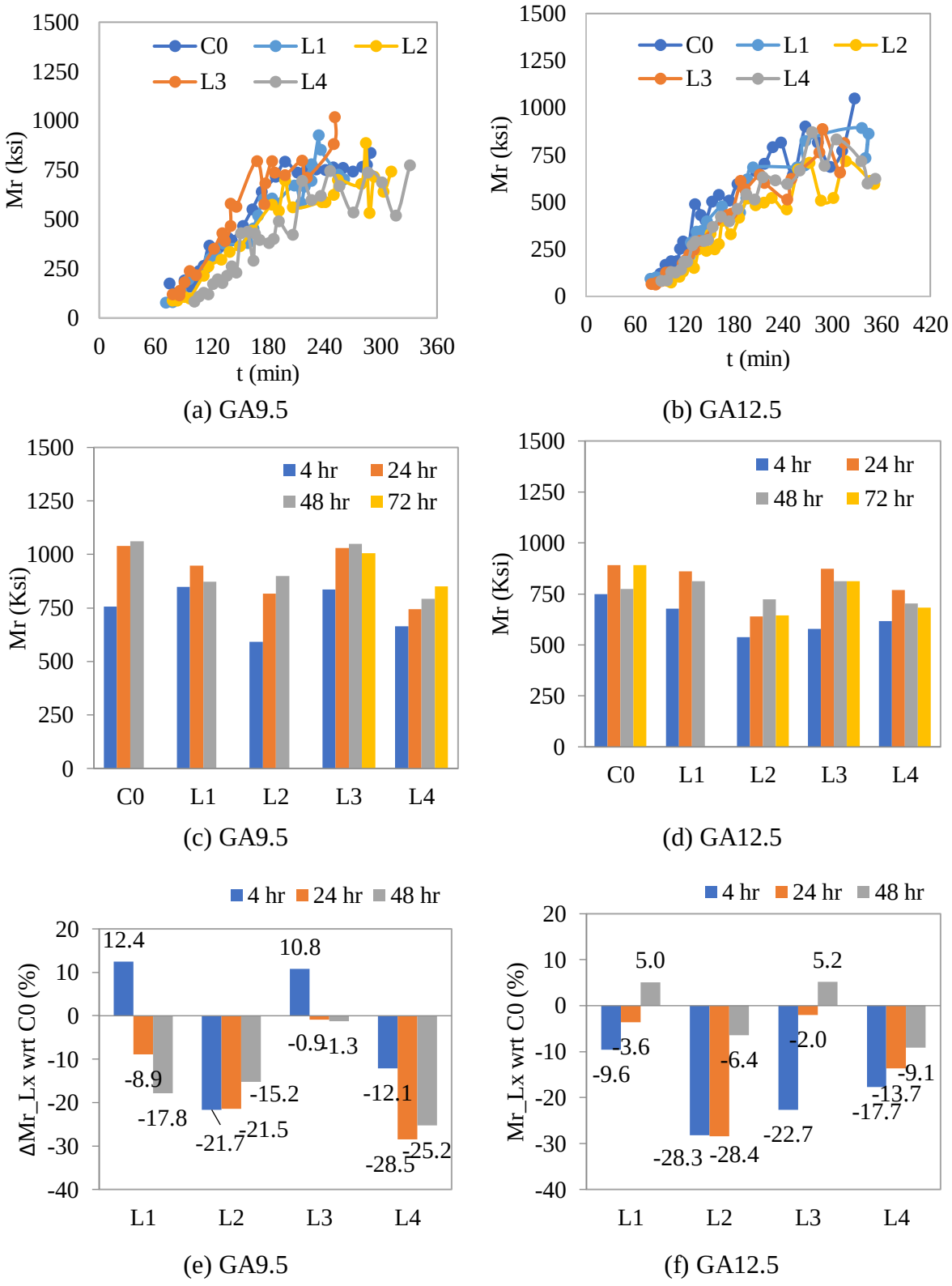

Figure 5-8. Resilient Modulus Test Results: (a-b) Moduli during 4-5 Hours of Cooling after Compaction, (c-d) Moduli after 4, 24, 48, and 72 Hours of Cooling after Compaction, and (e-f) Percent Difference in Moduli of Lx-Treated and Control Mixes

5.2.2 Cantabro Abrasion Loss Tests

The CAL test for asphalt mixtures involves the placement of SGC samples in an enclosed drum without steel spheres and rotating the drum for 300 revolutions at 30-33 cycles/min and the calculation of mass chafed away from the surface of the SGC samples [see Figure 5-9(a-b)] following AASHTO TP 108-14 (2018). The mass of samples weighed before and after the tests are used to calculate the abrasion loss percent, m_L:

$$m_L(\%) = \left(\frac{m_{\text{before}} - m_{\text{after}}}{m_{\text{before}}}\right) \times 100\% \qquad 5\text{-}2$$

where,

m_{before} = mass of compacted sample before CAL test

m_{after} = mass of compacted sample after CAL test

Ideally, asphalt mixtures with higher m_L percentages are considered less durable (or more prone to breakdown) as compared to asphalt mixtures with lower m_L percentages.

In this study, four SGC samples measuring 150.0 mm (5.91 in.) in diameter by 115.0 mm (4.53 in.) in height and 7.0% in target air void content were fabricated for these tests. The freshly compacted SGC samples were left undisturbed and allowed to cool down at the laboratory room temperature of 21.5°C for 2, 4, 6 and 24 hours before subjecting them to the CAL test. Since this test is destructive, separate SGC samples were used for each cooling interval.

The test results showed that the m_L value increased with longer cooling periods in most of the mixtures, while decreased in others [see Figure 5-9(c-d)]. The increasing and decreasing trends of m_L continued throughout the cooling process. As such, the m_L value did not show good correlation with cooling time. To determine the effect of liquid ASA on the m_L value, the percent difference between treated and control mixtures after 24 hours of cooling was also calculated:

$$\Delta m_{Lx,Co}\ (\%) = \left(\frac{(m_L)_{Lx} - (m_L)_{C0}}{(m_L)_{C0}}\right) \times 100\% \qquad 5\text{-}3$$

where,

$(m_L)_{Lx}$ = mass loss of Lx-treated mixture after 24 hours

$(m_L)_{C0}$ = mass loss of control mixture after 24 hours

The results of this analysis showed that the use of liquid ASA generally reduced the CAL. However, the liquid ASA-treated GA9.5 and GA 12.5 mixtures did not show the same ranking of the liquid ASA based on this parameter. In other words, this CAL test parameter was unable to consistently discriminate the effect of liquid ASA in mixture stability after compaction.

(a) Instrument

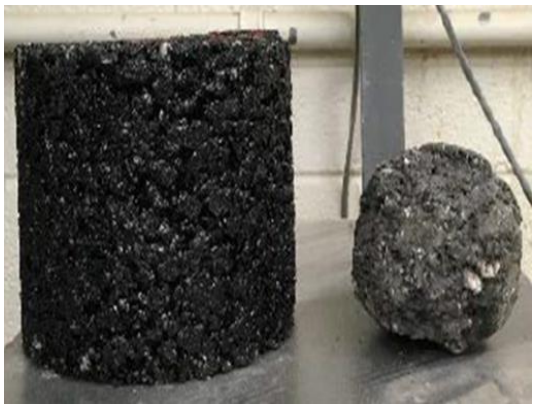

(b) Specimen before and after the Test

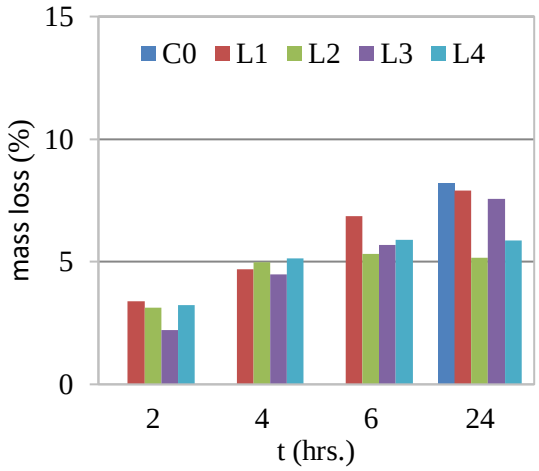

(c) GA9.5

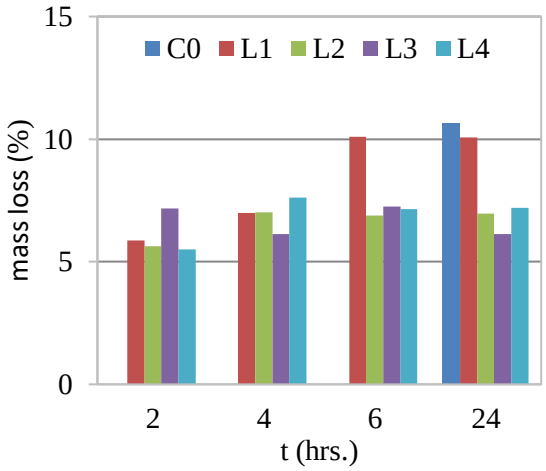

(d) GA12.5

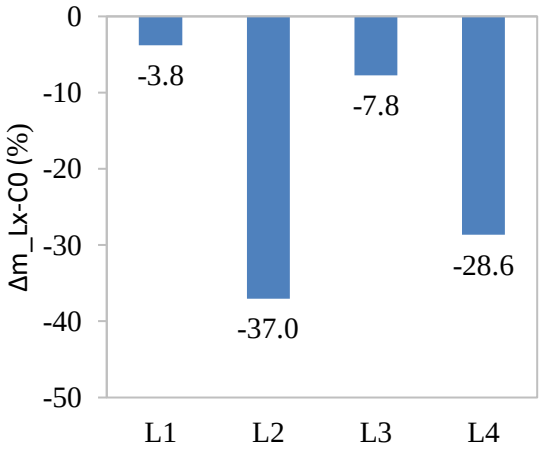

(e) GA9.5

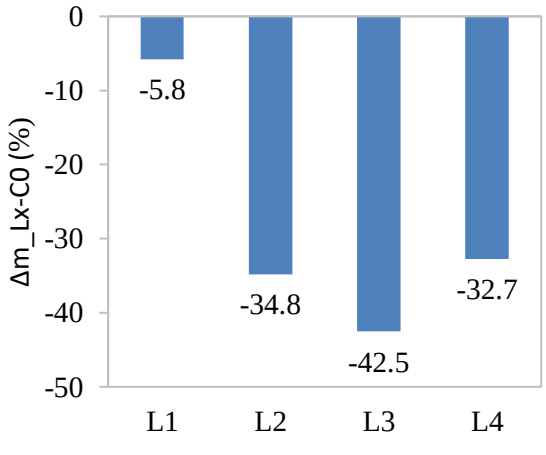

(f) GA12.5

Figure 5-9. CAL Test: (a) Instrument, (b) Specimen before and after the Test, (c-d) CAL Values, and (e-f) Percent Difference in CAL Values between Lx-Treated and Control Mixtures

5.2.3 Asphalt Pavement Analyzer Tests

The APA test involves the application of a wheel load (445 N or 100 lbf) on temperature-controlled SGC samples through a rubber hose (pressurized with 690 kPa or 100 psi) at a rate of 60 cycles per minute (see Figure 5-10) following AASHTO T 340 (2010b) until the total number of cycles (forward and backward pass of the wheels on the hoses) reaches the DOT-specified number (usually 8,000 cycles i.e., 16,000 wheel passes) or until the accumulated rut depth (d) reaches the DOT-specified depth (usually, 8 mm), whichever comes first. Mixtures that are rutting resistant have lower rut depths at a given number of cycles and need more cycles to reach same rut depth than their counterparts.

(a) Instrument

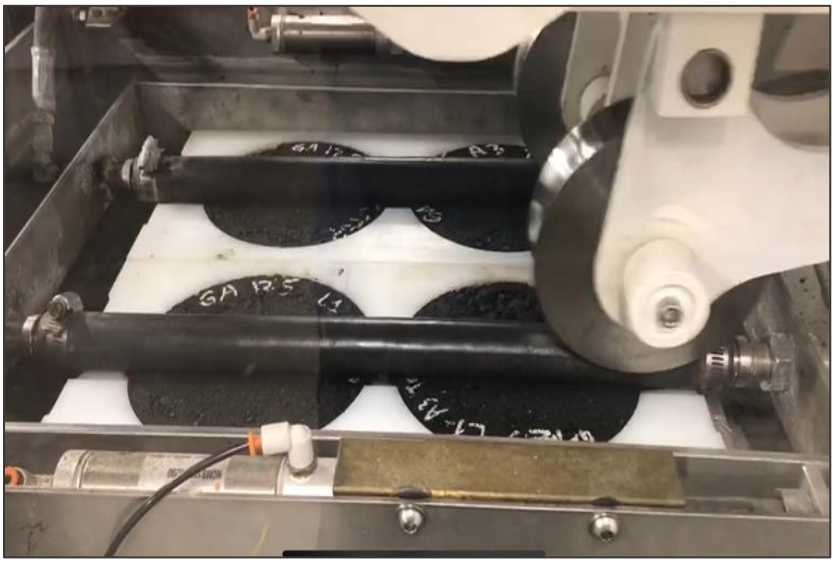

(b) Setup

Figure 5-10. APA Test: (a) Instrument; (b) Setup

In this study, two sets of SGC samples, each measuring 150.0 mm (5.91 in.) in diameter by 75.0 mm (2.95 in.) in height and 7.0% in target air void content were used for these tests. The first set was conditioned and tested at 64°C (147°F) while the other set was conditioned and tested at 74°C (165°F). The tests were continued until the total number of cycles reached 8,000 (i.e., 16,000-wheel passes) or until the rut depth reached 12.5 mm, whichever occurred first. Though rut depth criterion of 8.0 mm is usually used for this binder, the test termination criterion of 12.5 mm was selected in this study. Rut depths measured from the two sets of tests were used to determine the change in rut depth from 74°C to 64°C:

$$\Delta d_{7464}\ (\%) = \left(\frac{d_{74} - d_{64}}{d_{74}}\right) \times 100\% \qquad 5\text{-}4$$

where,

$d_{74°C}$ = Rut depth at 8,000 cycles of the selected asphalt binder at 74°C

$d_{64°C}$ = Rut depth at 8,000 cycles of the selected asphalt binder at 64°C

To better determine the effect of liquid ASA, the absolute values of rut depths at 8,000 cycles were then used to determine the effect of Lx:

$$\Delta d_{Lx,74°C}\ (\%) = \left[\frac{(d_{74})_{Lx} - (d_{74})_{C0}}{(d_{74})_{C0}}\right] \times 100\% \qquad 5\text{-}5$$

$$\Delta d_{Lx,64}\ (\%) = \left[\frac{(d_{64})_{Lx} - (d_{64})_{C0}}{(d_{64})_{C0}}\right] \times 100\% \qquad 5\text{-}6$$

Test results showed that rut depths of GA12.5 mixtures at 8,000 cycles were higher than rut depths of GA9.5 mixtures at 64°C in all but one case; however, the trend was not the same at 74°C [see Figure 5-11(a-b)]. Similarly, test results also showed that rut depths at 8,000 cycles were always higher at 74°C than at 64°C as illustrated by the percent increase in their values—an expected outcome resulting from an increase in test temperature [see Figure 5-11(c-d)].The difference in rut depths between control and liquid ASA-treated asphalt binders showed that, at 74°C, the use of liquid ASA reduced the rutting resistance (or increased the rut depths) of GA9.5 and GA12.5 mixtures in all but one case. However, at 64°C, the effect was the same in GA12.5 mixtures but opposite in GA9.5 mixtures, which negated the effectiveness of this parameter as an indicator of stability of asphalt mixtures after construction [see Figure 5-11(e-f)].

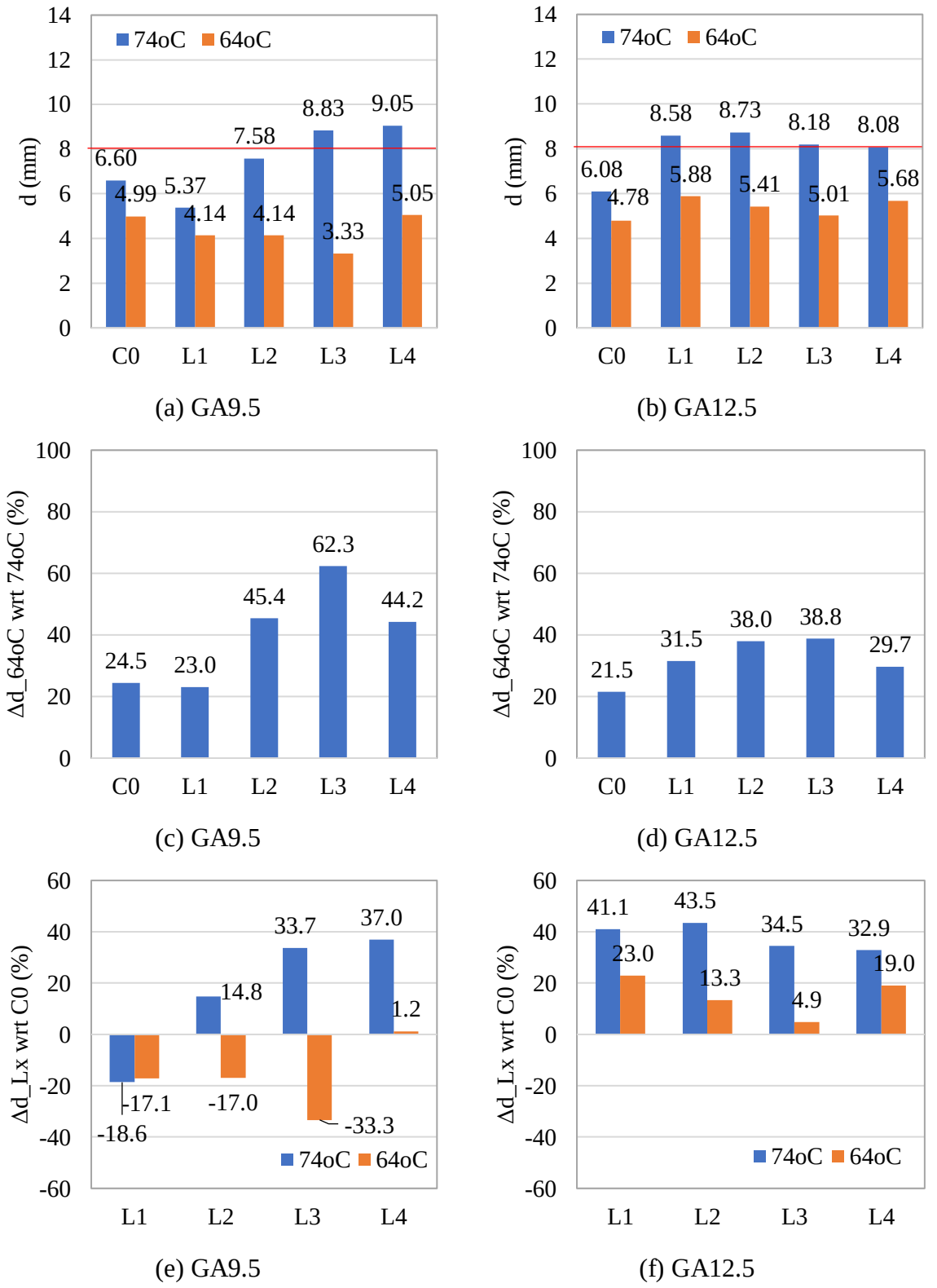

Figure 5-11. APA Test Results: (a-b) Rut Depths at 74°C and 64°C, (c-d) Percent Difference in Rut Depths between 74°C to 64°C, and (e-f) Percent Difference in Rut Depths between Lx-Treated and Control Mixtures

5.2.4 Hamburg Wheel-Track Tests

The HWT test involves the application of a steel wheel load (705 N or 158 lbf) on temperature-controlled, water-submerged SGC samples (see Figure 5-12) at a rate of 52 wheel passes per minute following AASHTO T 324 (2017b). The test is conducted until the total number of wheel passes reaches the DOT-specified number (usually 20,000) or until the accumulated rut depth (d) reaches the DOT-specified depth (usually 12.5 mm), whichever comes first.

(a) Instrument (b) Setup

Figure 5-12. HWT Test: (a) Instrument; (b) Setup

In this study, SGC samples measuring 150.0 mm (5.91 in.) in diameter by 63.5 mm (2.5 in.) in height and 7.0% in target air void content were fabricated for these tests. After cutting the samples in one side to fit them in testing molds, the samples were conditioned for two hours under water at 50°C (122°F) and then tested. The tests were continued until the wheel passes reached 20,000 or until the rut depth reached 12.5 mm, whichever occurred first.

HWT test results showed that of each of the five GA9.5 and five GA12.5 mixtures were able to withstand 20,000 wheel passes without any sign of stripping (i.e., stripping inflection point, SIP in the rut depth versus the number of pass curve), and without going beyond a rut depth of 12.5 mm, thereby confirming good performance of control and liquid ASA-treated mixtures [see Figure 5-13(a-b)].

Rut depths measured from these tests were then used to determine the percent difference in rut depths due to the use of liquid ASA with respect to the control mixture:

$$\Delta d_{Lx,50°C}\ (\%) = \left[\frac{(d_{50})_{Lx} - (d_{50})_{C0}}{(d_{50})_{C0}}\right] \times 100\% \qquad 5\text{-}7$$

where,

$(d_{50})_{Lx}$ = Rut depth at 20,000 passes of Lx-treated asphalt mixture at 50°C

$(d_{50})_{C0}$ = Rut depth at 20,000 passes of control asphalt mixture at 50°C

The results show that, in the case of GA9.5 mixtures, the rut depth value increased with the use of L2 and L4 but decreased with the use of L1 and L3 [see Figure 5-13(c-d)]. And in the case of GA12.5 mixtures, the rut depth value increased with the use of L1, L2 and L3 but negligibly decreased with the use of L4 [see Figure 5-13(c-d)]. The opposite rate of change in rut depth in GA9.5 and GA12.5 mixtures with respect to ASA showed that the HWT test and the proposed parameter could not be used to evaluate the effect of liquid ASA on the stability of the asphalt mixtures.

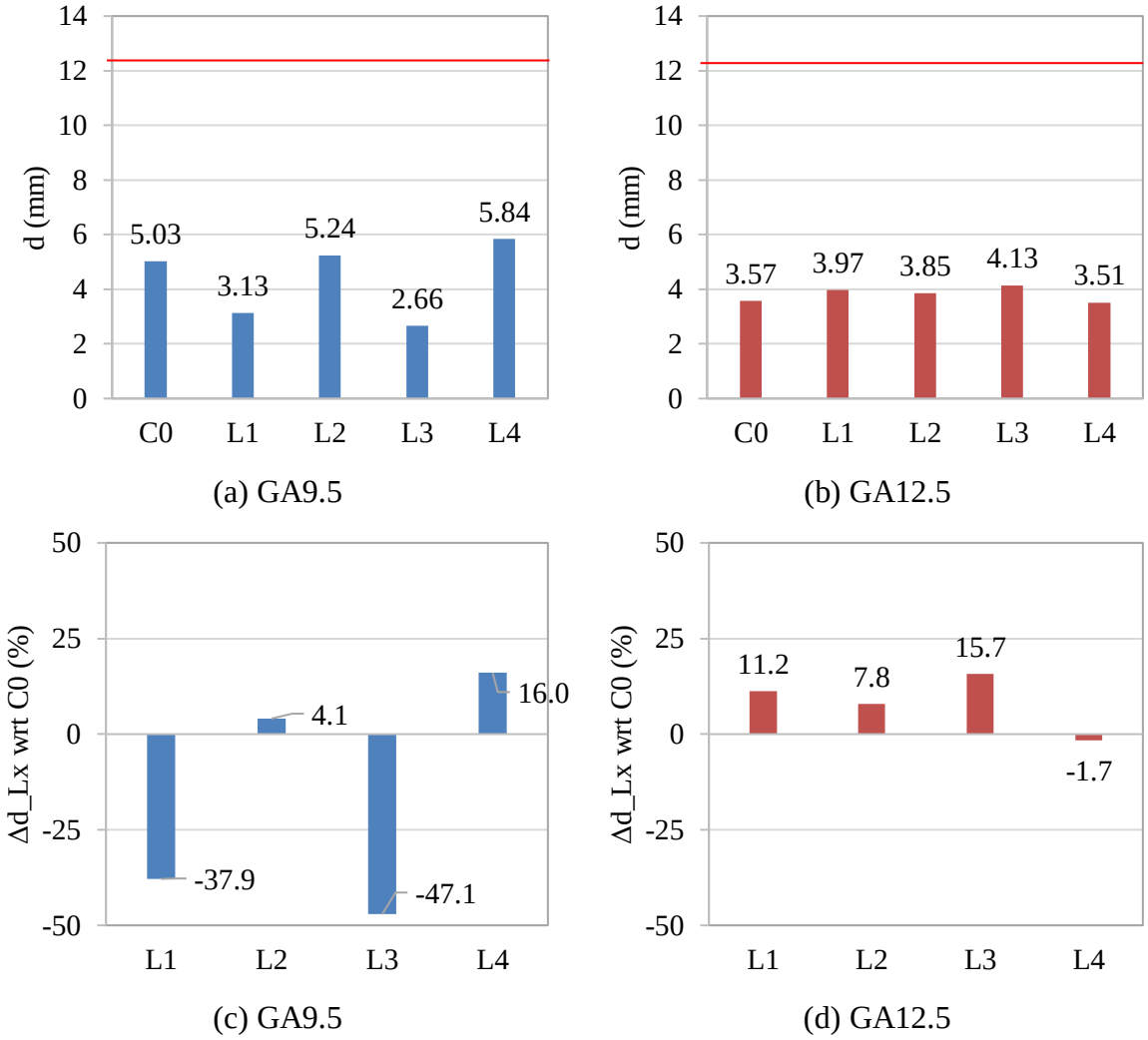

Figure 5-13. HWT Test Results: (a-b) Rut Depths at 50°C; (c-d) Percent Difference in Rut Depths between Lx-Treated and Control Mixtures

5.2.5 IDEAL Shear Rutting Tests

IDEAL shear rutting test was recently developed as an alternative method for evaluating rutting resistance of asphalt mixtures (Zhou et al., 2019). The test involves applying indirect tension on SGC samples of asphalt mixtures at a load-line displacement rate of 50 mm/min (2 inch/min) through a 19.0 mm (0.75 in.) wide strip until failure, measuring the peak force (P_{max})

experienced by the samples, and determining the value of shear strength (τ) using a unique relationship derived from shear stress (p) distribution (see Figure 5-14):

$$\tau = 0.356 \times p \quad \text{5-8}$$

where,

p =shear stress = $\frac{P_{\max}}{A}$

$P_{\max}$ = Peak force

A = Load application strip area = $h \times b$

h = Load application strip length = Compacted sample height

b = Load application strip width = 19.0 mm (0.75 in.)

Ideal shear rutting tests was selected for this study because shear strength is an indicator of rutting (shear) resistance of asphalt mixtures. Ideally, the greater the shear strength value, the more resistant to rutting is the asphalt mixture. Based on the correlation of shear strength with maximum allowable rut depth (Zhou et al., 2019), the asphalt mixtures that have good rutting performance usually have minimum shear strength of 1.2 MPa (which corresponds to 4.0 KN in peak load).

In this study, two set of SGC samples each measuring 150.0 mm (5.91 in.) in diameter by 63.5 mm (2.5 in.) in height and 7.0% in target air void content were produced for these tests. These specimens were identical to the ones used for the HWT test. After measuring the G_{mb} of these samples without any cutting and coring, the SGC samples were conditioned at 50°C or 122°F (the same temperature as used in the standard HWT test) in an environmental chamber for 2.5 hours.

Each specimen was then removed from the chamber and tested—the first set of two specimens each was tested immediately (i.e., at 50°C) while the second set was allowed to cool for 35 minutes at laboratory room temperature of 21.5°C before testing. The 35-minute of cooling corresponded to the time period required by the control mixture to cool down from 50°C to 40°C at the laboratory room temperature of 21.5°C. It is important to note that the 35-minute of cooling might not warrant the same amount of temperature drop in control and liquid ASA-treated mixtures.

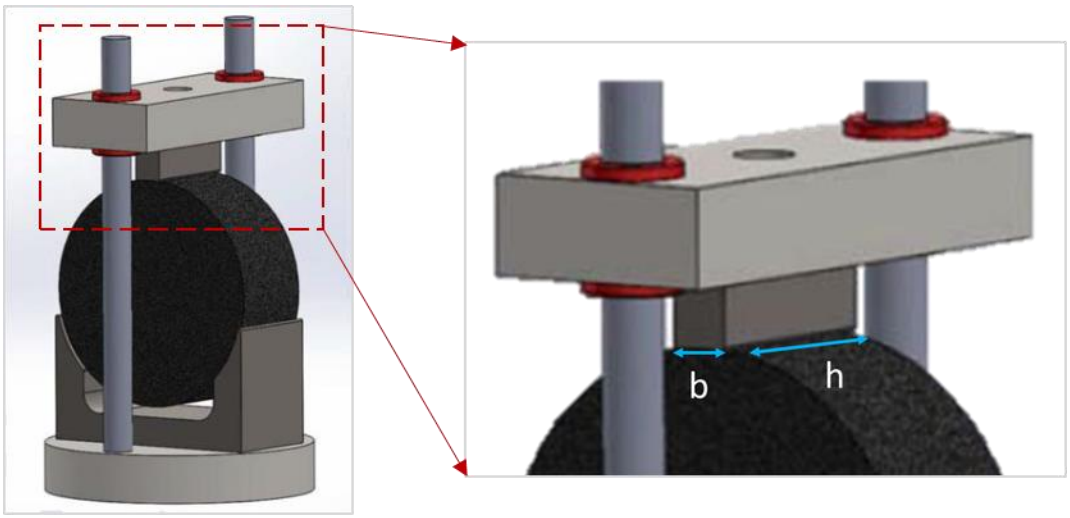

(a) Test Setup

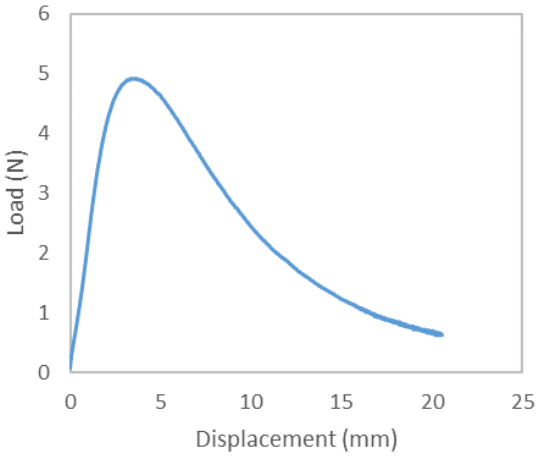

(b) Typical Test Result

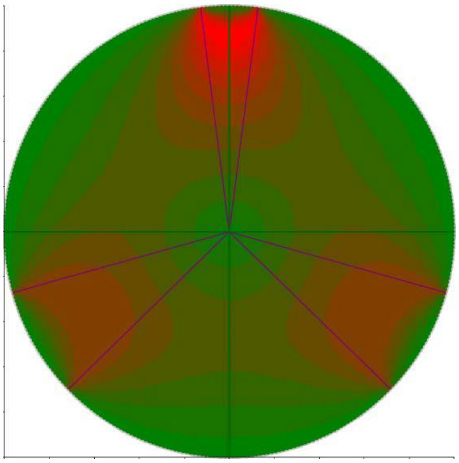

(c) Shear Stress Distribution

Figure 5-14. IDEAL Shear Rutting Test: (a) Setup, (b) Typical Result, and (c) Shear Stress Distribution (Zhou et al., 2019)

Test results also showed that the shear strength values measured after 35 minutes of cooling were higher than shear strength values measured without cooling (i.e., after 0 minutes of cooling) irrespective of the type of mix design and the use of liquid ASA [see Figure 5-15(c-d)]. This increase in shear strength during 35 minutes of cooling was essentially the result of the corresponding drop in effective temperature. To better understand this effect, the percent increase in shear strength over 35 minutes of cooling was determined using:

$$\Delta\tau\ (\%) = \left(\frac{\tau_{35\ min} - \tau_{0\ min}}{\tau_{0\ min}}\right) \times 100\% \qquad 5\text{-}9$$

where,

$\tau_{0\ min}$ = τ measured immediately after removing the sample from chamber

$\tau_{35\ min}$ = τ measured 35 minutes after removing the sample from the chamber

This analysis showed that the increase in shear strength values over 35 minutes of cooling was higher generally in L2 and L3 compared to C0, L1 and L4, possibly due to difference in temperature drop among them during this period [see Figure 5-15(c-d)]. More importantly, the test results also showed that liquid ASA-treated mixtures had lower shear strength than control mixtures irrespective of the type and dosage of liquid ASA, the type of mix design and the duration of cooling (see Figure 5-15(a-b)). Therefore, to better understand the effect of liquid ASA, the decrease in shear strength between the liquid ASA-treated and control mixtures were analyzed using:

$$\Delta\tau_{Lx,0\ min}\ (\%) = \left[\frac{(\tau_{0\ min})_{Lx} - (\tau_{0\ min})_{C0}}{(\tau_{0\ min})_{C0}}\right] \times\ 100\% \qquad 5\text{-}10$$

$$\Delta\tau_{Lx,35\ min}\ (\%) = \left[\frac{(\tau_{35\ min})_{Lx} - (\tau_{35\ min})_{C0}}{(\tau_{35\ min})_{C0}}\right] \times\ 100\% \qquad 5\text{-}11$$

This analysis showed that the shear strength values of liquid ASA-treated mixtures measured without allowing the samples to cool were lower than shear strength values of control mixtures in all but one case [see Figure 5-15(e-f)], highlighting the negative effect of liquid ASA on shear resistance and consequently on the stability of asphalt mixtures. This analysis also showed that the shear strength values of liquid ASA-treated mixtures measured after 35 minutes of cooling were lower than shear strength values of control mixtures by at least 9.0% and 8.6% in all but one GA9.5 and all GA12.5 mixtures without any exception, demonstrating the continuity of negative effect of liquid ASA on shear strength over cooling and the need to verify the results obtained from GA9.5 with GA12.5.

The negative effect of liquid ASA on shear strength irrespective of (a) whether the mixtures were tested 0 minute or 35 minutes following their removal from the environmental chamber and (b) whether the mixtures were SP/FC-9.5 or SP/FC-12.5 mm types revealed the applicability of the IDEAL shear rutting test to evaluate asphalt mixture stability. Since the second type of stability issue (i.e., the possibility of mixtures exhibiting markings of parked

vehicles and crumbling during inspection following a couple of days after compaction) is directly related to shear resistance, the shear strength obtained from the IDEAL shear rutting test can be used to evaluate the effect of liquid ASAs on this particular issue. Based on limited previously published data from other research projects and internal data, a threshold value of 1.2 MPa for shear strength at 50°C was selected as one of the parameters for evaluating and approving liquid ASAs. If the shear strength of the treated mixtures at 50°C (i.e., immediately after removing the samples from environmental chamber following 2.5 hours of conditioning period at 50°C) is equal to or higher than this value, the liquid ASA would be considered appropriate with respect to stability after construction.

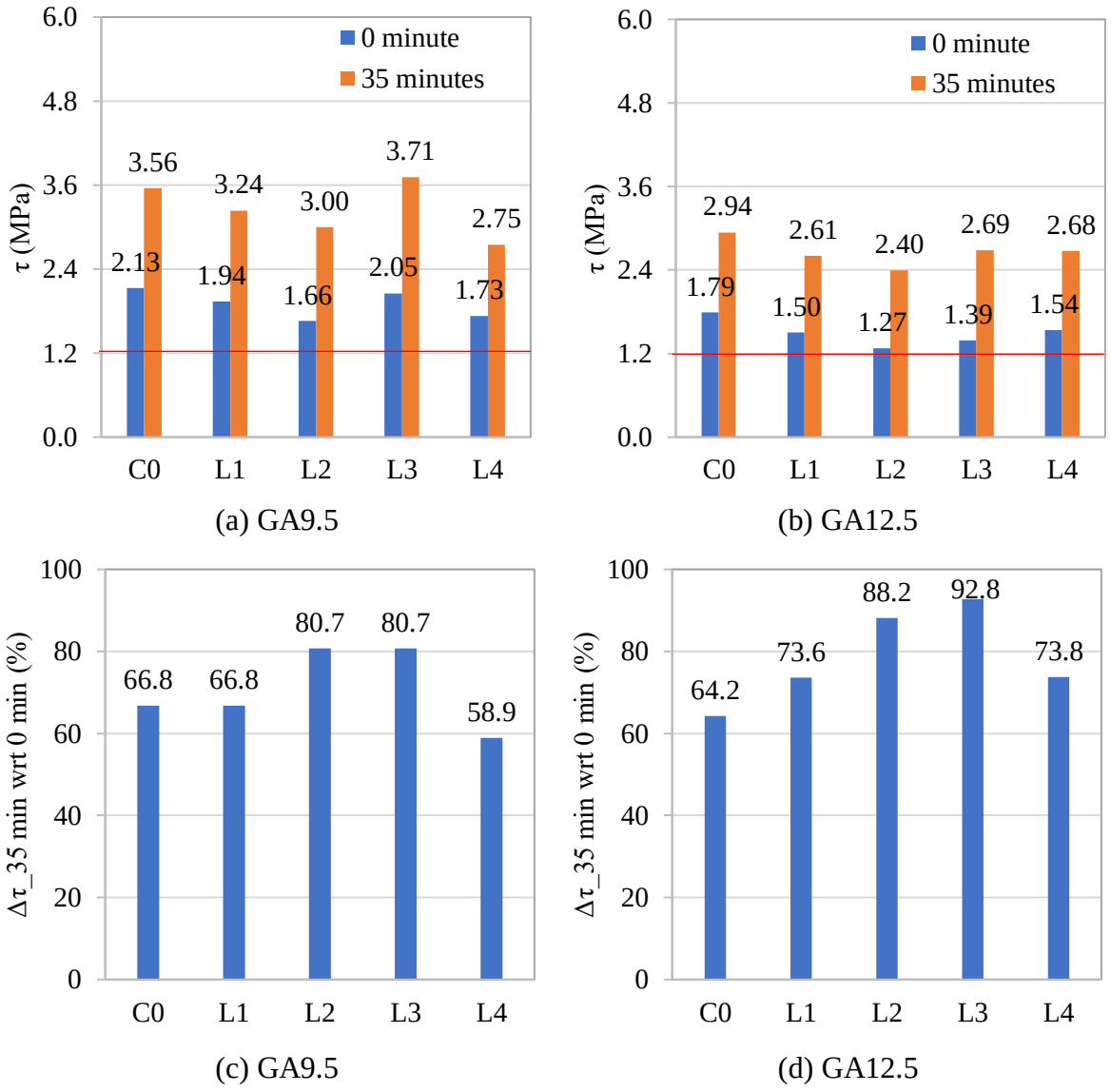

Figure 5-15. IDEAL Shear Rutting Test Results: (a-b) Shear Strengths after 0 and 35 Minutes of Cooling, (c-d) Percent Difference in Shear Strengths between 0 and 35 Minutes of Cooling, and (e-f) Percent Difference in Shear Strengths between Lx-Treated and Control Mixtures

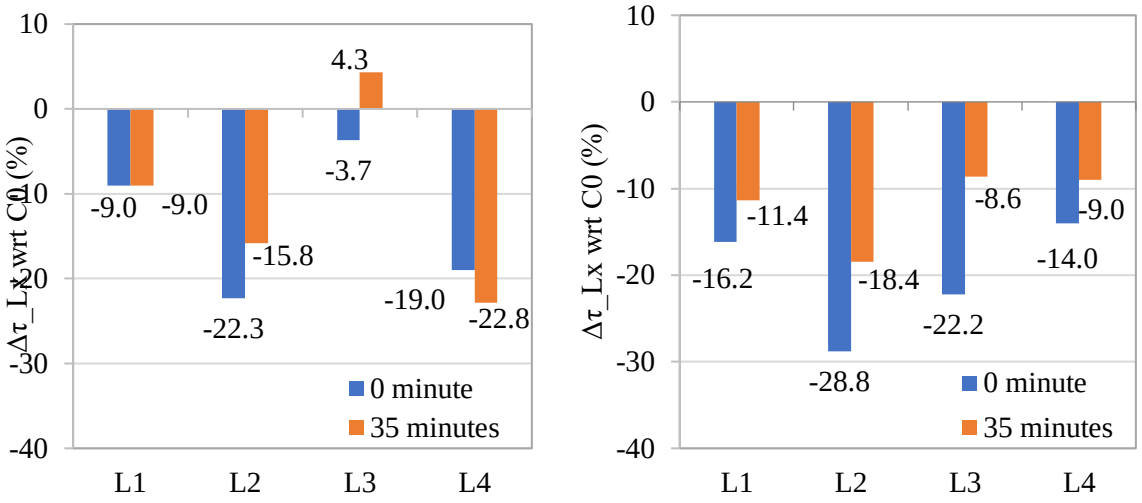

(e) GA9.5 (f) GA12.5

Figure 5-15. IDEAL Shear Rutting Test Results: (a-b) Shear Strengths after 0 and 35 Minutes of Cooling, (c-d) Percent Difference in Shear Strengths between 0 and 35 Minutes of Cooling, and (e-f) Percent Difference in Shear Strengths between Lx-Treated and Control Mixtures, Continued

5.3 Summary

Several different types of asphalt binders and asphalt mixture tests were performed in this part of the experimental plan to evaluate the stability of asphalt mixtures after compaction and determine the best test methods and parameters that could differentiate liquid ASA that yielded stable versus unstable asphalt mixtures after construction.

- FTIR test results revealed that liquid ASA-treated binders did not exhibit significant anomalies in chemical composition that could contribute to stability of mixtures during or after construction.
- Dynamic shear modulus tests showed that the liquid ASA-treated asphalt binders did not show significantly different G* and δ values at a given cooling interval or different rates of change in their values over a given period. Yet, the rate of change over a given period was different between the liquid ASA-treated asphalt binders and the control binder.
- Monotonic pull-off tests showed that liquid ASA-treated binder generally needed more pull-off force and work and demonstrated faster rates of increase in these values than control binder; however, the ranking of asphalt binders did not match the expected behavior based on limited field observations.
- Resilient modulus, CAL, APA, and HWT tests did not rank the selected four types of liquid ASA consistently for the GA9.5 and GA12.5 mixtures. However, the IDEAL shear rutting test showed that there was loss in shear strength due to the use of liquid ASA in all but one case, and implied that shear strength is a more appropriate parameter

to evaluate and approve the use of liquid ASA. Based on limited previously published data from other research projects and internal data, a threshold value of 1.2 MPa at 50°C can be used to evaluate effectiveness of liquid ASAs with respect to asphalt mixture stability after construction.

6 CONCLUSIONS AND RECOMMENDATIONS

6.1 Conclusions

6.1.1 Literature Review

The review of literature was focused on three main areas relevant to the objectives of this project: asphalt mixture stripping, asphalt mixture stability, and assessment tools (see Chapter 2). Based on this review, the following conclusions were drawn:

1. State highway agencies only use moisture damage susceptibility tests to approve the use and to estimate the required dose of hydrated lime and liquid ASA in their contracts; in other words, these agencies do not employ asphalt mixtures stability tests for product approval or dosing.
2. Researchers have recognized liquid ASA as one of the many mix design-related factors that can impact the stability of asphalt mixtures, but they have not studied the type and severity of such effects extensively.
3. Measures of workability and compactability during mixing and compaction have been employed to assess the stability of asphalt mixtures with minimal correlation between parameters.
4. Stability during construction while the asphalt mixture is still hot has been mostly assessed in the laboratory with parameters that can be obtained from the initial part of compaction curves and tied to workability and compactability of mixtures under rollers during construction.
5. Stability after construction while the asphalt mixture is partially cooled down has not been studied extensively.
6. Stability after construction when the asphalt mixture has already cooled down to ambient temperature has been mostly assessed in the laboratory with parameters that can be extracted from the latter part of compaction curves and tied to resistance to plastic deformation in the field. In addition, stiffness and wheel-track tests are commonly used in the laboratory to analyze the resistance to deformation.

6.1.2 Parameters Obtained from Compaction Data

Based on analysis of data accumulated during compaction of 20 mixtures (with a minimum 2 replicates each), the following conclusions were drawn (see Chapter 4):

1. Thirteen parameters—four compaction effort parameters ($N98$, $N98\text{-}NG1$, $GR_{log9895}$, and $GR_{log9896}$), one compaction density parameter (CLP), one compaction rate parameter (CI), four densification parameters (TDI_{NG1N98}, TI_{NG1N98}, TI_{NLPN96}, and TI_{NLPN98}) and three compaction energy parameters (SEI_{NLPN96}, SEI_{NLPN98}, and CEI_{N92N98}) —were able to differentiate C0 (stable), L1- and L2-treated mixtures from L3- and L4-treated mixtures.
2. Among them, $N98$, $GR_{log9895}$, $GR_{log9896}$, and CLP refer to either the absolute values of volumetric properties at certain conditions or their differences or ratios. However,

these parameters do not represent the overall behavior of mixture during or after compaction and were not used to develop approval system for liquid ASA.

3. Similarly, compaction index obtained from laboratory compaction data (CI) represents the rate of compaction from uncompacted air void level to 8% air void content or 92%G_{mm}. Since this parameter is obtained from the initial part of the compaction data where significant change in height or air void happens with minimal shear resistance, this parameter was used to develop approval system for liquid ASAs.
4. SEI_{NLPN96}, SEI_{NLPN98}, and CEI_{N92N98} represent energy required to compact mixtures against shear resistance after aggregates have reached locking point or mixes have reached 92%Gmm (i.e., area under the compaction energy versus gyration number curve). Among these three parameters, SEI_{NLPN96} is redundant because area used to calculate SEI_{NLPN98} (i.e., area from *NLP* to 98%G_{mm}) already includes area used to calculate SEI_{NLPN96} (i.e., area from *NLP* to 96% G_{mm}). Therefore, SEI_{NLPN98} and CEI_{N92N98} were used to develop approval system for liquid ASAs.

6.1.3 Parameters Obtained from Tests Conducted after Compaction

Based on the results of several tests conducted on 5 binders and 10 mixtures, the following conclusions were drawn (see Chapter 5):

6.1.3.1 Binder Tests

1. FTIR test results did not reveal any anomalies in the chemical composition of liquid ASA-treated asphalt binders that might be related to the stability of mixtures during or after construction.
2. Asphalt binder tests (dynamic shear modulus and monotonic pull-off tests) showed that the liquid ASA-treated asphalt binders exhibited slightly lower G^*, higher δ, lower $P_{\max}$, and lower W values. In addition, during the cooling process, the ASA-treated asphalt binders exhibited slower rates of change in these values than control binders, highlighting the negative effect of liquid ASA on stiffness, viscosity, tack properties of asphalt binders. However, these parameters obtained from these tests did not rank the liquid ASA consistently and therefore were not used to develop approval system for liquid ASAs.

6.1.3.2 Mixture Tests

1. The asphalt mixture performance tests selected for this project (namely, resilient modulus, CAL, APA, and HWT tests) ranked the four liquid ASA differently compared to control mixture for both mix types (i.e., granite and limestone).
2. The IDEAL shear rutting tests consistently showed that liquid ASA-treated mixtures always had lower shear strength than the control mixtures throughout the 35-minute long cooling period.
3. As such, shear strength values measured from two different types of mixtures were used to develop the protocol and additional criteria for evaluating of the effect of liquid ASA on the stability of asphalt mixtures after construction. The protocols and

criteria developed for evaluating the effect of liquid ASA on the stability of asphalt mixtures both before and after construction were then combined into one protocol as presented in Chapter 7.

6.2 Limitations

1. This study used only one source and grade of asphalt binder i.e., SBS-modified PG 76-22 (PMA) to develop the protocol presented in the Chapter 7. Since the liquid ASA is combined with the binder prior to mixing the asphalt mixture components, it is critical to verify the conclusions drawn from this study are applicable when other sources and grades of binder are used.
2. This study did not include a field test validation. As such, it is equally, if not even more critical to verify the conclusions drawn from this study with field observations.
3. The ranking of the ASA's (L3 and L4 being more prone to shoving and rutting than L1 and L2) were based on limited field reports prior to this research.
4. The recommended threshold value of shear strength is based on limited previously published data from other research projects and internal data.

6.3 Recommendations

1. Based on these conclusions, it is recommended using the Superpave compaction data analyses and the IDEAL rutting tests to identify liquid ASAs that can adversely affect mixture stability during construction and immediately after construction as presented in Chapter 7.
2. Based on the inability of M_r, APA, CAL and HWT tests to differentiate liquid ASAs that impact asphalt mixture stability versus those that do not impact asphalt mixture stability, it is recommended not using these tests for this particular purpose.
3. Based on the limitations of this study, it is recommended verifying the conclusions drawn from this study with other sources and grades of binders, revising the protocol, if needed and validate the results with field data.
4. Because the threshold value of 1.2 MPa for shear strength is based on limited data, it is also recommended to check whether other typical mixtures used in Florida pass this threshold value and, if warranted, revise it.
5. After this verification, it is recommended implementing the protocol as a part of FM 5-508 or a stand-alone test method.

7 LIQUID ANTI-STRIP AGENT APPROVAL SYSTEM

7.1 Scope

This method covers the preparation of gyratory compacted specimens, measurement of stability parameters extracted from data collected during Superpave gyratory compaction of bituminous mixtures in the laboratory and measurement of parameters extracted from tests conducted on the Superpave gyratory compacted samples after compacting, cooling and conditioning. The results may be used to predict the effect of liquid anti-strip agents on the stability of bituminous mixtures during construction and to approve liquid anti-strip agents. The values stated in SI units are to be regarded as the standard.

7.2 Referenced Documents

7.2.1 AASHTO Standards

- R 30 Standard Practice for Mixture Conditioning of Hot-Mix Asphalt (HMA)
- T 312 Standard Method for Preparing and Determining the Density of Hot-Mix Asphalt (HMA) by Means of the Superpave Gyratory Compactor
- T 245 Resistance to Plastic Flow of Asphalt Mixtures Using Marshall Apparatus

7.2.2 ASTM Standards

- D 3549 Standard Test Method for Thickness or Height of Compacted Bituminous Paving Mixture Specimens

7.2.3 Florida Method of Tests

- FM 1-T 166 Bulk Specific Gravity of Compacted Bituminous Mixtures
- FM 1-T 168 Sampling Bituminous Paving Mixtures
- FM 1-T 209 Maximum Specific Gravity of Bituminous Paving Mixtures
- FM 1-T 283 Resistance of Compacted Bituminous Mixture to Moisture-induced damage

7.2.4 Journal Articles

- Zhou, F., Crockford, B., Zhang, J., Hu, S., Epps, J., and Sun, L. “Development and Validation of an Ideal Shear Rutting Test for Asphalt Mix Design and QC/QA”. Proceedings of the Association of Asphalt Paving Technologists, 2019.

7.3 Significance and Use

As noted in the scope, this method is intended to evaluate the effects of liquid anti-strip agents on the stability of bituminous mixtures during and after compaction in the laboratory.

7.4 Summary of Method

Pre-batched aggregate samples and liquid anti-strip agents are obtained from the supplier. Three sets or groups of Superpave gyratory compacted specimens are prepared from each mix—one group with untreated asphalt binder and two groups with asphalt binder treated with the liquid anti-strip agents [see Figure 7-1(a)]. The untreated and the first sets of treated samples (two specimens each) are used to obtain three different parameters that describe asphalt mixture stability during and after construction. If the mixtures treated with the liquid anti-strip agents satisfy the criteria set for these parameters, the second sets of treated samples (four specimens each) from each mix type are subjected to the IDEAL shear rutting test at 50.0 ± 1.0°C (122 ± 2.0°F) to obtain one more parameter that can describe asphalt mixture stability after construction. The effectiveness of liquid anti-strip agent in terms of asphalt mixture stability is again analyzed in terms of this parameter. [**Note**: To check whether the untreated mixture itself passes the criteria set for this parameter, one additional pre-batched aggregate sample can be obtained from each mix type. From this additional batch, untreated mixture samples can be prepared and subjected to the IDEAL shear rutting test.]

7.5 Apparatus

- Equipment for determining the theoretical maximum specific gravity (G_{mm}) of the asphalt mixture in accordance to FM 1-T 209.
- Balance and water bath in accordance to FM 1-T 166.
- Environmental chamber capable of maintaining a temperature of 50 ± 1 °C (122 ± 2°F).
- Forced-draft oven in accordance to AASHTO R 30, thermostatically controlled, capable of maintaining any desired temperature setting from room temperature to 166 ± 3°C (330 ± 5°F).
- Loading jack and ring dynamometer in accordance to AASHTO T 245 to provide a range of accurately controllable rates of vertical deformation including 50 mm per minute (2 in. per minute).
- 19-mm wide loading strip and two-point support system in accordance to Zhou et al. (2019).

7.6 Submittal of Test Specimens

- Submit three pre-batched aggregate specimens of SP-9.5/FC-9.5 and three pre-batched aggregate specimens of SP-12.5/FC-12.5 of granite aggregates. Each batch shall be enough to prepare at least three mix design samples (115.0 ± 5.0 mm in height by 150.0 mm in diameter, 4.0 ± 0.5 air void content at design number of gyrations) or at least four IDEAL shear rutting tests (63.5 ± 0.5 mm in height by 150.0 mm in diameter, 7.0 ± 1.0 air void content) and at least two G_{mm} tests (1000-1100 grams), whichever is the largest. The pre-batched samples must be representative of an existing mix design

currently approved for use in the State of Florida by the Department. One out of three pre-batched aggregates from each mix design will be used to prepare samples with untreated asphalt binders and the rest will be used to prepare samples with liquid anti-strip agent treated asphalt binders as illustrated in Figure 7-1(a) and as described in Sections 7.7 and 7.8. [**Note**: To check whether the untreated mixture itself passes the criteria set for the parameters obtained from the IDEAL shear rutting test, one more pre-batched aggregate sample can be obtained from each mix type. From this batch, untreated mixture samples can be prepared following Section 7.8 and subjected to the IDEAL shear rutting test following Section 7.11.]

- Submit a sample of the liquid anti-strip agent to the Department. The Department will provide PG 76-22 (PMA) binder and blend it with the supplied liquid anti-strip agent at dosage as specified in the approved product list.

7.7 Preparation of Specimens to Analyze Stability Parameters from Compaction Data

- Preheat and mix the untreated asphalt binder and two out of three pre-batched SP-9.5/FC-9.5 and SP-12.5/FC-12.5 aggregates at mixing temperature of 166 ± 5°C (330 ± 5°F) [see Figure 7-1(a)].
- After mixing, condition the loose mixtures in a pan for two hours at the compaction temperature of 166 ± 5°C (330 ± 5°F) as per AASHTO R 30.
- Determine G_{mm} of the mixture using at least two specimens of untreated and treated mixtures by FM 1-T 209.
- Compact the first set of samples from each treated and untreated mix into 150.0-mm diameter cylindrical specimens (at least two) until the number of gyrations reaches $N_{\max}$ in accordance to AASHTO T 312.
- Record each compacted height, normal stress, shear stress at each gyration. The air void content of control sample shall satisfy 4.0 ± 0.5 percent (or 96.0 ± 0.5%G_{mm}) at the design number of gyrations N_{design}.

7.8 Preparation of Specimens to Analyze Stability Parameters from Tests Conducted after Compaction

These sets of specimens are prepared only if specimens prepared in Section 7.7 pass the approval criteria for liquid anti-strip agents set in Section 7.10 [see Figure 7-1(a)].

- Preheat and mix the treated asphalt binder and the remaining pre-batched SP-9.5/FC-9.5 and SP-12.5/FC-12.5 aggregates at mixing temperature of 166 ± 5°C (330 ± 5°F) [see Figure 7-1(a)].
- After mixing, condition the loose mixtures in a pan for two hours at the compaction temperature of 166 ± 5°C (330 ± 5°F) as per AASHTO R 30.
- Determine G_{mm} of the mixture using at least two specimens of treated mixtures by FM 1-T 209, if not determined in step 7.7.
- Compact the second set of samples from each treated mix into 150.0-mm diameter cylindrical specimens (at least four) until compacted height reaches 63.5 ± 0.5 mm. The air void content of each specimen shall satisfy 7.0 ± 1.0 percent or 93.0 ± 1.0%G_{mm}.

[**Note**: To check whether the untreated mixture itself passes the criteria set for the parameters obtained from the IDEAL shear rutting test, one more pre-batched aggregates can be obtained from each mix type. From this batch, untreated mixture samples can be fabricated following Section 7.8 and subjected to the IDEAL shear rutting test following Section 7.11. The sample can be fabricated and tested with treated mixture at the end of the protocol as shown in Figure 7-1(b) as a screening test at the beginning of the protocol as shown in see Figure 7-1(c). The protocol in Figure 7-1(b) approves the liquid anti-strip agent if both treated and untreated mixtures pass the criteria set for parameters obtained from both the compaction data analysis and the IDEAL shear rutting test. The protocol in Figure 7-1(c) first requires the treated mixture to pass the criteria set for parameter obtained from the IDEAL shear rutting test (i.e., shear strength > 1.2 MPa) and only then proceed to remaining steps.]

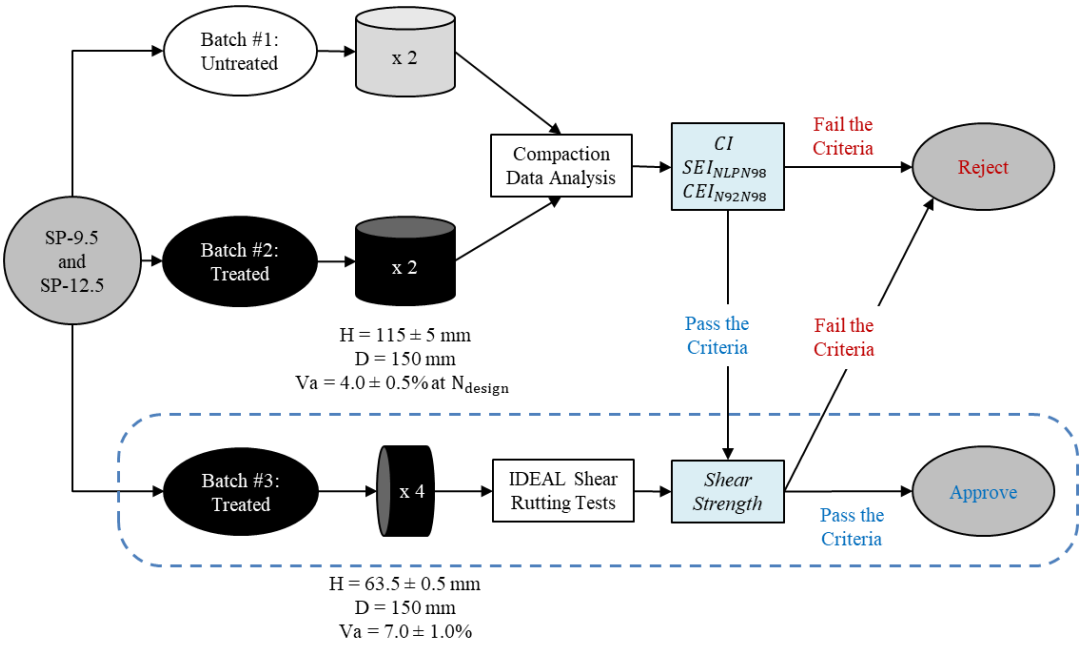

(a) Protocol that does not involve the IDEAL shear rutting tests of untreated mixtures

Figure 7-1. Sample Fabrication and Test Plan for Liquid Anti-Strip Agent Approval

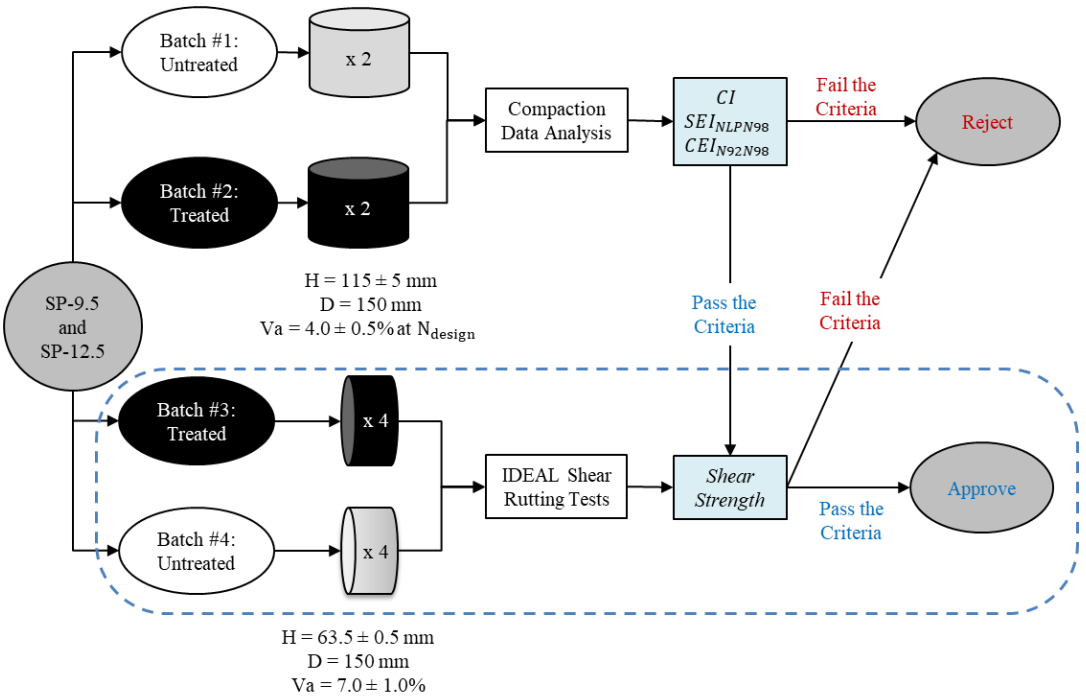

(b) Protocol that involves the IDEAL shear rutting tests of untreated mixtures at the end

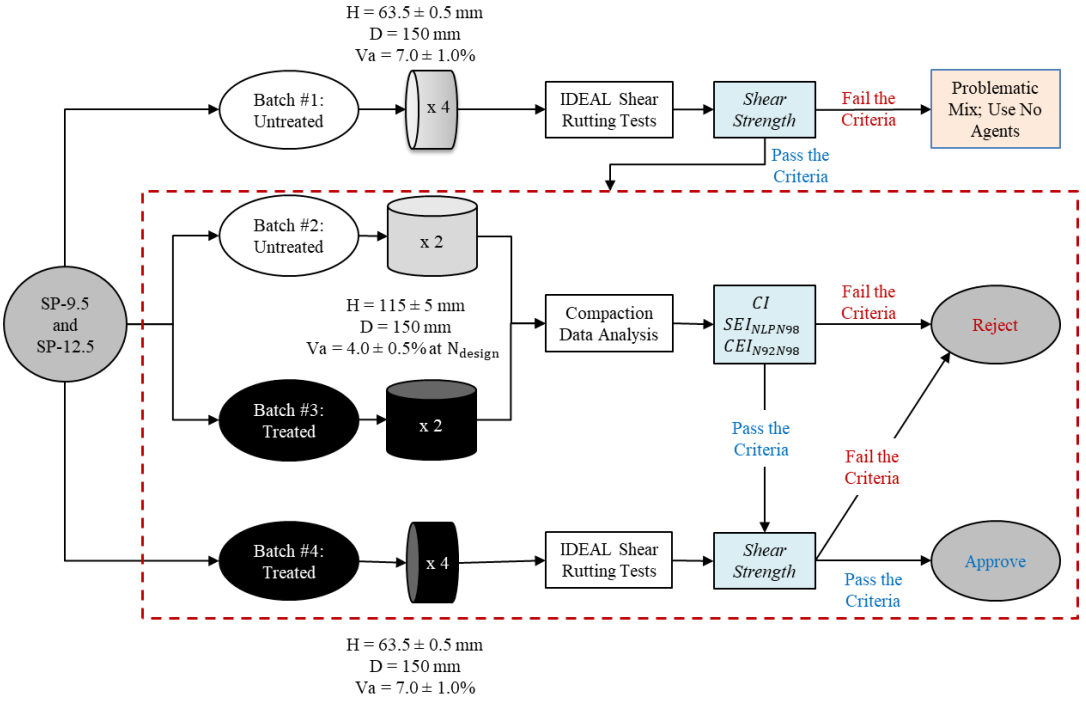

(c) Protocol that involves the IDEAL shear rutting tests of untreated mixtures at the beginning

Figure 7-1. Sample Fabrication and Test Plan for Liquid Anti-Strip Agent Approval, Continued

7.9 Evaluation of Test Specimens

- Determine specimen thickness by ASTM D 3549.
- Determine the bulk specific gravity, G_{mb} by FM 1-T 166 (nondestructive method).
- Calculate air void content:

$$Va\ (\%) = \frac{Gmm - Gmb}{Gmm} \times 100\% \qquad 7\text{-}1$$

7.10 Stability Parameters Obtained from Compaction Data

- Using compaction height versus gyration number data obtained from the first set of samples from each mix (samples with 4.0 ± 0.5 percent air voids at N_{design}), determine average and standard deviation values of laboratory compaction, shear energy and compactability energy indices for both control and treated asphalt mixtures:

$$CI = \frac{m^{1.2}}{c} \qquad 7\text{-}2$$

$$SEI_{NLPN98} = \sigma \times \left(\frac{\pi D^2}{4}\right) \times \sum_{NLP}^{N98} \Delta h_N \qquad 7\text{-}3$$

$$CEI_{N92N98} = \frac{SEI_{N92N98}}{N98 - N92} \qquad 7\text{-}4$$

where,

$$SEI_{N92N98} = \sigma \times \left(\frac{\pi D^2}{4}\right) \times \sum_{N92}^{N98} \Delta h_N \qquad 7\text{-}5$$

and,

CI = Compaction index obtained from laboratory compaction data

m = Slope of air void versus gyration curve until 92%G_{mm} = $\left|\frac{8\%-c}{log(N92)}\right|$

c = Intercept of air void content versus gyration curve until 92%G_{mm}= AV_0

$N92$ = Number of gyrations at 92%G_{mm}

SEI = Shear energy index

CEI = Compactability energy index

NLP = First number of gyrations that yields $\Delta h \leq 0.05$ mm

$N98$ = Number of gyrations at 98%G_{mm}

σ = Normal or vertical stress

$D =$ Diameter of the compacted sample

- Determine the upper and lower limits of selected parameter for control mix and liquid anti-strip agent-treated mix:

$$UL_{C0} = y_{C0} + z \times d_{C0} \quad 7\text{-}6$$

$$LL_{C0} = y_{C0} - z \times d_{C0} \quad 7\text{-}7$$

$$UL_{Lx} = y_{Lx} + z \times d_{Lx} \quad 7\text{-}8$$

$$LL_{Lx} = y_{C0} - z \times d_{Lx} \quad 7\text{-}9$$

where,

$UL =$ Upper limit of selected parameter

$LL =$ Lower limit of selected parameter

y= Average value of selected parameter

d= Standard deviation value of selected parameter

$C0 =$ Untreated, control (stable) mixture

$Lx =$ Liquid anti-strip agent-treated mixture

$z = 95\%$ confidence level variate $= 1.96$

- Determine whether selected liquid anti-strip agent-treated mixture will have instability issues during compaction:
  - If $UL_{Lx} \leq UL_{C0}$ and $LL_{Lx} \geq LL_{C0}$ are satisfied, Lx-treated mixture is equivalent to control mixture in terms of stability and therefore will not have issues during and after compaction.
  - If the above condition is not satisfied (i.e., if $UL_{Lx} > UL_{C0}$ or $LL_{Lx} < LL_{C0}$), Lx-treated mixture is not equivalent to control mixture in terms of stability.
    - If $y_{Lx} < y_{C0}$, where y = *CI* or *CEI*, Lx-treated mixture will have stability issues.
    - If $y_{Lx} > y_{C0}$, where y = *CI* or *CEI*, Lx-treated mixture will not have stability issues.

7.11 Stability Parameters Obtained from Tests Conducted after Compaction

These set of tests are conducted only if specimens prepared according to Section 7.7 pass approval criteria set for liquid anti-strip agents in Section 7.10 [see Figure 7-1(a)]. Specimens prepared in Section 7.8 are used for the tests mentioned in this section.

- Condition the set of compacted samples from each mix with 7.0 ± 1.0 percent air voids at 50.0 ± 1.0°C (122.0 ± 2.0°F) in an environmental chamber for a minimum 2.5 hours.
- Remove all compacted samples from the environmental chamber.
- Immediately run IDEAL shear rutting tests on each sample.
- Determine peak load from raw data and determine corresponding values of shear strengths:

$$\tau = 0.356 \times p \qquad 7\text{-}10$$

where,

p = Shear stress $= \frac{P_{\max}}{A}$

$P_{\max}$ = Peak force (in newton or lb.)

A = Load application strip area $= h \times b$

h = Load application strip length = Compacted sample height (in mm or in.)

b = Load application strip width =19.0 mm (0.75 in.)

- Determine whether selected liquid anti-strip agent-treated mixture will have instability issues after construction:
  - $\tau_{Lx} \geq 1.2\ MPa$ ➔ Lx-treated mixture will not have stability issues.
  - $\tau_{Lx} < 1.2\ MPa$ ➔ Lx-treated mixture will have stability issues.

  [Note: If $\tau_{C0} < 1.2\ MPa$ as determined following the protocols presented in Figure 7-1(b) or Figure 7-1(c), the treated mixture itself might be problematic and should not be used for this approval decision. In other words, the liquid anti-strip agent might not be alone responsible for failing the 1.2 MPa criteria of shear strength.]

7.12 Decision of Approval

- If the liquid anti-strip agent-treated mixture satisfies each of the criteria set for the stability of asphalt mixtures during and after compaction, the anti-strip agent shall be approved.

REFERENCES

American Association of State Highway and Transportation Officials (AASHTO), 2018. AASHTO TP 108-14 Standard Method of Test for Determining the Abrasion Loss of Asphalt Mixture Specimens. American Association of State Highway and Transportation Officials, Washington, DC.

American Association of State Highway and Transportation Officials (AASHTO), 2017a. AASHTO M 323 Standard Specification for Superpave Volumetric Mix Design. American Association of State Highway and Transportation Officials, Washington, DC.

American Association of State Highway and Transportation Officials (AASHTO), 2017b. AASHTO T 324 Standard Method of Test for Hamburg Wheel-Track Testing of Compacted Asphalt Mixtures. American Association of State Highway and Transportation Officials, Washington, DC.

American Association of State Highway and Transportation Officials (AASHTO), 2015. AASHTO T 312 Standard Method of Test for Preparing and Determining the Density of Asphalt Mixture Specimens by Means of the Superpave Gyratory Compactor. American Association of State Highway and Transportation Officials, Washington, DC.

American Association of State Highway and Transportation Officials (AASHTO), 2014a. AASHTO T 283 Standard Method of Test for Resistance of Compacted Asphalt Mixtures to Moisture-Induced Damage. American Association of State Highway and Transportation Officials, Washington, DC.

American Association of State Highway and Transportation Officials (AASHTO), 2014b. AASHTO T 350 Standard Method of Test for Multiple Stress Creep Recovery (MSCR) Test of Asphalt Binder Using a Dynamic Shear Rheometer (DSR). American Association of State Highway and Transportation Officials, Washington, DC.

American Association of State Highway and Transportation Officials (AASHTO), 2014c. AASHTO M 332 Standard Specification for Performance-Graded Asphalt Binder Using Multiple Stress Creep Recovery (MSCR) Test. American Association of State Highway and Transportation Officials, Washington, DC.

American Association of State Highway and Transportation Officials (AASHTO), 2014d. AASHTO R 30 Standard Practice for Mixture Conditioning of Hot Mix Asphalt (HMA). American Association of State Highway and Transportation Officials, Washington, DC.

American Association of State Highway and Transportation Officials (AASHTO), 2013. AASHTO T 240 Standard Method of Test for Effect of Heat and Air on a Moving Film of Asphalt. American Association of State Highway and Transportation Officials, Washington, DC.

American Association of State Highway and Transportation Officials (AASHTO), 2012a. AASHTO T 209 Standard Method of Test for Theoretical Maximum Specific Gravity (Gmm) and Density of Hot Mix Asphalt (HMA). American Association of State Highway and Transportation Officials, Washington, DC.

American Association of State Highway and Transportation Officials (AASHTO), 2012b. AASHTO R 28 Standard Practice for Accelerated Aging of Asphalt Binder Using a

Pressurized Aging Vessel. American Association of State Highway and Transportation Officials (AASHTO), Washington, DC.
American Association of State Highway and Transportation Officials (AASHTO), 2012c. AASHTO T 315 Standard Method of Test for Determining the Rheological Properties of Asphalt Binder Using a Dynamic Shear Rheometer (DSR). American Association of State Highway and Transportation Officials, Washington, DC.
American Association of State Highway and Transportation Officials (AASHTO), 2012d. AASHTO T 313 Standard Method of Test for Determining the Flexural Creep Stiffness of Asphalt Binder Using the Bending Beam Rheometer (BBR). American Association of State Highway and Transportation Officials, Washington, DC.
American Association of State Highway and Transportation Officials (AASHTO), 2010a. AASHTO M 303-89 Standard Specification for Lime for Asphalt Mixtures. American Association of State Highway and Transportation Officials, Washington, DC.
American Association of State Highway and Transportation Officials (AASHTO), 2010b. AASHTO T 340 Standard Method of Test for Determining Rutting Susceptibility of Hot Mix Asphalt (HMA) Using the Asphalt Pavement Analyzer (APA). American Association of State Highway and Transportation Officials, Washington, DC.
American Association of State Highway and Transportation Officials (AASHTO), 2002. AASHTO T 165 Standard Method of Test for Effect of Water on Cohesion of Compacted Bituminous Mixtures. American Association of State Highway and Transportation Officials, Washington, DC.
Abu Abdo, A.M., Bayomy, F., Nielsen, R., Weaver, T., Jung, S.J., Santi, M., 2010. Development and Evaluation of Hot Mix Asphalt Stability Index. International Journal of Pavement Engineering 11, 529–539. https://doi.org/10.1080/10298436.2010.488728
Alabama Department of Transportation (ALDOT), 2018. Standard Specifications for Highway Construction. Alabama Department of Transportation, Montgomery, AL.
Alabama Department of Transportation (ALDOT), 2008. ALDOT 361 Resistance of Compacted Hot-Mix Asphalt to Moisture Induced Damage. Alabama Department of Transportation, Montgomery, AL.
Al-Swailmi, S., Terrel, R.L., 1993. Evaluation of the Environmental Conditioning System (ECS) and Comparison with AASHTO T-283. Journal of the Association of Asphalt Paving Technologists 62, 150–171.
Al-Swailmi, S., Terrel, R.L., 1992. Evaluation of Water Damage of Asphalt Concrete Mixtures Using the Environmental Conditioning System (ECS). Journal of the Association of Asphalt Paving Technologists 61, 405–445.
Amirkhanian, S., Xiao, F., Corey, M., 2018. Laboratory Performance of Liquid Anti-Stripping Agents in Asphalt Mixtures used in South Carolina (Report No. FHWA-SC-18-01). Tri-County Technical College, Pendleton, SC.
Anderson, R., Bahia, H., 1997. Evaluation and Selection of Aggregate Gradations for Asphalt Mixtures Using Superpave. Transportation Research Record: Journal of the Transportation Research Board 1583, 91–97. https://doi.org/10.3141/1583-11
Anderson, R., Bukowski, J., Turner, P., 1999. Using Superpave Performance Tests to Evaluate Asphalt Mixtures. Transportation Research Record: Journal of the Transportation Research Board 1681, 106–112. https://doi.org/10.3141/1681-13
Anderson, R.M., Turner, P.A., Peterson, R.L., Mallick, R.B., 2002. Relationship of Superpave Gyratory Compaction Properties to HMA Rutting Behavior (NCHRP

Report No. 478). Transportation Research Board of the National Academies, Washington, DC.
Apeagyei, A.K., Buttlar, W.G., Reis, H., 2009. Assessment of Low-Temperature Embrittlement of Asphalt Binders Using an Acoustic Emission Approach. Insight - Non-Destructive Testing and Condition Monitoring 51, 129–136. https://doi.org/10.1784/insi.2009.51.3.129
Aragao, F.T.S., Lee, J., Kim, Y.-R., Karki, P., 2010. Material-Specific Effects of Hydrated Lime on the Properties and Performance Behavior of Asphalt Mixtures and Asphaltic Pavements. Construction and Building Materials 24, 538–544. https://doi.org/10.1016/j.conbuildmat.2009.10.005
Aschenbrenner, T., 2003. AASHTO Survey, in: Moisture Sensitivity of Asphalt Pavements: A National Seminar. National Academies of Sciences, Engineering, and Medicine, Washington, DC, pp. 29–42.
Aschenbrenner, T., McGennis, R.B., Terrel, R.L., 1995. Comparison of Several Moisture Susceptibility Tests to Pavement of Known Field Performance (with Discussion and Closure). Journal of the Association of Asphalt Paving Technologists 64, 163–208.
ASTM International (ASTM), 2016. ASTM D7643 Standard Practice for Determining the Continuous Grading Temperatures and Continuous Grades for PG Graded Asphalt Binders. ASTM International, West Conshohocken, PA.
ASTM International (ASTM), 2014. ASTM D4867 Standard Test Method for Effect of Moisture on Asphalt Concrete Paving Mixtures. ASTM International, West Conshohocken, PA.
ASTM International (ASTM), 2012. ASTM D3625 Standard Practice for Effect of Water on Bituminous-Coated Aggregate Using Boiling Water. ASTM International, West Conshohocken, PA.
ASTM International (ASTM), 2011a. ASTM D1075 Standard Test Method for Effect of Water on Compressive Strength of Compacted Bituminous Mixtures. ASTM International, West Conshohocken, PA.
ASTM International (ASTM), 2011b. ASTM D7369 Standard Test Method for Determining the Resilient Modulus of Bituminous Mixtures by Indirect Tension Test. ASTM International), West Conshohocken, PA.
Bahia, H.U., Faheem, A.F., 2007. Using the Superpave Gyratory Compactor to Estimate Rutting Resistance of Hot-Mix Asphalt, in: Transportation Research Circular E-C124: Practical Approaches to Hot-Mix Asphalt Mix Design and Production Quality Control Testing. Transportation Research Board, Washington, D.C., pp. 45–61.
Bahia, H.U., Friemel, T.P., Peterson, P.A., Russell, J.S., Poehnelt, B., 1998. Optimization of Constructability and Resistance to Traffic: A New Design Approach for HMA using the Superpave Compactor. Journal of the Association of Asphalt Paving Technologists 67, 189–232.
Bayomy, F., Abu Abdo, A.M., 2006. Development and Performance Prediction of Idaho Superpave Mixes (Final Report No. ITD-NIATT Project KLK464). National Institute for Advanced Transportation Technology, University of Idaho, Moscow, ID.
Bayomy, F., Masad, E., Dessouky, S., 2002. Development and Performance Prediction of Idaho Superpave Mixes (Interim Report No. ITD-NIATT Project KLK464). National Institute for Advanced Transportation Technology, University of Idaho, Moscow, ID.

Bennert, T., Reinke, G., Mogawer, W., Mooney, K., 2010. Assessment of Workability and Compactability of Warm-Mix Asphalt. Transportation Research Record: Journal of the Transportation Research Board 2180, 36–47. https://doi.org/10.3141/2180-05

Bikerman, J.J., 1947. The Fundamentals of Tackiness and Adhesion. Journal of Colloid Science 2, 163–175. https://doi.org/10.1016/0095-8522(47)90017-2

Birgisson, B., Roque, R., Tia, M., Masad, E.A., 2005. Development and Evaluation of Test Methods to Evaluate Water Damage and Effectiveness of Antistripping Agents (Report No. FDOT-BC354-11). University of Florida, Gainesville, FL.

Bissada, A., 1984. Resistance to Compaction of Asphalt Paving Mixtures and Its Relationship to Stiffness, in: Wagner, F. (Ed.), Placement and Compaction of Asphalt Mixtures. ASTM International, West Conshohocken, PA, pp. 131–145.

Brown, E.R., Lord, B., Decker, D., Newcomb, D., 2000. Hot Mix Asphalt Tender Zone (NCAT Report No. 00-02). National Center for Asphalt Technology (NCAT), Auburn, AL.

Buncher, M., 2009. PPA Modification and Performance Testing [WWW Document]. Asphalt: The Magazine of the Asphalt Institute. URL http://asphaltmagazine.com/ppa-modification-and-performance-testing/ (accessed 8.10.18).

Butcher, M., 1998. Determining Gyratory Compaction Characteristics Using Servopac Gyratory Compactor. Transportation Research Record: Journal of the Transportation Research Board 1630, 89–97. https://doi.org/10.3141/1630-11

Button, J.W., Chowdhury, A., Bhasin, A., 2005. Evaluation of Selected Laboratory Procedures and Development of Databases for HMA (Report No. FHWA/TX-05/0-4203-3). Texas Transportation Institute, College Station, TX.

Button, J.W., Chowdhury, A., Bhasin, A., 2004. Design of TxDOT Asphalt Mixtures using the Superpave Gyratory Compactor (Report No. FHWA/TX-05/0-4203-1). Texas Transportation Institute, College Station, TX.

Cabrera, J.G., 1996. Hot Bituminous Mixture: Design for Performance, in: Cabrera, J.G., Dixon, J.R. (Eds.), Performance and Durability of Bituminous Materials: Proceedings of Symposium, University of Leeds, March 1994. E & F. N. Spon, London, UK, pp. 101–113.

Cabrera, J.G., 1991. Assessment of the Workability of Bituminous Mixtures. Highways and Transportation, 38, 17–23.

Chadbourn, B.A., Newcomb, D.E., Voller, V.R., DeSombre, R.A., Luoma, J.A., Timm, D.H., 1998. An Asphalt Paving Tool for Adverse Conditions (Report No. MN/RC-1998-18). University of Minnesota, Minneapolis, MN.

Chang, C.-M., Chang, Y.-J., Chen, J.-S., 2009. Effect of Mixture Characteristics on Cooling Rate of Asphalt Pavements. Journal of Transportation Engineering 135, 297–304. https://doi.org/10.1061/(ASCE)TE.1943-5436.0000004

Christensen, D., Morris, D., Wang, W., 2015. Cost Benefit Analysis of Anti-Strip Additives in Hot Mix Asphalt with Various Aggregates (Report No. FHWA-PA-2015-004-110204). Advanced Asphalt Technologies, LLC, Kearneysville, WV.

Cominsky, R., Killingsworth, B.M., Anderson, R.M., Anderson, D.A., Crockford, W.W., 1998. Quality Control and Acceptance of Superpave-Designed Hot Mix Asphalt (NCHRP Report No. 409). Transportation Research Board, National Research Council, Washington, DC.

Cominsky, R., Leahy, R.B., Harrigan, E.T., 1994. Level One Mix Design: Materials Selection, Compaction, and Conditioning (Report No. SHRP-A-408). Strategic Highway Research Program, National Research Council, Washington, DC.

De Sombre, R., Newcomb, D.E., Chadbourn, B., Voller, V., 1998. Parameters to Define the Laboratory Compaction Temperature Range of Hot-Mix Asphalt. Journal of the Association of Asphalt Paving Technologists 67, 125–152.

Dessouky, S., 2015. Laboratory and Field Evaluation of Asphalt Concrete Mixture Workability and Compactability, in: Harvey, J., Chou, K.F. (Eds.), Airfield and Highway Pavements 2015: Innovative and Cost-Effective Pavements for a Sustainable Future. American Society of Civil Engineers, Reston, VA, pp. 97–106. https://doi.org/10.1061/9780784479216.010

Dessouky, S., Masad, E., Bayomy, F., 2004. Prediction of Hot Mix Asphalt Stability Using the Superpave Gyratory Compactor. Journal of Materials in Civil Engineering 16, 578–587. https://doi.org/10.1061/(ASCE)0899-1561(2004)16:6(578)

Dessouky, S., Masad, E., Bayomy, F., 2003. Evaluation of Asphalt Mix Stability Using Compaction Properties and Aggregate Structure Analysis. International Journal of Pavement Engineering 4, 87–103. https://doi.org/10.1080/10298430310001597043

Dessouky, S., Pothuganti, A.R., Walubita, L.F., Rand, D., 2013. Laboratory Evaluation of the Workability and Compactability of Asphaltic Materials Prior to Road Construction. Journal of Materials in Civil Engineering 25, 810–818. https://doi.org/10.1061/(ASCE)MT.1943-5533.0000551

Dickson, P.F., Corlew, J.S., 1970. Thermal Computations Related to the Study of Pavement Compaction Cessation Requirements, in: Proceedings of the Association of Asphalt Paving Technologists. Association of Asphalt Paving Technologists, Lino Lakes, MN, pp. 377–403.

Emery, J., Seddik, H., 1997. Moisture Damage of Asphalt Pavements and Antistripping Additives: Background Document. Transportation Association of Canada, Ottawa, Ontario, Canada.

Epps, J., Berger, E., Anagnos, J.N., 2003. Treatments, in: Moisture Sensitivity of Asphalt Pavements: A National Seminar. National Academies of Sciences, Engineering, and Medicine, Washington, DC, pp. 120–180. https://doi.org/10.17226/21957

Florida Department of Transportation (FDOT), 2020. Standard Specifications for Road and Bridge Construction. Florida Department of Transportation, Tallahassee, FL.

Florida Department of Transportation (FDOT), 2019. Standard Specifications for Road and Bridge Construction. Florida Department of Transportation, Tallahassee, FL.

Florida Department of Transportation (FDOT), 2018a. FM 5-508 Florida Method of Test for Laboratory Testing the Effectiveness of Anti-Strip Additives. Florida Department of Transportation, Tallahassee, FL.

Florida Department of Transportation (FDOT), 2018b. FM 1-T 283 Florida Method of Test for Resistance of Compacted Bituminous Mixture to Moisture-Induced Damage. Florida Department of Transportation, Tallahassee, FL.

Florida Department of Transportation (FDOT), 2017. FM 1-T 209 Florida Method of Test for Maximum Specific Gravity of Asphalt Paving Mixtures. Florida Department of Transportation, Tallahassee, FL.

Florida Department of Transportation (FDOT), 2016. FM 1-T166 Florida Method of Test for Bulk Specific Gravity of Compacted Asphalt Specimens. Florida Department of Transportation, Tallahassee, FL.

Garf, P.E., 1986. Factors Affecting Moisture Susceptibility of Asphalt Concrete Mixes, in: Proceedings of the Association of Asphalt Paving Technologists. Association of Asphalt Paving Technologists, Lino Lakes, MN, pp. 175–204.
Georgia Department of Transportation (GDOT), 2013. Standard Specifications Construction of Transportation Systems. Georgia Department of Transportation, Atlanta, GA.
Georgia Department of Transportation (GDOT), 2012. GDT 56 Heat Stable Anti-Strip Additive. Georgia Department of Transportation, Atlanta, GA.
Georgia Department of Transportation (GDOT), 2011. GDT 66 Evaluating the Moisture Susceptibility of Bituminous Mixtures by Diametral Tensile Splitting. Georgia Department of Transportation, Atlanta, GA.
Gorsuch, C., HogenDoorn, S., Daranga, C., Mckay, J., 2013. Measuring the Surface Tackiness of Modified Asphalt Binders and Emulsion Residues using a Dynamic Shear Rheometer, in: Proceedings of the Fifty-Eighth Annual Conference of the Canadian Technical Asphalt Association (CTAA): St. John's, Newfoundland and Labrador, November 2013. Canadian Technical Asphalt Association, Victoria, British Columbia, Canada, pp. 121–38.
Gudimettla, J., Cooley, L., Brown, E., 2004. Workability of Hot-Mix Asphalt. Transportation Research Record: Journal of the Transportation Research Board 1891, 229–237. https://doi.org/10.3141/1891-27
Gudimettla, J.M., Cooley, L.A., Brown, E.R., 2003. Workability of Hot Mix Asphalt (NCAT Report No. 03-03). National Center for Asphalt Technology (NCAT), Auburn, AL.
Guler, M., Bahia, H., Bosscher, P., Plesha, M., 2000. Device for Measuring Shear Resistance of Hot-Mix Asphalt in Gyratory Compactor. Transportation Research Record: Journal of the Transportation Research Board 1723, 116–124. https://doi.org/10.3141/1723-15
Heukelom, W., 1968. The Role of Filler in Bituminous Mixes, in: Proceedings of the Association of Asphalt Paving Technologists. Association of Asphalt Paving Technologists, Lino Lakes, MN, pp. 396–429.
Hicks, R.G., Leahy, R.B., Cook, M., Moulthrop, J.S., Button, J., 2003. Road Map for Mitigating National Moisture Sensitivity Concerns in Hot-Mix Pavements, in: Moisture Sensitivity of Asphalt Pavements: A National Seminar. National Academies of Sciences, Engineering, and Medicine, Washington, DC, pp. 331–340.
Hughes, C.S., 1989. NCHRP Program Synthesis of Highway Practice 152: Compaction of Asphalt Pavement. Transportation Research Board, National Research Council, Washington, DC.
Kaseem, E., Scullion, T., Masad, E., Chowdhury, A., Liu, W., Estakhri, C., Dessouky, S., 2012. Comprehensive Evaluation of Compaction of Asphalt Pavements and Development of Compaction Monitoring System (Report No. FHWA/TX-12/0-6992-2). Texas Transportation Institute, College Station, TX.
Kennedy, T.W., Anagnos, J.N., 1984. Techniques for Reducing Moisture Damage in Asphalt Mixtures (Report No. FHWA/TX-85/68+253-9F). Center for Transportation Research, Austin, TX.
Kennedy, T.W., Roberts, F.L., Anagnos, J.N., 1984a. Texas Boiling Test for Evaluating Moisture Susceptibility of Asphalt Mixtures (Report No. FHWA/TX-85/63+253-5). Center for Transportation Research, Austin, TX.

Kennedy, T.W., Roberts, F.L., McGennis, R.B., Anagnos, J.N., 1984b. Compaction of Asphalt Mixtures and the Use of Vibratory Rollers (Report No. 317-1). Center for Transportation Research, Austin, TX.
Kim, Y.-R., Lutif, J.S., Bhasin, A., Little, D.N., 2008. Evaluation of Moisture Damage Mechanisms and effects of Hydrated Lime in Asphalt Mixtures through Measurements of Mixture Component Properties and Performance Testing. Journal of Materials in Civil Engineering 20, 659–667.
Louisiana Department of Transportation and Development (LaDOTD), 2016. Standard Specifications for Roads and Bridges. Louisiana Department of Transportation and Development, Baton Rouge, LA.
Louisiana Department of Transportation and Development (LaDOTD), 2014a. DOTD TR 317 Method of Test for Water Susceptibility of Asphaltic Concrete Materials. Louisiana Department of Transportation and Development, Baton Rouge, LA.
Louisiana Department of Transportation and Development (LaDOTD), 2014b. DOTD TR 322 Method of Test for Determining the Effect of Moisture on Asphaltic Concrete Paving Mixtures. Louisiana Department of Transportation and Development, Baton Rouge, LA.
Louisiana Department of Transportation and Development (LaDOTD), 1994. DOTD TR 610 Method of Test for Infrared Spectophotometric Analysis. Louisiana Department of Transportation and Development, Baton Rouge, LA.
Ling, C., Moraes, R., Swiertz, D., Bahia, H., 2013. Measuring the Influence of Aggregate Coating on the Workability and Moisture Susceptibility of Cold-Mix Asphalt. Transportation Research Record: Journal of the Transportation Research Board 2372, 46–52. https://doi.org/10.3141/2372-06
Little, D., Epps, J., Sebaaly, P., 2006. The Benefits of Hydrated Lime in Hot Mix Asphalt. National Lime Association, Arlington, VA.
Lottman, T.P., 1982. Predicting Moisture-Induced Damage to Asphaltic Concrete: Field Evaluation (NCHRP Report No. 246). Transportation Research Board, National Research Council, Washington, DC.
Mallick, R., 1999. Use of Superpave Gyratory Compactor to Characterize Hot-Mix Asphalt. Transportation Research Record: Journal of the Transportation Research Board 1681, 86–96. https://doi.org/10.3141/1681-11
Marvillet, J., Bougault, P., 1979. Workability of Bituminous Mixes: Development of a Workability Meter. Journal of the Association of Asphalt Paving Technologists 48, 91–110.
McGennis, R., 1997. Evaluation of Materials from Northeast Texas using Superpave Mix Design Technology. Transportation Research Record: Journal of the Transportation Research Board 1583, 98–105. https://doi.org/10.3141/1583-12
McGennis, R.B., Kennedy, T.W., Machemehl, R.B., 1984. Stripping and Moisture Damage in Asphalt Mixtures (Interim Report No. FHWA/TX-85/55+253-1). Center for Transportation Research, Austin, TX.
McLeod, N.W., 1967. Influence of Viscosity of Asphalt-Cements on Compaction of Paving Mixtures in the Field. Highway Research Record 158, 76–115.
McRea, J.L., 1965. Gyratory Testing Machine Technical Manual. Engineering Developments Company, Inc., Vicksburg, MS.
McRea, J.L., 1962. Gyratory Compaction Method for Determining Density Requirements for Subgrade and Base of Flexible Pavements (Miscellaneous Paper No. 4-494). U.S.

Army Engineering Waterways Experiment Station, Corps of Engineering, Vicksburg, MS.
Mississippi Department of Transportation (MDOT), 2017. Standard Specifications for Road and Bridge Construction. Mississippi Department of Transportation, Jackson, MS.
Mississippi Department of Transportation (MDOT), 2010. MT 59 Determination of Loss of Coating of HMA (Boiling Water Test). Mississippi Department of Transportation, Jackson, MS.
Mississippi Department of Transportation (MDOT), 2005. MT 63 Resistance of Bituminous Paving Mixtures to Stripping (Vacuum Saturation Method). Mississippi Department of Transportation, Jackson, MS.
Ministry of Transportation (MTO), 2017. LS-283 Test for Resistance to Stripping of Asphalt Cement in Bitumen Mix by Marshall Immersion. Ministry of Transportation, Ontario, Canada.
Mohammad, L.N., Al Shamsi, K., 2007. A Look at the Bailey Method and Locking Point Concept in Superpave Mixture Design, in: Transportation Research Circular E-C124: Practical Approaches to Hot-Mix Asphalt Mix Design and Production Quality Control Testing. Transportation Research Board, Washington D.C., pp. 12–32.
National Lime Association (NLA), 2003. How to Add Hydrated Lime to Asphalt: An Overview of Current Methods. National Lime Association, Arlington, VA.
North Carolina Department of Transportation (NCDOT), 2018a. Specifications for Roads and Structures. North Carolina Department of Transportation, Raleigh, NC.
North Carolina Department of Transportation (NCDOT), 2018b. NCDOT T283 Tensile Strength Ratio (TSR) Test. North Carolina Department of Transportation, Raleigh, NC.
Newcomb, N., Arámbula, E., Zhang, J., Bhasin, A., Li, W., Arega, Z., 2015. Properties of Foamed Asphalt for Warm Mix Asphalt Applications (NCHRP Report No. 807). National Academies of Sciences, Engineering, and Medicine, Washington, DC.
Paul, H.R., 1995. Compatibility of Aggregate, Asphalt Cement and Antistrip Materials (Report No. 292). Louisiana Transportation Research Center, Baton Rouge, LA.
Pavement Interactive, 2020. Corrugation and Shoving [WWW Document]. Pavement Distresses. URL https://pavementinteractive.org/reference-desk/pavement-management/pavement-distresses/corrugation-and-shoving/ (accessed 4.20.20).
Poeran, N., Sluer, B., 2016. Workability of Asphalt Mixtures, in: Proceedings of the 6th Eurasphalt & Eurobitume Congress. Eurasphalt & Eurobitume Congress, Prague, Czech Republic. https://doi.org/dx.doi.org/10.14311/EE.2016.057
Putnam, B.J., Amirkhanian, S.N., 2006. Laboratory Evaluation of Anti-Strip Additives in Hot Mix Asphalt (Report No. FHWA-SC-06-07). Clemson University, Clemson, SC.
Ravi Shankar, A.U., Sarang, G., Lekha, B.M., Carlton-Carew, C., 2018. Investigation on the Effect of Anti Stripping Additives on the Moisture Sensitivity of Bituminous Concrete, in: Struble, L., Tebaldi, G. (Eds.), Materials for Sustainable Infrastructure: Proceedings of the 1st GeoMEast International Congress and Exhibition, Egypt 2017 on Sustainable Civil Infrastructures. Springer International Publishing, Cham, Switzerland, pp. 228–239.
Ruth, B., Shen, X., Wang, L.-H., 1992. Gyratory Evaluation of Aggregate Blends to Determine their Effect on Shear Resistance and Sensitivity to Asphalt Content, in: Meininger, R. (Ed.), Effects of Aggregates and Mineral Fillers on Asphalt Mixture

Performance. ASTM International, West Conshohocken, PA, pp. 252–264. https://doi.org/10.1520/STP24221S
Sánchez, M., Timm, D., 2014. Influence of Sustainable Recycled Asphalt Technologies on Pavement Construction Cooling Predictions. Transportation Research Record: Journal of the Transportation Research Board 2408, 69–77. https://doi.org/10.3141/2408-08
South Carolina Department of Transportation (SCDOT), 2009. SCT 70 Laboratory Determination of Moisture Susceptibility Based on Retained Strength of Asphalt Concrete Mixture. South Carolina Department of Transportation, Columbia, SC.
South Carolina Department of Transportation (SCDOT), 2008. SCT 69 Method of Determining the Effectiveness of Anti-Stripping Additives in Hot Asphalt Mixtures. South Carolina Department of Transportation, Columbia, SC.
South Carolina Department of Transportation (SCDOT), 2007. Specifications for Highway Construction. South Carolina Department of Transportation, Columbia, SC.
Scherocman, J.A., 2006. Compaction of Stiff and Tender Asphalt Concrete Mixes, in: Transportation Research Circular E-C105: Factors Affecting Compaction of Asphalt Pavements. Transportation Research Board, Washington, DC, pp. 69–84.
Sebaaly, P., Elie, H., Little, D., Shivakolunthar, S., Sathanathan, T., Vasconcelos, K., 2010. Evaluating the Impact of Lime on Pavement Performance. National Lime Association, Arlington, VA.
Sun, Z., Behnia, B., Buttlar, W., Reis, H., 2017. Assessment of Low-Temperature Cracking in Asphalt Materials Using an Acoustic Emission Approach. Journal of Testing and Evaluation 45, 1948–1958.
Tennessee Department of Transportation (TDOT), 2018. Ten Minute Boil Test (Stripping). Tennessee Department of Transportation, Nashville, TN.
Tennessee Department of Transportation (TDOT), 2015. Standard Specifications for Road and Bridge Construction. Tennessee Department of Transportation, Nashville, TN.
Timm, D.H., Voller, V.R., Lee, E., Harvey, J., 2001. Calcool: A Multi-Layer Asphalt Pavement Cooling Tool for Temperature Prediction During Construction. International Journal of Pavement Engineering 2, 169–185. https://doi.org/10.1080/10298430108901725
Tunnicliff, D.G., Root, R.E., 1984. Use of Antistripping Additives in Asphaltic Concrete Mixtures: Laboratory Phase (NCHRP Report No. 274). Transportation Research Board, Washington D.C.
Texas Department of Transportation (TxDOT), 2014. Standard Specifications for Construction and Maintenance of Highways, Streets, and Bridges. Texas Department of Transportation, Austin, TX.
Texas Department of Transportation (TxDOT), 2008. Tex-530-C Effect of Water in Bituminous Paving Mixtures. Texas Department of Transportation, Austin, TX.
Texas Department of Transportation (TxDOT), 1999. Tex-531-C Test Procedure for Prediction of Moisture-Induced Damage to Bituminous Paving Materials Using Molded Specimens. Texas Department of Transportation, Austin, TX.
Vargas-Nordcbeck, A., Timm, D.H., 2011. Validation of Cooling Curves Prediction Model for Nonconventional Asphalt Concrete Mixtures. Transportation Research Record 2228, 111–119. https://doi.org/10.3141/2228-13
Vavrik, W., Carpenter, S., 1998. Calculating Air Voids at Specified Number of Gyrations in Superpave Gyratory Compactor. Transportation Research Record: Journal of the Transportation Research Board 1630, 117–125. https://doi.org/10.3141/1630-14

Velasquez, R., Cuciniello, G., Swiertz, D., Bonaquist, R., Bahia, H., 2012. Methods to Evaluate Aggregate Coating for Asphalt Mixtures Produced at WMA Temperatures, in: Proceedings of the Fifty-Seventh Annual Conference of the Canadian Technical Asphalt Association. Canadian Technical Asphalt Association, Vancouver, British Columbia, Canada, pp. 225–238.

Wilson, B., Seo, A.Y., Sakhaeifar, M., 2016. Performance Evaluation and Specification of Trackless Tack (Report No. FHWA/TX-16/0-6814-1). Texas A&M Transportation Institute, College Station, TX.

Zhou, F., Crockford, B., Zhang, J., Hu, S., Epps, J., Sun, L., 2019. Development and Validation of an Ideal Shear Rutting Test for Asphalt Mix Design and QC/QA, in: Proceedings of the Association of Asphalt Paving Technologists. Association of Asphalt Paving Technologists, Lino Lakes, MN.

APPENDIX A PARAMETERS OBTAINED FROM COMPACTION DATA

Table A-1. Compaction Effort Parameters Obtained from Compaction Data

S.N.	Parameter	GA9.5						GA12.5						LS9.5						LS12.5					
		C0-Avg	C0-SD	L1	L2	L3	L4	C0-Avg	C0-SD	L1	L2	L3	L4	C0-Avg	C0-SD	L1	L2	L3	L4	C0-Avg	C0-SD	L1	L2	L3	L4
1	N87	3.67	0.58	2.33	2.00	2.00	2.00	2.00	0.00	1.00	1.00	1.00	1.00	2.00	0.00	2.00	2.00	2.00	2.00	1.50	0.71	1.00	1.00	1.50	1.50
2	N92	20.00	2.65	14.33	14.00	11.00	10.67	14.33	1.53	10.67	10.67	8.00	6.33	14.50	0.71	12.00	11.50	12.50	12.50	12.50	0.71	11.00	10.00	11.50	9.50
3	N93	28.00	4.36	20.33	20.00	15.33	15.00	21.00	2.65	16.67	15.67	11.67	9.33	21.50	0.71	17.00	17.50	18.50	18.50	19.00	1.41	16.50	15.00	17.00	13.50
4	N95	62.00	10.44	44.33	44.00	32.00	30.67	49.00	8.19	38.67	37.67	25.67	21.33	54.50	3.54	39.00	42.50	41.50	46.00	47.00	4.24	41.50	37.50	40.50	28.00
5	N96	90.67	11.02	69.67	69.33	49.00	46.00	77.33	11.68	63.33	61.67	40.33	33.33	90.00	4.24	64.50	74.00	67.50	81.50	79.00	5.66	71.00	62.50	65.50	43.00
6	N98	163.00	15.72	176.00	173.33	132.67	127.67	156.33	18.23	173.67	172.33	117.33	93.00	162.50	2.12	155.50	209.50	181.00	218.00	152.00	5.66	173.50	184.50	174.50	114.50
7	N100	234.33	44.81	290.00	284.00	253.00	255.33	236.67	49.10	296.33	296.33	246.00	223.67	231.50	0.71	251.00	348.00	302.00	354.00	221.00	5.66	275.50	320.00	294.00	229.50
8	NG1	33.67	0.58	33.00	33.00	33.00	33.00	33.00	0.00	32.00	32.00	32.67	32.33	32.50	0.71	33.00	32.00	33.00	32.00	32.00	0.00	32.00	32.00	32.00	33.00
9	NLP	64.33	3.06	56.33	57.33	55.00	57.00	59.33	2.52	50.67	50.00	51.33	56.00	51.00	2.83	52.00	50.50	53.50	50.50	53.50	0.71	47.00	48.50	53.00	52.50
10	Ntmax	93.00	38.11	52.00	51.33	43.00	43.33	100.67	24.83	67.67	68.33	54.33	72.67	82.50	45.96	102.50	75.00	90.50	54.50	115.00	0.00	109.50	100.50	90.50	53.00
11	NSRmax	94.67	35.22	52.00	51.33	46.33	43.33	100.67	24.83	67.67	68.33	54.33	72.67	82.50	45.96	102.50	75.00	90.50	54.50	115.00	0.00	111.50	100.50	90.50	53.00
12	N92-7	13.00	2.65	7.33	7.00	4.00	3.67	7.33	1.53	3.67	3.67	1.00	-0.67	7.50	0.71	5.00	4.50	5.50	5.50	5.50	0.71	4.00	3.00	4.50	2.50
13	N96-7	83.67	11.02	62.67	62.33	42.00	39.00	70.33	11.68	56.33	54.67	33.33	26.33	83.00	4.24	57.50	67.00	60.50	74.50	72.00	5.66	64.00	55.50	58.50	36.00
14	N96-N92	70.67	8.39	55.33	55.33	38.00	35.33	63.00	10.15	52.67	51.00	32.33	27.00	75.50	3.54	52.50	62.50	55.00	69.00	66.50	4.95	60.00	52.50	54.00	33.50
15	N96-NG1	57.00	10.44	36.67	36.33	16.00	13.00	44.33	11.68	31.33	29.67	7.67	1.00	57.50	3.54	31.50	42.00	34.50	49.50	47.00	5.66	39.00	30.50	33.50	10.00
16	N96-NLP	26.33	13.32	13.33	12.00	-6.00	-11.00	18.00	13.23	12.67	11.67	-11.00	-22.67	39.00	1.41	12.50	23.50	14.00	31.00	25.50	4.95	24.00	14.00	12.50	-9.50
17	N98-NG1	129.33	16.29	143.00	140.33	99.67	94.67	123.33	18.23	141.67	140.33	84.67	60.67	130.00	1.41	122.50	177.50	148.00	186.00	120.00	5.66	141.50	152.50	142.50	81.50
18	N98-NLP	98.67	13.28	119.67	116.00	77.67	70.67	97.00	19.52	123.00	122.33	66.00	37.00	111.50	0.71	103.50	159.00	127.50	167.50	98.50	4.95	126.50	136.00	121.50	62.00
19	N98-N92	143.00	18.25	161.67	159.33	121.67	117.00	142.00	19.00	163.00	161.67	109.33	86.67	148.00	1.41	143.50	198.00	168.50	205.50	139.50	4.95	162.50	174.50	163.00	105.00
20	N98-N96	72.33	26.58	106.33	104.00	83.67	81.67	79.00	26.00	110.33	110.67	77.00	59.67	72.50	2.12	91.00	135.50	113.50	136.50	73.00	0.00	102.50	122.00	109.00	71.50
21	Nd-NG1	41.33	0.58	42.00	42.00	42.00	42.00	42.00	0.00	43.00	43.00	42.33	42.67	42.50	0.71	42.00	43.00	42.00	43.00	43.00	0.00	43.00	43.00	43.00	42.00
22	Nd-NLP	10.67	3.06	18.67	17.67	20.00	18.00	15.67	2.52	24.33	25.00	23.67	19.00	24.00	2.83	23.00	24.50	21.50	24.50	21.50	0.71	28.00	26.50	22.00	22.50
23	Nm-NG1	81.33	0.58	82.00	82.00	82.00	82.00	82.00	0.00	83.00	83.00	82.33	82.67	82.50	0.71	82.00	83.00	82.00	83.00	83.00	0.00	83.00	83.00	83.00	82.00
24	Nm-NLP	50.67	3.06	58.67	57.67	60.00	58.00	55.67	2.52	64.33	65.00	63.67	59.00	64.00	2.83	63.00	64.50	61.50	64.50	61.50	0.71	68.00	66.50	62.00	62.50
25	Nm-Nd	40.00	0.00	40.00	40.00	40.00	40.00	40.00	0.00	40.00	40.00	40.00	40.00	40.00	0.00	40.00	40.00	40.00	40.00	40.00	0.00	40.00	40.00	40.00	40.00
26	GR_98/95	2.72	0.78	3.97	3.94	4.15	4.16	3.27	0.82	4.49	4.58	4.57	4.35	2.99	0.15	3.99	4.93	4.36	4.74	3.24	0.17	4.17	4.93	4.31	4.09
27	GR_98/96	1.83	0.42	2.53	2.50	2.71	2.78	2.06	0.49	2.74	2.80	2.91	2.78	1.81	0.06	2.41	2.83	2.68	2.67	1.93	0.07	2.43	2.95	2.67	2.66
28	GR_Log96/92	1.51	0.03	1.59	1.61	1.62	1.62	1.63	0.01	1.75	1.74	1.78	1.90	1.68	0.01	1.68	1.76	1.67	1.74	1.73	0.01	1.78	1.80	1.71	1.67
29	GR_Log98/95	1.24	0.08	1.36	1.36	1.41	1.42	1.30	0.07	1.41	1.42	1.47	1.48	1.27	0.02	1.38	1.43	1.40	1.41	1.31	0.02	1.38	1.44	1.39	1.42
30	GR_Log98/96	1.13	0.05	1.22	1.22	1.26	1.27	1.16	0.06	1.24	1.25	1.29	1.29	1.13	0.01	1.21	1.24	1.23	1.22	1.15	0.01	1.21	1.26	1.23	1.26
31	CR	4.41	0.75	5.95	6.07	7.93	8.08	5.86	0.69	7.28	7.80	10.42	13.15	5.63	0.20	7.10	6.90	6.54	6.52	6.37	0.46	7.32	8.06	7.10	8.96

Note: Units of Nx = gyrations; Units of GR and GR_{log} = None; Unit of CR = mm/gyrations

Table A-2. Compaction Density Parameters Obtained from Compaction Data

S.N.	Parameter	GA9.5						GA12.5						LS9.5						LS12.5					
		C0-Avg	C0-SD	L1	L2	L3	L4	C0-Avg	C0-SD	L1	L2	L3	L4	C0-Avg	C0-SD	L1	L2	L3	L4	C0-Avg	C0-SD	L1	L2	L3	L4
1	C1	82.65	0.32	83.81	83.93	84.52	84.35	84.32	0.07	85.28	85.41	86.01	86.49	84.16	0.09	84.39	84.76	84.33	84.59	84.98	0.28	85.35	85.45	84.99	85.10
2	C7	88.67	0.46	89.73	89.83	90.49	90.50	89.87	0.26	90.67	90.76	91.50	91.95	89.84	0.15	90.30	90.47	90.17	90.29	90.40	0.22	90.74	90.89	90.51	90.95
3	C8	89.09	0.46	90.15	90.24	90.91	90.94	90.26	0.28	91.03	91.13	91.88	92.33	90.23	0.15	90.71	90.86	90.58	90.67	90.76	0.21	91.10	91.25	90.89	91.35
4	C10	89.82	0.46	90.84	90.93	91.60	91.65	90.91	0.30	91.63	91.74	92.49	92.95	90.88	0.15	91.38	91.48	91.25	91.30	91.36	0.21	91.70	91.84	91.50	92.01
5	C75	95.44	0.40	96.15	96.15	96.91	97.04	95.90	0.36	96.31	96.35	97.23	97.62	95.58	0.10	96.29	96.01	96.18	95.85	95.86	0.16	96.08	96.30	96.26	97.18
6	C100	96.22	0.25	96.71	96.72	97.46	97.57	96.59	0.26	96.83	96.86	97.72	98.13	96.26	0.10	96.90	96.46	96.70	96.31	96.55	0.16	96.67	96.78	96.78	97.74
7	C115	96.66	0.11	96.96	96.98	97.70	97.79	96.99	0.22	97.05	97.09	97.96	98.34	96.67	0.09	97.22	96.67	96.94	96.52	96.96	0.16	96.98	96.99	97.01	98.00
8	CNG1	93.47	0.38	94.24	94.28	95.02	95.15	94.10	0.37	94.55	94.63	95.52	95.91	93.91	0.08	94.58	94.38	94.44	94.22	94.18	0.17	94.46	94.66	94.46	95.32
9	CLP	95.09	0.49	95.53	95.58	96.25	96.46	95.41	0.41	95.54	95.58	96.49	97.07	94.86	0.00	95.57	95.30	95.51	95.14	95.24	0.13	95.23	95.51	95.56	96.43
10	Cτmax	96.04	0.97	95.31	95.30	95.61	95.78	96.70	0.53	96.10	96.17	96.60	97.54	95.75	1.21	97.01	96.01	96.52	95.27	96.96	0.16	96.90	96.77	96.59	96.44
11	CSRmax	96.12	0.83	95.31	95.30	95.78	95.78	96.70	0.53	96.10	96.17	96.60	97.54	95.75	1.21	97.01	96.01	96.52	95.27	96.96	0.16	96.94	96.77	96.59	96.44

Note: Units of Cx = percent

Table A-3. Compaction Slope Parameters Obtained from Compaction Data

S.N.	Parameter	GA9.5						GA12.5						LS9.5						LS12.5					
		C0-Avg	C0-SD	L1	L2	L3	L4	C0-Avg	C0-SD	L1	L2	L3	L4	C0-Avg	C0-SD	L1	L2	L3	L4	C0-Avg	C0-SD	L1	L2	L3	L4
1	Gmm_0	82.52	0.40	83.74	83.86	84.45	84.28	84.25	0.07	85.25	85.36	85.98	86.46	84.13	0.12	84.34	84.74	84.26	84.58	84.98	0.27	85.36	85.45	84.96	85.04
2	k	7.29	0.11	7.09	7.05	7.13	7.35	6.65	0.27	6.39	6.37	6.53	6.48	6.74	0.04	7.03	6.75	6.97	6.72	6.39	0.06	6.36	6.41	6.55	6.97
3	PI	1.21	0.01	1.19	1.19	1.18	1.19	1.19	0.00	1.17	1.17	1.16	1.16	1.19	0.00	1.19	1.18	1.19	1.18	1.18	0.00	1.17	1.17	1.18	1.18
4	k x AV75	33.22	2.62	27.28	27.14	22.02	21.74	27.22	1.27	23.57	23.26	18.10	15.39	29.80	0.53	26.10	26.93	26.61	27.90	26.43	1.25	24.88	23.73	24.52	19.65
5	c	17.48	0.40	16.26	16.14	15.55	15.72	15.75	0.07	14.75	14.64	14.02	13.54	15.87	0.12	15.66	15.26	15.74	15.42	15.02	0.27	14.64	14.55	15.04	14.96
6	m	7.29	0.11	7.09	7.05	7.13	7.35	6.65	0.27	6.39	6.37	6.53	6.48	6.74	0.04	7.03	6.75	6.97	6.72	6.39	0.06	6.36	6.41	6.55	6.97
7	CI	62.08	2.19	64.46	64.56	67.96	69.70	61.66	3.12	62.78	63.06	67.74	69.55	62.14	0.90	66.28	64.80	65.27	63.79	61.61	0.41	62.85	63.93	63.40	68.72

Note: Units of Gmm_0, and c = %; Units of m, k, and $k\ x\ AV75$ = %/gyrations, Unit of PI= 1/%, Unit of CI = None

Table A-4. Densification Parameters Obtained from Compaction Data

S.N.	Parameter	GA9.5						GA12.5						LS9.5						LS12.5					
		C0-Avg	C0-SD	L1	L2	L3	L4	C0-Avg	C0-SD	L1	L2	L3	L4	C0-Avg	C0-SD	L1	L2	L3	L4	C0-Avg	C0-SD	L1	L2	L3	L4
1	CDI_N1N92	16.97	2.35	11.93	11.63	8.95	8.64	11.95	1.37	8.67	8.68	6.29	4.79	12.09	0.63	9.85	9.41	10.30	10.31	10.33	0.62	8.99	8.08	9.42	7.62
2	CDI_N1NG1	29.65	0.40	29.34	29.36	29.58	29.60	29.34	0.10	28.61	28.64	29.52	29.34	28.85	0.62	29.49	28.55	29.44	28.50	28.51	0.06	28.61	28.66	28.57	29.71
3	CDI_N1NLP	58.61	3.11	51.49	52.48	50.64	52.62	54.32	2.52	46.36	45.77	47.45	52.19	46.32	2.62	47.56	46.11	48.92	46.02	48.89	0.57	42.84	44.36	48.54	48.41
4	CDI_N1Nd	68.77	0.31	69.39	69.42	69.96	70.03	69.30	0.25	69.71	69.77	70.38	70.69	69.17	0.10	69.63	69.55	69.54	69.43	69.44	0.13	69.64	69.78	69.64	70.20
5	CDI_N7N92	11.78	2.38	6.67	6.37	3.65	3.34	6.67	1.38	3.35	3.35	0.92	0.61	6.83	0.64	4.56	4.11	5.01	5.02	5.02	0.64	3.66	2.74	4.11	2.29
6	CDI_N7N96	78.56	10.24	59.01	58.71	39.57	36.73	66.26	10.95	53.17	51.61	31.49	24.89	78.27	3.97	54.24	63.28	57.05	70.37	67.96	5.30	60.47	52.43	55.20	33.94
7	WI_N1N92	0.85	0.01	0.83	0.83	0.81	0.81	0.83	0.01	0.81	0.81	0.79	0.76	0.83	0.00	0.82	0.82	0.82	0.82	0.83	0.00	0.82	0.81	0.82	0.80
8	WI_N1NG1	0.88	0.00	0.89	0.89	0.90	0.90	0.89	0.00	0.89	0.89	0.90	0.91	0.89	0.00	0.89	0.89	0.89	0.89	0.89	0.00	0.89	0.90	0.89	0.90
9	WI_N1NLP	0.91	0.01	0.91	0.92	0.92	0.92	0.92	0.00	0.91	0.92	0.92	0.93	0.91	0.00	0.91	0.91	0.91	0.91	0.91	0.00	0.91	0.91	0.92	0.92
10	WI_N1Nd	0.92	0.00	0.93	0.93	0.93	0.93	0.92	0.00	0.93	0.93	0.94	0.94	0.92	0.00	0.93	0.93	0.93	0.93	0.93	0.00	0.93	0.93	0.93	0.94
11	WI_N8N92	0.91	0.00	0.91	0.91	0.91	0.91	0.91	0.00	0.91	0.91	0.92		0.91	0.00	0.91	0.91	0.91	0.91	0.91	0.00	0.91	0.91	0.91	0.91
12	WI_N8N96	0.94	0.00	0.94	0.94	0.94	0.94	0.94	0.00	0.94	0.94	0.94	0.95	0.94	0.00	0.94	0.94	0.94	0.94	0.94	0.00	0.94	0.94	0.94	0.94
13	TDI_N92N96	66.78	7.87	52.34	52.34	35.92	33.39	59.58	9.57	49.82	48.26	30.57	25.51	71.45	3.33	49.68	59.18	52.04	65.35	62.95	4.67	56.81	49.68	51.09	31.66
14	TDI_N92N98	136.95	18.00	155.56	153.29	117.23	112.77	136.23	18.62	156.94	155.71	105.42	83.50	141.76	1.28	138.00	190.66	162.21	197.78	133.74	4.66	156.26	168.13	156.91	101.14
15	TDI_N96N98	70.17	25.81	103.22	100.95	81.31	79.39	76.65	25.28	107.12	107.45	74.85	57.99	70.31	2.05	88.31	131.48	110.17	132.42	70.80	0.00	99.45	118.44	105.82	69.49
16	TDI_NdNm	38.43	0.11	38.64	38.64	38.94	38.98	38.58	0.11	38.69	38.70	39.05	39.21	38.45	0.04	38.71	38.55	38.64	38.49	38.57	0.06	38.62	38.67	38.67	39.05
17	TDI_NG1N96	54.09	9.82	34.93	34.61	15.29	12.43	42.19	11.04	29.88	28.30	7.34	2.24	54.69	3.34	30.05	40.04	32.89	47.16	44.76	5.35	37.18	29.10	31.94	9.57
18	TDI_NG1N98	124.26	16.14	138.15	135.56	96.60	91.81	118.83	17.86	137.01	135.75	82.19	58.95	125.01	1.29	118.36	171.52	143.06	179.59	115.55	5.35	136.63	147.54	137.75	79.05
19	TDI_NG1Nd	39.11	0.71	40.05	40.06	40.38	40.43	39.96	0.15	41.10	41.13	40.86	41.35	40.33	0.71	40.14	41.00	40.09	40.93	40.92	0.07	41.03	41.12	41.07	40.49
20	TDI_NG1Nm	77.54	0.82	78.69	78.70	79.31	79.41	78.54	0.26	79.79	79.83	79.91	80.56	78.78	0.75	78.85	79.54	78.73	79.42	79.49	0.13	79.65	79.79	79.74	79.54
21	TDI_NLPN96	25.14	12.67	12.77	11.49	5.77	10.59	17.21	12.61	12.13	11.18	10.59	21.90	37.23	1.35	11.97	22.48	13.41	29.64	24.38	4.72	22.95	13.41	11.97	9.14
22	TDI_NLPN98	95.30	13.15	115.99	112.44	75.55	68.80	93.85	19.03	119.25	118.62	64.26	36.10	107.54	0.71	100.29	153.97	123.58	162.06	95.18	4.71	122.40	131.85	117.79	60.35
23	TDI_NLPNd	10.16	2.88	17.89	16.94	19.32	17.42	14.98	2.37	23.35	24.00	22.93	18.50	22.86	2.71	22.07	23.44	20.61	23.40	20.55	0.71	26.80	25.42	21.10	21.79
24	TDI_NLPNm	48.58	2.80	56.53	55.58	58.26	56.40	53.57	2.29	62.03	62.70	61.98	57.71	61.31	2.75	60.78	61.99	59.25	61.89	59.11	0.77	65.41	64.09	59.77	60.84
25	TI_N92N96	0.95	0.00	0.95	0.95	0.95	0.94	0.95	0.00	0.95	0.95	0.95	0.94	0.95	0.00	0.95	0.95	0.95	0.95	0.95	0.00	0.95	0.95	0.95	0.94
26	TI_N92N98	0.96	0.00	0.96	0.96	0.96	0.96	0.96	0.00	0.96	0.96	0.96	0.96	0.96	0.00	0.96	0.96	0.96	0.96	0.96	0.00	0.96	0.96	0.96	0.96
27	TI_N96N98	0.97	0.00	0.97	0.97	0.97	0.97	0.97	0.00	0.97	0.97	0.97	0.97	0.97	0.00	0.97	0.97	0.97	0.97	0.97	0.00	0.97	0.97	0.97	0.97
28	TI_NdNm	0.96	0.00	0.97	0.97	0.97	0.97	0.96	0.00	0.97	0.97	0.98	0.98	0.96	0.00	0.97	0.96	0.97	0.96	0.96	0.00	0.97	0.97	0.97	0.98
29	TI_NG1N96	0.95	0.00	0.95	0.95	0.96	0.96	0.95	0.00	0.95	0.95	0.96	0.96	0.95	0.00	0.95	0.95	0.95	0.95	0.95	0.00	0.95	0.95	0.95	0.96
30	TI_NG1N98	0.96	0.00	0.97	0.97	0.97	0.97	0.96	0.00	0.97	0.97	0.97	0.97	0.96	0.00	0.97	0.97	0.97	0.97	0.96	0.00	0.97	0.97	0.97	0.97
31	TI_NG1Nd	0.95	0.00	0.95	0.95	0.96	0.96	0.95	0.00	0.96	0.96	0.97	0.97	0.95	0.00	0.96	0.95	0.95	0.95	0.95	0.00	0.95	0.96	0.96	0.96
32	TI_NG1Nm	0.95	0.00	0.96	0.96	0.97	0.97	0.96	0.00	0.96	0.96	0.97	0.97	0.95	0.00	0.96	0.96	0.96	0.96	0.96	0.00	0.96	0.96	0.96	0.97
33	TI_NLPN96	0.96	0.00	0.96	0.96	0.96	0.96	0.96	0.00	0.96	0.96	0.96	0.97	0.95	0.00	0.96	0.96	0.96	0.96	0.96	0.00	0.96	0.96	0.96	0.96
34	TI_NLPN98	0.97	0.00	0.97	0.97	0.97	0.97	0.97	0.00	0.97	0.97	0.97	0.98	0.96	0.00	0.97	0.97	0.97	0.97	0.97	0.00	0.97	0.97	0.97	0.97
35	TI_NLPNd	0.95	0.00	0.96	0.96	0.97	0.97	0.96	0.00	0.96	0.96	0.97	0.97	0.95	0.00	0.96	0.96	0.96	0.96	0.96	0.00	0.96	0.96	0.96	0.97
36	TI_NLPNm	0.96	0.00	0.96	0.96	0.97	0.97	0.96	0.00	0.96	0.96	0.97	0.98	0.96	0.00	0.96	0.96	0.96	0.96	0.96	0.00	0.96	0.96	0.96	0.97

Note: Units of CDI, WI, TDI, and TI = N.mm

Table A-5. Compaction Energy Parameters Obtained from Compaction Data

S.N.	Parameter	GA9.5						GA12.5						LS9.5						LS12.5					
		C0-Avg	C0-SD	L1	L2	L3	L4	C0-Avg	C0-SD	L1	L2	L3	L4	C0-Avg	C0-SD	L1	L2	L3	L4	C0-Avg	C0-SD	L1	L2	L3	L4
1	VEI_N1N92	146.39	5.41	125.30	123.89	113.34	115.38	117.64	0.37	99.40	99.47	88.70	78.38	119.25	0.97	115.13	108.34	116.16	111.57	105.76	4.06	99.77	96.38	104.42	102.83
2	VEI_N1NG1	167.31	1.22	157.18	156.26	156.22	160.53	147.94	4.35	137.27	137.08	138.35	136.61	146.92	0.06	151.79	142.92	151.22	143.31	136.61	2.56	134.14	134.83	139.55	149.84
3	VEI_N1NLP	189.24	2.34	174.24	173.53	172.34	177.70	165.56	4.70	150.30	149.67	150.94	151.63	159.59	1.03	164.80	155.06	165.35	155.50	150.68	3.23	144.36	145.92	153.98	164.15
4	VEI_N1Nd	193.80	1.07	182.28	180.99	180.87	185.10	171.90	4.06	160.39	159.75	160.32	158.64	169.04	0.32	174.04	164.28	174.11	164.73	158.76	2.93	155.48	156.16	162.90	173.70
5	VEI_N7N92	48.49	6.77	31.68	30.43	20.14	19.32	29.79	3.29	16.29	16.51	5.36	4.17	29.80	1.86	23.00	19.90	24.69	23.13	21.92	2.41	17.10	13.57	19.65	13.03
6	VEI_N7N96	102.99	6.84	86.58	85.51	75.70	75.26	85.13	3.94	73.11	72.16	61.06	54.81	84.94	2.08	78.13	75.53	80.04	77.99	76.37	3.34	71.54	69.28	74.68	68.52
7	WEI_N1N92	7.39	0.77	8.75	8.85	10.30	10.83	8.27	0.86	9.33	9.34	11.09	12.42	8.23	0.33	9.59	9.42	9.30	8.93	8.46	0.15	9.07	9.66	9.09	10.83
8	WEI_N1NG1	4.97	0.09	4.76	4.74	4.73	4.86	4.48	0.13	4.29	4.28	4.24	4.23	4.52	0.10	4.60	4.47	4.58	4.48	4.27	0.08	4.19	4.21	4.36	4.54
9	WEI_N1NLP	2.94	0.11	3.09	3.04	3.14	3.13	2.79	0.09	2.98	3.00	2.95	2.71	3.13	0.15	3.17	3.07	3.09	3.08	2.82	0.02	3.07	3.01	2.91	3.13
10	WEI_N1Nd	2.58	0.01	2.43	2.41	2.41	2.47	2.29	0.05	2.14	2.13	2.14	2.12	2.25	0.00	2.32	2.19	2.32	2.20	2.12	0.04	2.07	2.08	2.17	2.32
11	WEI_N8N92	3.77	0.28	4.32	4.35	5.03	5.28	4.12	0.39	4.46	4.52	5.36	-	3.98	0.13	4.60	4.42	4.50	4.21	3.99	0.07	4.27	4.57	4.38	5.21
12	WEI_N8N96	1.24	0.09	1.38	1.37	1.80	1.93	1.23	0.14	1.30	1.32	1.83	2.10	1.02	0.03	1.36	1.13	1.32	1.05	1.06	0.04	1.12	1.25	1.28	1.90
13	SEI_N92N96	54.50	0.76	54.90	55.08	55.57	55.94	55.34	0.67	56.82	55.65	55.69	58.97	55.14	0.21	55.13	55.63	55.35	54.86	54.45	0.92	54.45	55.70	55.03	55.49
14	SEI_N92N98	80.05	0.72	80.41	80.58	81.17	81.66	80.96	0.56	82.34	81.21	81.23	84.87	80.63	0.01	80.44	81.01	80.95	80.23	80.08	0.94	79.85	80.98	80.29	80.90
15	SEI_N96N98	25.55	0.05	25.51	25.50	25.60	25.72	25.62	0.16	25.52	25.56	25.53	25.90	25.50	0.23	25.31	25.38	25.60	25.38	25.63	0.01	25.41	25.28	25.26	25.42
16	SEI_NdNm	15.88	3.89	10.34	10.65	9.99	9.46	14.11	3.39	9.50	9.52	9.17	9.07	14.12	0.19	11.91	8.43	9.67	8.60	14.12	0.03	11.37	8.81	9.61	10.19
17	SEI_NG1N96	33.58	5.00	23.01	22.71	12.68	10.80	25.04	4.98	18.94	18.04	6.05	2.09	27.47	1.12	18.48	21.05	20.29	23.12	23.59	2.43	20.08	17.25	19.90	8.48
18	SEI_NG1N98	59.13	5.01	48.53	48.21	38.28	36.52	50.66	4.84	44.47	43.60	31.58	26.64	52.96	0.89	43.79	46.43	45.89	48.50	49.23	2.44	45.48	42.53	45.16	33.90
19	SEI_NG1Nd	26.50	0.18	25.10	24.73	24.65	24.58	23.96	0.29	23.12	22.67	21.97	22.03	22.13	0.38	22.25	21.36	22.89	21.42	22.14	0.37	21.35	21.33	23.35	23.87
20	SEI_NG1Nm	42.38	3.78	35.45	35.38	34.65	34.04	38.08	3.62	32.63	32.19	31.13	31.11	36.25	0.20	34.16	29.79	32.56	30.02	36.26	0.41	32.72	30.14	32.96	34.06
21	SEI_NLPN96	11.65	6.35	5.95	5.45	3.44	6.38	7.41	5.44	5.91	5.45	6.54	14.27	14.79	0.15	5.47	8.91	6.16	10.93	9.52	1.75	9.85	6.16	5.47	5.84
22	SEI_NLPN98	37.21	6.36	31.46	30.95	22.17	19.34	33.03	5.31	31.44	31.01	18.99	11.62	40.29	0.08	30.78	34.29	31.76	36.30	35.16	1.77	35.26	31.44	30.73	19.58
23	SEI_NLPNd	4.57	1.56	8.04	7.46	8.54	7.40	6.33	1.24	10.10	10.08	9.38	7.02	9.45	1.35	9.24	9.22	8.76	9.23	8.07	0.30	11.12	10.24	8.91	9.55
24	SEI_NLPNm	20.45	5.24	18.38	18.12	18.53	16.87	20.45	3.49	19.60	19.61	18.54	16.09	23.57	1.17	21.15	17.65	18.43	17.82	22.19	0.27	22.49	19.05	18.53	19.74
25	CEI_N92N96	0.78	0.10	0.99	1.00	1.46	1.58	0.89	0.13	1.08	1.09	1.73	2.20	0.73	0.03	1.05	0.89	1.01	0.79	0.82	0.05	0.91	1.06	1.02	1.66
26	CEI_N92N98	0.57	0.07	0.50	0.51	0.67	0.70	0.58	0.07	0.51	0.50	0.75	0.99	0.54	0.01	0.57	0.41	0.48	0.39	0.57	0.01	0.51	0.46	0.49	0.77
27	CEI_N96N98	0.38	0.12	0.24	0.25	0.31	0.31	0.34	0.09	0.23	0.23	0.33	0.44	0.35	0.01	0.29	0.19	0.23	0.19	0.35	0.00	0.27	0.21	0.23	0.36
28	CEI_NdNm	0.40	0.10	0.26	0.27	0.25	0.24	0.35	0.08	0.24	0.24	0.23	0.23	0.35	0.00	0.30	0.21	0.24	0.21	0.35	0.00	0.28	0.22	0.24	0.25
29	CEI_NG1N96	0.59	0.02	0.63	0.63	0.79	0.83	0.57	0.04	0.61	0.61	0.79	0.96	0.48	0.01	0.59	0.50	0.59	0.47	0.50	0.01	0.52	0.56	0.59	0.85
30	CEI_NG1N98	0.46	0.09	0.34	0.34	0.38	0.39	0.42	0.08	0.31	0.31	0.37	0.45	0.41	0.00	0.37	0.26	0.31	0.26	0.41	0.00	0.34	0.28	0.32	0.42
31	CEI_NG1Nd	0.64	0.01	0.60	0.59	0.59	0.59	0.57	0.01	0.54	0.53	0.52	0.52	0.52	0.00	0.53	0.50	0.54	0.50	0.51	0.01	0.50	0.50	0.54	0.57
32	CEI_NG1Nm	0.52	0.05	0.43	0.43	0.42	0.42	0.46	0.04	0.39	0.39	0.38	0.38	0.44	0.00	0.42	0.36	0.40	0.36	0.44	0.00	0.39	0.36	0.40	0.42
33	CEI_NLPN96	0.43	0.03	0.45	0.45	0.57	0.59	0.42	0.03	0.47	0.47	0.60	0.62	0.38	0.01	0.44	0.38	0.44	0.35	0.37	0.00	0.41	0.44	0.44	0.61
34	CEI_NLPN98	0.39	0.11	0.26	0.27	0.29	0.27	0.35	0.09	0.26	0.25	0.29	0.32	0.36	0.00	0.31	0.22	0.25	0.22	0.36	0.00	0.30	0.23	0.25	0.32
35	CEI_NLPNd	0.42	0.02	0.43	0.42	0.43	0.41	0.40	0.02	0.41	0.40	0.39	0.37	0.39	0.01	0.40	0.38	0.41	0.38	0.38	0.00	0.40	0.39	0.40	0.42
36	CEI_NLPNm	0.40	0.08	0.31	0.31	0.31	0.29	0.37	0.06	0.30	0.30	0.29	0.27	0.37	0.00	0.34	0.27	0.30	0.28	0.36	0.00	0.33	0.29	0.30	0.32

Note: Units of VEI, WEI, SEI, and CEI = N.mm